UNIVERSITAT DE BARCELONA

Refining prognosis capacity and implementing principles of personalized therapies for Neurofibromatosis Type 2
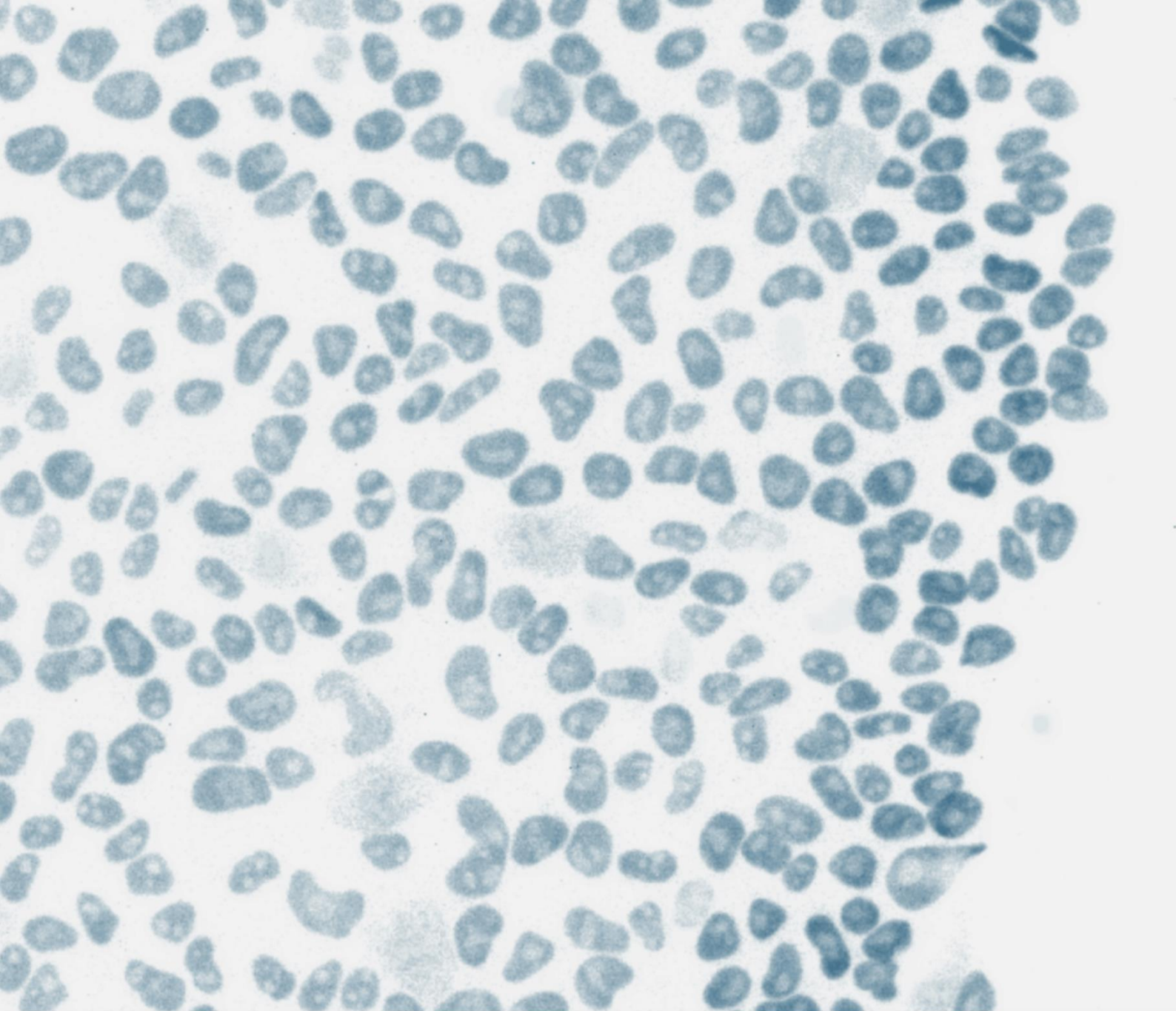
Núria Catasús Segura
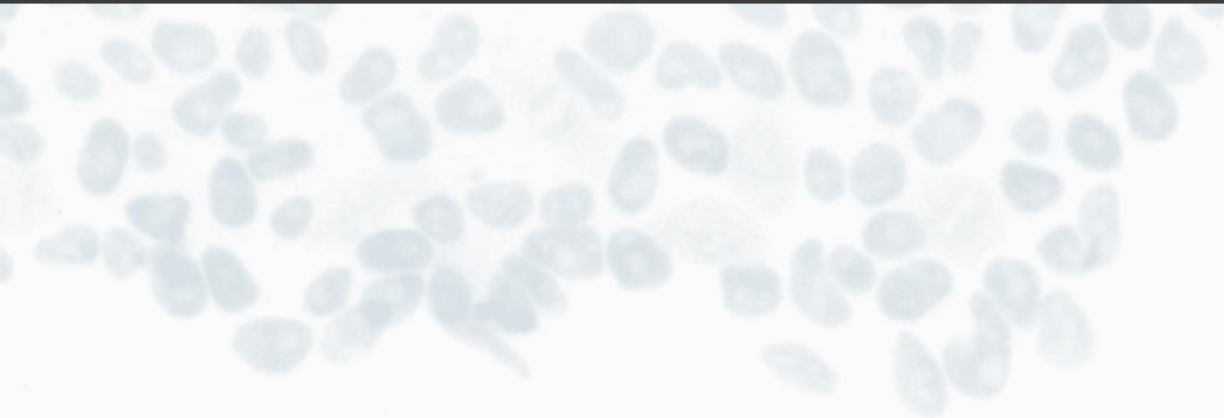
Refining prognosis capacity and implementing
principles of personalized therapies for

NEUROFIBROMATOSIS TYPE 2

Doctoral Thesis
Núria Catasús Segura

Refining prognosis capacity and implementing principles of personalized therapies for Neurofibromatosis Type 2

Memòria presentada per

Núria Catasús Segura

per optar al grau de

Doctora per la Universitat de Barcelona

Programa de Genètica

Tesi realitzada a l'Institut d'Investigació Germans Trias I Pujol

sota la direcció de la **Dra. Elisabeth Castellanos Pérez** i el **Dr. Ignacio Blanco Guillermo**
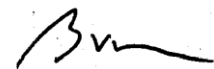
i tutoritzada pel Dr. Bru Cormand Rifa

Dr. Elisabeth Castellanos Pérez

Co-director

Dr. Ignacio Blanco Guillermo

Co-director

Dr. Bru Cormand Rifa

Tutor

Núria Catasús Segura

Barcelona 2022

I was taught that the way of progress was neither swift nor easy.

Marie Curie

Acknowledgments

"In the long history of humankind (and animal kind, too) those who learned to collaborate and improvise most effectively have prevailed" – **Charles Darwin**

No podria començar d'una altra manera que mostrant el més sincer agraïment a la Dra. Elisabeth Castellanos i al Dr. Ignacio Blanco, per brindar-me l'oportunitat de desenvolupar aquesta tesi i, sobretot, per la vostra confiança i dedicació durant aquesta etapa. A l'Ignacio, gràcies per compartir els teus coneixements i inavaluables consells. I a l'Eli, sincerament gràcies. Sense la teva perseverança i motivació no podria haver dut a terme aquesta tesi. Per les infinites vegades que m'has recolzat quan no veia per on seguir. Ha estat un plaer i un honor ser la primera *Padawan*.

S'allarguen els agraïments a tots els que heu patit aquesta tesi dia a dia. Inma, que difícil es agradecer en unas líneas lo que has hecho por mi durante estos años, seguro será insuficiente. Gracias por tu paciencia en enseñar, pero sobre todo por tu cariño, empatía y ser el hombro donde apoyarse. Me quedo con una frase que espero reconozcas: "*tenía la rara virtud de no existir por completo sino en el momento oportuno*". Gracias. Álex, por el soporte técnico, pero sobre todo moral. Por estar dispuesto día a día a colaborar y ayudar, gracias por todo lo que has aportado a esta tesis y a mí a nivel personal. Sandra, és una sort saber que només cal mirar al costat per trobar recolzament i una dosi de confiança, gràcies per la paciència. Mercedes i Arturo, gràcies per tot el suport i tots els moments compartits. A tots els membres del CSUR, en especial a la Belén, gràcies per fer que treballar amb tu sigui tant fàcil.

M'agradaria mostrar un especial agraïment al Dr. Eduard Serra i la Dra. Meritxell Carrió. Gràcies per tot el que he pogut aprendre de vosaltres. Gràcies Edu per estar sempre disposat a transmetre i compartir coneixement; Meri, per la paciència en ensenyar, ajudar i pel gran recolzament brindat aquests anys. L'agraïment és extensible a la resta de membres del Serra Lab i el grup BCN-NF, especialment a l'Helena pel suport i consells.

Agraeixo poder comptar amb elles, que m'agafen de la mà, sempre atentes, tant diferents i úniques: Cristina, Ariadna, Sara, Carlota, Ingrid, Gemma, Mònica i Mireia, gràcies. Laura, Nico i Pol, gràcies per fer sempre el camí una mica més fàcil.

A la Teresa, Pere Joan, Gemma, Xavi i als dos petits. Gràcies pel suport i fer-me sentir una més.

A tu Joan, és insuficient qualsevol agraïment que pugui escriure. Gràcies per fer-ho fàcil, per ser inspiració i motivació, per recolzar-me i sempre creure en mi.

I el major agraïment a la meva família. A les meves àvies per ser exemple de superació i generositat. Al Xavi, i sobretot a la meva germana, no podria haver tingut un millor exemple a seguir. Als meus pares Jaume i Anna. Gràcies pel vostre amor i suport incondicional, per confiar en mi i acompanyar-me en cada etapa.

Abstract

Neurofibromatosis type 2 (NF2) is an autosomal dominant condition caused by loss of function variants in the *NF2* gene. The pathognomonic feature of the disease is the development of bilateral vestibular schwannomas (VS), benign tumours that result from the overgrowth of Schwann cells (SC) on the vestibulocochlear nerves. Affected individuals are at high risk of developing schwannomas in other cranial, spinal and peripheral nerves, as well meningiomas and ependymomas, tumours that are responsible for significant morbidity. The clinical management of these patients is complex due to the limited treatment options and the broad and variable clinical spectrum of the disease, strongly associated with the type of variant inherited in the *NF2* gene.

The general objective of this thesis was to contribute to the development of strategies for a personalized medicine for Neurofibromatosis Type 2. Specifically, the three aims were to assess and improve the prognosis capacity of the disease, to evaluate the use of antisense gene therapy approaches *in vitro* for pathogenic variants causing NF2 and finally, to develop an induced pluripotent stem cell-based model for further studies on the *NF2* gene role and the development of targeted therapies.

In 2017, the UK NF2 Reference Group established a Genetic Severity Score (GSS) to predict the severity of the disease considering the *NF2* pathogenic variant. In the present work, we validated the GSS in a cohort of NF2 patients from the Spanish National Reference Centre (CSUR) of Phacomatoses. In addition, data from the identification of potential novel prognostic molecular markers were considered to suggest a revision of the GSS, called the Functional Genetic Severity Score (FGSS). The FGSS includes data from functional assays and the predicted effect of pathogenic variants on merlin, the *NF2* protein.

With the aim to develop a personalized therapeutic approach for NF2 patients, we evaluated the use of antisense oligonucleotides for *NF2* loss of function variants in patients' primary fibroblast cell cultures. First, we tested the use of phosphorodiamidate morpholino oligomers (PMOs) to modulate the effect of *NF2* splice site variants, although the approach proved unsuccessful to restore merlin levels. The second strategy consisted of reducing the severe effect of truncating variants affecting the *NF2* gene. We used PMOs to induce the skipping of an in-frame exon harbouring a nonsense or frameshift variant to generate novel, and potentially functional, merlin forms. Encouraging results emerged for germline truncating variants in exon 11 of *NF2*, for which it was possible to generate a hypomorphic merlin (merlin-e11) that partially rescued the NF2 phenotype in primary fibroblasts cultures. This result constitutes an *in vitro* proof of concept of the use of PMOs as a personalized therapy for *NF2* patients.

Finally, due to the limited preclinical models available for NF2, we generated induced pluripotent stem cell (iPSC) lines with single or bi-allelic loss of function of *NF2* through combining direct reprogramming of VS cells with the use of CRISPR/Cas9 genome editing. In our experience, the *NF2* gene could be essential for reprogramming and maintaining pluripotency. Despite difficulties encountered in maintaining pure merlin-deficient pluripotent cultures, iPSCs lines were characterized and differentiated towards the Neural Crest – Schwann cell axis. The application of a 3D Schwann cell differentiation protocol led to the successful generation of *NF2* (+/-) and *NF2* (-/-) spheroids that co-expressed the classical lineage markers p75 and S100B, potentially representing a genuine VS model.

Table of contents

List of figures and tables

Abbreviations

AAV - adeno-associated virus

AJs – adherens junctions

AMOT – angiomiotin

ASOs - antisense oligonucleotides

BMP - bone morphogenetic protein

BSA - Bovine Serum Albumin

B-SCB - Barcelona Stem Cell Bank

BVS - bilateral vestibular schwannoma

CAL - café-au-lait

Cas9 –CRISPR associated protein 9

cDNA – complementary DNA

CNA – copy number alterations

CNS – central nervous system

CNV – copy number variation

CPA - cerebellopontine angle

CRISPR - clustered regularly interspaced short palindromic repeats

CSUR - Centros, Servicios y Unidades de Referencia del Sistema Nacional de Salud

CTD – C-terminal domain

DNA - deoxyribonucleic acid

EGFR - epidermal growth factor receptor

ES – exon skipping

FGSS – Functional Genetic Severity Score

FiPS - fibroblast induced pluripotent stem cells

GSS – Genetic Severity Score

HDAC - histone deacetylases

hESC - human embryonic stem cells

iPSC - induced pluripotent stem cell

iSC(s) – immature Schwann cell(s)

Kb – Kilobases

kDa – Kilodalton

KO – knockout

LOF – loss of function

LOH – loss of heterozygosity

MLPA - multiplex ligation-dependent probe amplification

mRNA - messenger RNA

mTORC - mammalian target of rapamycin complex

NC – neural crest

NCSC – neural crest stem cell

NC-SC – Neural Crest-Schwann Cell

NF2 - Neurofibromatosis Type 2

NGFR - nerve growth factor receptor

NGS – next generation sequencing

NPE – normalized protein expression

NRG1 - neuregulin 1

PBS - phosphate buffered saline

PCA - principal component analysis

PI3K - phospho-inositide 3-kinase

PKA - cyclic AMP-dependent protein kinase

PMO(s) - phosphorodiamidate morpholino oligomer(s)

PS – phosphorothioate

RISC - RNA inducing complex

RNA - ribonucleic acid

RNAse H - ribonuclease H

RT – room temperature

RTKs - receptor tyrosine kinases

S100β - S100 calcium-binding protein B

SC(s) – Schwann cell(s)

SCP(s) – Schwann cell Precursor(s)

siRNA - small interfering RNA

SPS - schwannoma predisposition syndrome

SWNTS – Schwannomatosis

TGF-β - transforming growth factor β

TJs – tight junctions

UK - United Kingdom

UPL - Universal Probe Library

UT – untreated

VEGFR - vascular endothelial growth factor receptor

VS(s) – vestibular schwannoma(s)

WES – Whole exome sequencing

WGS – Whole genome sequencing

WHO - World Health Organization

WT - wild type

Introduction

1. Genetic diseases

The genetic component is involved, to a greater or lesser extent, in all disorders. Alterations in the DNA, whether inherited or influenced by environmental factors, are the basis of many, if not most, diseases.

The completion of the Human Genome Project in 2003 [1,2], evolving technologies and development of DNA sequencing techniques led to the identification of genes and genetic variants associated with genetic disorders, knowledge that is still in continuous progress. The understanding of concepts underlying genetic conditions has made possible to advance towards an era in which molecular diagnosis is in the present-day clinical practice, broadly used in any health-care area.

Molecular diagnostics opens the door to early and predictive diagnosis of many pathologies. In this way, identification of the disease-causing genetic variant in an individual and cascade testing of relatives can lead to early detection, possible prevention of associated symptoms and transmission of the disease. Beyond this, the implementation of molecular diagnostics has also allowed a better understanding of the relationship between the molecular biological basis of a disease and its clinical expression, unveiling genotype-phenotype associations that can be applied to establish clinical prognosis [3,4].

Insights in genetics have likewise enabled substantial progress in the development of therapeutic approaches for genetic conditions, from pharmacogenetics to gene therapy, focusing on the amelioration or prevention of diseases by considering specific genetic factors. In addition, genetic engineering techniques have provided powerful tools for establishing disease models that are essential to achieve a better understanding of malignancies and, among other purposes, may provide platforms for drug discovery.

Of all genetically based conditions, cancer predisposition syndromes constitute about 5-10% of cancer cases and are the result of germline pathogenic variants in cancer susceptibility genes. Among the most frequent are hereditary breast and ovarian cancer syndrome or Lynch syndrome, but there are also less frequent forms, including Neurofibromatosis type 2.

2. Neurofibromatosis Type 2

Neurofibromatosis type 2 (NF2) (OMIM 101000) is an autosomal dominant disorder caused by the loss of function (LOF) of the *NF2* tumour suppressor gene, located on the chromosome 22q [5]. NF2 is characterized by the development of multiple schwannomas and meningiomas. The clinical expression of the disease is variable and closely related to the disease-causing genetic variant. Clinical management of NF2 patients requires multidisciplinary approaches due to the anatomical location and number of lesions.

2.1. Epidemiology

The incidence of the disease is around 1 in 28.000-40.000 live births and although showing phenotypic variability, it has nearly complete penetrance by the age of 60 [6,7].

It has been estimated that around 50% of the cases are familial and the remaining 50% are due to *de novo* variants. *De novo* pathogenic variants in the *NF2* gene can be prezygotic or postzygotic, giving rise in the latter case to different cell populations and constituting somatic mosaicisms, estimated in around 30% of NF2 cases, although with the use of Next Generation Sequencing (NGS) techniques, it has been found to be as high as 50-60% [8,9]. Hence, the estimated prevalence is 1 in 60.000, although possibly underestimated due to high frequencies of somatic mosaicism forms presenting milder phenotypes with and delayed onsets [10,11].

2.2. Clinical presentation

NF2 predisposes to the development of tumours of the nervous system, being the pathognomonic feature of the disease the presence of vestibular schwannomas (VSs). It is also common that affected patients develop cranial, spinal, peripheral nerve and intradermal schwannomas, cranial or spinal meningiomas and other central nervous system (CNS) tumours, most typically ependymomas. Tumour-independent peripheral neuropathies, ophthalmological and cutaneous lesions are also frequent [5,12]. Despite being histologically non-malignant tumours, their number and location cause significant morbidity to affected individuals as well as a reduction in quality of life and life expectancy [13]. An overview of NF2 associated lesions is shown in **Figure I.1** and its estimated frequency is summarized in **Table I.1**.

Figure I.1. Overview of NF2 associated lesions. *Adapted from: Asthagiri AR et al. Neurofibromatosis type 2. Lancet 2009;373:1974–86 [14] and National Institutes of Health.*
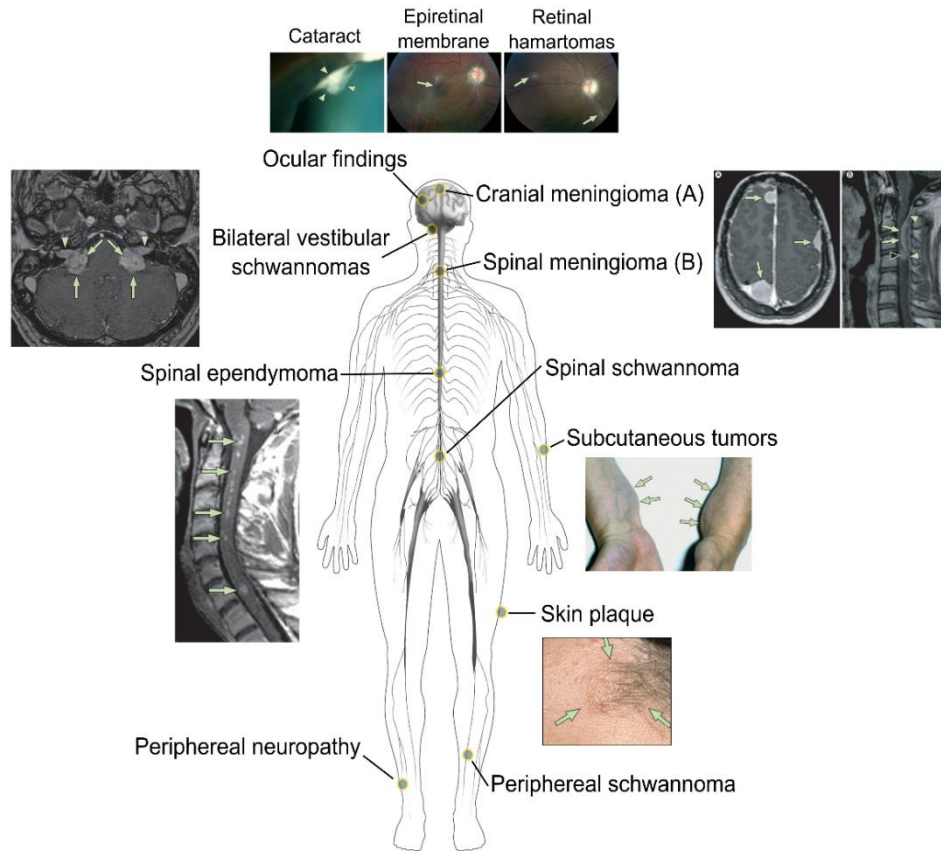
Table I.1. NF2 associated lesions and their frequency in NF2 patients

NF2 Associated lesions	Frequency in NF2 patients
Neurological	
Bilateral vestibular schwannomas	90–95%
Other cranial nerve schwannomas	24–51%
Intracranial meningiomas	45–58%
Spinal tumours	63–90%
Extramedullary	55–90%
Intramedullary	18–53%
Peripheral neuropathy	Up to 66%
Ophthalmological	
Cataracts	60–81%
Epiretinal membranes	12–40%
Retinal hamartomas	6–22%
Dermatological	
Skin tumours	59–68%
Skin plaques	41–48%
Subcutaneous tumours	43–48%
Intradermal tumours	Rare

Adapted from: Asthagiri AR, et al. Neurofibromatosis type 2. Lancet 2009;373:1974–86 [14]

2.2.1. Schwannomas

Schwannomas are benign tumours (WHO grade I) that arise from Schwann cells of the peripheral nervous system as a result of the loss of function of the *NF2* gene. Its microenvironment includes macrophages, fibroblasts, endothelial and T cells that could contribute to schwannoma pathology. Distinctively from other tumours arising in Schwann cells, schwannomas grow with no more trapped axons than those associated with Schwann cells from which they are originated [15].

Histopathologically, schwannomas show Antoni A tissue, characterized by the proliferation of bipolar spindle-cell lesions with high densely cellular areas showing frequent nuclear palisading and Verocay bodies. During tumour progression, it may be transformed to Antoni B tissue leading to lose cellular arrangements [14,16].

Schwannoma formation has been suggested to be due to a nerve regeneration failure, most commonly found among the vestibular, trigeminal and hypoglossal cranial nerves [17], although these tumours can also arise in spinal nerve roots or related to big nerves of the extremities [18]. These are associated with peripheral neuropathy, covered in detail in a separate section below.

2.2.2. Vestibular schwannomas

Bilateral vestibular schwannomas (BVS) are the hallmark of NF2, responsible for significant disease morbidity due to the mass effect involving several intracranial structures (**Figure I.2**). Vestibular schwannomas (VSs) are clinically manifested during young adulthood (20-30 years) with hearing loss, dizziness or disabling imbalance. The progressively tumour growth can lead to facial paraesthesia, ataxia, tinnitus and vertigo. Eventually, VSs can also cause brainstem and cerebellar compression, increasing the risk of mortality in the absence of treatment [5,19].

VSs arise from the cochleovestibular nerve sheath, surrounding sensory and motor neurons. They account for 85% of intracranial tumours in the cerebellopontine angle (CPA) and show variable tumour growth patterns [20–23]. No genotype-phenotype associations have been established regarding hearing loss in schwannomas, besides that tumour growth or size do not predict the hearing outcome of NF2 patients [24].
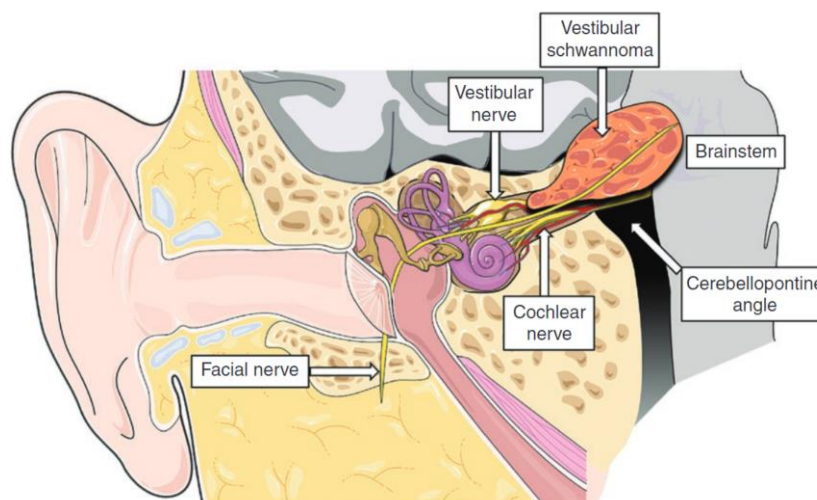
Figure I.2. Schematic representation of a vestibular schwannoma. *Extracted from: Ren Y, et al. New developments in neurofibromatosis type 2 and vestibular schwannoma. Neuro-Oncology Advances 2021;3:1–13* [25]*.*

2.2.3. Meningiomas

Meningiomas are the most common type of primary intracranial tumours and constitute the second most frequent tumour type in NF2. Often multiple and developed at earlier ages, meningiomas may exhibit heterogenous behaviours and asynchronous growth patterns [14]. Most meningiomas are slow growing tumours and persist stable in size, only a few show more aggressive growing patterns and therefore, require resection. For NF2, the presence of meningiomas has been determined as a disease severity indicator, with a 2.5-fold increased risk of mortality compared with individuals without these lesions [26].

Significantly, up to 60% of sporadic meningiomas also exhibit inactivation of *NF2*, thus indicating that it may be an early tumorigenic event, occurring before there is a commitment to a particular histopathological subtype [27,28].

2.2.4. Ependymomas

Ependymomas are primary CNS tumours that histologically, molecularly and structurally resemble ependymal cells of the ventricles and the spinal cord. They are diagnosed in 33-53% of patients with NF2 [14,29], sometimes multiple, most commonly in the posterior fossa and the spinal cord, in contrast to sporadic cases that are more frequently identified intracranially. The great majority of these tumours when associated with NF2 are WHO grade II and asymptomatic, with a recommended conservative management due to the morbidity associated with its resection, rarely cases require intervention [30,31].

While for years the presence of diffuse or plioid gliomas were associated with NF2, subsequent characterizations of these tumours have shown them to be ependymomas [32], and thereafter, a revision of diagnosis criteria suggested that the replacement of the term glioma for ependymoma could result in an improved diagnostic capacity [33].

Ependymomas have been more recorded in patients that harbour truncating mutations in the *NF2* gene, indicating that the presence of these tumours could be an indicator of the disease severity, as similar as meningiomas.

2.2.5. Peripheral neuropathy

Neuropathy can be associated with the presence of schwannomas, which produce pain through a mass compressive effect and impair axonal integrity of nerves. However, studies have shown that most NF2 patients may develop non-tumour related peripheral neuropathy that eventually appears years earlier than other NF2-related symptoms, suggesting that factors other than tumour burden must be considered [34]. Polyneuropathy related to NF2 usually involves more than two nerves, commonly peripheral nerves of the extremities [35,36]. The management of peripheral neuropathy includes medical treatment for pain and preventive or palliative cares.

The pathogenic mechanisms to explain peripheral neuropathy consider the presence of tumourlets, hyperproliferative Schwann cells that compress the nerve, or the development of schwannosis, Schwann cell proliferation without a formation of a tumour yet with entangled axons. Although in cases in which these lesions are absent, a Schwann cell dysfunction due to NF2 protein deficiency has also been considered [37].

2.2.6. Ophthalmological manifestations

Ocular manifestations for NF2 have been well described, being an onset symptom in paediatric patients and typically presenting with loss of visual acuity or diplopia. The presence of juvenile subcapsular or cortical cataracts interfere with vision in 10-25% of patients and has been established as a diagnostic criterion for NF2 [17,38].

Other lesions include epiretinal membranes (ERM) and retinal hamartomas. ERMs are semi-translucent fibro-cellular tissues that arise on the inner surface of the retina, which are present in up to 40% of patients with NF2 but usually do not compromise visual acuity. Presence of ERM before the age of 40 is considered a minor criterion for NF2 diagnosis. Retinal hamartomas are

benign, glial tumours of the retinal nerve fiber layer that can grow over time causing vision difficulties [39].

It has been possible to stablish a correlation between eye-disease and the *NF2* genotype, in which it has been described that patients harbouring mutations associated with a more severe form of the disease are at increased risk of combined hamartoma, ERMs and optic atrophy [40].

2.2.7. Cutaneous lesions

Skin lesions are present in 70% of patients with NF2, constituting a useful resource for diagnosis, and include skin plaques and subcutaneous or intradermal tumours. The most frequent are intracutaneous plaque-like lesions, characterized by slight hyperpigmentation and hypertrichosis. Subcutaneous tumours are usually found in peripheral nerves and are often palpable [41,42]. Café-au-lait (CAL) spots have also been observed, yet with a similar incidence as in general population and lower frequencies compared with other similar genetic diseases as Neurofibromatosis type 1. The vast majority of these tumours are schwannomas, although hybrid schwannomas, eventually erroneously classified as neurofibromas, have been identified [43].

2.3. Paediatric NF2

The clinical presentation of NF2 and its natural history differs between adults and children. The first symptoms when the disease appears in a pre-pubertal age are more related to skin tumours and the diagnosis of small posterior capsular or cortical edge cataracts, rather than signs secondary to vestibular nerve disfunction [44,45]. Most reported skin lesions during childhood cutaneous or nodular schwannomas and NF2-plaques. The latter, usually appearing in upper and lower limbs in contrast to the expected in adults, for whom are more prevalent in the trunk. Skin lesions constitute a useful diagnostic tool in the paediatric age group [41,46].

Cataracts are the main ophthalmologic manifestation, recorded in 40% of the children, being the most frequent the posterior subcapsular or cortical type with approximately 20% of patients presenting affection of visual acuity. Retinal hamartomas are found in 25% of the cases [44,45,47].

Neurological manifestations appear as a result of cranial or spinal lesions, which extent depends of localization, size and region of the tumours. These include motor or sensory deficits, and visual affection, that can appear related to the presence of meningiomas, schwannomas or

ependymomas, either intracranial or spinal. Peripheral neuropathy is also common and results from the presence of schwannomas [47,48].

2.4. The clinical overlap with Schwannomatosis

NF2 has a significant phenotypic overlap with Schwannomatosis (SWNTS; OMIM 162091), a dominantly inherited condition that predisposes to the development of schwannomas in peripheral and spinal nerves (found in 90% and 75% of patients, respectively). SWNTS is associated with severe chronic pain and great impact on patients' quality of life [49].

Although schwannomas from NF2 and SWNTS have indistinguishable phenotypic and histopathological features, their genetic aetiology has been differentiated, thus molecular analysis of these tumours is recommended with diagnosis purposes [50–52]. Genetics underlying SWNTS involves germline genetic variants in *SMARCB1* (22q11.23), found in 48% of familial and 10% of sporadic SWNTS, or *LZTR1* (22q11.21) accounting for 38% of familial and 30% of sporadic SWNTS, additionally to the loss of function of *NF2* [53–59].

For non-NF2 associated schwannomas, a four-hit, three step model has been described, consisting of a constitutional *SMARCB1* or *LZTR1* pathogenic variant, followed by the total or partial loss of chromosome 22 (involving *SMARCB1* or *LZTR1* and *NF2* loci), and finally, a somatic mutation in the remaining wild type allele of *NF2* occurs [60]. This model highlights that loss of function of the *NF2* gene is essential for the development of schwannomas, including those unrelated to NF2.

The genetic aetiology of some patients with SWNTS remains unknown, suggesting that other genes may be responsible for the disease. Recently, a new candidate gene has been suggested, *DGCR* (22q11.21), reported in a family affected of SWNTS and euthyroid multinodular goiter syndrome [61].

2.5. Disease progression and survival

NF2 is a progressive and life-threatening condition for which an early age of onset, the presence of multiple meningiomas or spinal tumours and harbouring a truncating *NF2* variant are factors associated with poor prognosis [62]. In the 1990s, patients had a 15-year life expectancy from the time of diagnosis [63], although this output has improved due to early diagnosis and multidisciplinary medical management offered at specialized centres, with an average life expectancy of 62 years [26].

3. Diagnostic criteria for Neurofibromatosis type 2

Diagnostic criteria for NF2 were first published in 1992 as the Manchester Criteria [64], which established that a NF2 individual must meet one of the following:

- Bilateral vestibular schwannomas
- First-degree relative with NF2 and unilateral VS
- First-degree relative with NF2 or unilateral VS and two of: meningioma, cataract, glioma, neurofibroma, schwannoma or cerebral calcification
- Multiple meningiomas (2 or more) and two of: unilateral VS, cataract, glioma, neurofibroma, schwannoma, cerebral calcification

The identification of other pathologies with phenotypic similarities, genes involved in the disease, new clinical data and genetic testing have led to identify some limitations in the current criteria. First, a significant overlap in phenotypic features between NF2 and SWNTS has been identified, finding that 9% of patients clinically diagnosed of SWNTS resulted to be NF2 after genetic analysis and contrarily, 1-2% of patients diagnosed of NF2 had SWNTS upon genetic analysis. It is also considered that the presence of bilateral vestibular schwannomas in patients older than 50 years can be due to sporadic cases. Finally, it has been observed that development of high-grade gliomas or neurofibromas are not NF2 related features [13,65–67].

Currently there is an experts' recommendation to group and rename NF2 and SWNTS with the aim to improve diagnostic accuracy for these diseases, proposing an umbrella term that includes both diseases: Schwannoma Predisposition Syndromes (SPS). In this way, it is indicated that both syndromes predispose to schwannoma formation. A molecular analysis would be clinically indicated to classify the type of SPS according to the pathogenic genetic variant (*NF2*, *SMARCB1*, *LZTR1*, 22q, or not found) [68].

Overall, there is a current proposal that recommends changes in the diagnostic criteria for NF2, shown in blue in **Table I.2**. It is important to highlight that genetic testing may be relevant for diagnosis but it is not currently a requirement; it is still possible to diagnose NF2 clinically. Besides, genetic analysis will not be sufficient to stablish a diagnosis, since a clinical NF2 diagnostic feature or family history of NF2 is required.

Table I.2. NF2 diagnostic criteria (2019 NF Conference Revision)	
Finding	Additional features required for diagnosis
Bilateral VS	None
Identical NF2 pathogenic variant in at least 2 anatomically distinct NF2-related tumours (schwannoma, meningioma and/or ependymoma)	None
Major criteria	**Minor Criteria**
Unilateral VS	Can count more than one of each type: ependymoma, schwannoma (at least one dermal if major criterion is unilateral VS)
First-degree relative, other than sibling, with NF2	
Multiple meningiomas	Can count each type only once: juvenile subcapsular/cortical cataract, retinal hamartoma, epiretinal membrane if age <40, meningioma
NF2 pathogenic variant in an unaffected tissue	

Adapted from: Evans G, et al. Revision of Diagnostic Criteria for Neurofibromatosis. 2019 [68] and Dinh CT, et al. Genomics, Epigenetics, and Hearing Loss in Neurofibromatosis Type 2. Otology and Neurotology. 2020;41:e529–37 [69].

4. Molecular biology of Neurofibromatosis type 2

4.1. The *NF2* gene

NF2 is a tumour suppressor gene (Gene ID: 4771), first cloned in 1993, located at the centre of the long arm of chromosome 22 (chr22q12.2) and with an estimated mutation rate of 6.5×10^{-6} [70,71]. Its approximately 95 kilobases of DNA code for 17 exons that can be alternatively spliced to generate two predominant isoforms of the protein merlin (exons 1-15&17 or exons 1-16) [72]. The autosomal dominant inheritance pattern of NF2 was first described in 1930 in a study of five generations in a total of 38 affected individuals, which indicated that the likelihood of vertical transmission is 50% [73]. However, *de novo* germline mutations appear in approximately 50% of the patients [74].

Following Knudson's "Two-Hit" model of tumour suppressor gene activity [75], NF2 is caused by inherited or early zygotic constitutional mutations in the *NF2* gene, arising the tumour through a second mutational event, or second hit, that results in the bi-allelic inactivation of the gene. It will likely occur in Schwann cells of target tissues, particularly on vestibular nerves.

When the mutation in the *NF2* gene occurs *de novo* in a subpopulation of cells during the post-zygotic stage of embryogenesis, different cell lineages arise and result in somatic mosaicism, highly reported in NF2. The estimation of mosaicism among NF2 patients is 33% in *de novo*

patients with unilateral VS or 24.8% in patients with bilateral VS [76–78]. However, a recent study estimates that the incidence of mosaicism could be underrated. With the use of high read depth NGS analysis, Evans and colleagues stablished that for disorders expressed as a result of heterozygous variants, and nonlethal, *NF2* could have the highest rate of *de novo* mosaicism, estimated in 50-60% [9]. The risk of transmitting NF2 to offspring is substantially lower for mosaic patients and probably correlate with the frequency in which the variant can be detected in blood [9].

4.2. Mutational spectrum of the *NF2* gene

Since the cloning of the gene in 1993, the mutational spectrum for *NF2* has been studied. Given its function as a tumour suppressor gene, most of the reported variants are predicted to be truncating, whether nonsense or frameshift, or to shorten the protein through splice-site variants.

4.2.1. *NF2* germline variants

The germline or constitutional alterations are those that appear in the germ cells, thus, present in all the cells composing an individual with the possibility of being transmitted to offspring. Germline variants are considered when detected in unaffected tissue.

NF2 has a broad mutational spectrum in which 85-90% account for point mutations and the remaining 10-15% are large deletions, being nonsense variants more frequent than frameshift in a 3:1 ratio as germline mutations [79].

Ahronowitz and colleagues reported in 2007 that predominantly, constitutional point mutations were nonsense (39%), followed by frameshift (27%), splice site (25%), and the remaining were whether non-truncating or undetermined. Large deletions were less frequent (14%), being the most reported the removal of exons 15 and 16, while indels and complex rearrangements have been rarely reported [80]. This mutational spectrum also accounts for variants detected in mosaicism, although not affecting the germline, and represent the first hit thus, the disease-causing variant.

C>T transitions in the CGA codons (Arginine) into stop codons (TGA) leading to nonsense variants are the most common variations found among exons 1-15, while no mutations have been reported in exons 16 and 17, with no proteins known to interact with these exons. Constitutional mutations affecting exon 9 are reported in low frequencies, probably due to a relation between the function and structure of the protein [80,81].

4.2.2. *NF2* somatic variants

According to Knudson's "Two-Hit" model [75], second mutations or second hits in tumour suppressor genes occur in somatic tissues and are referred as somatic variants. These events are expected in target tissues and cause loss of function of the remaining wild type allele, with the consequent appearance of a tumour.

For *NF2*, somatic variants show a different mutation spectrum than constitutional or germline events. The most frequently reported second hit in NF2-related tumours is the loss of all or most of chromosome 22, causing loss of heterozygosity (LOH). Somatic mutations reported in *NF2* are point mutations, single or multi-exon deletions or duplications and mainly, as mentioned above, LOH due to whether the loss of chromosome 22, the 22q12 locus or mitotic recombination. Contrary to *NF2* constitutional variants, frameshift mutations are more frequent than nonsense [81,82] and with more predominance in tumours of older individuals. This shift related to age has been hypothesized to be due to defects in DNA repair pathways acquired with age [79].

In NF2-related and sporadic schwannomas, LOH of the 22q chromosomal region is the most common feature. The frequency of the different point mutations and large rearrangements in NF2-related and sporadic schwannomas in the UK cohort, the largest described, was reported by Hexter and Evans and is shown in **Table I.3** [83]. A study in sporadic schwannomas reported recurrent mutations in other genes: *ARID1A*, *ARID1B* and *DDR1* and an in-frame fusion, *SH3PD2A-HTRA1*, in addition to the bi-allelic inactivation of *NF2* [84].

Both sporadic and NF2-related meningiomas are also characterized by LOH of chromosome 22, with the consequent loss of function of the *NF2* gene. NF2-associated meningiomas do not show clear recurrent alterations, with the exemption of *NF2* inactivation, and do not tend to become malignant. However, these tumours are responsible for significant morbidity and an increased risk of mortality depending on their location and size. For sporadic meningiomas, *NF2* inactivation has been suggested as an early step in its development, reported in between 20%–60% of the cases [27,85]. In addition, sporadic meningiomas can acquire mutations in other tumour suppressor genes that contribute to its malignant progression (WHO grade II or III), and four mutational subgroups have been established determined by pathogenic variants in *NF2*, *TRAF7*, the Hedgehog pathway or *POLR2A* [86].

NF2 variants have also been detected in diverse malignant cancers, being the most common the mesothelioma, with *NF2* mutations occurring in 30-50% of these tumours. In much lower rates, *NF2* mutations have been detected in hepatocellular tumours, melanomas, lung, thyroid, prostate and breast cancers among others [87,88].

Table I.3. Germline and somatic variants found in the Manchester (UK) genetics laboratory in NF2 and sporadic VSs				
	NF2 VS first hit (germline)	NF2 VS second hit (somatic)	Sporadic VS first hit	Sporadic VS second hit
Point mutations				
Nonsense	155 (29%)	3 (2%)	29 (22%)	3 (2,5%)
Frameshift insertions/deletions	125 (25%)	9 (6%)	1 (7,5%)	7 (5,5%)
Missense	24 (4,5%)	0	1 (7,5%)	1 (7,5%)
In-frame deletions	5 (1%)	0	1 (7,5%)	0
Splice site	115 (22%)	5 (3,5%)	13 (10%)	3 (2,5%)
Large rearrangements				
Ring 22	3 (0,5%)	NA	NA	NA
Chromosome translocation	2 (0,5%)	NA	NA	NA
MLPA exon/multiexon deletions/duplications	102 (19%)	3 (2%)	2 (1,5%)	2 (1,5%)
Loss of chromosome 22q or most all chromosome	0	80 (55%)	0	70 (53%)
Mitotic recombination	0	20 (14%)	0	9 (7%)
Methylation	0	0	0	0
Total	**351**	**146**	**131**	**131**

NA: no karyotypic analysis was performed for these tumours

Adapted from Hexter AT, Evans DG. The Genetics of Vestibular Schwannoma. Current Otorhinolaryngology Reports. 2014;2:226–34 [83].

4.3. Molecular diagnosis

Molecular diagnosis is currently a common clinical practice and allows the determination of a disease-causing variant, either to confirm a clinical diagnosis or to stablish a differential diagnosis in case of phenotypic overlap with other pathologies, such as NF2 and SWNT. Thus, genetic testing for *SMARCB1* and *LZTR1* are frequently incorporated in genetic screenings of individuals at risk for NF2. Molecular diagnosis plays an important role to confirm clinical diagnosis in adult and paediatric ages, when there are still no conclusive signs of the disease, as well as in cases of segmental mosaicism [89].

Molecular diagnostic challenges in *NF2* reside in the high incidence of mosaicism, preventing in more than 30% of cases to detect the genetic disease-causing variant in blood. If so, at least two lesions need to be studied to understand which is the constitutional variant [90,91].

The identification of the pathogenic variant also allows genetic testing for at-risk relatives and the possibility of family planning to prevent vertical transmission. Furthermore, there is a well-known genotype-phenotype relationship for NF2 (further assessed in Section 5) and therefore, determining the disease-causing variant also allows to stablish a more accurate prognosis. Over the years, genetic diagnosis of NF2 is becoming increasingly relevant, as it is currently being

proposed as a diagnostic criterion and the affected gene would give the name to the disease (see Section 3).

Nowadays, genetic testing allows detection of *NF2* germline pathogenic variants, both sequence and copy number alterations, and possibly mosaicism, depending on the representation of the mutation in blood. The extended used technology is NGS, while alternative techniques are used to validate the results: Sanger sequencing, multiplex ligation-dependent probe amplification (MLPA), quantitative real-time PCR or comparative genomic hybridization [11,92].

Recently, Dinh and colleagues suggested an algorithm to fully characterize alterations in the *NF2* gene [69] (**Figure I.3**), yet studies at RNA level would be necessary to identify deep intronic variants.
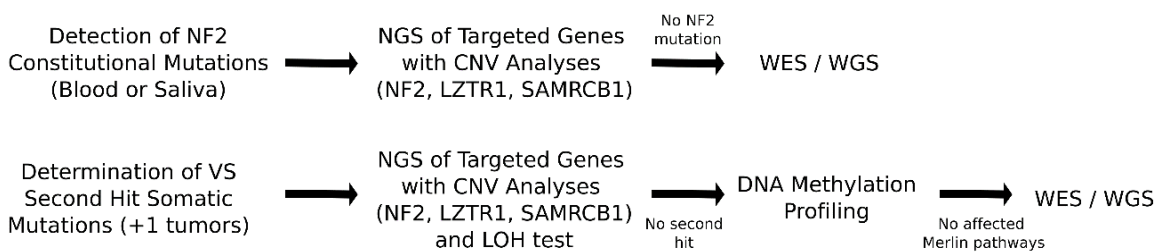
Figure I.3. Genetic workflow for mutational analysis of *NF2* and tumour profiling. NGS: Next Generation Sequencing; CNV: Copy Number Variation; LOH: Loss of Heterozygosity; WES: Whole Exome Sequencing; WGS: Whole Genome Sequencing**.** *Adapted from Dinh CT, et al. Genomics, Epigenetics, and Hearing Loss in Neurofibromatosis Type 2. Otology and Neurotology. 2020;41:e529–37* [69].

4.4. Merlin

The *NF2* gene encodes for the protein merlin (<u>m</u>oesin-<u>e</u>zrin-<u>r</u>adixin-<u>l</u>ike prote<u>in</u>), a 70-kDa member of the ERM (Ezrin, Radixin and Moesin) protein family, sharing a 64% of sequence identity with the canonical ERM domain. Merlin is preferably located in the plasma membrane associated with lipid rafts and regulated thorough its attachment to the extracellular matrix and intracellular adhesions [70,93,94]. Given the high similarity to ERM proteins, merlin was assumed to perform its tumour suppressor activity by inhibiting mitogenic signals in the cell cortex through contact inhibition, although further studies showed that merlin can also be regulated by other non-contact mediated signals [95].

The alternative splicing of the *NF2* gene generates two main forms of merlin, which differ in the C-terminal region. Isoform I is constituted by exons 1-15 and 17, coding for 595 amino acids, while isoform 2 is encoded by exons 1-16 and contains 590 residues, identically as merlin-I in the first 579 [72,96]. The lack of the carboxy-terminal domain in Isoform II was initially thought to prevent intramolecular binding and to prompt an open conformation with no activity,

however, it has been further observed that both isoforms can equally exert tumour suppressor activity [97,98].

Merlin is composed of three structural regions: a N-terminal FERM domain divided in three subdomains (A, B and C), an α-helical coiled-coil domain and a C-terminal hydrophilic domain (CTD). Differences in merlin regarding ERM proteins reside in the lack of the canonical C-terminal actin binding site, fundamental for their activity at the cortical cytoskeleton. In contrast, merlin can interact with actin fibers through residues 1-27 and 280-232 and has an important role in regulating the structure and function of microvilli and membrane ruffles. In addition, merlin has a 7-residue conserved blue box motif (residues 177-183 in human merlin) in which alterations in Drosophila and mammals have result in mutants with a dominant-negative activity [99–101]. An overview of merlin domain organization is shown in **Figure I.4**.
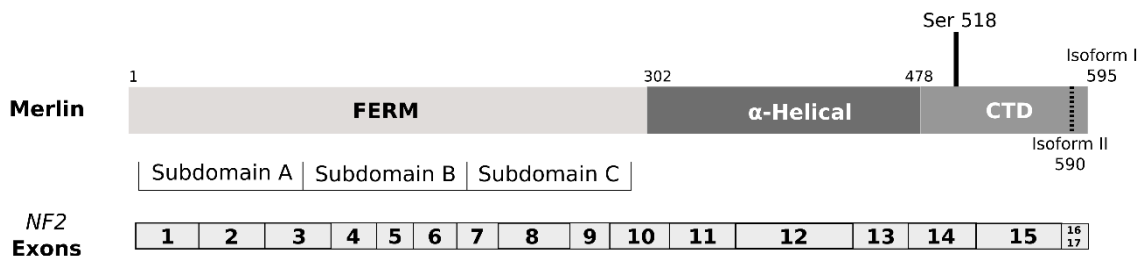
Figure I.4. Merlin domain organization and overview of the *NF2* gene. Merlin is organized in three domains: N-terminal FERM domain, consisting of three subdomains (A, B and C), a central helical domain and a C-terminal domain (CTD). Phosphorylation of Ser518 is the most well characterized post-translational modification. Merlin two main isoforms have been identified, resulting from the alternative splicing of the *NF2* gene. *Adapted from:* Sato T, Sekido Y. NF2/merlin inactivation and potential therapeutic targets in mesothelioma. *International Journal of Molecular Sciences* 2018;19 *and Cooper J, Giancotti FG. Molecular insights into NF2/Merlin tumour suppressor function. FEBS Letters. 2014;588:2743–52* [88,102].

Merlin performs and regulates its activity as a tumour suppressor protein in three different ways: (I) through its molecular conformation and post-translational modifications, (II) cell contact inhibition and (III) by the interaction with other effector proteins, with a known role in several oncogenic signalling pathways [102].

4.4.1. Molecular conformations and post-translational modifications of merlin

The intramolecular association and activation states of merlin have been studied for years. Merlin's intramolecular association occur between the CTD and FERM domains, masking great part of the FERM domain and resulting in a closed head-to-tail conformation. Through phosphorylation of Serine residue 518 (Ser518), these domains are released and merlin adopts an opened conformation that renders the FERM domain accessible for interaction with binding partners [103–106].

Merlin was thought to be active (growth suppressive) when found in a closed conformation and its inactivation (growth permissive) was the result of phosphorylation of Ser18 adopting an opened conformation (**Figure I.5**). However, this model has raised much controversy: evidences suggested that it was much more complex and merlin could have multiple conformational variants with varying degrees of head-tail association. Instead, it has been shown that phosphorylation could lead to a strengthen intramolecular association [98]. Fluorescence resonance energy transfer (FRET) assays suggested that the C-terminal and FERM domains could be found constitutionally closely located and that post-translational modifications could induce just minor modifications in proximity [105]. In addition, subsequent studies have determined that both merlin-II and S518A mutants, both lacking the CTD, can also adopt a closed conformation and maintain tumour suppressor activity [97,107].
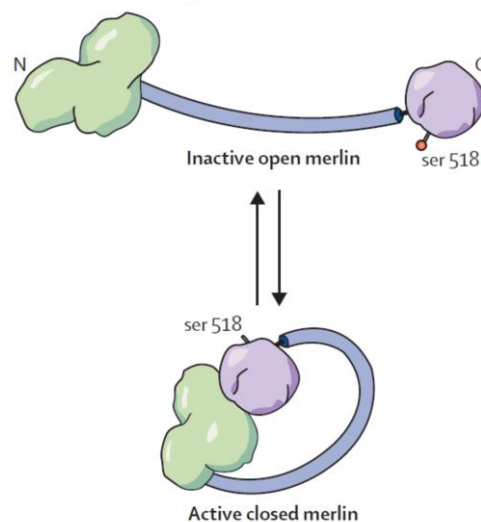
Figure I.5. Conformational and post-translational modifications of merlin. Conformational changes of merlin are described to regulate its tumour suppressor activity. *Adapted from: Asthagiri AR, et al. Neurofibromatosis type 2. Lancet 2009;373:1974–86* [14].

The most relevant and well characterized post-translational modification is the Ser518 phosphorylation, that may be in turn necessary for phosphorylation of other residues [108,109]. Phosphorylation of Ser518 is mediated by a feedback regulation loop with p21-activated kinase (PAK) and consequent activation of Rho small GTPases (Rac1/Cdc42) [95]. Ser518 is also substrate for the cyclic AMP-dependent protein kinase (PKA), in both cases phosphorylation leads to the inactivation of the tumour suppressor activity [110]. Contrarily, merlin is thought to be activated through the myosin phosphatase MYPT1-PP1δ dephosphorylation [111].

Recent studies have reported that merlin could dimerize when found in an opened conformation, via FERM-FERM interaction, giving rise to the possibility that some mutant merlin proteins could act in a dominant negative manner that impair the activity of the wild type merlin. Dimerization would be inhibited by phosphorylation at Ser518 and enhanced by interactions with phosphatidylinositol 4,5-bisphosphate (PIP2). Dimerization thus, would constitute a new mechanism by which merlin controls interaction with binding partners to exert an anti-proliferative activity [112,113].

Overall, it is well stablished that conformation and activity of merlin is regulated through post-translational modifications, although much remains to be elucidated about the underlying mechanisms.

4.4.2.   Merlin as a mediator of contact-dependent inhibition

In confluent cells, merlin is recruited at the cell cortex, where it interacts with membrane-associated proteins including other ERM proteins, α-catenin and β-catenin at adherens junctions (AJs), angiomiotin (AMOT) at tight junctions (TJs) or the intracellular domain CD44 [102]. Concretely, dephosphorylated and active merlin negatively regulates CD44 function, a cell surface molecule involved in cell-cell interaction, cell adhesion and activated by extracellular hyaluronic acid, resulting in the inhibition of cell growth through contact inhibition. This regulation is modulated by interactions with Rac1 (Rac Family Small GTPase 1) and its downstream kinase PAK1. Merlin, in its active form, prevents activation of Rac1 and PAK1 by suppressing the recruitment of Rac1 to the plasma membrane. However, PAK1 can phosphorylate merlin to revert the inhibitory effect on Rac1 [95].

Therefore, interaction with signalling proteins involved in cell-cell adhesion enables merlin to sense cell environment and perform its function of inhibiting growth upon confluence (**Figure I.6**).
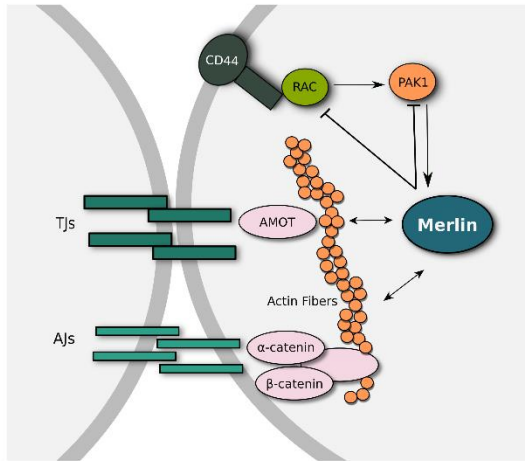
Figure I.6. Merlin mediates contact inhibition through interaction with membrane-associated proteins. *Adapted from: Lee et al. The role of merlin/NF2 loss in meningioma biology, Cancers 2019* [114] *and: J. Cooper, F.G. Giancotti/FEBS Letters 588 (2014) 2743–2752* [102].

4.4.3. Merlin signalling pathways

The Hippo tumour suppressor pathway

Merlin is known to activate the Hippo tumour suppressor pathway, an evolutionary conserved signalling pathway responsible for inhibiting proliferation, promoting apoptosis and involved in development and tumorigenesis [115]. When located in the nucleus, the transcriptional coactivators YAP/TAZ can regulate gene expression by interactions with DNA-binding factors of the TEAD family and promote cell proliferation. Merlin can inhibit YAP and TAZ through various signalling pathways: (1) at the adherens and tight junctions by interactions with α and β-catenins; (2) requiting Lats kinases at the plasma membrane and regulating its activation through Mst1; (3) recruiting Angiomiotin (AMOT), directly linked with Hippo pathway components and (4) in the nucleus, where merlin can be translocated to inhibit CRL4^{DCAF1}, a E3 ubiquitin ligase that prevents ubiquitination of Lats1/2 inhibiting tumorigenesis (**Figure I.7**) [102].
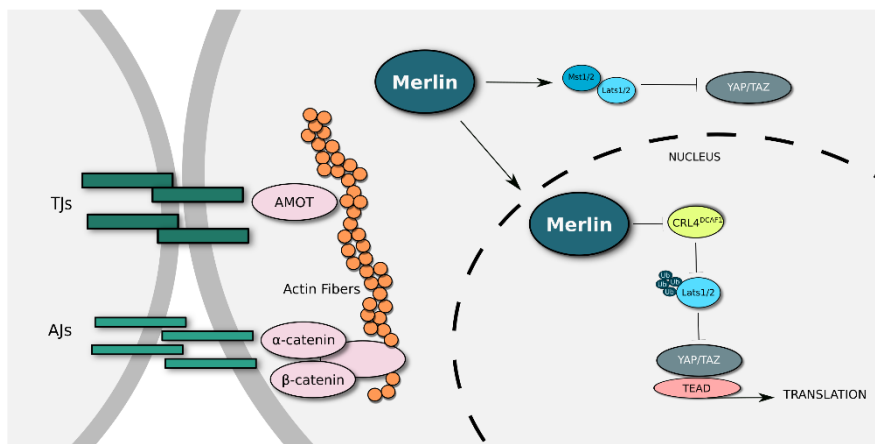
Figure I.7. Merlin is as an upstream regulator of the Hippo tumour suppressor pathway. Merlin can suppress the transcriptional coactivators YAP/TAZ through interactions with adherens and tight junctions, Mst1/2, AMOT and by suppressing CRL4^{DCAF1}. *Adapted from: J. Cooper, F.G. Giancotti/FEBS Letters 588 (2014) 2743–2752* [102].

PI3K/AKT/mTOR Pathway

Loss of merlin in schwannomas and meningiomas results in the activation of the phospho-inositide 3-kinase (PI3K)/Akt pathway leading to increased Schwann cell proliferation. Merlin suppresses the PI3K activity by binding the phosphatidylinositol 3-kinase enhancer L (PIKE-L), inhibiting its capacity to stimulate and activate PI3K, which in turn fail to activate AKT and the mammalian target of rapamycin complex (mTORC) (**Figure I.8**) [116–118]. Phosphorylation of AKT is also regulated by histone deacetylases (HDAC) through Protein Phosphatase 1 (PP1). HDAC inhibitors have shown to reduce cell proliferation in NF2-related tumours [119]. In addition, merlin can negatively regulate mTORC1 independently of PI3K/Akt and ERK upstream signalling, although this mechanism remains unclear, as does the interaction with mTORC2 [120,121].
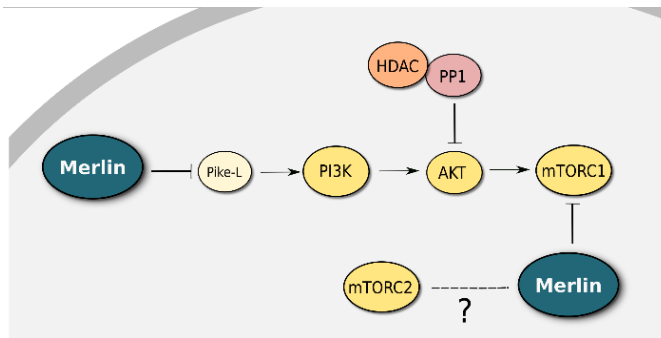
Figure I.8. Merlin mediates inhibition of the PI3K/mTORC1/Akt signalling pathway. *Adapted from: AM Petrilli and C Fernández-Valle, NF2 in tumour biology Oncogene (2016) 537–548* [122].

Ras/MAPK signalling pathway

Loss of merlin is associated with a sustained activation of the well characterized Ras/MAPK signalling pathway, with a critical role during tumorigenesis [122]. Merlin can assemble a complex with paxillin, erbB2 and β1-integrin. The binding of merlin into the complex allows inhibition of the Akt and MAPK (ERK) signalling by preventing the activation of Ras and Rac (**Figure I.9**) [123,124]. The mechanisms by which merlin can interfere with Ras activation remain unclear, although recent reports show that merlin could directly interact with Ras and Ras-GAP to regulate Ras signalling [125]. In addition, merlin could interact with neurofibromin, a negatively regulator of Ras, forming complex with spred1, to interfere in the Ras pathway [126].
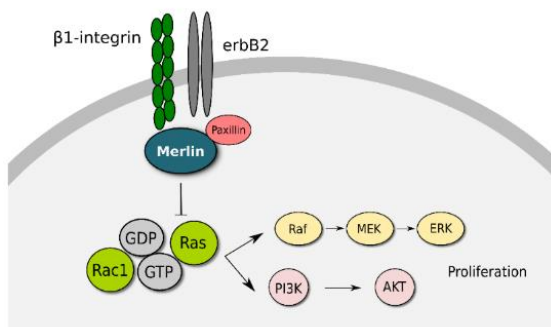
Figure I.9. Merlin is an inhibitor of the Ras/MAPK signalling pathway. *Adapted from: AM Petrilli and C Fernández-Valle, NF2 in tumour biology Oncogene (2016) 537–548* [122].

Receptor tyrosine kinases (RTKs)

Mainly located in the lipid rafts, merlin has an important interaction with receptor tyrosine kinases (RTKs) [90]. Among the most relevant are ErbB, already mentioned in the previous section, insulin-like growth factor 1 receptor (IGF-1), platelet-derived growth factor receptor β (PDGFR-β), and vascular endothelial growth factor receptors (VEGFR). It is through inhibition of integrin signalling and RTKs where merlin initiates the activation of several of the anti-mitogenic pathways mentioned in the previous sections [127,128].

Other signalling pathways

Given the certain parallelism between embryonic development and oncogenesis, merlin has been reported as an important protein in development, influencing the signalling of different pathways: Wnt/β-catenin, TGF- β, Notch or Hedgehog signalling pathways are examples [129].

4.5. Epigenetics

Beyond the genetics associated with VSs, epigenetic changes have also been described, being the most frequent modifications by methylation of CpG dinucleotides, and possibly related to the gene loss of function. However, there are strong discrepancies in literature. While studies have been showing that methylation of the promotor regulatory sites can result in gene silencing, others report that the pattern is relatively rare and could not be associated with the formation of vestibular schwannomas [130–132].

Methylation could have a role in the progression of hearing loss associated with VSs [133]. Aberrant methylation patterns have been observed in the tumour suppressor gene *TP73* [134], involved in apoptosis or *HOX* genes, linked with cancer [135], among others. However, mechanisms behind these associations remain unclear.

Epigenetic studies in meningiomas are further ahead. For these tumours, methylation profiles enable to establish six groups, clinically relevant, that better predict the risks of tumour progression and recurrence than the WHO classification [136] .

5. Genotype-phenotype correlations in Neurofibromatosis Type 2

Neurofibromatosis Type 2 has a variable clinical expression, as already mentioned in previous sections. Thus, identification of prognostic factors or genotype-phenotype associations can provide useful tools to individualize the clinical management according to the expected severity.

Prior to the understanding of the molecular aetiology of the disease, a first clinical classification of NF2 led to the identification of two clinical subtypes, Gardner [73] and Wishart [137], according to disease severity.

The Wishart subtype was associated with an early onset of the disease, usually pre-pubertal, with rapid course progression and higher predisposition to meningiomas and spinal tumours, besides the presence of VS. Further characterizations have identified that its primary presentation includes NF2-plaques, predominantly in the limbs, and intracranial nervous system tumours prior to the development of VSs [45,47]. Ophthalmologic features, usually posterior capsular o cortical edge cataracts are related to this subtype [44].

Contrarily, the Gardner subtype or adult form shows milder phenotypes with the onset during young adulthood, benign courses and low incidence of extra-vestibular tumour burden. The typical presentation is hearing loss, tinnitus or imbalance due to the presence of VSs [138,139].

Progress in molecular analysis resulted in the determination of genotype-phenotype associations that better represent the broad clinical expression of the disease. In these correlations, truncating variants are associated with severe phenotypes of NF2 predisposing to high tumour burden [140], while large or small in-frame deletions and missense variants are more likely to present with milder forms [140,141]. Splice site variants show more phenotypic variability, with evidences suggesting that the associated severity can be related to their location within the gene. Hence, variants located in exons 1-5 of the gene are associated with a more severe phenotype that when found in exons 11-15 [142,143]. The positional effect could be relevant in other mutation types, as seen in individuals harbouring a germline mutation in exons 14-15, who are at lower risk of meningioma development [144].

Individuals with mosaicism often present milder forms of the disease yet with certain phenotypic variability. For these group, the age of onset is estimated to be nearly eight years later than patients with constitutional variants. NF2 mosaicism can present with unilateral VS or no VS tumours but with meningiomas and peripheral schwannomas [138,145], being sometimes challenging to differentiate from a schwannomatosis diagnosis. It is estimated that mutation in blood lymphocytes can be detected in 50% of patients, while for the remaining, two distinct tumour tissues need to be studied [143].

In 2017, a study of 142 NF2 patients from the UK cohort led to the development of the Genetic Severity Score (GSS) [146]. This score enabled the stratification of NF2 patients into severity groups based on genotype-phenotype associations, considering the type of mutation, its position within the gene and the proportion of cells carrying the genetic variant. Halliday and

colleagues established 4 genetic subcategories that correlated across 10 measures: 1) mean age at diagnosis, 2) proportion of patients with bilateral vestibular schwannomas, 3) presence of intracranial meningioma, 4) spinal meningioma and 5) spinal schwannoma, 6) NF2 eye features, 7) hearing grade, 8) age at first radiotherapy, 9) age at first surgery and 10) age starting bevacizumab. Moderate or weak but significant correlations were also found in age at hearing loss, mean age at death, quality of life, last optimum Speech Discrimination Score and the total number of major interventions.

Therefore, the GSS was based on the germline *NF2* pathogenic variant to predict disease severity. Patients considered in the subcategories 1A and 1B were those with no pathogenic variant identified in blood (presumed or confirmed tissue mosaicism), showing mild phenotypes. Groups 2A, 2B and 3 included full or mosaic variants identified in blood and were associated with mild, moderate and severe phenotypes, respectively (**Table I.4**). Genetic variants considered in each group are indicated in **Appendix A**, **Table A1.1.**

Table I.4. UK Neurofibromatosis Type 2 (NF2) Genetic Severity Score			
Genetic Severity	Subcategory	Clinical characteristics	Definition
Tissue mosaic	1A	Presumed tissue mosaicism	Meets clinical criteria for sporadic NF2 but not confirmed molecularly with identical NF2 mutations detected in two separate tissue samples
	1B	Confirmed tissue mosaicism	Mosaic NF2 confirmed molecularly with identical NF2 mutations detected in two or more separate tissue samples
2 Classic	2A	Mild NF2	Full or mosaic NF2 mutation identified in blood excluding those found in group 2B or 3: missense mutations; in-frame deletions and duplications; deletions involving the promoter region or exon 1; splice site mutations in exons 8–15; truncating mutations of exon 1; mosaicism in blood for mutations other than truncating mutations in exons 2–13. Inherited NF2 but no NF2, SMARCB1 or LZTR1 mutation identified in blood
	2B	Moderate NF2	Full or mosaic NF2 mutation identified in blood including: splicing mutation involving exons 1–7; large deletion not including the promoter or exon 1; truncating mutations in exons 14–15; mosaic in blood for a truncating mutation in exons 2–13
3 Severe	3	Severe NF2	Full NF2 truncating mutation exons 2–13

Extracted from Halliday D, et al. Genetic severity score predicts clinical phenotype in NF2. Journal of Medical Genetics 2017;54:657–64 [146].

In 2018, the GSS was assessed in the UK paediatric cohort in a total of 87 children, the largest reported [147]. First, this study revealed that more than 90% of the patients harboured a constitutional variant, rather than what is observed in adult cohorts in which there is significant presence of mosaic cases. Thus, no patients were found in group 1. Furthermore, all groups showed significant tumour burden and the need of major interventions, although with the same trend observed in adults, in which group 3 patients had more severe manifestations when compared with group 2A.

They conclude that NF2 paediatric patients included in group 3 manifested clinical presentations earlier, with greater tumour load, poorer visual outcomes and required more interventions. Overall, the genotype-phenotype trend could be already noticed in early ages.

Whilst it has been possible to establish a very good genotype-phenotype relationship and the GSS is a powerful tool to stablish disease prognosis, there are still cases that do not fit in this score and constitute a challenge in the clinics, where currently the score is gently used [148]. Furthermore, much remains unknown on the cellular and molecular mechanisms by which the genetic variant can prompt the appearance of particular NF2-associated lesions.

6. Therapeutic approaches for Neurofibromatosis Type 2

6.1. Current treatment options

Clinical manifestations associated with NF2 are diverse, as already seen up to this section, which makes the clinical management of these patients complex [14]. It is recommended that these patients are managed in specialty centres as they usually require multidisciplinary approaches [62].

Treatment recommendations for VSs consider patient age, tumour size, diagnosis of NF2, symptomatology, patients' preferences and other coexisting comorbidities, although management for sporadic VS differs from VS associated with NF2. For sporadic VS, observation with serial MRI is considered in small and asymptomatic tumours, as typically present a slow growing pattern, although with an associated risk of tumour progression and progressive hearing loss. Thus, patients with a conservative management need to consider hearing loss risk and the possibility to require future treatment, either surgery or radiotherapy [149].

Management of NF2 related VS require a different strategy as these are usually bilateral. Treatment decision-making should balance morbidities associated with treatment and observation, with the aim to preserve function and quality of life. However, surgery is required

upon brainstem compression, deterioration of the facial nerve and loss of useful hearing, unfortunately with high risk of recurrence. Auditory brainstem or cochlear implants can be used for hearing rehabilitation after VS resection [41,62,149].

Improved understanding on molecular and cellular mechanisms underlying the pathophysiology of these tumours has led to the identification of potential therapeutic targets. The most successful has been Bevacizumab, a monoclonal antibody against the vascular endothelial growth factor (VEGF), targeting angiogenesis. It has proven to be effective in more than 50% of progressive vestibular schwannomas of NF2 patients, resulting in VSs size reduction and improved hearing outcomes [150]. However, beneficial responses of VSs to treatment are limited to a sustained treatment, which cannot be extended in time due to its associated toxicity (amenorrhea, proteinuria or hypertension), constituting a clinical challenge for a treatment of a long-course disease [151]. Little responses to meningiomas and no beneficial clinical effects for ependymomas have been described related to Bevacizumab [152,153].

In the case of meningiomas, the gold-standard treatment is observation while the tumour remains asymptomatic and with slow growing patterns, although tumour resection or radiotherapy is indicated in symptomatic and rapid growing tumours. NF2-related meningiomas, that appear usually multiple, with an asynchronous growing pattern can present symptoms independently [62].

The main traits of NF2 and their management are summarized in **Table I.5**.

Table I.5. Clinical presentation and therapeutic options for NF2-related lesions

NF2 tumour type	Incidence (%)	Clinical presentation	Treatment	Complications
Vestibular Schwannomas	~90%	Tinnitus Hearing loss Ataxia	Radiosurgery Chemotherapy Bevacizumab	Facial nerve injury
Peripheral Schwannomas	~70%	Neuropathic pain Loss of sensation Weakness Tumours on skin, head and neck region	Intraneural dissection Excision	Risk of nerve infiltration
Meningiomas	~50%	Headache	Surgical excision Radiosurgery	Malignant transformation (not common in NF2 meningiomas) Invasion to vascular brain structures Compression effect
Ependymoma	~30%	Asymptomatic	Monitoring/ surveillance Surgical resection if symptomatic	Malignant transformation is rare
Retinal Hamartomas	Common	Asymptomatic	Surveillance and monitoring	None

Adapted from: Bachir S, et al. Neurofibromatosis type 2 (NF2) and the implications for vestibular schwannoma and meningioma pathogenesis. International Journal of Molecular Sciences. 2021;22:1–12 [154].

6.2. Development of drug treatments

Due to the lack of effective treatment for NF2 patients, there is a need to identify new potential therapies for the treatment of NF2-related tumours. The increasing knowledge in the role of merlin in multiple molecular pathways is leading to the development of new therapeutic approaches, a few are described below [155,156].

Angiogenesis inhibitors

Bevacizumab, targeting VEGF, is in current use in the clinics and has shown tumour shrinkage and improved or stabilized hearing in 39–55% and 45–57% of the patients, respectively. However, adverse effects are common and can result in treatment interruptions. In addition, long periods of treatment are limited due to cumulative toxicities [157,158]. Another drug targeting angiogenesis is Axitinib (VEGFR, PDGFR, and c-KIT inhibitor), for which preclinical studies have shown to induce inhibition of schwannoma cell growth [159,160].

Tyrosine kinase inhibitors

Merlin can regulate the Epidermal Growth Factor (EGFR) receptor tyrosine kinases (RTKs) ErbB2 and ErbB3, which are involved in Schwann cell differentiation and proliferation, and remain constitutively active upon merlin loss, thus, constituting a target for NF2-related tumours [101]. Lapatinib is a dual EGFR/ErbB2 inhibitor that blocks the phosphorylation and activation of Erk1/2 and Akt, proven to successfully inhibit growth of VSs in phase II of clinical trials [161] and to reduce growth rate of NF2-related meningiomas in some patients [162].

Crizotinib is a focal adhesion kinase (FAK) inhibitor that proved significant reduction in proliferation rates in NF2-deficient Schwan cells and is currently in phase II of clinical trials [163].

Brigatinib is a multi-tyrosine kinase inhibitor. Treatment with Brigatinib in mouse models showed reduction of tumour burden and hearing loss, results that led drug usage to be tested in clinical trials [164].

Mammalian target of Rapamycin (mTOR) inhibitors

Potential targets for NF2-related tumours are also components of the PI3k/Akt/mTORC1. In preclinical studies, inhibition of mTORC1 with rapamycin achieved VS shrinkage and prevented meningioma growth [121,165]. Everolimus, a rapamycin analogue has been studied in clinical trials and resulted in stabilization of VSs, delaying tumour progression in 50% of patients. However, discontinuation of treatment resulted in a rebound effect in the tumour growth rate. Stabilization of meningiomas has also been observed [166].

AZD2014 is an mTORC1/2 inhibitor that has proven to be more effective than the inhibition of mTORC1 alone, resulting in decreased proliferation rates in meningioma cells in vitro [167]. This drug is currently in phase II of clinical trials [168,169].

Histone deacetylase (HDAC) inhibitors

A histone deacetylase (HDAC) inhibitor (AR-12) has been described to regulate Akt phosphorylation through the activity of the Protein Phosphatase 1 (PP1). In preclinical studies in schwannoma and meningioma cells, Akt inhibition resulted in reduced cellular proliferation and increased cellular apoptosis, that was later confirmed in mice xenografts [170].

MEK - Mitogen-activated protein kinase- inhibitors

Selumetinib, a FDA recently approved drug as a treatment for Neurofibromatosis type 1 tumours, is a MEK1/2 inhibitor that halted proliferation of human schwannoma cells in vitro, currently in clinical trials [171].

Anti-inflammatory drugs

Losartan, an antihypertensive drug responsible for blocking angiotensin II, is a new approach currently being studied. This drug has proven to normalize the tumour microenvironment by reducing neuroinflammatory signalling, normalizing tumour vasculature and increasing oxygen delivery in NF2 schwannoma rodent models, which results in the prevention of hearing loss and an augmented radiation efficacy [172].

Some of the drug candidates currently in clinical trials are shown in **Appendix A**, **Table A1.2**.

6.3. Gene therapy

Gene therapy involves modulating expression of affected genes in targeted cells, a powerful approach that has garnered much effort in recent decades and remains a central goal for many diseases. In recent years, several therapies have been approved for neuromuscular diseases, inherited blindness and cancer, evidencing that these targeted therapies could be effective for other pathologies. Gene therapy approaches range from the replacement of the affected gene by viral vectors, modulation of gene expression through antisense therapies and ultimately, gene editing with the use of the CRISPR/Cas9 system [173].

For NF2, preclinical approaches have been focused on trying to prevent schwannoma progression with potential encouraging results. A study with an adeno-associated virus (AAV) serotype 1 vector encoding caspase-1 (ICE) under the Schwann-cell specific promoter, P0, lead to schwannoma regression in a mouse model, with no-vector mediated neuropathy [174]. The use of AAV has been also recently used with an encoded apoptosis-associated speck-like protein, a newly described schwannoma tumour suppressor, and reported to inhibit schwannoma growth in a xenograft model [175]. Nanoparticles have been tested in primary human vestibular schwannoma cultures as a tumour-targeted delivery of small interfering RNA (siRNA), directed against TNFα, resulting in a silenced gene expression [176]. However, none of these approaches target *NF2*.

6.3.1. Antisense therapy

Antisense technologies constitute a RNA-based therapy that aims to modulate gene expression by the use of chemically engineered oligonucleotides, antisense oligonucleotides (ASOs). ASOs are usually 12–30 nucleotides in length and can be designed to bind RNA and form a mRNA-ASO duplex via Watson-Crick binding, leading to the inhibition of the expression of the gene of interest. This approach represents a promising advancement towards personalized genomics

which can potentially be used to treat not only hereditary or genetic diseases, but also viral diseases or cancers [177].

Over the years, there has been an evolution in the chemistry of oligonucleotides by modifications of the phosphodiester backbone in order to improve its performance in terms of pharmacokinetics, tolerability and target binding affinity. The two most relevant modifications have resulted from two phosphate changes, the phosphorothioate (PS) and the phosphorodiamidate morpholino oligomer (PMO) for their resistance to nucleases and enhanced cell uptake (**Figure I.10**) [178].
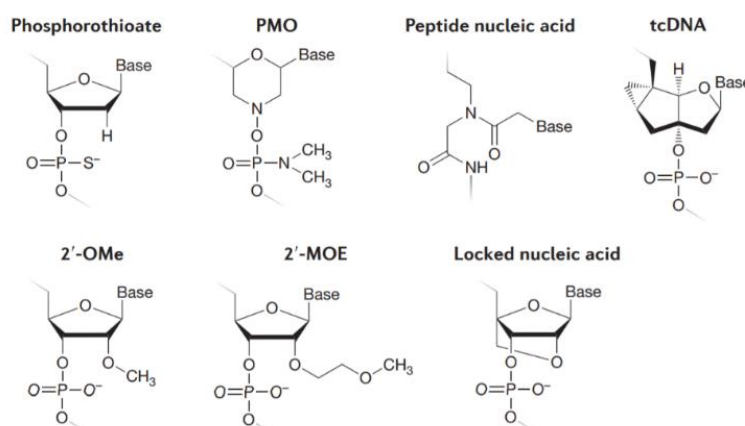
Figure I.10. Types of antisense oligonucleotides according to chemistry modifications. *Extracted from Rinaldi C, Wood MJA. Antisense oligonucleotides: The next frontier for treatment of neurological disorders. Nature Reviews Neurology. 2018;14:9–22* [178].

There are several mechanisms of action by which ASOs modulate gene expression depending on the nature of the targeted sequence and the ASOs chemistry, entailing multiple therapeutic opportunities. In general, they can be distinguished for inducing RNA cleavage (e.g., PS) or RNA blockage (e.g., PMO) [179].

The most common mechanism of action related to RNA cleavage is recruitment of RNAse-H. In this, the ASO binds the RNA target and form a DNA-RNA duplex that is substrate for the RNAse H, responsible to hydrolyse the RNA strand from the DNA-RNA hybrid. Thus, residual products are cleaved and processed through cell degradation pathways resulting in the impairment of protein synthesis (**Figure I.11A**). Cleavage can also be induced by exogenous small interfering RNAs (siRNAs), double-stranded nucleotide modified-RNA sequences that associate with a ribonucleoprotein (Argonaute 2, Ago2) to form the RNA inducing complex (RISC), in which one of the strands will be degraded. In this mechanism, the guide strand enables the RISC to bind

complementary to the target mRNA, where Ago2 cleaves the mRNA, leading to a reduced gene expression (**Figure I.11B**) [179]. These strategies can likewise be used to modulate splice signalling or eliminate RNAs that harbour aberrant splicing patterns.

Regarding RNA blockage, a first mechanism consists of the allosteric blocking of the ribosomal machinery, preventing the assembly of the 40S and 60S ribosomal subunits, leading to a reduced protein expression by translational arrest (**Figure I.11C**). With this mechanism, it is possible to modulate splice signalling. Thus, for frameshift or nonsense variants that code for an aberrant pre-mRNA, resulting in truncating proteins, ASOs can alter the splice signals by binding to the pre-mRNA and induce the skipping of the exon harbouring the pathogenic variant to produce a shorter, yet potentially functional, protein (**Figure I.11D**). In the contrary, for exon inclusion, ASOs prevent the spliceosome to access the transcript sites. In case of genetic variants that induce aberrant splice signalling, ASOs could be used to mask the pathogenic genetic variant and therefore, correct the splice pattern to restore protein synthesis (**Figure I.11E**) [178].

Hence, by means of RNA-blockage is possible to reduce protein expression, restore normal gene function or modulate alternative splicing, both through exon skipping or exon inclusion. However, while RNAse H dependent ASOs can be used to target expression of any protein, only determined regions can be used with ASOs with a steric block activity, as the steric hindrance is related to the binding affinity of ASOs to target sequences [180].

Other described mechanisms involve masking of polyadenylation signals in pre-mRNAs or inhibition of intron excision [178].
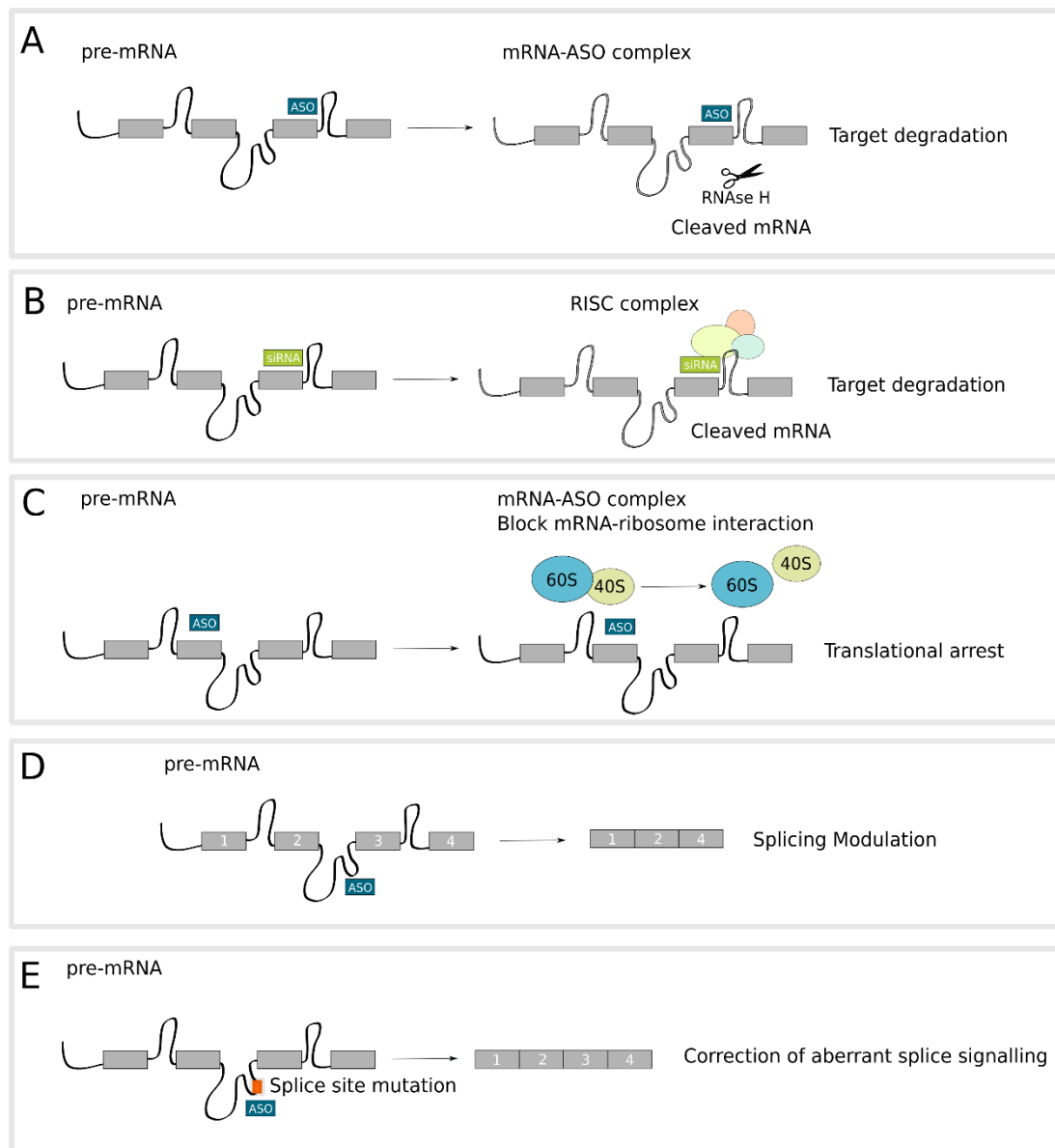
Figure I.11. Molecular mechanisms of antisense oligonucleotides. (A) RNAse-H dependent ASO induce degradation of the mRNA target. (B) siRNA induce degradation of RNA target by activating the RISC complex. (C) hindrance blocking effect of ASOs resulting in translational effect. (D) ASOs' modulation of splice signalling to induce exon skipping. (E) ASOs can mask and correct aberrant splice signalling. *Adapted from: Rinaldi C, Wood MJA. Antisense oligonucleotides: The next frontier for treatment of neurological disorders. Nature Reviews Neurology. 2018;14:9–22 [178] and Dhuri K, et al. Antisense oligonucleotides: An emerging area in drug discovery and development. Journal of Clinical Medicine. 2020;9:1–24 [179].*

One of the main limitations of ASOs to broaden their applications has been its delivery. Bypassing biological barriers and avoiding cell degradation mechanisms is a major concern. Several strategies have been developed and are continuously evolving: the chemical modifications of ASOs, as previously seen, the use of nanoparticles or lipid-based delivery are some examples. Currently, strategies are focused on targeted delivery to specific tissues and cells [181].

Several antisense drugs have been approved by regulatory agencies and are currently used in the clinics (**Appendix A**, **Table A1.3**), while many others are in clinical trials for a wide range of diseases such as Huntington disease, cancers or metabolic diseases, to name a few [182].

For NF2, a first approach was performed by investigating the use of antisense oligonucleotides in a NF2 patient harbouring a germline deep intronic variant. The variant induced the inclusion of a cryptic exon, which truncated the NF2 protein. The use of ASOs in this study resulted in correction of the aberrant splice signalling, restoration of merlin levels and recovery of the phenotype *in vitro*, demonstrating the potential use of these molecules as a therapy to correct splicing defects for NF2 patients [206].

Overall, there is still considerable work ahead in the development of treatments for NF2, being one of the challenges for the advancement in therapeutic options the lack of study models that precisely recapitulate the complexity of the disease.

7. Preclinical models for Neurofibromatosis type 2

Development of new therapies require preclinical models that reproduce the underlying genetics of the disease as well as the tumour biology, and the current available for NF2 are not very extensive.

7.1. *In vivo* models

Several genetically engineered mouse models have been developed for the study of NF2. In the late 1990s, attempts in the development of a homozygous knockout (KO) mice demonstrated that *NF2* deficiency in mice led to early death during embryonic development. *NF2* null mice showed absence of organized extraembryonic ectoderm and failure to initiate gastrulation, suggesting a critical role of *NF2* during differentiation and cell-cell signalling for extraembryonic formation [184,185]. Mutants in heterozygosis showed predisposition to develop osteosarcomas, harbouring the bi-allelic inactivation of the gene, with a high tendency to metastasize [186]. Hence, these mice model did not show clinical features that recapitulate human NF2, although was later achieved with the conditional *NF2* KO Mice. The model was generated through a conditional *NF2* allele (Nf2^{flox2}) under the Schwann-cell-specific promoter P0 and resulted in Schwann cell hyperplasia, Schwann cell tumours, cataracts and cerebral calcifications. However, histological differences were found among mice and human tumours [187]. The development of meningiomas was obtained by selective inactivation of *NF2* in homozygosis in leptomeningeal cells, in a conditional KO mice model [185,188].

Xenograft mouse models have been developed using *NF2* deficiency Schwann cells from mouse or an immortalized human schwannnoma cell line (HEI-193, see below), although with different levels of success in recapitulating histological and biological characteristics of NF2 patients (**Table I.6**).

Table I.6. Xenograft mouse models for NF2		
Animal model	**Advantage**	**Disadvantage**
HEI-193 cells xenografted into mouse sciatic nerve	Rapid tumour formation, ease of access and measurement of tumour growth	Not anatomically accurate, limited neurological assessment possible
HEI-193 cells with fluorescent protein and luciferase reporters, xenografted into mouse sciatic nerve	Rapid tumour formation, ease of access, reporter provided a non-invasive and reliable means to monitor growth *in vivo* by bioluminescence and to locate tumour cells by fluorescence microscopy	Not anatomically accurate, limited neurological assessment possible
Mouse *NF2-/-* or HEI-193 cells xenografted in meninges	Intracranial window present for longitudinal imaging; intravital microscopy of blood vessels	Superficial implantation, cannot assess hearing loss or vestibular dysfunction
Mouse *NF2-/-* Schwann cells grafted into mouse CPA	Appropriate tumour microenvironment, hearing loss and vestibular dysfunction present, intravital microscopy and ultrasound through intracranial window	Not NF2
Mouse SC4 Schwannoma cell line implanted into auditory-vestibular nerve complex	Appropriate tumour microenvironment, hearing loss, bioluminescence and MRI monitoring tumour growth	Significant hearing at implantation and long recovery, sacrificed at 21 days
Mouse *NF2-/-* Schwann cells grafted into CPA of rats	Appropriate tumour microenvironment, hearing loss and vestibular dysfunction present	Not NF2, no intravital microscopy or ultrasound

Adapted from: Ren Y, *et al.* New developments in Neurofibromatosis type 2 and vestibular schwannoma. *Neuro-Oncology Advances* 2021;**3**:1–13 [25].

7.2. *In vitro* models

Cellular resources for the study of NF2 are limited. Primary Schwann cell cultures derived from VSs have been established, constituting probably the most accurately reproduction of tumour genetics and biology *in vitro* [189,190]. The limitation of these cultures, derived from benign tumours, is that they have a finite number of passages, as they progressively loose proliferation capacity and undergo senescence, what hinders its use for large experiments. In addition, obtention of the culture relies on the accessibility to material from a resected tumour, being sometimes challenging, not only because it is a rare disease, but also because tumour resection is avoided when possible, and more notably since treatment with Bevacizumab.

Overcoming the limitations of primary cultures, an immortalized cell line derived from a vestibular schwannoma was isolated (HEI-193) and has been the platform for many studies [191]. HEI-193 was originated from a VS of a 56-year-old patient with bilateral VS, harbouring a splicing variant in *NF2*, and generated by the use of retrovirus-mediated transfer of the human papilloma virus *E6* and *E7* genes. More recently, it has been reported a schwannoma cell line (JEI-001) derived from a 41-year-old sporadic VS patient, harbouring a heterozygous mutation in exon 5 of *NF2* that was immortalized using the lentivirus-mediated hTERT gene transduction technique [215]. The major drawback in the use of these lines results from the cell immortalization process, that leads to unclear alterations in the underlying physiology of cells. Additionally, HEI-193 cells expressed aggressive growing patterns that distinctively differ from the VS benign behaviour.

Low-grade meningioma models for NF2 undergo a similar scenario. Primary cultures of leptomeningeal cells derived meningiomas have been established, sharing limitation of senescence with derived VS cell cultures. The most characterized cell line derived from a benign meningioma is the Ben-Men-1 cell line, immortalized by retroviral expression of hTERT harbouring the loss of one chromosome 22 [193].

7.3. Induced pluripotent stem cells as a disease model

Stem cells are undifferentiated, self-renewal cells with the ability to differentiate into any cell of an organism. They are found in embryos and in many adult tissues with distinct degrees of specialization. While totipotent cells are capable to differentiate to all cell types of the organism, with the largest differentiation potential to form embryonic and extra-embryonic structures, pluripotent stem cells are those that can differentiate into cells of the three germ layers although not capable to generate extra-embryonic structures. More specialized are multipotent stem cells, being able to differentiate to specific lineages, and even more are oligopotent or unipotent stem cells, characterized by a narrowed differentiation capacity although maintaining the self-renewal property [194].

Takahashi and Yamanaka reported in 2006 a major breakthrough in science. They defined four transcription factors (Oct4, Sox2, Klf4, and c-Myc) with which terminally differentiated cells can be reprogrammed to a pluripotent state (induced pluripotent stem cells, iPSC), with similar capabilities to human embryonic stem cells (hESC), able to generate tissues of the three germ layers. That finding provided an opportunity for regenerative medicine, disease modelling and drug screening [195].

iPSCs can be obtained from an affected individual, constituting an inexhaustible source of cells that carry disease-specific genetic information. More advantages in the use of iPSCs rely on their human origin, expandability capacity and the ability to potentially give rise to any cell type, overcoming the ethical concerns regarding the use of hESCs for research. In addition, the development and advancement in gene editing technologies in the recent years, notably the CRISPR-Cas9 technology, has enhanced opportunities in manipulating genes to define disease iPSC-based models. Thus, variability among cell lines caused by genetic heterogeneity can be solved using the CRISPR-Cas9 system by the generation of isogenic cell lines, enhancing the use of iPSCs for disease modelling and the development of personalized-based therapies [196].

Reprogramming efficiency may depend on the delivery methods used to induce pluripotency. The delivery of Yamanaka transcription factors was originally achieved with the use of viral delivery systems (retroviral or lentiviral), which were integrative methods that led to an increased risk of tumour formation. The most common strategies used nowadays are non-integrative approaches that include adenovirus, Sendai virus, episomal vectors and direct protein or RNA delivery. The donor cell type could also influence in efficiency and kinetics of reprogramming, being fibroblasts the most common cellular type used due to its ease and high reprogramming efficiencies. In contrast, reprogramming of cancer cells has been achieved in low efficiencies, possibly due to their altered epigenetic state, chromosomal aberrations and genetic mutations [197,198].

To model human cells and tissues, it is required that iPSCs-derived systems recapitulate the pathophysiological *in vivo* conditions. Understanding signalling pathways involved in differentiation has allowed to stablish directed-differentiation protocols, that use recombinant factors or small molecules to manipulate culture conditions and induce a specific differentiation pathway that mimic stages of human developmental processes. These protocols have been traditionally stablished in two-dimensional (2D) cultures, adherent surfaces usually coated with substrates that enhance cell adhesion or differentiation. However, it is stated that these cultures may not provide a representation of *in vivo* physiological environment due to altered morphologies, modified gene expression and limited cell-cell interaction stablished in side-by-side contact. Three-dimensional (3D) cultures can overcome these limitations by the generation of spheroids or organoids, that allow increased cell-cell interaction and spatial organization [196].

Since 2006, many efforts have been invested in the development of patient specific iPSC-based models: spinal muscular atrophy, Parkinson disease or familial long-QT are just some examples [199–202]. In cancer predisposition syndromes, iPSCs generated from affected tumoral cells represent a valuable resource to develop gene therapy approaches or type-specific drugs and study tumour initiation and progression (**Figure I.12**) [203]. The unique approach of an iPSC-based model for NF2 has been recently reported with a cell line (UMi031-A-2) that harbour a homozygous variant in *NF2* generated by CRISPR/Cas9 in a non-affected pluripotent cell line [204].
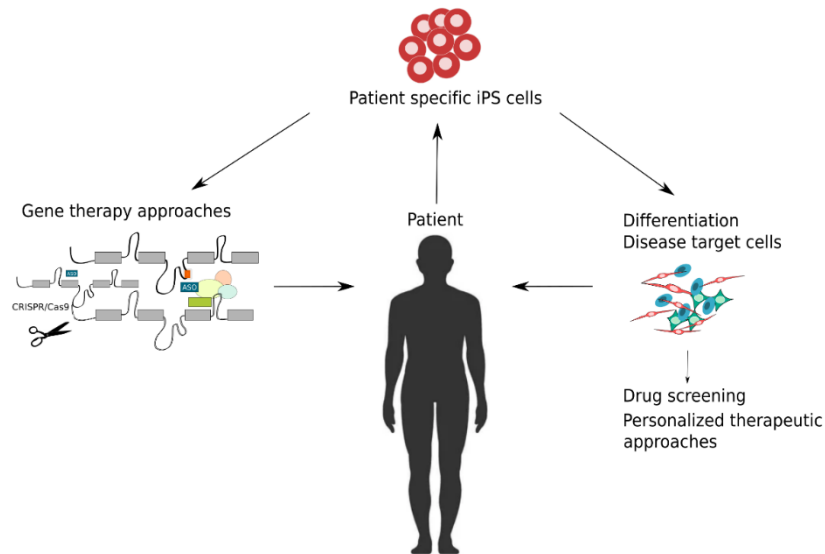
Figure I.12. Schematic representation of iPSCs for disease modelling and their possible applications in personalized medicine. iPSCs can be generated from an affected individual to study potential gene therapy approaches. These cells have the potential to differentiate towards the disease target cells, in which drug screening to develop personalized therapeutic approaches could be performed.

7.3.1. iPSC differentiation towards the Neural Crest - Schwann Cell lineage

Predominantly, cells affected in NF2-related tumours are Schwann cells (SCs), glial cells from the peripheral nervous system. They are involved in the myelin-sheath formation to facilitate neuroconduction processes and in the support of the peripheral axons via secretion of neurotrophic factors and extracellular matrix components [205].

Embryologically, SCs derive from Neural Crest Stem Cells (NCSC) or Neural Crest (NC), a migratory multipotent stem cell population originated in the neural tube that can develop ectodermal derivatives including mesenchymal, neuronal, secretory and pigmented cells [206,207]. During embryogenesis, in the gastrula stage, NC progenitors are found at the neural plate border. Upon formation of the neural tube, NC cells can leave the central nervous system through epithelial-mesenchymal transition and migrate to differentiate into specific cell types

(**Figure I.13**). Neural crest induction depends on the signalling from surrounding embryonic tissues including the Bone Morphogenetic Protein (BMP), Wnt, Notch/Delta, and FGF pathways [208]. Hence, several protocols have been developed in order to efficiently differentiate NC cells from iPSCs *in vitro* [209]. The most common approach is the combination of small molecules that modulate key signalling pathways in NC development, which include the activation of the Wnt signalling and inhibition of the BMP and transforming growth factor β (TGF-β) signalling [210,211]. Characterization of the differentiated cell population after the application of the protocol can be accessed via immunocytochemistry or flow cytometry assays of classical lineage markers, that include transcription factors (Sox 10 and AP2α/TFAP2α) or cytoplasmatic and membrane markers (NGFR/p75 and Hnk1). Sox10 is a master transcription factor essential during specification of NC and Schwann cells, although is also expressed in other NC derivatives, such as melanocytes. AP2α is expressed during embryogenesis in migrating NC and crucial for SC development. Other well characterized markers of NC populations are the Nerve Growth Factor Receptor (NGFR), also named p75, which is expressed along the NC-SC lineage, and the CD57 antigen or Hnk1 [212].
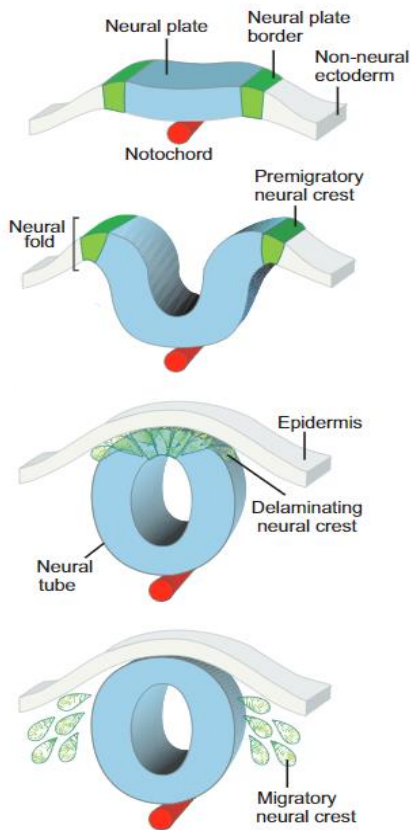
Figure I.13. Embryological development of the multipotent neural crest population. Neural crest development begins at the neural plate border. The neural plate is closed to form the neural tube and neural crest progenitors can migrate upon epithelial-mesenchymal transition to differentiate to specific cell types. *Extracted from Simões-Costa M, Bronner ME. Establishing neural crest identity: a gene regulatory recipe. Development. 2015;142:242–57* [213].

The NC population can differentiate *in vivo* to myelinating and non-myelinating (Remak) Schwann cells. This differentiation is a multistep process that include transitions from NC to Schwann cell precursors (SCP), immature Schwann cells (iSC) and finally give rise to myelinating or non-myelinating Schwann cells (**Figure I.14**). Transcription factors and the signalling underlying the generation of SCP from NC have been poorly described, although some have been reported as Sox10, Neuregulin 1 or the Noch signalling pathway. Expression of Sox10 has been characterized to be required for SCP generation, yet its expression is not specific from the glia. Neuregulin 1 has also been considered as it is required for SC development and maintenance. It is a pleiotropic growth factor expressed naturally in the axon membrane and responsible for inducing the activation of the ErbB2/ErbB3 receptor complex. Notch signalling has been described to promote generation of SC from SCP [212].
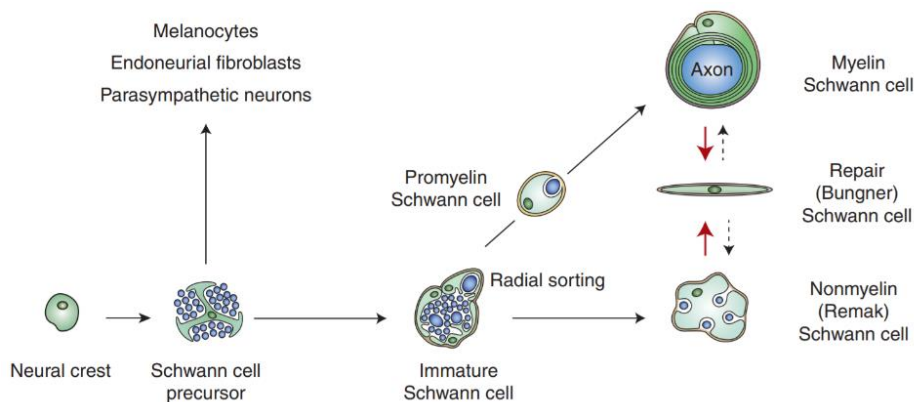
Figure I.14. Schwann cell differentiation process in mice. NC differentiate towards Schwann cell precursors, immature Schwann cells to finally derive to Myelinating or non-myelinating SC. *Extracted from Jessen KR, Mirsky R, Lloyd AC. Schwann cells: Development and role in nerve repair. Cold Spring Harbor Perspectives in Biology 2015;7:1–15* [212].

Several protocols have been defined to induce SC differentiation from NC *in vitro*, frequently with the use of neuregulin 1 (NRG1), also referred as Heregulin [214]. In addition, there are markers that allow the characterization of the SC identity in a stage-specific manner during or after the application of the differentiation protocol. Specifically expressed at the SCP stage can be found Cadherin 19 (CDH19) and Alpha4 integrin (ITGA4). Regarding myelin composition, the markers Myelin Protein Zero (MPZ), Proteolipid Protein 1 (PLP1) and Peripheral Myelin Protein 22 (PMP22) are considered, that together with the Growth Associated Protein 43 (GAP43) are initially expressed at the SCP stage [215]. The Nerve Growth Factor Receptor (NGFR) or p75 expression is found along the NC-SC lineage, in conjunction with Krox20 or the early growth response protein-2 (EGR2). Finally, one of the most commonly used markers to determine the SC identity is the S100 calcium-binding protein B (S100β) expressed in iSC and both myelinating and non-myelinating SC [212].

Objectives

The ultimate goal of this thesis is to provide new insights that could contribute to the development of a personalized medicine for Neurofibromatosis type 2 (NF2). The three specific objectives of the present work are:

1. To improve the prognostic capacity for NF2 patients by refining the published Genetic Severity Score (GSS) and include functional variables.

    1.1. To validate the NF2 Genetic Severity Score published by the UK reference group in a Spanish cohort.

    1.2. To identify novel molecular prognostic factors in NF2 derived patients' fibroblasts.

    1.3. To propose improvements in the GSS by incorporating data from novel molecular prognostic factors for a more accurate classification of NF2 patients according to disease severity.

2. To evaluate the use of antisense therapeutic strategies *in vitro* as a personalized therapy for NF2 patients.

    2.1. To test the use of Phosphorodiamidate Morpholino Oligomers (PMOs) to modulate and correct the aberrant splicing of the *NF2* gene originating from point-mutations located near the canonical splice site and restore protein levels.

    2.2. To force the skipping of in-frame *NF2* exons harbouring frameshift or nonsense variants and generate hypomorphic, less deleterious protein forms using PMOs.

3. To develop a cellular model that precisely recapitulate tumour genetics and biology of vestibular schwannomas (VSs).

    3.1. To generate an induced pluripotent stem cell (iPSC)-based model from reprogramming VSs.

    3.2. To develop and characterize the differentiation towards the Neural Crest-Schwann Cell lineage from iPSC harbouring single o bi-allelic inactivation of the *NF2* gene.

Chapter 1

Revisiting the UK Genetic Severity Score for NF2: a proposal for the addition of a functional genetic component

This chapter presents the work performed on the first objective of the thesis, in which the aim was to find improvements in the prognostic capacity of Neurofibromatosis Type 2 (NF2). It includes the validation of the UK NF2 Genetic Severity Score (GSS) in a Spanish cohort, as well as the results from functional assays performed in order to identify novel molecular prognostic factors for the disease. Finally, we present a revision of the GSS, named Functional Genetic Severity Score.

Abstract

Background: Neurofibromatosis Type 2 (NF2) is an autosomal dominant disorder characterized by the development of multiple schwannomas, especially on vestibular nerves, and meningiomas. The UK NF2 Genetic Severity Score (GSS) is useful to predict the progression of the disease from germline *NF2* pathogenic variants, which allows the clinical follow-up and the genetic counselling offered to affected families to be optimized.

Methods: 52 Spanish patients were classified using the GSS, and patients' clinical severity was measured and compared between GSS groups. The GSS was reviewed with the addition of phenotype quantification, genetic variant classification and functional assays of merlin and its downstream pathways. PCA and regression models were used to evaluate the differences between severity and the effect of *NF2* germline variants.

Results: The GSS was validated in the Spanish NF2 cohort. However, for 25% of mosaic patients and patients harbouring variants associated with mild and moderate phenotypes, it did not perform as well for predicting clinical outcomes as it did for pathogenic variants associated with severe phenotypes. We studied the possibility of modifying the mutation classification in the GSS by adding the impact of pathogenic variants on the function of merlin in 27 cases. This revision helped to reduced variability within *NF2* mutation classes and moderately enhanced the correlation between patient phenotype and the different prognosis parameters analysed ($R2=0,38$ vs $R2=0,32$, $p>0,001$).

Conclusions: We validated the UK NF2 GSS in a Spanish NF2 cohort, despite the significant phenotypic variability identified within it. The revision of the GSS, named FGSS, could add value for the classification of mosaic patients and patients showing mild and moderate phenotypes once it has been validated in other cohorts.

1. Introduction

Neurofibromatosis type 2 (NF2) (MIM 101000) is an autosomal-dominant syndrome caused by mutations in the *NF2* gene that affects 1 in 28,000-40,000 births worldwide [1,2]. Approximately 50% of the cases are due to *de novo* variants, while the other 50% are familial cases. NF2 typically presents with vestibular schwannomas (VS) on addition to multiples schwannomas in other cranial, peripheral and spinal nerves, as well as meningiomas, ependymomas, congenital cataracts, and it is also associated with focal neurological deficits. Due to the development of bilateral VS, NF2 disease will progress in most patients causing hearing loss, tinnitus and balance problems [3]. Despite the benign nature of these tumours, their multiplicity and anatomical location causes highly increased morbidity and early death. Therapeutic management is challenging in these patients due to the recurrence of treated tumours. Surgery, radiotherapy and Bevacizumab are the current gold standard treatments [4,5] .

The clinical expression of the disease is highly variable, which makes the clinical management of these patients complex and challenging [6]. Phenotype differences found among patients led to a clinical classification in which two subgroups of adult patients were established into Gardner and Wishart subtypes (mild and severe phenotypes, respectively). Further studies have resulted in the identification of several prognostic markers [7,8] and a good genotype-phenotype correlation [9–11].

In this context, the UK NF2 Reference Group established a Genetic Severity Score (GSS) to predict the severity of the disease based on the type of *NF2* germline variant in the patient [12]. This score stratifies NF2 patients into four groups: in groups 1A and 1B no pathogenic variant is identified in blood and patients show a very mild phenotype, while patients in group 3 carry truncating variants in exons 2-13 of the *NF2* gene and present a severe phenotype. Group 2B harbour mosaic in blood for a truncating variant in exons 2–13, splicing variant involving exons 1–7, large deletions not including the promoter or exon 1, truncating variants in exons 14–15 and patients present a moderate phenotype. Finally, group 2A includes full or mosaic NF2 variants identified in blood, excluding those found in group 2B or 3, and is associated with mild phenotypes. Therefore, the GSS represents a tool by which it is possible to establish a trend in NF2 prognosis from the patient' germline variant and thus, improve the clinical follow-up and the genetic counselling offered to affected families [12,13].

Around 50% of NF2 *de novo* cases are mosaic (groups 1A and 1B) and present highly variable phenotypes [14,15]. Specifically, more than 15% of the *de novo* NF2 patients show bilateral VS

before the age of 20 and with no variant identified in blood [14,16] . Therefore, despite the good performance of the UK NF2 GSS, this complicates the day-to-day application of it in the clinical context, as some mosaic cases may develop multiple tumours at early ages [8,17–19]. Similarly, some patients harbouring splicing and missense variants could also show significant differences in their clinical manifestations [7,9,10,20–24]. Hence, the GSS is useful for classifying NF2 patients in general terms but there is room for improvement in stratifying some patients.

The *NF2* gene encodes for the protein merlin. Merlin can be considered to be a scaffold protein as it indirectly links F-actin, transmembrane receptors and intracellular effectors to modulate receptor mediated signalling pathways and integrates extracellular signals to modulate morphology, motility, proliferation and survival [25–27]. Understanding the impact of the pathogenic *NF2* variant on the stability of merlin, and on the regulation of its associated signalling pathways could be a better way of accounting for variant pathogenicity. In this context, analysing the status of small GTPases (Rac1 and Ras), mTOR, PI3K/Akt and Hippo pathways in NF2 patients could help to determine the functional impact of the germline variant and therefore this data could be used to improve the capacity to predict the prognosis of NF2 patients.

In this study, we present the validation of the UK NF2 GSS [12] in the NF2 patients attended in the Spanish National Reference Centre (CSUR) of Phacomatoses and we propose a revised version, called Functional Genetic Severity Score (FGSS), considering data obtained from functional assays and the predicted mutational effect on merlin. We describe here the performance of the FGSS in comparison to GSS and show the changes observed in the behaviour of some clinical prognosis markers analysed in our cohort.

2. Materials and Methods

Patients

Written informed consent was obtained from all individuals included in the study. Clinical diagnosis was established following the Manchester Criteria [28]. Clinical data was recorded, five domains were assessed: patient demographics, tumour load, ocular features, hearing capacity and major interventions. Genetic testing was performed using the customized I2HCP panel [29] in blood or tissue when available.

Functional assay

The pathways downstream of merlin were analysed in 27 out of 52 NF2 patients through a Western Blot assay. Cultured fibroblasts from skin biopsies were processed as described in [23]. Three primary cultures from healthy donors were included as control samples (Ctrl1, Ctrl2 and Ctrl3) and grouped together with the tissue mosaic patients for the statistical analysis. Primary antibodies (Supplemental Material and Methods) were incubated at 4°C overnight and secondary antibodies during 1h at room temperature (IRDye 680LT and IRDye 800CW, 1:1000 dilution, LI-COR). The statistical threshold that allowed the differentiation between controls or mosaic patients and the patients in group 3 (severe) was established through the ±2SD limits method.

Statistics

All statistical analyses of the validation of the GSS were reproduced from the study of Halliday et al [12] with minor modifications. In order to study differences between protein expression levels in the functional assay, Kruskal-Wallis and Mann-Whitney U statistical tests were performed among genetic severity groups and pathogenic variant classes. Analysis of variance (ANOVA) of FGSS and *NF2* mutations was performed to test differences of severity between NF2 mutations groups. Backward stepwise regression analysis was performed to evaluate the contribution of merlin and pERK levels in the ANOVA model. Spearman Correlation (ρ) was used to calculate the correlation between merlin and pMerlin. Statistical analyses were performed using R software.

For more information, see **Supplemental Material and Methods** at the end of the reference section of this chapter.

3. Results

Validation of the UK NF2 Genetic Severity Score (GSS) in a Spanish cohort

Fifty-two NF2 patients from the Spanish National Reference Centre (CSUR) for Phacomatoses cohort were included in the GSS validation group. This cohort consisted of 19 men and 33 women, all of them with a clinical diagnosis of NF2 [28] at a mean age of 28.9 (range 9 - 70), 44 patients showed bilateral VS, 39 presented spinal tumours, and 30 had intracranial meningiomas with a mean age of the cohort of 41,87 (range 12-79). We stratified the whole cohort following the GSS classification. Nineteen cases of the cohort (35%) were assigned to group 1, including 4

confirmed tissue mosaics (group 1B, two or more affected tissue samples studied) and 15 to group 1A as presumed mosaics, since no variant was identified in blood and affected tissues were not available. Twelve out of nineteen patients were clinically diagnosed by the presence of bilateral vestibular schwannomas, while 6 cases (4 from 1A and 2 from 1B) showed a unilateral vestibular schwannoma in addition to multiple schwannomas and/or meningiomas. Only one case did not develop vestibular schwannomas at the moment of data collection and NF2 diagnosis was confirmed by genetic testing (patient 435) (**Supplemental Table S1.1**). Finally, the 33 patients with a constitutional *NF2* pathogenic variant were classified in group 2A, 2B or 3 following GSS criteria (**Tables 1.1 and 1.2**).

When analysing demographic data (**Table 1.1**), we observed the mean age at diagnosis in individuals in group 1 (39.88 ±16.48, range: 17-70) was significantly statistically different from that of patients in group 3 (18.79 ±6.45, range: 14-35; p<0.001). The mean age at diagnosis for the group 2A was ~31 (range 14-50) and lower in group 2B ~23 (range 9-37) with no significant differences between these groups. Regarding the age at hearing loss, significant differences were also found between groups 1 and 3 (p<0.0005); we observed a linear correlation between the age at hearing loss and the severity group as established by the GSS (**Table 1.2**). Therefore, these results showed the same tendency as the English cohort and that features related to poor prognosis such as the age at diagnosis and age at hearing loss correlated with the four groups established.

When studying tumour burden, the highest incidence of intracranial meningiomas was found in groups 2B and 3 (~70%), with a lower incidence in group 2A (22.2%) and a remarkably high incidence in group 1 (58%). Similarly, intracranial schwannomas were also present in patients classified into groups associated with mild phenotypes. Spinal meningioma was reported in groups 1, 2B and 3 of our cohort, specifically, six mosaic patients from our cohort developed multiple spinal meningiomas. A fairly even distribution of the presence of spinal schwannomas was seen in the groups 1 and 2 (52 to 66%) and a higher incidence was found in group 3 (79%) with no statistically significant differences. Regarding spinal ependymomas, a higher incidence was found in patients from groups 2B and 3 (40% and 36% respectively), but there was also considerable variability in the other groups and no clear linear trend was observed. Finally, considering the number of major interventions in our cohort we did not observe significant differences between groups (**Table 1.2**, **Supplemental Tables S1.1 - S1.2**).

Table 1.1. Demographic data according to Genetic Severity Score

Genetic Severity			1 Tissue Mosaic	2A Mild	2B Moderate	3 Severe	Correlation
N (% total)	Number of patients		19 (36,54%)	9 (17,3%)	10 (19,23%)	14 (26,9%)	
N (% gender)	Gender	Male	4 (21,1%)	3 (15,8%)	7 (36,8%)	5 (26,3%)	
		Female	15 (45,45%)	6 (18,2%)	3 (9%)	9 (27,3%)	$X^2(3) = 4.91$, p = 0.17
Mean (SD)	Age at diagnosis		39,88 (16,48)	30,80 (13,40)	22,82 (9,13)	18,79 (6,45)	$r_s(50) = -0.60$, p < 0.001
	Current age		52,29 (17,16)	44,80 (12,10)	36,55 (11,09)	30,79 (12,07)	$r_s(50) = -0.53$, p < 0.001
	Years since diagnosis		12,35 (8,41)	14 (12,18)	13,73 (8,13)	12 (8,26)	$r_s(50) = 0.02$, p = 0.89
	Age at NF2-related death			53	40	42	
N (% score category)	NF2-related deaths			1	1	1 (7,14%)	
	Familial NF2		0 (0%)	2 (22,22)	1 (9,09%)	3 (21,43%)	
	Sporadic NF2		19 (100%)	7 (77,77%)	9 (90%)	11 (78,57%)	$X^2(3) = 5.93$, p = 0.11

NF2, Neurofibromatosis Type 2.

Table 1.2. Tumour burden, presence of ocular features and hearing outcome according to Genetic Severity Score							
Genetic Severity				**1 Tissue Mosaic**	**2A Mild**	**2B Moderate**	**3 Severe**	**Statistics**
Number of patients				19	9	10	14	
Tumour load	N (%)	Bilateral VS		11 (57,89%)	9 (100%)	10 (100%)	14 (100%)	$X^2(1) = 8.38$, p = 0.003
		Unilateral VS		6 (31,58%)	0 (0%)	0 (0%)	0 (0%)	$X^2(1) = 5.18$, p = 0.022
		Intracranial meningioma		11 (57,89%)	2 (22,2%)	7 (70%)	10 (71,4%)	$X^2(1) = 0.79$, p = 0.37
		Intracranial Schwannoma		5 (26,3%)	3 (33,3%)	4 (40%)	7 (50%)	$X^2(1) = 1.56$, p = 0.21
		Spinal meningioma		6 (31,58%)	0 (0%)	4 (40%)	5 (35,7%)	$X^2(1) = 0.23$, p = 0.62
		Spinal Schwannoma		10 (52,63%)	6 (66,7%)	6 (60%)	11 (78,6%)	$X^2(1) = 2.46$, p = 0.11
		Spinal ependymoma		4 (21,05%)	1 (11,1%)	4 (40%)	5 (35,7%)	$X^2(1) = 1.23$, p = 0.26
Ocular Features	N (%)	Epiretinal membranes		0 (0%)	0 (0%)	0 (0%)	0 (0%)	NA
		Cataract		4 (21,05%)	2 (22,2%)	2 (22,2%)	3 (21,42%)	$X^2(1) = 0.01$, p = 0.90
		Combined hamartoma		0 (0%)	0 (0%)	0 (0%)	2 (14,28%)	$X^2(1) = 3.35$, p = 0.06
		Optic nerve meningioma		0 (0%)	0 (0%)	1 (10%)	0 (0%)	$X^2(1) = 0.24$, p = 0.62
	Mean (SD)	Total eye features		0,27	0,2	0,33	0,4	$r_s(49) = 0.05$, p = 0.69
Hearing Outcomes	N (%)	Hearing grade	1	13 (68,4%)	5 (55,5%)	4 (40%)	6 (42,9%)	$X^2(1) = 2.05$, p = 0.15
			2	1 (5,26%)	0 (0%)	0 (0%)	0 (0%)	$X^2(1) = 1.33$, p = 0.24
			3 o 4	0 (0%)	0 (0%)	2 (20%)	1 (7,1%)	$X^2(1) = 1.83$, p = 0.17
			5	2 (10,52%)	2 (22,2%)	1 (10%)	4 (28,6%)	$X^2(1) = 1.01$, p = 0.31
			6	2 (10,52%)	3 (33,3%)	3 (30%)	3 (21,4%)	$X^2(1) = 0.50$, p = 0.47
	Mean (SD)	Age of loss of useful hearing		48,59 (18,57)	38 (11,96)	30,27 (9,88)	26,23 (12,58)	$r_s(48) = -0.56$, p<0.001
Cutaneous manifestations	N (%)			6 (31,57%)	2 (22,2%)	6 (60%)	9 (64,3%)	$X^2(1) = 3,94$, p = 0.047

NA, not available; VS, Vestibular Schwannoma.

Functional analysis of merlin and associated signalling pathways in patient skin fibroblasts

To better interpret the pathogenicity of *NF2* constitutional variants in relation to the phenotype variability observed within GSS categories, a functional assay in primary cultured fibroblasts from patients was developed to analyse the activation state of merlin and some of its downstream pathways. In particular, we analysed PAK1 and RAC total protein amount, and total protein and the phosphorylated forms of merlin, ERK, PKA, YAP and AKT.

As expected, all patients that harboured a germline pathogenic variant, and therefore had one *NF2* mutated allele, showed lower merlin levels compared with healthy controls or tissue mosaics ($p < 0.05$). No significant differences were found inter-groups with a pathogenic variant in the *NF2* gene, regardless the variant type or location within the gene, meaning that the effect on merlin levels were very similar in patients carrying truncating and splicing variants or large deletions (**Figure 1.1A and 1.1B**, **Supplemental Table S1.1**). When studying the status of phosphorylated merlin (pMerlin), we observed the same tendency as merlin, suggesting that decreased levels of pMerlin could be due to the lower levels of merlin rather than a dysregulation of merlin activation (**Supplemental Figure S1.1**).

Results did not indicate any differences in the status of the PI3K, PAK, YAP or RAC pathways, neither in the total protein levels nor in the phosphorylated forms. In contrast, pERK levels in patients' fibroblasts with truncating variants were statistically significantly lower than pERK levels in tissue mosaics or healthy controls, while ERK levels remained constant between groups (**Figure 1.1C and 1.1D**, **Supplemental Figure S1.2**). These results allowed a statistically significant discrimination of patients with severe phenotypes from healthy controls ($p=0.0042$). The group with intermediate phenotype showed greater variability, as did the group of mosaic patients (SD 2A=1.999, SD 2B=2.332, 1A&B=2.624).

Figure 1.1. Merlin and pERK levels in patient's fibroblasts according to the GSS. (A) Merlin levels in NF2 patients' fibroblasts. (B) Average of merlin levels according to Genetic Severity Groups. (C) pERK levels in NF2 patients' fibroblasts. (D) Average of pERK levels according to Genetic Severity Groups. Column's grey scale indicates the Genetic Severity Group; NPE stands for Normalized Protein Expression; Bars represent the SD from three independent experiments. (*p <0.05; **p <0.005; ***p <0.001). Symbol legend: □ presumed mosaicism; ■ generalized mosaicism; ◆ tissue mosaicism; • missense.

Reviewing GSS mutation categorization

Due to the unexpected tendency among groups 1 and 2 in the clinical manifestations of the studied cohort, we revised the GSS considering the predicted mutation effect on merlin, its position within the gene and its effect on merlin and pERK activity based on functional assays results.

First, qualitative clinical data recorded were coded to quantitative variables in order to measure the NF2 phenotype, independently of the *NF2* variant type and the mosaicism status. Quantification of the phenotype was based on well-known NF2 prognosis markers (**Supplemental Table S1.3**) and was presented in a numeric ten-scale based on the sum of the transformed quantitative variables. In this way, a patient younger than 25 years old, presenting bilateral VS, peripheral schwannomas, and multiple spinal/cerebral tumours was classified with the most severe score (10).

Second, we analysed the relation between the GSS predicted phenotype and the outcome of the phenotype quantification in the patients of our cohort. We observed that some tissue mosaic patients did not show the expected very mild phenotype. In addition, patients carrying large deletions including or excluding the 5' of the gene did not show phenotypic differences and neither did the patients harbouring splice variants in exons 1-7 or 8-13 (**Supplemental Table S1.4**).

Taking into account the mentioned observations, we revised the GSS categorization of *NF2* mutations and propose a modified criteria based on six mutation classes (1-6), which was referred to as Functional Genetic Severity Score (FGSS). In general terms, presumed mosaics or patients carrying a Ring22 were scored as 1 and related to very mild phenotypes, while truncating variants in exons 2-13 were associated with a severe phenotype and scored as 6. Other types of pathogenic variants were scored in between considering the proportion of cells carrying the mutation and when the variant induced a frameshift alteration. However, we did not take into account the position of the altered exons, except for exon 1, since no differences were observed in merlin levels when comparing variants affecting 5' or 3' of the *NF2* gene (**Table 1.3**, **Supplemental Table S1.4**, **Supplemental Material and Methods**).

Table 1.3. Categorization of *NF2* mutation according to Functional Genetic Severity Score

NF2 Germline variants	GSS subcategory	FGSS mutation class	Phenotype Quantification	Disease Severity
Ring 22 (n=1)	NA	1	<5	Very mild phenotype
Missense variants (n=1)	2A	3	6-7	Mild
Large and small deletions				
Small in-frame deletion or duplication (n=1)	2A	3	6-7	Mild
large deletion (>1 exon) including promoter or exon 1				
maintaining reading frame	2A	3	6-7	Mild
causing frameshift alteration (n=2)	2A	4	7-7,8	Moderate
Whole *NF2* gene	2A	4	7-7,8	Moderate
large deletion (> 1 exon) excluding promoter or exon 1				
maintaining reading frame	2B	3	6-7	Mild
causing frameshift alteration (n=2)	2B	4	7-7,8	Moderate
Whole *NF2* gene	2B	4	7-7,8	Moderate
Splicing mutation				
Exons 1-7 (in frame)	2B	4	7-7,8	Moderate
Exons 8-13 (in frame)	2A	4	7-7,8	Moderate
Exons 1-7 (frameshift) (n=3)	2B	5	7,8-8,5	Moderate-Severe
Exons 8-13 (frameshift) (n=1)	2A	5	7,8-8,5	Moderate-Severe
Exons 14-17 (n=2)	2A	4	7-7,8	Moderate
Truncating mutation				
Exon 1	2A	5	7,8-8,5	Moderate-Severe
Exons 2–13 (n=14)	3	6	>8,5 - 10	Severe
Exons 14–15	2B	5	7,8-8,5	Moderate-Severe

NF2 Generalized mosaic variants[1]	GSS subcategory	FGSS mutation class	Phenotype Quantification	Disease Severity
Ring 22	NA	1	<5	Very mild phenotype
Missense variants	2A	2	<5	Very mild phenotype
Large and small deletions				
Small in-frame deletion or duplication	2A	2	<5	Very mild phenotype
large deletion (> 1 exon) including promoter or exon 1				
maintaining reading frame	2A	2	<5	Very mild phenotype
causing frameshift alteration	2A	3	6-7	Mild
Whole *NF2* gene (n=1)		3	6-7	Mild
large deletion (> 1 exon) excluding promoter or exon 1				
maintaining reading frame	2A	2	<5	Very mild phenotype
causing frameshift alteration (n=1)	2A	3	6-7	Mild

Table 1.3. Continued

Splicing mutation

Exons 1-7 (in frame)	2A	**3**	6-7	Mild
Exons 8-13 (in frame)	2A	**3**	6-7	Mild
Exons 1-7 (frameshift)	2A	**4**	7-7,8	Moderate
Exons 8-13 (frameshift)	2A	**4**	7-7,8	Moderate
Exons 14-17	2A	**3**	6-7	Mild

Truncating mutation

Exon 1 mosaic	2A	**4**	7-7,8	Moderate
Exons 2–13 mosaic (n=4)	2B	**5**	7,8-8,5	Moderate-Severe
Exons 14–15 mosaic	2A	**4**	7-7,8	Moderate

[1]Generalized mosaic variants: >2,5% of reads, 5% of cells

NF2 Tissue mosaic variants[2]	GSS subcategory	FGSS mutation class	Phenotype Quantification	Disease Severity
Variants classified as 3	1B	**1**	<5	Very mild phenotype
Variants classified as 4 (n=1)	1B	**2**	<5	Very mild phenotype
Variants classified as 5-6 (n=3)	1B	**3**	6-7	Mild

[1]Generalised mosaic variants: >2,5% of reads, 5% of cells
[2]Detected in two affected tissues. In addition, 15 patients with an inconclusive genetic test.
FGSS, Functional Genetic Severity Score; GSS, Genetic Severity Score; NF2, neurofibromatosis type 2.

Analysis of the added value of incorporating functional genetic information to GSS

When stratifying our cohort with the proposed criteria, patients harbouring genetic variants scored as 5 or 6 showed a severe phenotype, while patients harbouring *NF2* mutation class 4 behaved in a fairly similar way, although fewer extravestibular lesions were observed. In contrast, patients classified as class 3 presented a greater clinical heterogeneity, because class 3 included generalized and tissue mosaicisms as well as patients carrying constitutional variants associated with a mild phenotype. Finally, patients of classes 1 or 2 showed very mild phenotypes since these groups contain presumed mosaic and tissue mosaic patients, who harbour less deleterious variants. The FGSS showed stronger correlation between classes when studying the appearance of vestibular schwannomas, the presence of intracranial meningiomas, as well as in hearing outcomes and cutaneous manifestations. The age at first surgery and several of the parameters related to major interventions analysed also showed larger means between classes when compared with the GSS (**Table 1.2 and Supplemental Tables S1.1, S1.5-7**). In addition, the proposed revision to classify patient phenotype based on the *NF2* genetic variant reduced the intragroup variability, improved the classification of mosaic patients and moderately improved the correlation between patient phenotype and some of the prognostic

parameters analysed (**Figure 1.2**, **Supplemental Tables S1.4-7**). All these phenomena could indicate that the revised criteria could add value to the GSS.
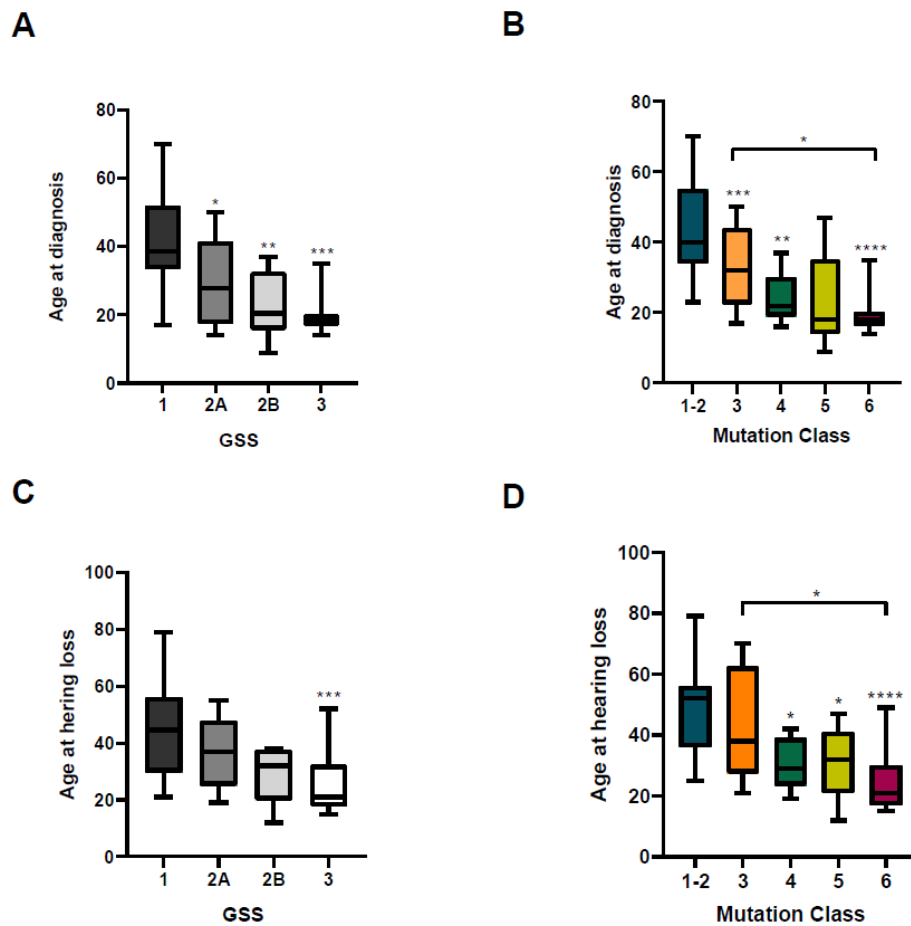
Figure 1.2. Comparison of the age diagnosis and age at hearing loss according to GSS or FGSS. (A) Average age at diagnosis according to the GSS classification. (B) Average age at diagnosis according to the FGSS. (C) Average age at hearing loss according to the GSS. (D) Average age at hearing loss according to the FGSS. Column's grey scale indicates the Genetic Severity Group; Blue stands for the healthy controls and mutation classes 1 and 2; orange stands for mutation class 3; dark green stands for mutation class 4; light green stands for mutation class 5 and purple stands for mutation class 6. Bars represent the SD; (*p<0.05; **p<0.005; ***p<0.001, ****p<0.0005).

Similarly, Merlin and pERK levels showed the same trend as when classified through the GSS but the intragroup variability decreased in classes associated with mild phenotypes. In addition, merlin levels were similar in groups 4-6, and significantly lower in groups 1-3 (p<0.005), since these three last groups contained mosaic patients. Furthermore, the levels of pERK in classes 5 and 6 and were statistically significantly lower compared with class 4 and below (p<0.005). As mentioned before, class 3 showed higher variability due to the phenotypic variability detected in tissue mosaic patients (σ=1.884) (**Figure 1.3**, **Table S1.8**).
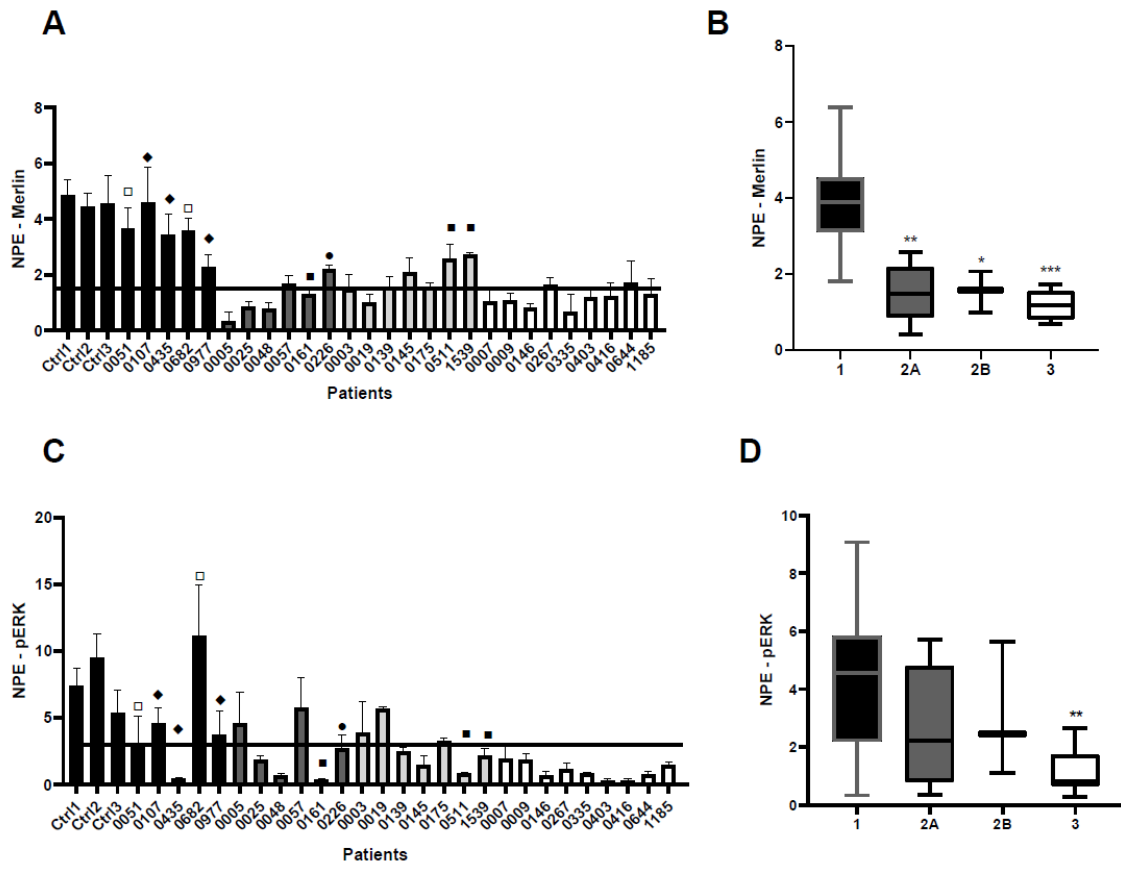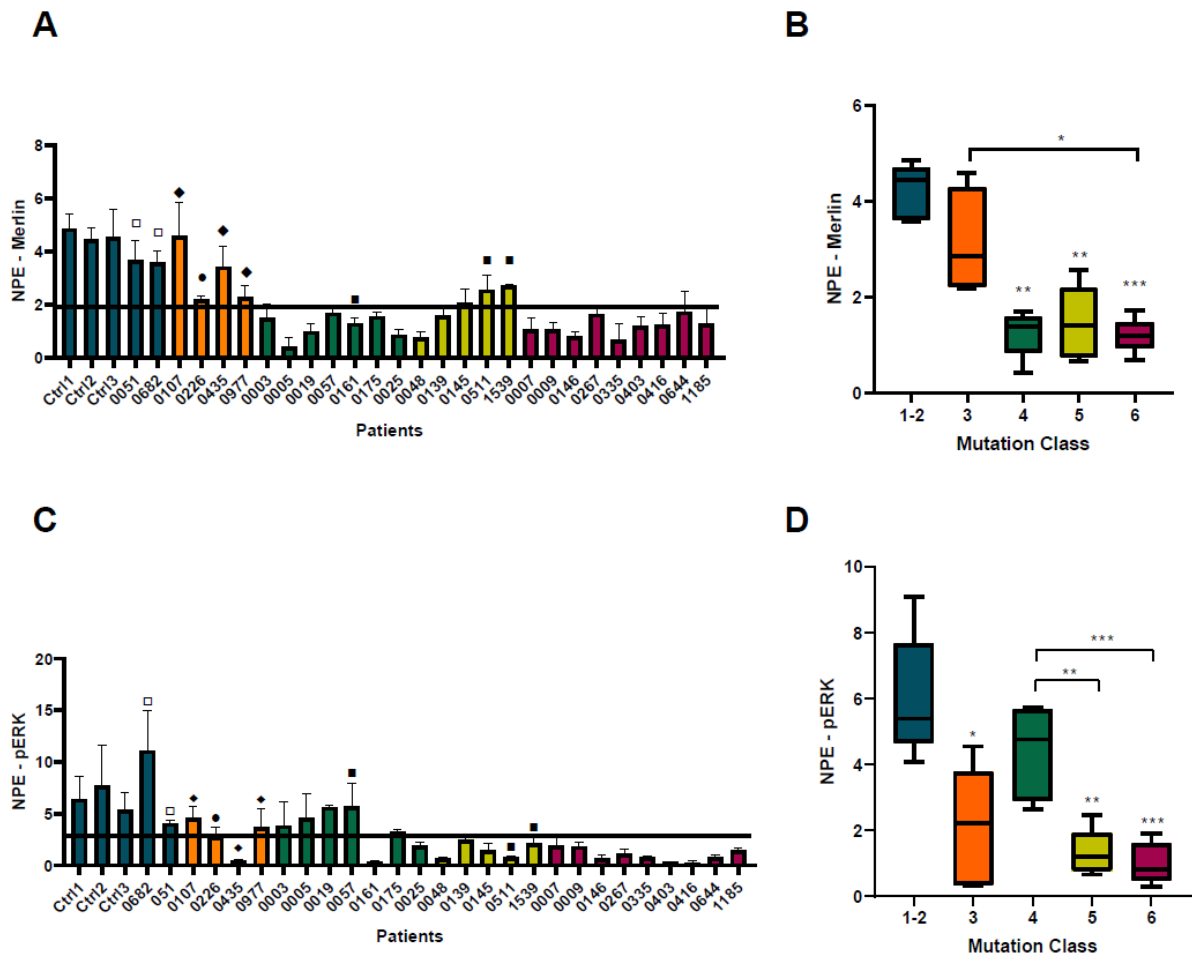
Figure 1.3. Merlin and pERK levels in patient's fibroblasts according to the FGSS. (A) Merlin levels in NF2 patients' fibroblasts. (B) Average of merlin levels according to Mutation Class. (C) pERK levels in NF2 patients' fibroblasts; (D) Average of pERK levels according to Mutation Class. Blue stands for the healthy controls and mutation classes 1 and 2; orange stands for mutation class 3; dark green stands for mutation class 4; light green stands for mutation class 5 and purple stands for mutation class 6. NPE stands for Normalized Protein Expression; Bars represent the SD from three independent experiments; (*p<0.05; **p<0.005; ***p<0.001). Symbol legend: □ presumed mosaicism; ■ generalized mosaicism; ◆ tissue mosaicism; • missense.

In addition, we explored the variability of phenotypical data by principal component analysis (PCA) (**Supplemental Figure S1.3**). The PCA-biplot suggested that patients in the first quadrant mainly had *NF2* mutations of classes 4, 5 and 6; early age at diagnosis and presented extravestibular affection, vestibular and peripheral schwannomas, whereas patients with negative values in the PCA-biplot presented late age at diagnosis and mainly NF2 variants of class 1. To evaluate the tendency observed using the FGSS and taking into account the different number of genetic subcategories between GSS and FGSS, we performed a regression model

(ANOVA) between the quantitative phenotype and *NF2* disease-causing variant class to evaluate quantitatively the NF2 phenotype in base of the *NF2* variant (**Supplemental Table S1.9A**, Shapiro-Wilk p=0.67, Levene test p=0.16). We observed that NF2 phenotype could be explained partially by the *NF2* germline variant, specifically by variants classified as 3 or higher scores (R2=0.38, p=0.0001). Therefore, variants classified as 6 were associated with patients showing the severest phenotypes (phenotype > 8.5), while variants classified as 3 were associated with patients presenting milder phenotypes (phenotype ~7). These results agreed with the observations that some mosaic patients showed a severe phenotype. In this regard, the fact that the *NF2* pathogenic variant could explain no more than 40% of the phenotype, indicated that many other variables could explain the resulting phenotype of the patient. Due to the differences observed in ERK activation, the incorporation of functional data from 27 patients to the statistical model was analysed. Yet, using this sample set, the incorporation of pERK levels into the ANOVA model in addition to *NF2* germline mutation class data did not seem to improve the capacity to explain the NF2 phenotype (p>0.05, **Supplemental Table S1.9**).

In contrast, the regression model between GSS and *NF2* disease-causing variant showed a R^2=0.32 (p=0.001) and was only statistically significant in groups 2B and 3 (**Supplemental Table S1.9B**). Unfortunately, none of these models could explain presumed mosaics or some of the tissue mosaic patients. However, taken overall, these results indicate that FGSS would improve the contribution of the *NF2* variant in predicting the NF2 phenotype and could improve the prognosis prediction capacity of patients with NF2 in comparison with GSS.

4. Discussion

The clinical management of NF2 is complex, it not only requires a specialized multidisciplinary team, but it also presents challenges due to the phenotypic variability found among patients. A huge effort has been made to determine NF2 prognosis markers [7,8] and to establish a good genotype-phenotype relationship in order to be able to predict NF2 prognosis [9–11]. Improvement in determining patient prognosis allows an optimization of the patients' clinical follow-up and ameliorate the genetic counselling offered to affected families.

The UK NF2 Genetic Severity Score (GSS) [12] is an objective tool for predicting the trend of NF2 prognosis based on the patient germline genetic variant type. The application of the GSS in our Spanish cohort confirmed significant differences in several prognostic markers between groups 1 and 3, thus, allowing the GSS validation to determine the prognosis of patients carrying

variants associated with the severest phenotypes. However, in our cohort the GSS had difficulty in classifying patients harbouring variants associated with mild or moderate NF2 phenotypes accurately enough, and neither could it differentiate the mosaic patients amongst them, since not all of this group presented a mild clinical presentation. Certain inconsistencies have been detected, as in the case of four patients from group 2A and one mosaic patient (group 1B), who were clinically diagnosed close to the age of 20 and who have recently developed multiple central nervous system tumours in addition to vestibular schwannomas, three of them before their thirties. These disparities could be due to the cohort size (n=52) or due to a possible bias since the largest number of patients in the cohort belong to the severe phenotype group. In contrast to the UK health system, the Spanish Reference Centre is responsible for the management of NF2 patients in its healthcare region, and patients attending their region centre are generally only referred to the CSUR when their clinical management is complex. Hence, our cohort could be biased due to the low representation of mild phenotypes. In addition, other factors need to be taken into consideration in addition to *NF2* pathogenic variant, as there is a wide range of evidence for heterogeneity in the mild-moderate phenotypes, even in patients harbouring the same *NF2* variant [10,11,14,15,21–23], which was also observed in our statistical model. Although the GSS, is entirely appropriate for establishing general trends, there is scope for improvement by harnessing other types of data to establish a personalized NF2 prognosis score.

Understanding the status of merlin and its regulated pathways might provide data that could help in the interpretation of the NF2 genotype-phenotype relationship. With this aim, a functional assay in patient primary cultured fibroblast was developed. As expected, merlin levels showed significant differences between group 1 (no variant identified in blood), compared with the groups harbouring a constitutional *NF2* genetic variant. Furthermore, no differences were found regardless of the type or the location of variant within the gene. Although evidence in Schwann cells or immortalized tumour cells show the opposite effect, in this study, significantly lower levels of pERK in merlin haploinsufficient primary fibroblasts were observed in comparison with healthy controls and tissue mosaics [26,30–32]. Hence, these results, if validated in other cohorts and in larger sample sizes, would establish that pERK levels in patient fibroblast are associated with severe phenotypes, and thus are susceptible for use as an NF2 prognostic marker.

In this study, we decided to quantify the NF2 phenotype using a ten-scale system based on well-known NF2 prognostic markers [7]. This scale not only allows an easy quantification of the NF2 phenotype, which is held to be more accurate than using a qualitative system (mild-moderate-

severe), but also the quantification of mosaic phenotypes. Additionally, this quantitative method makes it possible to model the NF2 phenotypes according to the *NF2* genetic variant, as has been done in other studies [33–35].

Subsequently, with the aim of improving the NF2 prognostic capacity based on the germline variant, and also to assess if functional data could be incorporated into the UK NF2 GSS, we reviewed the classification of variants proposed by Halliday et al. [12]. Similarly to GSS, we propose that in addition to the predicted mutation effect on merlin function and the functional assays results, the mosaicism extension and the published NF2 genotype-phenotype evidence [9,10,12,14,16] be taken into account. We classified *NF2* genetic variants in six classes, where truncating variants in exons 2-13 were scored 6, missense and in frame deletions as 3, presumed mosaics or patients carrying a Ring22 as 1, while the other type of pathogenic variants were scored in between. The main dissimilarities to GSS are the classification of large deletions and splicing variants, where the position in the *NF2* gene were contemplated differently, because considerable evidence indicates that splicing variants affecting the N-term or C-term of *NF2* gene are associated with both severe and moderate phenotypes respectively [5,7,8,20–22], and variants that do not alter the reading frame have lower scores in comparison as those generating a frameshift alteration, assuming that in-frame alterations could generate a hypomorphic merlin preventing the activation of nonsense-mediated mRNA decay.

Within our cohort, the reviewed GSS, called Functional Genetic Severity Score (FGSS) seems to reduce the intragroup variability, to improve mosaic patient stratification and slightly upgrade the correlation between patient phenotype and the different prognostic parameters analysed in relation to the GSS. Furthermore, the modelling of the NF2 phenotype in terms of the *NF2* mutation classification in our cohort corroborates that *NF2* variants can partially explain patient phenotype therefore, the GSS with this added value could be more precise when determining a prognosis trend in patients with NF2.

Similar to the GSS, FGSS is unable to properly classify presumed and some tissue mosaic patients. Although mosaic patients are generally associated with mild phenotypes, some of these patients show a rather severe phenotype, indicating that the extension of mosaicism should also be considered. Regarding this point, we observed that *NF2* analysis on blood may not represent the degree of affectation, given that in some patients the *NF2* variant was undetectable in blood, but was present in the skin fibroblasts (**Supplemental Figure S1.4**). In addition, it is known that tissue mosaic NF2 patients are at risk of transmitting the disease, even though the variant was not detected in blood [14,16]. These outcomes could indicate that hematopoietic primordial

stem cells harbouring *NF2* mutations may have a selective growth disadvantage over normal stem cells, reducing their representation in this tissue, contrarily to what it has been shown for *NF1* mutations [36,37].

In addition, both GSS and FGSS identify similar levels of merlin and pERK, but using FGSS there is an increased correlation with the NF2 phenotype and a decreased intragroup variability in groups associated with mild phenotypes. However, although pERK levels could represent a potential NF2 prognosis marker, its incorporation into the genetic score does not improve the capacity to explain NF2 phenotype. This could be due to the small sample set included in the model (n=27) or because the contribution of pERK on NF2 phenotype is too low when compared with the contribution of the *NF2* variant in the phenotype description, thus, its addition does not increase the statistical significance of the model. Although discouraging, these results should be tested in larger sets of samples because the inclusion tendency of pERK levels does appear to be a promising approach.

To conclude, with the data obtained from this study, we propose a review of the UK NF2 GSS to continue the advance towards a personalised assessment of NF2 prognosis. This revision considers the type of germline pathogenic variant, the extent of mosaicism, genotype-phenotype evidence and statistically significant correlations already published, and the predicted effect of mutation on the function of merlin and its effect on merlin and pERK activity.

5. Acknowledgements

6. References

1   Evans DG, Bowers NL, Tobi S, *et al.* Schwannomatosis: A genetic and epidemiological study. *Journal of Neurology, Neurosurgery and Psychiatry* Published Online First: 14 June 2018. doi:10.1136/jnnp-2018-318538

2   Evans DGR, Huson SM, Donnai D, *et al.* A genetic study of type 2 neurofibromatosis in the United Kingdom . II . Guidelines for genetic counselling. 1992;:847–52.

3   Ferner RE, Bakker A, Elgersma Y, *et al.* From process to progress—2017 International Conference on Neurofibromatosis 1, Neurofibromatosis 2 and Schwannomatosis. *American Journal of Medical Genetics Part A* 2019;:ajmg.a.61112. doi:10.1002/ajmg.a.61112

4   Lloyd SKW, Evans DGR. *Neurofibromatosis type 2 (NF2): diagnosis and management.* 1st ed. Elsevier B.V. 2013. doi:10.1016/B978-0-444-52902-2.00054-0

5   Plotkin SR, Duda DG, Muzikansky A, *et al.* Multicenter, prospective, phase II and biomarker study of high-dose bevacizumab as induction therapy in patients with neurofibromatosis type 2 and progressive vestibular schwannoma. *Journal of Clinical Oncology* 2019;**37**:3446–54. doi:10.1200/JCO.19.01367

6   Asthagiri AR, Parry DM, Butman JA, *et al.* Neurofibromatosis type 2. *Lancet* 2009;**373**:1974–86. doi:10.1016/S0140-6736(09)60259-2

7   Hexter A, Jones A, Joe H, *et al.* Clinical and molecular predictors of mortality in neurofibromatosis 2: a UK national analysis of 1192 patients. *Journal of Medical Genetics* 2015;**52**:699–705. doi:10.1136/jmedgenet-2015-103290

8   Baser ME, Friedman JM, Aeschliman D, *et al.* Predictors of the Risk of Mortality in Neurofibromatosis 2. 2002.

9   Baser ME, Kuramoto L, Joe H, *et al.* Genotype-Phenotype Correlations for Nervous System Tumors in Neurofibromatosis 2: A Population-Based Study. *The American Journal of Human Genetics* 2004;**75**:231–9. doi:10.1086/422700

10   Kluwe L, MacCollin M, Tatagiba M, *et al.* Phenotypic variability associated with 14 splice-site mutations in the NF2 gene. *American Journal of Medical Genetics* 1998;**77**:228–33. doi:10.1002/(SICI)1096-8628(19980518)77:3<228::AID-AJMG8>3.0.CO;2-L

11   Ruttledge MH, Andermann a a, Phelan CM, *et al.* Type of mutation in the neurofibromatosis type 2 gene (NF2) frequently determines severity of disease. *American Journal of Human Genetics* 1996;**59**:331–42.

12   Halliday D, Emmanouil B, Pretorius P, *et al.* Genetic severity score predicts clinical phenotype in NF2. *Journal of Medical Genetics* 2017;**54**:657–64. doi:10.1136/jmedgenet-2017-104519

13   Halliday D, Emmanouil B, Vassallo G, *et al.* Trends in phenotype in the English paediatric neurofibromatosis type 2 cohort stratified by genetic severity. *Clinical Genetics* 2019;**96**:151–62. doi:10.1111/cge.13551

14   Gareth Evans D, Hartley CL, Smith PT, *et al.* Incidence of mosaicism in 1055 de novo NF2 cases: much higher than previous estimates with high utility of next-generation sequencing. Published Online First: 2020. doi:10.1038/s41436

15   Kluwe L, Mautner V-F. Mosaicism in sporadic neurofibromatosis 2 patients. 1998.

16   Evans DG, Raymond FL, Barwell JG, *et al.* Genetic testing and screening of individuals at risk of NF2. *Clinical Genetics* 2012;**82**:416–24. doi:10.1111/j.1399-0004.2011.01816.x

17   Hagel C, Lindenau M, Lamszus K, *et al.* Polyneuropathy in neurofibromatosis 2: Clinical findings, molecular genetics and neuropathological alterations in sural nerve biopsy specimens. *Acta Neuropathologica* 2002;**104**:179–87. doi:10.1007/s00401-002-0535-7

18   Otsuka G, Saito K, Nagatani T, *et al.* Age at symptom onset and long-term survival in patients with neurofibromatosis Type 2. *Journal of Neurosurgery* 2003;**99**:480–3. doi:10.3171/jns.2003.99.3.0480

19   Baser ME, Makariou E v., Parry DM. Predictors of vestibular schwannoma growth in patients with neurofibromatosis Type 2. *Journal of Neurosurgery* 2002;**96**:217–22. doi:10.3171/jns.2002.96.2.0217

20   Kluwe L, Mautner VF. A missense mutation in the NF2 gene results in moderate and mild clinical phenotypes of neurofibromatosis type 2. *Human Genetics* 1996;**97**:224–7. doi:10.1007/BF02265270

21   Heineman TE, Evans DGR, Campagne F, *et al.* In Silico Analysis of NF2 Gene Missense Mutations in Neurofibromatosis Type 2 : From Genotype to Phenotype. 2015;:908–14.

22   Mautner VF, Baser ME, Kluwe L. Phenotypic variability in two families with novel splice-site and frameshift NF2 mutations. *Human Genetics* 1996;**98**:203–6. doi:10.1007/s004390050191

23   Castellanos E, Rosas I, Solanes A, *et al.* In vitro antisense therapeutics for a deep intronic mutation causing Neurofibromatosis type 2. *European Journal of Human Genetics* 2013;**21**:769–73. doi:10.1038/ejhg.2012.261

24   Baser ME, Kuramoto L, Woods R, *et al.* The location of constitutional neurofibromatosis 2 (NF2) splice site mutations is associated with the severity of NF2. Journal of Medical Genetics. 2005;**42**:540–6. doi:10.1136/jmg.2004.029504

25   Li W, Cooper J, Karajannis MA, *et al.* Merlin: A tumour suppressor with functions at the cell cortex and in the nucleus. *EMBO Reports* 2012;**13**:204–15. doi:10.1038/embor.2012.11

26   Petrilli AM, Fernández-Valle C. Role of Merlin/NF2 inactivation in tumor biology. *Oncogene* 2015;**35**:537–48. doi:10.1038/onc.2015.125

27   Cooper J, Giancotti FG. Molecular insights into NF2/Merlin tumor suppressor function. *FEBS Letters* 2014;**588**:2743–52. doi:10.1016/j.febslet.2014.04.001

28   Baser ME, Friedman JM, Wallace AJ, *et al.* Evaluation of clinical diagnostic criteria for neurofibromatosis 2. *Neurology* 2002;**59**:1759–65. doi:10.1212/01.WNL.0000035638.74084.F4

29   Castellanos E, Gel B, Rosas I, *et al.* A comprehensive custom panel design for routine hereditary cancer testing : preserving control , improving diagnostics and revealing a complex variation landscape. *Nature Publishing Group* 2017;:1–12. doi:10.1038/srep39348

30   Cui Y, Groth S, Troutman S, *et al.* The NF2 tumor suppressor merlin interacts with Ras and RasGAP, which may modulate Ras signaling. *Oncogene* 2019;**38**:6370–81. doi:10.1038/s41388-019-0883-6

31   Morrison H, Sperka T, Manent J, *et al.* Merlin / Neurofibromatosis Type 2 Suppresses Growth by Inhibiting the Activation of Ras and Rac. 2007;:520–8. doi:10.1158/0008-5472.CAN-06-1608

32   Hilton DA, Ristic N, Hanemann CO. Activation of ERK, AKT and JNK signalling pathways in human schwannomas *in situ*. *Histopathology* 2009;**55**:744–9. doi:10.1111/j.1365-2559.2009.03440.x

33   Painter SL, Sipkova Z, Emmanouil B, *et al.* Neurofibromatosis Type 2-Related Eye Disease Correlated With Genetic Severity Type. *Journal of Neuro-Ophthalmology* 2019;**39**:44–9. doi:10.1097/WNO.0000000000000675

34   Emmanouil B, Houston R, May A, *et al.* Progression of hearing loss in neurofibromatosis type 2 according to genetic severity. *Laryngoscope* 2019;**129**:974–80. doi:10.1002/lary.27586

35   Abi Jaoude S, Peyre M, Degos V, *et al.* Validation of a scoring system to evaluate the risk of rapid growth of intracranial meningiomas in neurofibromatosis type 2 patients. *Journal of Neurosurgery* 2020;:1–9. doi:10.3171/2020.3.jns192382

36   Roehl AC, Mussotter T, Cooper DN, *et al.* Tissue-Specific Differences in the Proportion of Mosaic Large NF1 Deletions are Suggestive of a Selective Growth Advantage of Hematopoietic del (+/−) Stem Cells. 2011;:1–10. doi:10.1002/humu.22013

37   Fernández-Rodríguez J, Castellsagué J, Benito L, *et al.* A mild neurofibromatosis type 1 phenotype produced by the combination of the benign nature of a leaky NF1-splice mutation and the presence of a complex mosaicism. *Human Mutation* 2011;**32**:705–9. doi:10.1002/humu.21500

7. Supplemental Material and Methods

NF2 diagnosis and clinical data collection

Patients included in the study are clinically followed-up in the NF2 Spanish reference centre. Our multidisciplinary team consists of physicians with different specialties responsible for NF2 patients' follow-up in their area of expertise (Neurologists, Neurosurgeons, Otolaryngologists, Dermatologists, Paediatricians, Oncologists, Clinical Geneticist, Genetic Counselling, Radiotherapists, Radiologists, etc.). Neurofibromatosis and Schwannomatosis (probable) patients are followed-up yearly by all clinical specialists required and when the patient informs of new symptomatology or clinical problem. Records from patient's follow-up were reviewed according to five domains: patient demographics, tumour load, ocular features, hearing capacity and major interventions. All clinical data collected was from the last clinical patient assessment. Patients included met the Manchester NF2 diagnostic criteria [28]. The age at diagnosis also includes patients that were detected asymptomatically on scan although most of them were symptomatic.

Tumour burden was determined by reviews of gadolinium-enhanced brain and spine MRI scans performed. In case of NF2 patients, a brain and spine MRI scan is usually offered once the patient is clinically diagnosed and afterwards, a yearly brain scan is performed. In addition, a spine or whole-body scan is offered if the patient needs tumour growth follow-up or shows new symptomatology related to the development or growth of a tumour. Type of lesions was determined taking into account the most likely lesion radiologically although histological diagnosis was used when available. **Hearing** was evaluated at every appointment using speech audiometry and pure tone audiometry. **Hearing grade** was classified on a score of 1-6 according to Halliday et al. Grades 1, 2, 3-4 represents those patients with an optimum **Speech Discrimination Score** (SDS) in the better hearing ear of >70%, 50%–70% and below 50%, respectively. Patients with hearing implant are classified as grade 5 and those with bilaterally dead ears as grade 6. **Hearing loss** was defined as the age of loss of useful hearing which it was described by Halliday et al. as hearing grade 3 or worse.

The clinical assessment of **cutaneous abnormalities** consisted of examination for CAL spots as well as the type, location and number of dermal tumours clinically suggestive of cutaneous schwannomas. However, for this study only the number of patients that present tumours suggestive of cutaneous schwannomas, most of them confirmed by a histopathological analysis are considered. Tumour histopathological features were classified using the World Health Organization criteria for central nervous system and soft tissue tumours. Schwannomas were defined as encapsulated tumours composed of spindle-shaped neoplastic Schwann cells. The study was based on haematoxylin and eosin–stained slides and the immunocytochemical analysis of S100B and MelanA.

The **number and type of major interventions** for each patient was also collected. The indication of intervention is decided by the multidisciplinary team committee, taking into account patient's symptomatology, tumour location and growth rate. In the case of vestibular schwannomas, the hearing grade of the affected ear and the contralateral one is considered.

Genetic *NF2* test

Genetic test was performed using the customized I2HCP panel [29] in blood or tissue when available and validated by Sanger sequencing in all primary cultures established. In mosaic patients, a deep sequencing with a >700 depth of coverage was performed in primary culture fibroblasts. Only variants detected above 5% of the cells were considered.

Functional assay, Western Blot analysis

Merlin's downstream pathways were analysed in 27 out of 30 NF2 patients included in the validation of the Genetic Severity Score. We obtained cultured fibroblasts from skin biopsies that were processes as described in Castellanos et al., 2013 [23]. 50 µg of protein extracted from these primary cultures at 50%, 80% and 100% of confluence was load to SDS-PAGE (150V) and transferred onto PVDF membranes (1 hour 350 mA at 4°C). Odyssey Blocking Buffer TBS (LI-COR) was used to block the resulting membranes. Three primary cultures from healthy donors were included as control samples (Ctrl1, Ctrl2 and Ctrl3). When grouping for the statistical studies, the control healthy donors and the mosaics as a control group were been taken into account, since none of these show the constitutional *NF2* mutation in the analysed tissue. Primary antibodies were incubated at 4°C overnight. Membranes were later incubated with IRDye 680LT and IRDye 800CW secondary antibodies (1:1000 dilution, LI-COR) for 1h at room temperature and scanned and analysed using the Odyssey Infrared Imaging System (LI-COR). The statistical threshold that allows the differentiation between healthy controls or mosaic patients and the patients in group 3 (severe) is established through the ±2SD limits method. **Primary antibodies: α-pERK**:

phospho-p44/42; APK (Erk1/2) (Thr202/Tyr204) (E10) #9106 α-mouse (Cell Signaling Technology), **α-ERK**: p44/42; APK (Erk1/2) Antibody #9102 – α – rabbit (Cell Signaling Technology, **α-pAKT:** Phospho Akt (Ser 473) (587F11) Mouse ab #4051 α-mouse (Cell Signaling Technology), **α-AKT** Akt Antibody #9272– α –rabbit (Cell Signaling Technology, **α-pNF2:** Phospho NF2/Merlin (phospho S518) antibody (ab131473) α-rabbit (Abcam), **α-NF2:** NF2/Merlin antibody (ab88957) α-mouse (Abcam), **α -PAK1:** Anti-PAK1 antibody (ab154284) α-rabbit (Abcam), **α -RAC1:** Anti-RAC1 antibody (ab33186) α-mouse (Abcam), **α-pYAP1**: anti-YAP1 (phospho S127) antibody [EP1675Y] (ab76252) – α – rabbit (Abcam), **α-YAP1**: anti-YAP1 antibody (ab56701) – α – mouse (Abcam), **α-pPKA:** Phospho PKA. Anti PKA alpha+beta (phospho T197) antibody (ab5815) – α – rabbit (Abcam), **α-PKA:** PKA C alpha beta antibody Clone #515741 (MAB5908) – α – mouse (Abcam). **α-vinculin:** anti-vinculin antibody [EPR8185] (ab129002) – α – rabbit (Abcam) was used to normalize protein expression among samples

NF2 phenotype quantification

Clinical phenotype was recorded as follows: age of diagnosis was rated as 3 if it was below 25, 2 between 25 and 35 and 1 if patient was diagnosed after the age of 35; the presence of peripheral and vestibular schwannomas were scored as 0, 1 or 2 if they were absent, unique or multiple, while extravestibular lesions were scored between 1 if we detected single intracranial or intra-spinal lesion, 2 if the patients showed multiple intracranial or intra-spinal schwannomas or meningiomas, or 3 when patient developed multiple intra-spinal or intracerebral different lesion types or multiple intra-spinal and intracerebral schwannomas or meningiomas (**Supplemental Table S1.3**).

NF2 pathogenic variant score

Truncating mutations in exons 2-13 were scored 6, missense and in frame deletions as 3, presumed mosaics or patients carrying a Ring22 as 1. Based on [7,10,14], the predicted effect of *NF2* mutation on the function of merlin, our observations on the phenotype shown by patients harbouring mutations in the most terminal region of the gene and the results from the pERK functional analysis, we decided to rate differently when mutations are located in first exons, as merlin could start its translation using another methionine, or if the variant does not alter *NF2* reading frame because some merlin residual function could be maintained. In addition, when the variant affects exon 14 or the followings due to its association to good prognosis was also considered [7,8]. In addition, in the absence of more evidence, we scored all missense variants as 3, since in our functional assays and as published before [21], missense mutations result in the quantitative loss of merlin protein, and we assume they might minimally affect the intrinsic

protein function unless when altering specific positions, which would be rated differently once the association to a severe phenotype is demonstrated. In contrast to GSS, we scored those splicing and copy number alterations (CNA) at exon level that do not alter the reading frame as less severe, in comparison to those generating a frameshift alteration assuming that in frame alterations could generate an hypomorphic merlin, although we do not consider them different when variants are located at exons 1-7 or 8-13. We also scored generalized mosaicism, if *NF2* variant was detected in blood or unaffected tissue, differently from tissue mosaicism if it was detected only in two independent tumours, since the degree of affectation could be different. Finally, patients with an inconclusive blood test without any tumour analysed were considered presumed tissue mosaics and scored as 1 (**Table 1.3**).

Statistics

All statistical analyses of the validation of the GSS were reproduced from the study of Halliday et al. In brief, an NF2 Genetic Severity Score (GSS) was determined based on the phenotype of patients. Genetic Severity Score consists of a 3-point classification into tissue mosaicism, classic and severe disease. χ2 statistics were used to compare the distribution of GSS by gender and NF2-related deaths (sporadic or familial). Trends with genetic severity were investigated using Mantel-Haenszel linear-by-linear χ2 tests of association for tumour load, ocular features, hearing outcomes and major interventions of the patients. Spearman's rank-order correlations were run to assess the relationship between age of patients, eye features, number of interventions, ratio of interventions to age and genetic severity. In our study, minor variations were applied in comparison to Halliday et al. and quality of life was not considered. Principal component analysis (PCA) of age at diagnosis, extravestibular affection, vestibular and peripheral schwannomas was performed to explore variability of NF2 type mutations of patients.

In our study, minor variations were applied. Mutation data, tumour load, ocular features, hearing outcomes and major interventions of the patients were defined as categorical variables. Quality of life was not considered in our study. Principal component analysis (PCA) of age at diagnosis, extravestibular affection, vestibular and peripheral schwannomas was performed to explore variability of NF2 type mutations of patients.

In order to study differences between protein expression levels in the functional assay, Kruskal-Wallis and Mann-Whitney U statistical tests were performed among genetic severity groups and mutation classes. Fibroblast protein levels from healthy controls have been included in group 1 for the statistics analysis. Analysis of variance (ANOVA) of FGSS and *NF2* mutations was

performed to test differences of severity between *NF2* mutations groups. Shapiro Wilk and Levene tests were applied for testing Normality of residuals and homoscedasticity of groups respectively. Backward stepwise regression analysis was performed to evaluate the contribution of merlin and pERK levels in the ANOVA model. Statistical analyses were performed using R software.

Chapter 2

Antisense oligonucleotides targeting exon 11 are able to partially rescue the Neurofibromatosis Type 2 phenotype *in vitro*

This chapter presents the evaluation of the use of antisense therapeutic strategies *in vitro* for the purpose of advancing in the development of personalized therapies for NF2 patients. First, we present an approach to target splice site variants affecting the *NF2* gene, using antisense oligonucleotides to correct the aberrant splice patterns and restore merlin protein levels. The second proposed approach addresses truncating variants in *NF2* with the aim of reducing the pathogenicity of their effect.

Supplemental figures and tables are available at the end of the chapter.

Abstract

Neurofibromatosis type 2 (NF2) is an autosomal dominant condition characterized by the development of multiple tumours of the nervous system caused by loss of function variants in the *NF2* gene. The clinical presentation of the disease is variable and related to the type of the inherited constitutional mutation. Here, we evaluated the use of antisense oligonucleotides, specifically phosphorodiamidate morpholino oligomers (PMOs), to reduce the severity of the effects of *NF2* truncating variants by converting them to milder hypomorphic forms *in vitro*. Our results showed that the PMOs designed for variants located at +/- 13 from the intron-exon boundary region interfered with the correct splicing signalling of both *NF2* wild-type and mutated alleles. On the other hand, we were able to specifically induce the skipping of exons 4, 8 and 11 of both the mutated and the WT allele maintaining the *NF2* gene reading frame at cDNA level. Only the skipping of exon 11 produced a hypomorphic merlin (merlin-e11) able to partially rescue the phenotype observed in primary fibroblast cultures from NF2 patients harbouring a germline loss of function variant. This encouraging result is an *in vitro* proof of concept of the use of antisense therapy to develop personalized therapies for NF2.

1. Introduction

Neurofibromatosis type 2 (NF2) (OMIM 101000) is an autosomal dominant (AD) disease caused by loss-of-function (LOF) variants in the *NF2* tumour suppressor gene (22q12.2) [1,2]. The reported incidence is between 1 in 28,000-40,000 [3] and the hallmark of the disease is the presence of bilateral vestibular schwannomas (BVS) which clinically present with hearing loss, tinnitus and imbalance [4]. Common features of NF2 include cranial, spinal, peripheral nerve, and intradermal schwannomas; cranial and spinal meningiomas; and intrinsic central nervous system (CNS) tumours, usually spinal ependymomas [5,6]. Despite their benign nature, tumours are associated with high morbidity due to their multiplicity and anatomical location, which cause pain and nerve dysfunction leading to a reduced quality of life and life expectancy [7].

There are limited therapies available for these patients and radiotherapy and surgery for tumour resection are the classical treatments [8]. Currently, medical therapy is also an option since Bevacizumab, an anti-angiogenic monoclonal antibody, has been demonstrated to be an effective treatment for vestibular schwannomas (VS) inducing the reduction of tumour growth and an improvement in hearing in adult NF2 patients [6,9]. However, Bevacizumab does not seem to be equally effective in all NF2 patients and, in addition, it has no effect on other types of tumours present due to the disease, such as meningiomas [10]. Efforts have been made to develop other therapies for NF2-related tumours, such as Losartan (antihypertensive), Lapatinib (tyrosine kinase inhibitor) or AR-42 (Histone deacetylase (HDAC) inhibitor) [11–14], but there still remains a need to identify clinically relevant therapeutic targets to treat NF2 patients.

The *NF2* gene consists of 17 exons [15,16] with a wide mutational spectrum, 85-90% are germline point mutations and 10-15% are large deletions distributed throughout the entire gene [17,18]. *NF2* encodes for merlin (Moesin-Ezrin-Radixin-Like protein), a 595aa scaffold protein involved in membrane protein organization, regulation of cell-cell adhesion and with a regulatory role in the cytoskeleton architecture [19,20]. Merlin is comprised of three structural regions: a N-terminal FERM domain which is subdivided into three globular domains (F1, F2 and F3), an α-helical coiled-coil domain and a C-terminal hydrophilic tail [21].

The genotype-phenotype correlation of NF2 has long been studied [22–30]. For NF2, it is well reported that nonsense variants and large deletions, which account for around 30% of cases, are associated with severe manifestations of the disease, whereas missense, or in-frame variants present a milder form of NF2. Besides, about 25% of the point mutations affect the correct splicing of the *NF2* gene, and this mechanism is associated with a variable severity of the disease

[27,29,31]. The well-known association between the genetic variant type and disease severity may constitute an opportunity to develop personalized gene therapies based on the specific variant of the *NF2* gene.

Antisense gene therapy has been successfully used to regulate gene expression in some pathologies. Most of the target diseases are inherited in an autosomal recessive manner, such as Spinal Muscular Atrophy (SMA) [32], homozygous familial hypercholesterolemia (HoFH) [33], or Duchenne muscular dystrophy (DMD) [34] the latter two have been approved by the FDA and are amongst others currently in the advanced stages of clinical trials, [35,36]. Furthermore, there are also examples for AD diseases, such as Retinitis pigmentosa (RP) [37], amyotrophic lateral sclerosis [38] or Huntington's disease [39]. In all cases, antisense oligonucleotides (ASOs) have been used. These are single-stranded modified DNA-like molecules of 15 to 30 nucleotides that act at RNA level by specifically correcting or changing the expression of the target protein to a less deleterious form [40,41]. ASOs have been therapeutically used to reduce protein production whether via RNase H cleavage or mRNA-ASO complex to block mRNA-ribosome interaction. It is also possible to modulate the splice signalling and among the different types of ASOs, Phosphorodiamidate Morpholino Oligomers (PMOs) have highly desirable molecular properties that make them suitable for this last approach. In PMOs the deoxyribose sugar element is replaced by a six-member morpholino ring, and the phosphodiester inter-subunit bonds are replaced by phosphorodiamidate linkages; all of which produce a structure that provides high-targeting specificity, stability, low toxicity and resistance to nucleases, assuring the maintenance of a good long-term activity within the cell [42].

In this study we assessed two different approaches to test *in vitro* antisense therapy for NF2: the first consisted of modulating and correcting the aberrant splicing of the *NF2* gene originating from different point-mutations located near the canonical splice site; the second consisted of forcing the skipping of those exons that carry a frameshift or a nonsense variant, while preserving the reading frame. Thus, taking into consideration the NF2 genotype-phenotype association, nonsense variants that generate a more severe phenotype could be altered at RNA level to generate less deleterious protein forms.

2. Materials and Methods

All procedures performed were in accordance with the ethical standards of the IGTP Institutional Review Board, which approved this study and with the 1964 Helsinki declaration and its later amendments.

Samples

Samples from 14 NF2 patients from the Spanish Reference Centre were included in the study (**Supplemental Table S2.1**) after providing written informed consent. Samples included in the study were those harbouring a splicing variant or a truncating variant in an in-frame exon of *NF2*.

Genetic *NF2* test

Genetic testing was performed using the customized I2HCP panel [43] in blood or tissue when available. To detect *NF2* splicing variants, patients were studied both at RNA and DNA levels. Variants were validated by Sanger sequencing and analysed using CLC-workbench (Qiagen, Hilden, Germany) in all primary cultures established.

Variant analysis

Human Genome Variation Society (www.hgvs.org) nomenclature guidelines were used to name the mutation at the DNA level, its effect at the mRNA level, and the predicted resulting protein. The first nucleotide of the ATG translation initiation codon is denoted position þ1 according to the *NF2* mRNA sequence NM_000268.3 5. and NM_016418.

Primary cell culture

For fibroblast isolation, a skin punch was disaggregated into small pieces and digested with 160U/ml collagenase type 1 (Worthington, Lakewood, NJ, USA) and 0.8U/ml dispase grade 1 (Worthington). Fibroblast were grown in Dulbecco's modified Eagle's medium (DMEM; PAA), 10% fetal bovine serum (FBS; Gibco, Paisley, UK), 500U/ml penicillin and 500mg/mL streptomycin antibiotics (Gibco, Paisley, UK) at 37ºC and 5% CO_2.

DNA and RNA preparation and RT-PCR

Total DNA from peripheral blood was extracted using Flexigene DNA KIT (Qiagen, Hilden, Germany) and DNA from patient-derived cultured fibroblasts was extracted using Maxwell® 16 Cell DNA purification kit according to manufacturer's instructions. For RNA isolation, fibroblasts were treated with 250mg/ml puromycin (Sigma-Aldrich, St Louis, MO, USA) 4–6 h to circumvent the nonsense-mediated decay (NMD) mechanism and extracted using 16 LEV simplyRNA

Purification Kit, from Maxwell technology (Promega, Madison, Wisconsin, USA). Total RNA was reverse-transcribed using SuperScript III reverse transcriptase (Invitrogen, Paisley, UK) and random hexamers (Invitrogen).

Antisense molecules treatment conditions

In order to test the PMO treatment, cells were seeded at $3 \cdot 10^5$ cells in a six-well plate. 24h later, culture medium was replaced with fresh medium containing the indicated concentration of PMOs (see Results section) plus 6mM of Endo-Porter. PMO reported in Castellanos et al. 2013 was used as an experimental control (PMO_Ctrl). Each experiment was performed in triplicate.

Antisense specificity and efficacy

25-mer specific Phosphorodiamidate Morpholino Oligomers (PMOs) for four patients with splicing variants, and a pair of PMOs to induce exon skipping of exons 4, 8, and 11 of the *NF2* gene were designed, synthesized and purified by Gene Tools (Philomath, OR, USA). Endo-Porter (Gene Tools) was used as vehicle to deliver PMOs into cells, according to the manufacturer's instructions. Patient primary fibroblasts carrying *NF2* germline pathogenic variants were treated with the specific single or paired PMOs. A dose-response and a time course study were performed to set-up treatment conditions and the effect of PMOs was assessed by RT-PCR and Sanger sequencing. Levels of merlin after PMO treatment were analysed by Western Blot. For all experiments, the correct effect of the treatment at RNA level was confirmed prior to Western Blot analysis.

Western Blotting

Cells were lysed with RIPA buffer (50 mM Tris-HCl (pH 7.4), 150 mM NaCl, 1mM EDTA, 0.5% Igepal CA-630) supplemented with 3mM DTT (Roche, Mannheim, Germany), 1mM PMSF (Thermofisher, Waltham, Massachusetts, USA), 1mM sodium orthovanadate (Sigma-Aldrich), 5mM NaF (Thermofisher), 10 ug/ml leupeptin (Sigma-Aldrich), 5ug/ml aprotinin (Sigma-Aldrich) and 1xPhosSTOP (Roche). 50 µg of protein extracted from primary cultures was loaded to SDS-PAGE (150V) and transferred onto PVDF membranes (1 hour 350 mA at 4°C). Odyssey Blocking Buffer TBS (LI-COR, Lincoln, Nebraska, USA) was used to block the membranes. Primary antibodies were incubated at 4°C overnight. Membranes were later incubated with IRDye 680LT and IRDye 800CW secondary antibodies (1:1000 dilution, LI-COR) for 1h at room temperature and scanned and analysed using the Odyssey Infrared Imaging System (LI-COR). **Western Blot Primary antibodies:** α-NF2: NF2/Merlin antibody (ab88957) α-mouse (Abcam). α-vinculin: anti-vinculin antibody [EPR8185] (ab129002) – α – rabbit (Abcam) was used to normalize protein expression among samples.

NF2 Cloning and expression

NF2 gene was cloned using the Gateway® Gene Cloning system (Invitrogen) after treatment to induce the exon-skipping to a FLAG® Tag Expression Vector. The expression vector was transfected into HeLa cells (Lipofectamine LTX with Plus Reagent, Invitrogen) according to the manufacturer's instructions. Flag expression was assessed by Western Blot (Monoclonal ANTI-FLAG® M2 antibody, Sigma-Aldrich).

Immunofluorescence

Cells were fixed in 4% para-formaldehyde in PBS for 15 min at RT, permeabilized with 0.1%Triton-X 100 in PBS for 10 min at RT, blocked in 10% FBS in PBS for 15 min at RT and stained Alexa Fluor 594 Phalloidin (Molecular Probes, Invitrogen). Nuclei were stained with DAPI and images captured using LEICA DMIL6000 and LASAF software.

Cell proliferation

Cell proliferation was determined using the Click-iT™ EdU Alexa Fluor™ 488 Flow Cytometry Assay Kit (Molecular Probes, Invitrogen) according to the manufacturer's protocol and DNA content was studied with DAPI. $1 \cdot 10^5$ cells were seeded in a six-well plate, treated 24h later with the corresponding concentration of PMO. 48h after treatment, 5uM of EdU was added to the cell culture media and incubated for 24h. After 72h of PMO treatment and 24h of EdU incubation, cells were recollected, proceeding according to the manufacturer's instructions and analysed by FACS. Data was analysed using an BD FACSCanto™ and BD FACSDiva 6.2 software.

Cell viability

Cell viability was assessed using RealTime-Glo™ MT Cell Viability Assay (Promega) according to the manufacturer's instructions. 500 cells were seeded in a ninety-six well plate, treated 24h later with the corresponding concentration of PMO and analysed at 24h, 48h and 72h after treatment using Flash Thermo Scientific Varioskan® (Thermofisher).

Statistics

Statistical analysis was carried out using GraphPad Prism software v7. The Shapiro–Wilk test was used to test normality and for multiple group comparisons, a two-tailed unpaired t test was performed. Statistical significance is indicated by *p<0.05, **p<0.01, and ***p<0.001.

3. Results

Antisense therapy for *NF2* splicing variants

The experimental approach for *NF2* splicing variants consisted of designing specific PMOs for each variant to be tested in order to mask the aberrant splice signalling triggered by the pathogenic variant and promote the spliceosome to properly recognize the correct splice site without altering the wild type (WT) allele (**Figure 2.1**).
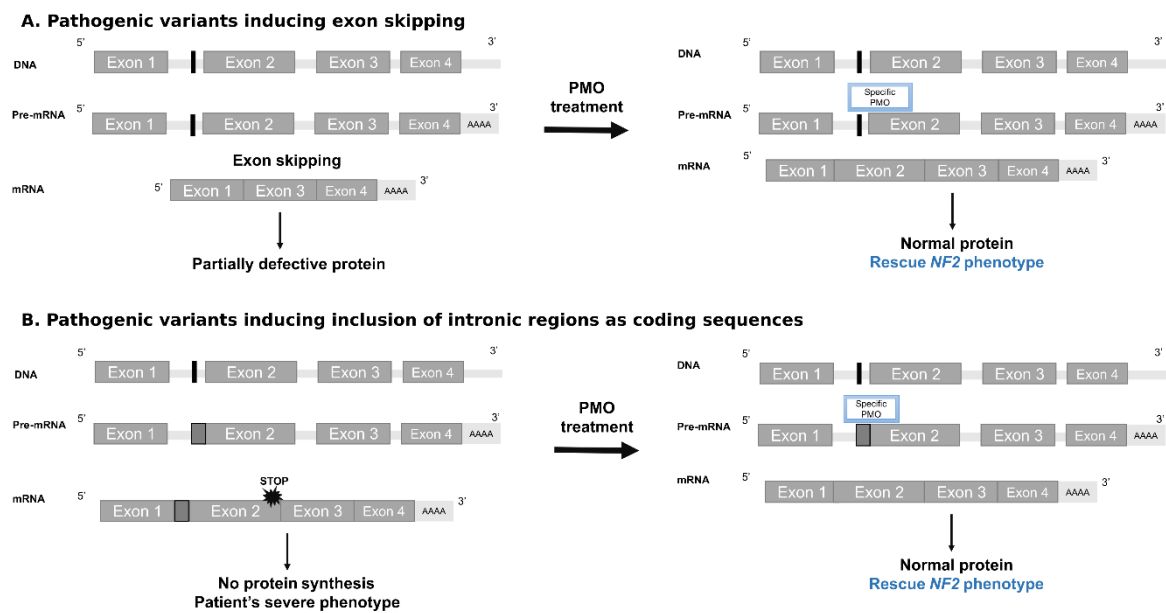
Figure 2.1. Experimental approach to test antisense therapy for splicing *NF2* variants. In blue, expected outcome after PMO treatment. **(A)** Experimental design for splicing variants that induce exon skipping and result in a truncating protein. **(B)** Experimental design for variants inducing the inclusion of intronic regions as coding sequences, resulting in alterations in the gene reading frame that finally generate a truncating protein. In both approaches, the PMO is expected to mask the aberrant splicing signal and rescue the NF2 phenotype in vitro.

Two different PMOs were designed for each variant. The first design was a 25-mer variant-specific facilitated by Gene Tools according to their guidelines for intron and exon binding subunits and self-complementary moieties. We made a second design using splice site predictors to study the variant surrounding sequence (acceptor splicing sites, exonic splicing enhancers (ESEs) or exonic splicing silencers (ESSs)) (Human Splice Finder) in order to avoid the induction of possible new splicing signals due to the effect of the PMO. In addition, the design avoided masking the canonical splicing GT-AG sites and branch points (YNYYRAY) when possible (**Table 2.1, Figure 2.2A**).

We tested the PMOs' efficacy in primary fibroblasts from NF2 patients harbouring heterozygous germline variants located near the canonical splice site of exons 3, 8 and 15 (**Supplemental Table S2.1**) from the Spanish National Reference Centre (CSUR) on Phacomatoses. A dose-response study was performed to test the effect on splicing of different concentrations of PMOs after 24h of treatment and the efficiency was assessed at cDNA level by RT-PCR. The effect of PMOs on the splicing of *NF2* was analysed by electrophoresis and confirmed by Sanger sequencing, revealing a maximum effect at 20µM. A time course was carried out treating fibroblasts with 20µM PMO during 24h, 48h and 72h. PMO treatment in Patient_Spl_1 and Patient_Spl_2 increased the skipping of exons 15 and 8 respectively in both of the designs, in contrast to the expected effect of blocking only the germline variant and restoring the NF2 correct splicing without altering the transcription of the WT allele (**Figure 2.2B, B.I and B.II**). Similarly, the treatment of PMOs of patients Patient_Spl_3 and Patient_Spl_4, both with nearby variants near the canonical splice site of exon 2, revealed that the variant-specific PMO caused the skipping of both exons 2 and 3 of the NF2 gene instead of correcting the aberrant NF2 splicing due to germline variants (**Figure 2.2B, B.III and B.IV**). The same effect was observed with the two different designs and the effect was confirmed by Sanger sequencing (**Supplemental Table S2.1**). Fibroblasts from healthy donors (FibCtrl) were also treated with each designed variant-specific PMO and they showed the same effect as fibroblasts derived from patients. The effect of the treatment on merlin was assayed by Western Blot and no improvement in merlin levels was detected after the treatment at the studied time points (**Supplemental Figure S2.2**).
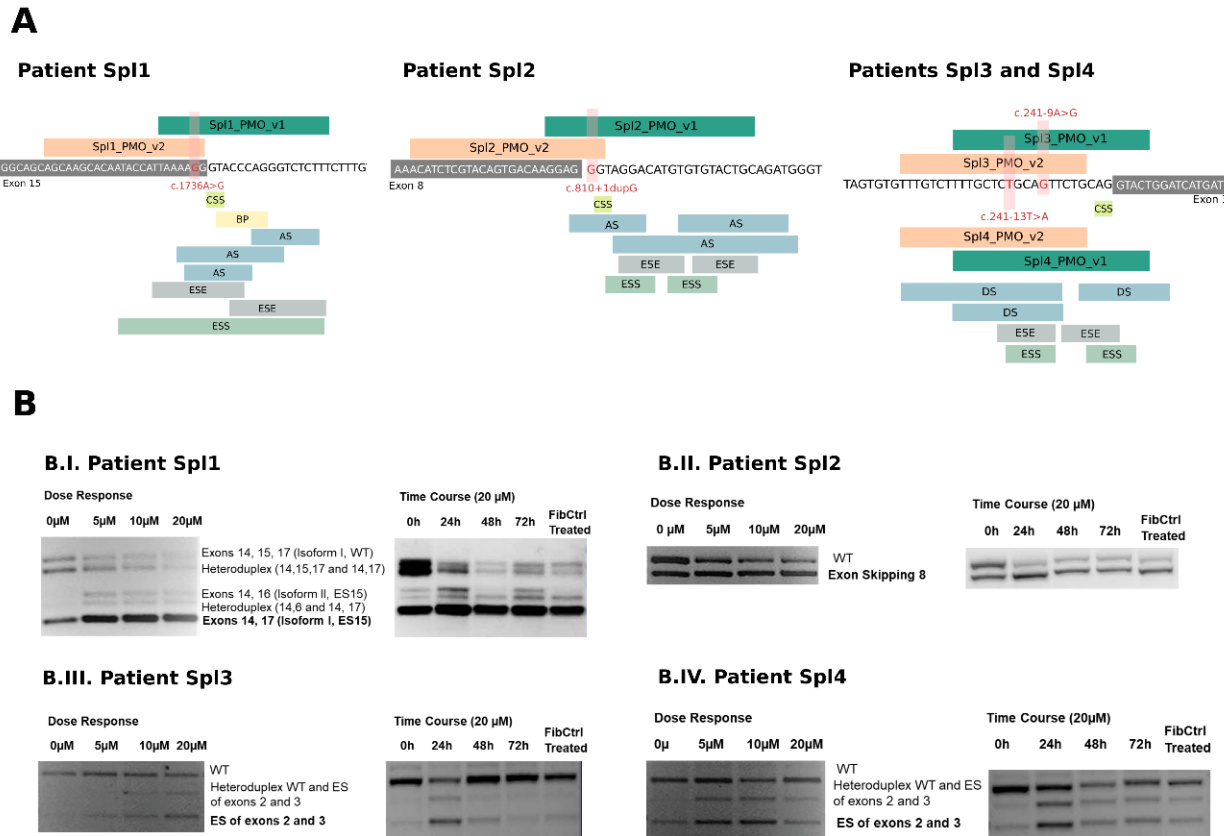
Figure 2.2. (A) Design of the PMO specific for each variant. For the second design (v2), Canonical Splice Sites (CSS), Branch Points (BR), Acceptor and Donor Sites (AS and DS), Exonic Splicing Enhancer sequences (ESE) and Exonic Splicing Silencer (ESS) sequences indicated were taken into account and excluded, when possible, for the sequence design in order to avoid masking the correct splicing signals. The exonic part of the sequence is shown in a grey box and the unlabelled part constitute intronic regions. Tested genetic variants are highlighted in red. **(B) The use of variant-specific PMO did not allow correction of the aberrant splicing signalling.** The effect of the PMOs is shown at cDNA level through dose response and time course experiments. As the same effect was observed in both of the PMO designs (v1 and v2), only results from the second design (v2) are shown. Forms of merlin according to the expected molecular weight are indicated next to the bands in the agarose gel. PMO_Ctrl was used as an experiment control. Fib_Ctrl stands for fibroblasts without *NF2* mutation, ES for Exon Skipping and UT for Untreated. 0µM are samples treated with Endo-Porter.

Table 2.1. NF2 splicing variants PMO design						
Patient's code	c.	g.	p.	Variant Effect	PMO_Design 1	PMO_Design 2
Patient_Spl_Ctrl (Experimental Control) (PMO_Ctrl)	c.1446_1477ins	g.74409T>A	p.Pro482Profs*39	Insertion of a cryptic exon of 167pb between exons 13 and 14	CATCCCTCAAATCTCT**T**ACCGTTCT*	
Patient_Spl_1	c.1736A>G	g.83045A>G	p.Lys525Asnfs*19	ES of exon 15	**Spl1_PMO_v1**: AGAAAGAGACCCTGGGTAC**C**TTTTT	**Spl1_PMO_v2**: C**C**TTTTAATGGTATTGTGCTTGCTG
Patient_Spl_2	c.810+1dupG	g.62785dupG	p.Phe271_295del	ES of exon 8	**Spl2_PMO_v1**: GCAGTACACACATGTCCTA**C**CCTCC	**Spl2_PMO_v2:** **C**CCTCCTTGTCACTGTACGAGATGT
Patient_Spl_3	c.241-9A>G	g.35526A>G	p.Val81Phefs*44	New acceptor site. Inclusion of 8 intronic nucleotides as coding sequence	**Spl3_PMO_v1**: AGTACCTGCAGAA**C**TGCAGAGCAAA	**Spl3_PMO_v2**: GCAGAA**C**TGCAGAGCAAAAGACAAA
Patient_Spl_4	c.241-13T>A	g.35522T>A	p.Val81Phefs*44	New acceptor site. Inclusion of 10 intronic nucleotides as coding sequence	**Spl4_PMO_v1**: AGTACCTGCAGAATTGC**T**GAGCAAA	**Spl4_PMO_v2**: GCAGAATTGC**T**GAGCAAAAGACAAA

*Exon Skipping (ES). * Published in Castellanos et al. 2013*

Antisense therapy for *NF2* truncating variants

Differently from the previous approach, this aimed to test if PMOs could be used to specifically force the skipping of in-frame exons carrying a frameshift or nonsense variant, thus maintaining the *NF2* gene reading frame, and test if the generated merlin protein could act as an hypomorphic form, still preserving partial function and to some extent able to rescue an *in vitro* phenotype. In this way, taking into account the genotype-phenotype association in which nonsense or truncating variants are related to more severe phenotypes than in-frame variants, those that generate a more severe phenotype could be modified to less deleterious forms (**Figure 2.3**), assessing if the effect of the exon skipping on both alleles was more beneficial than a truncating variant in heterozygosis. A pair of PMOs were designed to be complementary to both 5'- and 3'- intron-exon boundaries to induce skipping of exons 4, 8 or 11 of the *NF2* gene (Exon-Specific PMOs) (**Table 2.2**).
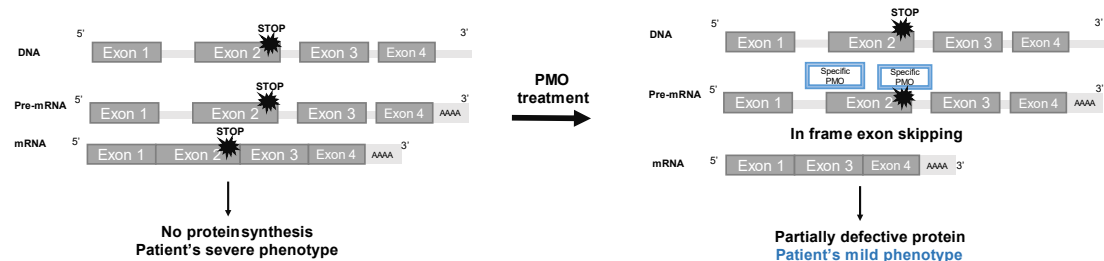
Figure 2.3. Experimental approach to test antisense therapy for truncating *NF2* variants. In blue, expected outcome after PMO treatment**.** PMOs are designed at the donor and acceptor sites of an in-frame exon to induce skipping of exons harbouring truncating variants. The generated in-frame deletion is expected to ameliorate the phenotype *in vitro*.

Fibroblasts from healthy donors were treated with a pair of PMOs designed to target the acceptor and the donor sites of each exon. A dose response study confirmed the efficiency of the treatment showing full skipping of exons 4 and 8 at 20μM (**Supplemental Figure S2.3 A and B**). For exon 11, two different designs were tested (**Table 2.2**; PMO_ES11_v1 and PMO_ES11_v2), while the first (PMO_ES11_v1) failed to induce skipping (data not shown), the second design (PMO_ES11_v2) showed a maximum effect when inducing the skipping of exon 11 at 40μM, and the cells showed an expression of more than 50% of the exon-less form (**Supplemental Figure S2.3C**). As for the splicing variants, a time course experiment was performed to test the effect at distinct time points (24h, 48h and 72h). In all cases, no differences were observed over time, indicating that the maximum effect of the treatment at RNA level was reached at 24h and maintained at 72h (**Supplemental Figure S2.3**).

We analysed whether the skipping of both the in-frame *NF2* exon harbouring a truncating variant and the wild-type *NF2* allele, was less deleterious than harbouring a non-functional allele in primary NF2 patients' derived fibroblasts. First, we studied the capacity of restoring merlin levels *in vitro* after the PMO treatment (**Figure 2.4**). Unexpectedly, merlin western blot showed progressive loss of protein signal when targeting exons 4 (merlin-e4) or 8 (merlin-e8), studied in two and five samples respectively at the 24h, 48h and 72h time points (**Figure 2.4, A and B**). In order to elucidate if the induced skipping of exons 4 or 8 caused a reduction of merlin levels; or if there was a loss in the detection of merlin by the antibody used, possibly due to a misfolded protein; the exon-less NF2 cDNAs were cloned to a N-terminal FLAG® Tag Expression Vector and transfected to HeLa cells. Flag-Merlin Western Blot showed that there was little or no expression of merlin-e4 or merlin-e8, indicating that these new merlin forms could not be synthesized or were degraded shortly after synthesis (**Supplemental Figure S2.4**).

The skipping of exon 11 generated a shorter form of merlin, indicating that a potential hypomorphic merlin could be resulting from the skipping of this exon (merlin-e11) (**Figure 2.4C**).

A. Truncating mutation in exon 4: inducing skipping of exon 4 (ES4)
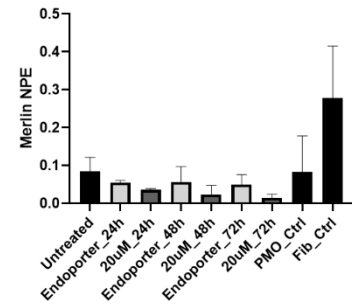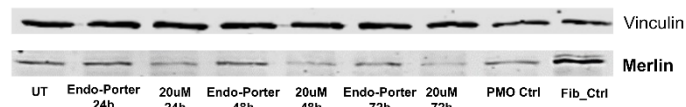
B. Truncating mutation in exon 8: inducing skipping of exon 8 (ES8)
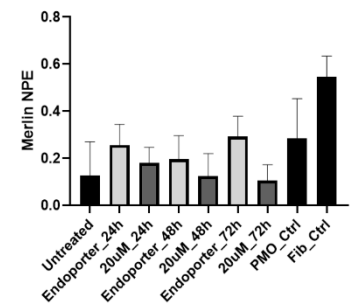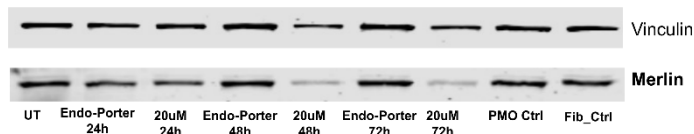
C. Truncating mutation in exon 11: inducing skipping of exon 11 (ES11)
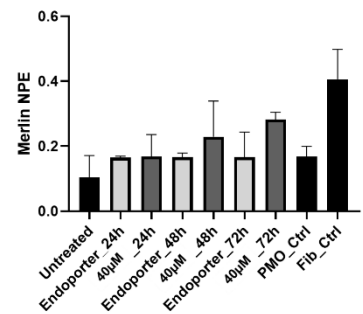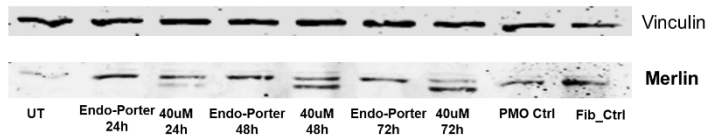
Figure 2.4. Merlin levels after inducing skipping of in-frame exons harbouring truncating variants. Merlin Western Blot after exon-specific PMOs treatment showed a decrease in Merlin total levels and no presence of exon-less, shorter forms of merlin-e4 (A) and merlin-e8 (B). Merlin-e11 was detected and a slight increase was determined in total merlin levels (C). Increases or decreases in merlin levels are considered with respect to the untreated sample. Fibroblast control, with no *NF2* mutation, are used as experimental control. UT stands for Untreated. NPE stands for Normalized Protein Expression.

Table 2.2. Exon-specific PMOs design to target NF2 truncating variants

Exon	Target *NF2* variant	Target region	PMOs designed	PMO_Design 1	PMO_Design 2
4 (n=2)	Any truncating at exon 4	Exon 4_5'	PMO Pair	**PMO_5'ES4**: ACCTGAAAGGAGCAACAAGGGAGAC	
		Exon 4_3'		**PMO_3'ES4**: TTTCTTCTTTGAGCCTACCTTGGCC	
8 (n=5)	Any truncating at exon 8	Exon 8_5'	PMO Pair	**PMO_5'ES8**: TTTATTCTGTGGATCCAATAAGAAC	
		Exon 8_3'		**PMO_3'ES8**: TGCAGTACACACATGTCCTACCTCC	
11 (n=2)	Any truncating at exon 11	Exon 11_5'	PMO Pair	**PMO_5'ES11_v1**: CGCTCCATCTGCGAGGGGTGAAGAA	**PMO_5'ES11_v2**: CGCTCCATCTGCGAGGGGTGAAGAA
		Exon 11_3'		**PMO_3'ES11_v1**: CCTCAGAAATCACCAGTGCTTCGTT	**PMO_3'ES11_v2**: CCTCAGAAATCACCAGTGCTTCGTT

n indicates the number of patients derived fibroblasts in which PMOs is tested

E11 PMO treatment of *NF2*$^{+/-}$ fibroblasts partially rescued the phenotype *in vitro*

Functionality of merlin-e11 was studied in primary fibroblasts harbouring a heterozygous truncating variant in exon 11: one from an adult patient (Patient_ES11_1) and another from a paediatric patient (Patient_ES11_2) (**Supplemental Table S2.1**). Given the complexity of determining differences in severity in the phenotype from studying the signalling pathways in which merlin is involved [29], physiological read outs were assessed. Due to the role of merlin in cytoskeletal organization [38,39], merlin-e11's functional activity was first tested through actin immunofluorescence. Phalloidin staining revealed an improvement of the organizational capacity of the cytoskeleton after PMO treatment, although the phenotype observed in both samples was slightly different: patient_ES11_1 showed prominent membrane ruffles that decreased in response to treatment, (**Figure 2.5A**) while in patient_ES11_2 we observed an improvement in the cell-cell contact organization (**Figure 2.5B**). Specifically, paediatric derived NF2+/- fibroblasts showed an improvement in cell culture, as it seemed that the treatment and expression of merlin-e11 allowed fibroblasts to recover part of the cell-cell contact inhibition and grow as a monolayer instead of growing overlapped.
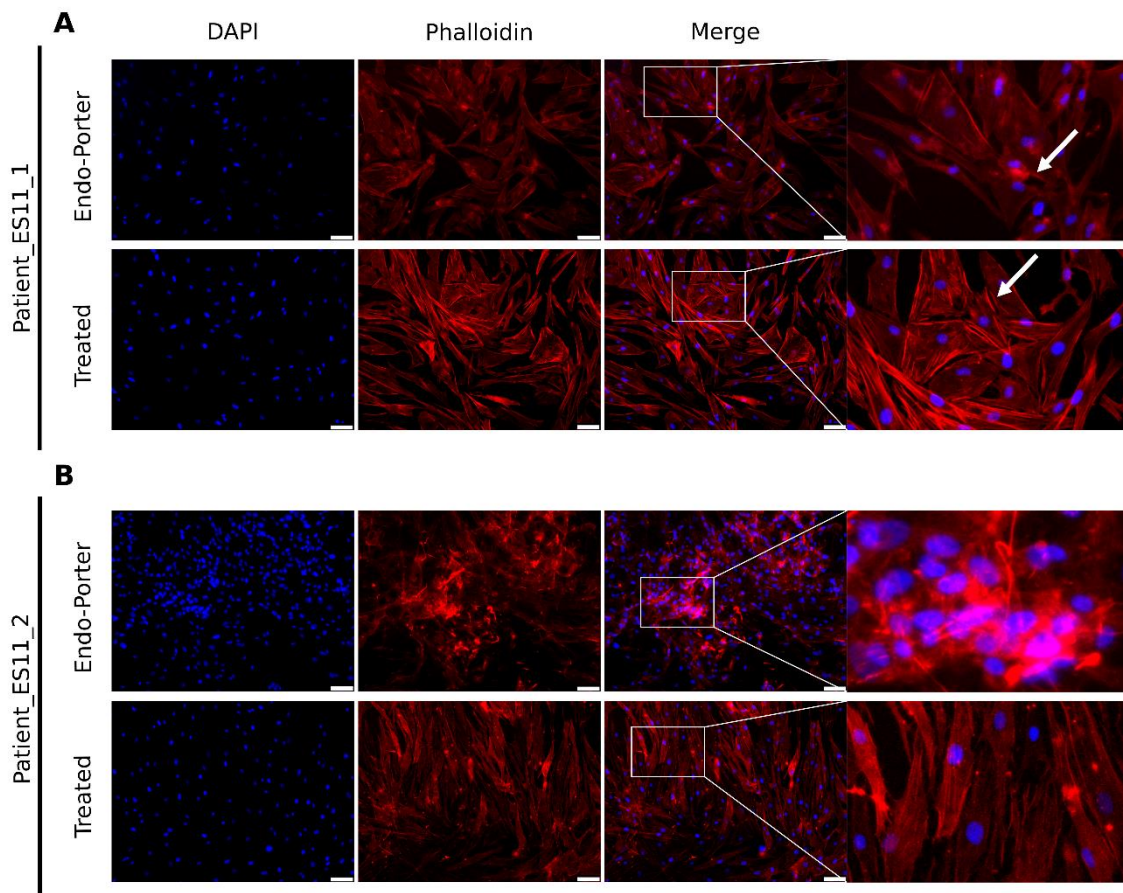
Figure 2.5. E11 PMO treatment of *NF2*$^{+/-}$ fibroblasts induced improvement in actin cytoskeleton organization. Actin immunocytochemistry analysis revealed cytoskeletal abnormalities in patient's derived fibroblasts. Patient_ES11_1 (A) showed a decrease in membrane ruffle formation and Patient_ES11_2 (B) responded to the treatment showing improved culture organization. DAPI (blue) was used to stain cell nuclei and Phalloidin is shown in red. Scale bar: 75µm.

In addition, proliferation rates were tested after 72h of treatment by flow cytometry. patient_ES11_1 showed a statistically significant depletion of proliferation when treated with PMOs (65.6%, $p<0.05$) (**Figure 2.6A**) while patient_ES11_2 showed a less pronounced decrease (25.1%) (**Figure 2.6B**). Considering both samples, primary fibroblasts with a truncating variant in exon 11 showed a 51% reduction in proliferation when compared with the vehicle (Endo-Porter, $p<0.01$) and 39.7% compared with treatment control ($p<0.01$), on average (**Figure 2.6C, Supplemental Figure S2.5**). PMO treatment did not induce significant differences in cell viability (**Supplemental Figure S2.6**).
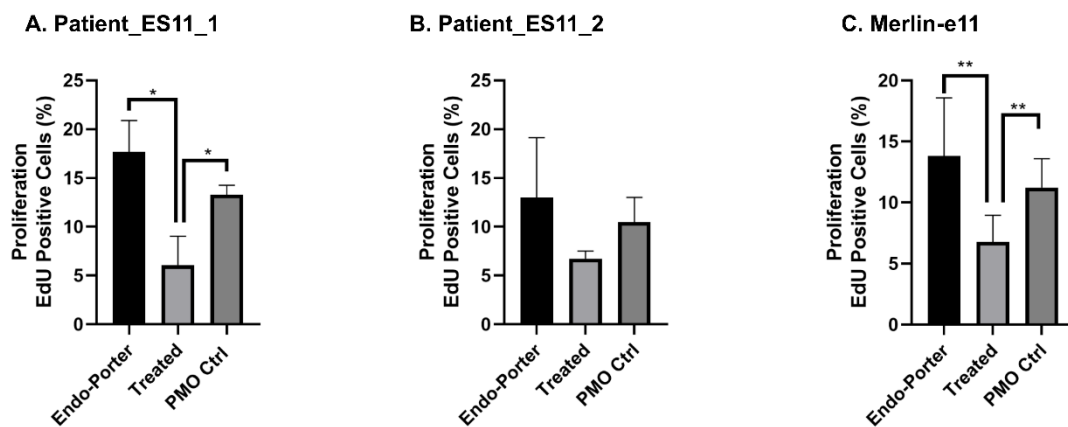
Figure 2.6. Expression of merlin-e11 was able to reduce the proliferation capacity of patient fibroblasts. Quantification of EdU-positive cells (percentage over DAPI-positive nuclei). A significant decrease was detected in the proliferation rate of treated fibroblasts when compared with Endo-Porter for Patient_ES11_1 (A). Patient_ES11_2 (B) showed the same tendency. (C) Representation of the mean values of both patients. Mean±SD is represented in the bar, representing three independent experiments. *$p<0.05$, **$p<0.01$ denotes statistical significance using unpaired t-test. See also Figure S5.

4. Discussion

Neurofibromatosis type 2 (NF2) is a multisystem genetic disorder for which the development of effective therapeutic options with no adverse consequences is needed. The clinical presentation of the disease is variable and related to the type of germline variant inherited in the *NF2* gene [8]. In this context, the development of personalized therapies based on the type of *NF2* variant constitutes an opportunity. In this study, we tested the use of PMOs as antisense therapy to reduce the severity of the effects of *NF2* truncating and splicing variants by changing them to milder hypomorphic forms *in vitro* by two different approaches.

The first approach targeted the splicing variants with the aim of concealing the erroneous splice signal caused by the pathogenic variant and restoring levels of merlin, in a similar way to the approach that our group used for a *NF2* deep intronic variant [44]. In this study it has not been possible to design PMOs that permit correction of the splicing signalling and furthermore, it was not possible to achieve specificity to target the mutated allele as the same effect was observed in both patient-derived fibroblasts and control fibroblasts. We hypothesize that when the splicing variant is within +/- 13 nucleotides of the acceptor or donor splice site, the PMO could allosterically interfere with the branch point and the U2 snRNA incorporation into the spliceosome [45]. The spatiotemporal localization of the two alleles during splicing could prevent the PMO from specifically targeting the mutated allele and thus it would interfere in the cis-regulation of RNA elements of both alleles equally, resulting in an increased pathogenic effect [46]. Since the approach requires the PMO to be specific for the allele harbouring the pathogenic variant, there is little room for variation in the PMO design.

As far as we know, there are no studies in the literature that have been able to repair the LOF variant effect and recover gene function through the use of ASOs for a splicing mutation located in the canonical splice regions in genes causing autosomal dominant diseases. It has only been possible through CRISPR/Cas9 technology by the induction of single nucleotide substitutions [47,48]. Allele-specific approaches have been successfully tested for intronic variants through splice modulation ASOs that mask the erroneous signalling and given their intronic location and distance to splicing regulatory regions, proper protein synthesis can be recovered [49–53].

Furthermore, the approach for the truncating variants tried to benefit from the fact that these variants are associated with more severe phenotypes in comparison to in-frame variants in *NF2* [28,30,54]. Thus, we proposed inducing skipping of the exon carrying the variant with the hypothesis of generating potential homozygous hypomorphic forms of merlin, still aiming to ameliorate the pathogenicity of the heterozygous truncating variant *in vitro*. The skipping of

exons 4 or 8 harbouring *NF2* LOF variants was not able to generate an exon-less merlin, because merlin-e4 and merlin-48 were degraded. Exons 4 and 8 of the *NF2* gene code for the subdomains B and C respectively of the FERM domain, where the majority of reported pathogenic variants occur; and which has the most potential for anti-mitogenic signalling and tumour suppressor function [17,21]. The observed results could be due to the fact that the lack of an exon coding for the FERM domain would cause an unbearable aberrant folding of the protein and its synthesis would be prevented or it would be forcibly degraded. In addition, the FERM domain is responsible for the intramolecular interaction with the C-terminal domain, which results in merlin being in a closed and active conformation [55–57], thus, if this folding fails, it is possible that the resulting protein would not be able to execute the suppressor activity.

For autosomal recessive diseases, such as SMA or DMD [58,59], an autosomal dominant with a dominant negative effect, Frontotemporal dementia with parkinsonism-17 (FTDP-17) or RP, allele specific ASOs have been used to induce degradation of the disease-causing allele via RNAse H activity and for this purpose, the native DNA backbone is not modified [45,60–62]. Recent evidence suggests that merlin could act in a negative dominant manner through its self-dimerization through FERM-FERM interactions [63], so the use of RNAse H dependent ASOs could be a possible antisense approach for mutations located in the FERM domain, in both in-frame and out of frame exons. In addition, in contrast to the approach tested in this study, we hypothesize that the degradation of the mutant transcript could prevent interference with the spliceosome during the splicing of the wild-type allele, and therefore, the use of RNAse H dependent ASOs should be also taken into consideration for patients harbouring splicing variants in the *NF2* gene. In the light of our findings, the degradation of the *NF2* mutated allele could bring an improvement in the *in vitro* phenotype and open the door for future gene therapy approaches.

When targeting exon 11 of the *NF2* gene, an exon-less merlin was expressed (merlin-e11). Merlin, as a member of the ERM protein family, is involved in the link between actin cytoskeleton and adherent junctions with a relevant role in dynamic cytoskeleton remodelling, such as in membrane ruffling or in the formation of actin micro-spikes. Consistent with other studies which found that merlin loss leads to a dramatic increase of membrane ruffles [64], here we showed a decrease in membrane ruffle formation in response to the expression of merlin-e11 that could be associated with a partial rescue of the phenotype. Additionally, we showed an improvement in the cytoskeleton organization after treatment, which could be due to a recovery of the merlin function as a scaffold protein regulating the linkage between membrane proteins and the cortical cytoskeleton [53,65,66]. Consistent with the role as a tumour suppressor

protein, merlin-deficient cells loose contact inhibition of proliferation [55,67,68] and although much remains to be discovered about the adhesive signalling pathways involved, in this study we showed that the induction of merlin-e11 by PMO treatment contributed to the recovery of cell-cell contact inhibition of proliferation in fibroblasts derived from NF2 patients harbouring truncating mutations in exon 11.

This work is a proof of concept of the use antisense therapy *in vitro* as a personalized therapy for NF2 patients harbouring truncating variants at exon 11 of the *NF2* gene. Further studies will be needed to elucidate whether there are other mechanisms or designs to apply ASOs as a therapeutic approach for this disease, as in our experience it has not been possible to recover merlin levels for variants located at in-frame exons 4 or 8, or to correct splicing signals *in vitro* in the four variants located near canonical splice sites tested, although other splicing variants should be tested to confirm these results.

On the other hand, our approach has shown encouraging results when targeting exon 11, although further characterization assays need to be performed to better characterize the function of merlin-e11 before considering it for further *in vivo* or pre-clinical assays.

5. Acknowledgements

6. References

1   Evans DGR, Huson SM, Donnai D, *et al.* A genetic study of type 2 neurofibromatosis in the United Kingdom . II . Guidelines for genetic counselling. 1992;:847–52.

2   Evans DG, Howard E, Giblin C, *et al.* Birth incidence and prevalence of tumor-prone syndromes: Estimates from a UK family genetic register service. *American Journal of Medical Genetics, Part A* 2010;**152**:327–32. doi:10.1002/ajmg.a.33139

3   Evans DG, Bowers NL, Tobi S, *et al.* Schwannomatosis: a genetic and epidemiological study. *Journal of Neurology, Neurosurgery & Psychiatry* 2018;**89**:1215–9. doi:10.1136/jnnp-2018-318538

4   Lloyd SKW, Evans DGR. *Neurofibromatosis type 2 (NF2): diagnosis and management*. 1st ed. Elsevier B.V. 2013. doi:10.1016/B978-0-444-52902-2.00054-0

5   Evans DGR. Orphanet Journal of Rare Diseases. 2009;**2**:1–11. doi:10.1186/1750-1172-4-16

6   Forde C, King AT, Rutherford SA, *et al.* Disease course of neurofibromatosis type 2: A 30-year follow-up study of 353 patients seen at a single institution. *Neuro-Oncology* 2021;**23**:1113–24. doi:10.1093/neuonc/noaa284

7   Lloyd SKW, Evans DGR. *Neurofibromatosis type 2 (NF2): diagnosis and management.* 1st ed. Elsevier B.V. 2013. doi:10.1016/B978-0-444-52902-2.00054-0

8   Lloyd SKW, Evans DGR. *Neurofibromatosis type 2 (NF2): diagnosis and management*. 1st ed. Elsevier B.V. 2013. doi:10.1016/B978-0-444-52902-2.00054-0

9   Plotkin SR, Duda DG, Muzikansky A, *et al.* Multicenter, Prospective, Phase II and Biomarker Study of High-Dose Bevacizumab as Induction Therapy in Patients With Neurofibromatosis Type 2 and Progressive Vestibular Schwannoma. *Journal of Clinical Oncology* 2019;:JCO.19.01367. doi:10.1200/jco.19.01367

10 Nunes FP, Merker VL, Jennings D, *et al.* Bevacizumab Treatment for Meningiomas in NF2: A Retrospective Analysis of 15 Patients. *PLoS ONE* 2013;**8**. doi:10.1371/journal.pone.0059941

11 Wu L, Vasilijic S, Sun Y, *et al.* Losartan prevents tumor-induced hearing loss and augments radiation efficacy in NF2 schwannoma rodent models. 2021. https://www.science.org

12 Karajannis MA, Legault G, Hagiwara M, *et al.* Phase II trial of lapatinib in adult and pediatric patients with neurofibromatosis type 2 and progressive vestibular schwannomas. *Neuro-Oncology* 2012;**14**:1163–70. doi:10.1093/neuonc/nos146

13 Osorio DS, Hu J, Mitchell C, *et al.* Effect of lapatinib on meningioma growth in adults with neurofibromatosis type 2. *Journal of Neuro-Oncology* 2018;**139**:749–55. doi:10.1007/s11060-018-2922-5

14 Welling DB, Collier KA, Burns SS, *et al.* Early phase clinical studies of AR-42, a histone deacetylase inhibitor, for neurofibromatosis type 2-associated vestibular schwannomas and meningiomas. *Laryngoscope Investigative Otolaryngology* 2021;**6**:1008–19. doi:10.1002/lio2.643

15 Schmucker B, Tang Y, Kressel M. Novel alternatively spliced isoforms of the neurofibromatosis type 2 tumor suppressor are targeted to the nucleus and cytoplasmic granules. *Human Molecular Genetics* 1999;**8**:1561–70. doi:10.1093/hmg/8.8.1561

16 Su F, Zhou Z, Su W, *et al.* A novel alternative splicing isoform of NF2 identified in human schwann cells. *Oncology Letters* 2016;**12**:977–82. doi:10.3892/ol.2016.4685

17 Ahronowitz I, Xin W, Kiely R, *et al.* Mutational Spectrum of the NF2 Gene : A Meta-Analysis of 12 Years of Research and Diagnostic Laboratory Findings. 2007;**28**. doi:10.1002/humu

18 Halliday D, Parry A, Evans DG. Neurofibromatosis type 2 and related disorders. *Current Opinion in Oncology* 2019;**31**:562–7. doi:10.1097/CCO.0000000000000579

19   Asthagiri AR, Parry DM, Butman JA, *et al.* Neurofibromatosis type 2. *Lancet* 2009;**373**:1974–86. doi:10.1016/S0140-6736(09)60259-2

20   Chiasson-MacKenzie C, Morris ZS, Baca Q, *et al.* NF2/Merlin mediates contact-dependent inhibition of EGFR mobility and internalization via cortical actomyosin. *Journal of Cell Biology* 2015;**211**:391–405. doi:10.1083/jcb.201503081

21   Cooper J, Giancotti FG. Molecular insights into NF2/Merlin tumor suppressor function. *FEBS Letters* 2014;**588**:2743–52. doi:10.1016/j.febslet.2014.04.001

22   Evans DGR, Trueman L, Wallace A, *et al.* Genotype / phenotype correlations in type 2 neurofibromatosis (NF2): evidence for more severe disease associated with truncating mutations. 1998;:450–5.

23   Heineman TE, Evans DGR, Campagne F, *et al.* In silico analysis of NF2 gene missense mutations in neurofibromatosis type 2: From genotype to phenotype. *Otology and Neurotology* 2015;**36**:908–14. doi:10.1097/MAO.0000000000000639

24   Selvanathan SK, Shenton A, Ferner R, *et al.* Further genotype - phenotype correlations in neurofibromatosis 2. *Clinical Genetics* 2010;**77**:163–70. doi:10.1111/j.1399-0004.2009.01315.x

25   Halliday D, Emmanouil B, Pretorius P, *et al.* Genetic severity score predicts clinical phenotype in NF2. *Journal of Medical Genetics* 2017;**54**:657–64. doi:10.1136/jmedgenet-2017-104519

26   Emmanouil B, Houston R, May A, *et al.* Progression of hearing loss in neurofibromatosis type 2 according to genetic severity. *Laryngoscope* 2019;**129**:974–80. doi:10.1002/lary.27586

27   Halliday D, Emmanouil B, Vassallo G, *et al.* Trends in phenotype in the English paediatric neurofibromatosis type 2 cohort stratified by genetic severity. *Clinical Genetics* 2019;**96**:151–62. doi:10.1111/cge.13551

28   Baser ME, Kuramoto L, Joe H, *et al.* Genotype-Phenotype Correlations for Nervous System Tumors in Neurofibromatosis 2: A Population-Based Study. *The American Journal of Human Genetics* 2004;**75**:231–9. doi:10.1086/422700

29   Catasús N, Garcia B, Galván-Femenía I, *et al.* Revisiting the UK genetic severity score for NF2: A proposal for the addition of a functional genetic component. *Journal of Medical Genetics* 2021;:1–9. doi:10.1136/jmedgenet-2020-107548

30   Ruttledge MH, Andermann a a, Phelan CM, *et al.* Type of mutation in the neurofibromatosis type 2 gene (NF2) frequently determines severity of disease. *American Journal of Human Genetics* 1996;**59**:331–42.

31   Halliday D, Emmanouil B, Pretorius P, *et al.* Genetic Severity Score predicts clinical phenotype in NF2. 2017;:657–64. doi:10.1136/jmedgenet-2017-104519

32   Hua Y, Vickers TA, Baker BF, *et al.* Enhancement of SMN2 exon 7 inclusion by antisense oligonucleotides targeting the exon. *PLoS Biology* 2007;**5**:729–44. doi:10.1371/journal.pbio.0050073

33   Crooke RM, Graham MJ, Lemonidis KM, *et al.* An apolipoprotein B antisense oligonucleotide lowers LDL cholesterol in hyperlipidemic mice without causing hepatic steatosis. *Journal of Lipid Research* 2005;**46**:872–84. doi:10.1194/jlr.M400492-JLR200

34   McClorey G, Moulton HM, Iversen PL, *et al.* Antisense oligonucleotide-induced exon skipping restores dystrophin expression in vitro in a canine model of DMD. *Gene Therapy* 2006;**13**:1373–81. doi:10.1038/sj.gt.3302800

35   Stein CA, Castanotto D. FDA-Approved Oligonucleotide Therapies in 2017. *Molecular Therapy* 2017;**25**:1069–75. doi:10.1016/j.ymthe.2017.03.023

36   Xiong H, Veedu RN, Diermeier SD. Recent advances in oligonucleotide therapeutics in oncology. *International Journal of Molecular Sciences* 2021;**22**. doi:10.3390/ijms22073295

37   Dominant NREA. Antisense Oligonucleotide-Based Downregulation of. ;**3**:1–12.

38   Miller T, Cudkowicz M, Shaw PJ, *et al.* Phase 1–2 Trial of Antisense Oligonucleotide Tofersen for SOD1 ALS . *New England Journal of Medicine* 2020;**383**:109–19. doi:10.1056/nejmoa2003715

39   Tabrizi SJ, Leavitt BR, Landwehrmeyer GB, *et al.* Targeting Huntingtin Expression in Patients with Huntington's Disease. *New England Journal of Medicine* 2019;**380**:2307–16. doi:10.1056/nejmoa1900907

40   Gleave ME, Monia BP. Antisense therapy for cancer. *Nature Reviews Cancer* 2005;**5**:468–79. doi:10.1038/nrc1631

41   Levin AA. Treating Disease at the RNA Level with Oligonucleotides. *New England Journal of Medicine* 2019;**380**:57–70. doi:10.1056/nejmra1705346

42   Sazani P, Kang SH, Maier MA, *et al.* Nuclear antisense effects of neutral, anionic and cationic oligonucleotide analogs. *Nucleic acids research* 2001;**29**:3965–74. doi:10.1093/nar/29.19.3965

43   Castellanos E, Gel B, Rosas I, *et al.* A comprehensive custom panel design for routine hereditary cancer testing: Preserving control, improving diagnostics and revealing a complex variation landscape. *Scientific Reports* 2017;**7**. doi:10.1038/srep39348

44   Castellanos E, Rosas I, Solanes A, *et al.* In vitro antisense therapeutics for a deep intronic mutation causing Neurofibromatosis type 2. *European Journal of Human Genetics* 2013;**21**:769–73. doi:10.1038/ejhg.2012.261

45   Tang Z, Zhao J, Pearson ZJ, *et al.* Rna-targeting splicing modifiers: Drug development and screening assays. *Molecules* 2021;**26**. doi:10.3390/molecules26082263

46   Maass PG, Barutcu AR, Shechner DM, *et al.* Spatiotemporal allele organization by allele-specific CRISPR live-cell imaging (SNP-CLING). *Nature Structural and Molecular Biology* 2018;**25**:176–84. doi:10.1038/s41594-017-0015-3

47   György B, Nist-Lund C, Pan B, *et al.* Allele-specific gene editing prevents deafness in a model of dominant progressive hearing loss. *Nature Medicine* 2019;**25**:1123–30. doi:10.1038/s41591-019-0500-9

48   Kocher T, Peking P, Klausegger A, *et al.* Cut and Paste: Efficient Homology-Directed Repair of a Dominant Negative KRT14 Mutation via CRISPR/Cas9 Nickases. *Molecular Therapy* 2017;**25**:2585–98. doi:10.1016/j.ymthe.2017.08.015

49   Tomkiewicz TZ, Suárez-Herrera N, Cremers FPM, *et al.* Antisense oligonucleotide-based rescue of aberrant splicing defects caused by 15 pathogenic variants in abca4. *International Journal of Molecular Sciences* 2021;**22**. doi:10.3390/ijms22094621

50   Aguti S, Bolduc V, Ala P, *et al.* Exon-Skipping Oligonucleotides Restore Functional Collagen VI by Correcting a Common COL6A1 Mutation in Ullrich CMD. *Molecular Therapy - Nucleic Acids* 2020;**21**:205–16. doi:10.1016/j.omtn.2020.05.029

51   Panagiotopoulos AL, Karguth N, Pavlou M, *et al.* Antisense Oligonucleotide- and CRISPR-Cas9-Mediated Rescue of mRNA Splicing for a Deep Intronic CLRN1 Mutation. *Molecular Therapy - Nucleic Acids* 2020;**21**:1050–61. doi:10.1016/j.omtn.2020.07.036

52   Pros E, Fernández-Rodríguez J, Canet B, *et al.* Antisense therapeutics for neurofibromatosis type 1 caused by deep intronic mutations. *Human Mutation* 2009;**30**:454–62. doi:10.1002/humu.20933

53   Castellanos E, Carrato C, Rosas I, *et al.* In vitro antisense therapeutics for a deep intronic mutation causing Neurofibromatosis type 2. 2013;:769–73. doi:10.1038/ejhg.2012.261

54   Kluwe L, MacCollin M, Tatagiba M, *et al.* Phenotypic variability associated with 14 splice-site mutations in the NF2 gene. *American Journal of Medical Genetics* 1998;**77**:228–33. doi:10.1002/(SICI)1096-8628(19980518)77:3<228::AID-AJMG8>3.0.CO;2-L

55   Morrison H, Sherman LS, Legg J, *et al.* The NF2 tumor suppressor gene product, merlin, mediates contact inhibition of growth through interactions with CD44. *Genes and Development* 2001;**15**:968–80. doi:10.1101/gad.189601

56   Scoles DR. The merlin interacting proteins reveal multiple targets for NF2 therapy. 2008;**1785**:32–54. doi:10.1016/j.bbcan.2007.10.001

57   Li Q, Nance MR, Kulikauskas R, *et al.* Self-masking in an Intact ERM-merlin Protein: An Active Role for the Central α-Helical Domain. *Journal of Molecular Biology* 2007;**365**:1446–59. doi:10.1016/j.jmb.2006.10.075

58   Passini MA, Bu J, Richards AM, *et al.* Antisense oligonucleotides delivered to the mouse CNS ameliorate symptoms of severe spinal muscular atrophy. *Science Translational Medicine* 2011;**3**. doi:10.1126/scitranslmed.3001777

59   Wheeler TM, Leger AJ, Pandey SK, *et al.* Targeting nuclear RNA for in vivo correction of myotonic dystrophy. *Nature* 2012;**488**:111–7. doi:10.1038/nature11362

60   Panza F, Lozupone M, Seripa D, *et al.* Development of disease-modifying drugs for frontotemporal dementia spectrum disorders. *Nature Reviews Neurology* 2020;**16**:213–28. doi:10.1038/s41582-020-0330-x

61   Murray SF, Jazayeri A, Matthes MT, *et al.* Allele-specific inhibition of rhodopsin with an antisense oligonucleotide slows photoreceptor cell degeneration. *Investigative Ophthalmology and Visual Science* 2015;**56**:6362–75. doi:10.1167/iovs.15-16400

62   DeVos SL, Miller RL, Schoch KM, *et al.* Tau reduction prevents neuronal loss and reverses pathological tau deposition and seeding in mice with tauopathy. *Science Translational Medicine* 2017;**9**. doi:10.1126/scitranslmed.aag0481

63   Hennigan RF, Thomson CS, Ratner N. Merlin Tumor Suppressor Function is Regulated by PIP 2 -Mediated Dimerization . 2021;:1–24.

64   The Nf2 Tumor Suppressor, Merlin, Functions in Rac-Dependent Signaling. http://www.developmental.

65   Chiasson-Mackenzie C, Morris ZS, Liu CH, *et al.* Merlin/ERM proteins regulate growth factor-induced macropinocytosis and receptor recycling by organizing the plasma membrane:Cytoskeleton interface. *Genes and Development* 2018;**32**:1201–14. doi:10.1101/gad.317354.118

66   McClatchey AI, Fehon RG. Merlin and the ERM proteins - regulators of receptor distribution and signaling at the cell cortex. Trends in Cell Biology. 2009;**19**:198–206. doi:10.1016/j.tcb.2009.02.006

67   Johnson KC, Kissil JL, Fry JL, *et al.* Cellular transformation by a FERM domain mutant of the Nf2 tumor suppressor gene. *Oncogene* 2002;**21**:5990–7. doi:10.1038/sj.onc.1205693

68   Lallemand D, Curto M, Saotome I, *et al.* NF2 deficiency promotes tumorigenesis and metastasis by destabilizing adherens junctions. *Genes and Development* 2003;**17**:1090–100. doi:10.1101/gad.1054603

7. Supplemental Figures and Tables

Figure S2.1. Sanger sequencing confirmed the effect of the variant-specific PMOs.

A. Patient_Spl_1

B. Patient_Spl_2

C. Patient_Spl_3

D. Patient_Spl_4
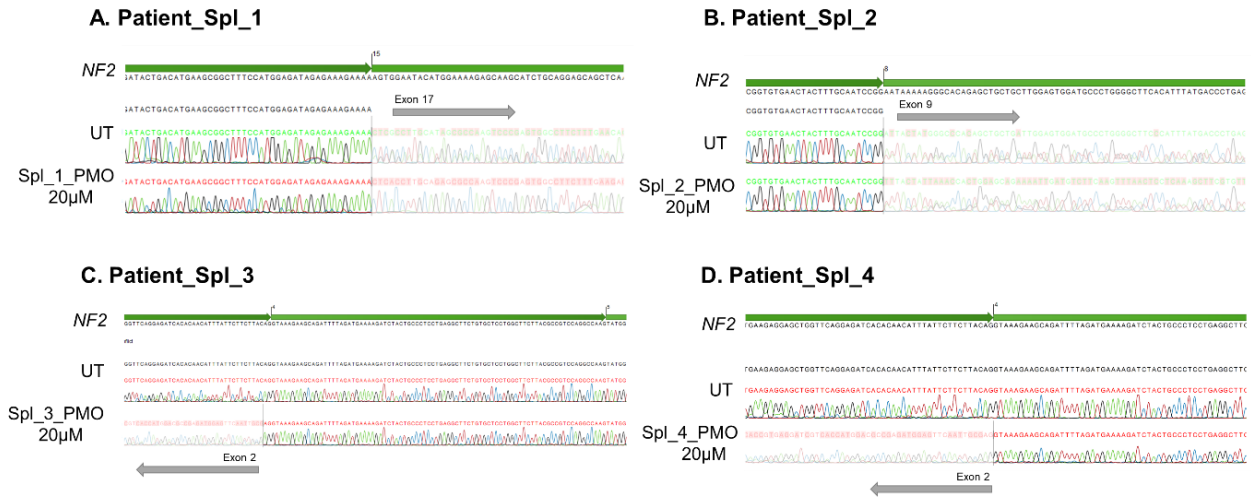
Figure S2.2. Testing variant-specific PMOs targeting *NF2* splicing variants. Merlin Western Blot decreased upon PMO treatment. Increases and decreases in levels of merlin are considered in respect to the untreated sample. Fibroblasts Control (Fib_Ctrl), with no mutation in *NF2* are used as experimental controls. UT stands for Untreated; NPE stands for Normalized Protein Expression.

Figure S2.3. Testing the effect of the PMOs to induce exon skipping by a dose-response and a time-course analysis. The bands in the electrophoretic gel revealed a maximum effect of the treatment of exon-skipping 4 and 8 (ES4 and ES8) at 20µM and effect was maintained over 72h at cDNA level (panels A and B). For the skipping of exon 11 (ES11), 40µM of the PMO_5'ES11_v2 and PMO_3'ES11_v2 were used the induce the maximum effect and it was maintained over 72h (panel C) at cDNA level. Treatment effect was confirmed by Sanger sequencing.

Figure S2.4. Flag-Merlin Western Blot. Flag-Merlin Western Blot was performed to detect expression of the possible generated hypomorphic forms of merlin after PMOs treatment. Wild-type merlin (merlin-WT) and the potential hypomorphic form of merlin skipping exon 11 (merlin-e11) cloned in the N-terminal FLAG® Tag Expression Vector were correctly detected, in contrast to the induced merlin forms with the skipping exon 4 or exon 8. NPE stands for Normalized Protein Expression.
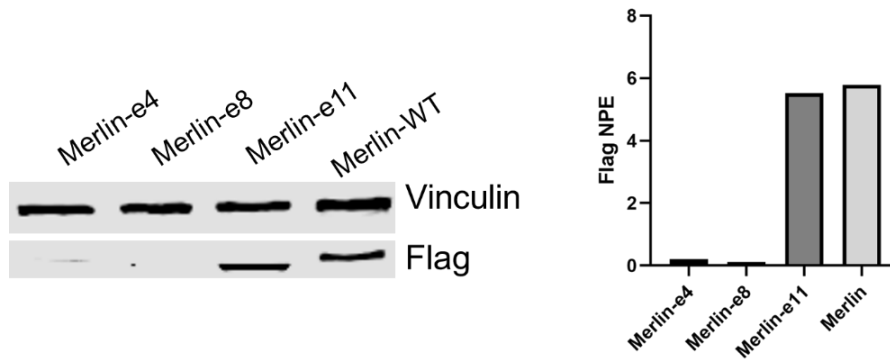
Figure S2.5. Quantification of EdU-positive cells by flow cytometry (percentage over total DAPI-positive nuclei). Gate were established considering EdU-positive cells and DNA content. Green gate represents EdU-positive cells in S phase, phases G0 and G1 are represented in yellow and red for phases G2 and M. R1, R2 and R3 stand for three independent experiments.
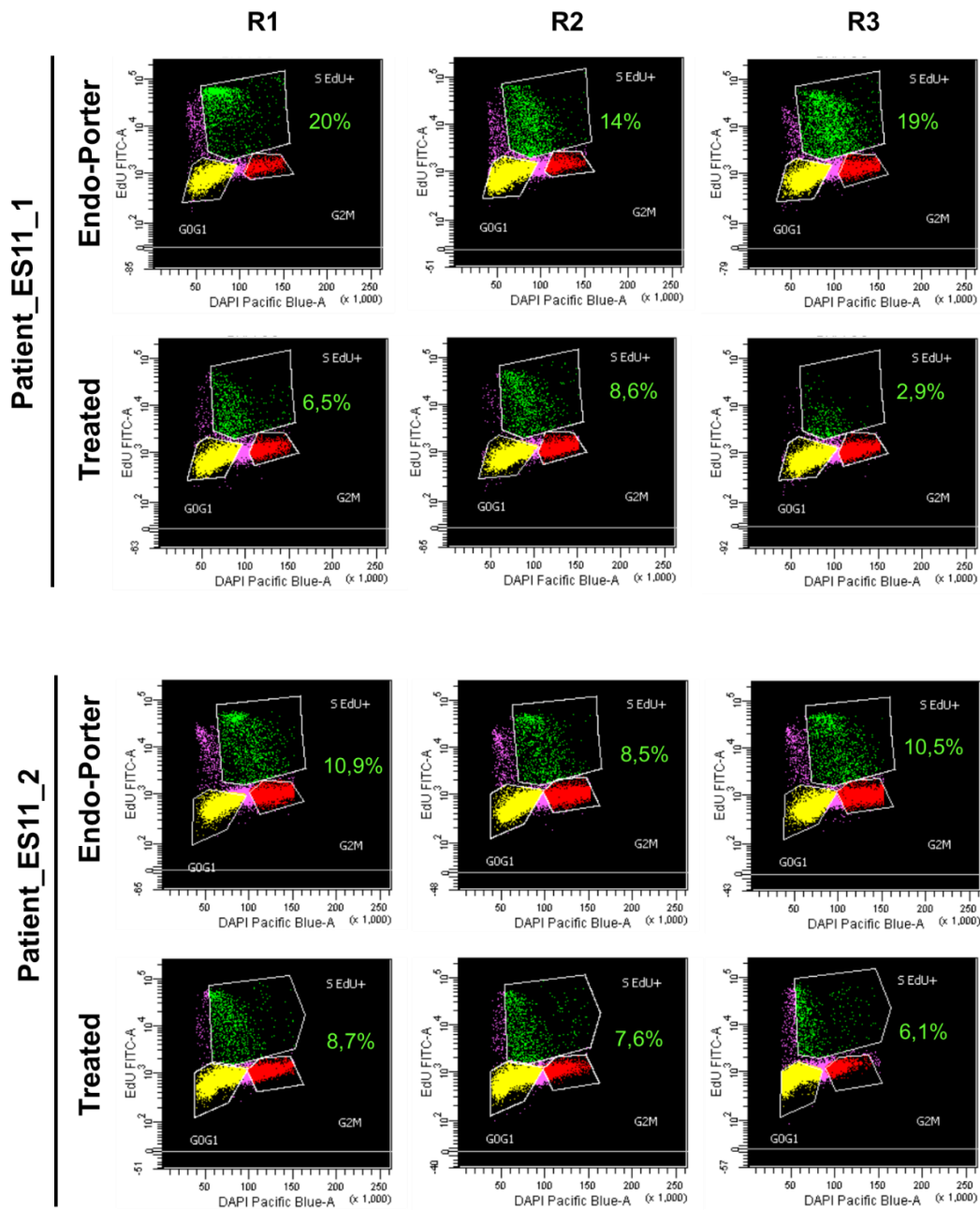
Figure S2.6. Cell viability assay. Results showed no significant differences in cell viability after PMO treatment. The mean of relative luminescence units (RLU) from three independent experiments is represented.
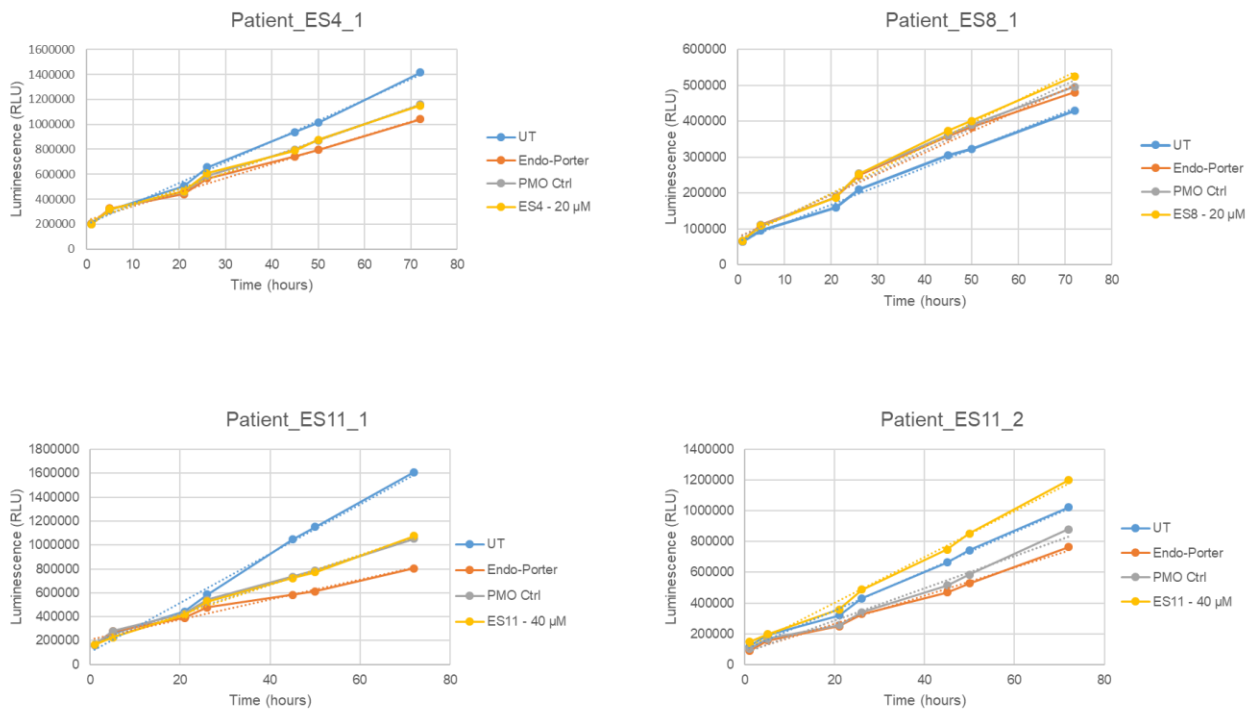
Table S2.1. Samples from NF2 patients included in the study and description of the pathogenic variants

Sample Patient	g.	c.	p.	Affected Exon
Patient_ES4_1	g.38716C>G	c.432C>G	p.Tyr144X	4
Patient_ES4_2	g.43663_43679dup	c.380_396dup	p.Cys133*	4
Patient_ES8_1	g.57759C>T	c.784C>T	p.Arg262X	8
Patient_ES8_2	g.57759C>T	c.784C>T	p.Arg262X	8
Patient_ES8_3	g.57759C>T	c.784C>T	p.Arg262X	8
Patient_ES8_4	g.57759C>T	c.784C>T	p.Arg262X	8
Patient_ES8_5	g.57759C>T	c.784C>T	p.Arg262X	8
Patient_ES11_1	g.73367_73373del	c.1096_1102del	p.Glu366Glnfs*7	11
Patient_ES11_2	g.30067836C>T	c.1021C>T	p.Arg341*	11
Patient_Spl_1	g.83045A>G	c.1736A>G	p.Lys525Asnfs*19	15
Patient_Spl_2	g.62785dupG	c.810+1dupG	p.Phe271_295del	8
Patient_Spl_3	g.35526A>G	c.241-9A>G	p.Val81Phefs*44	3
Patient_Spl_4	g.35522T>A	c.241-13T>A	p.Val81Phefs*44	3
Patient_Spl_Ctrl (PMO_Ctrl)	*positive control (g. 74409T4A)	c.1446_1477ins	p.Pro482Profs*39	13

Chapter 3

Generation of *NF2* (+/-) and *NF2* (-/-) induced pluripotent stem cells through vestibular schwannoma reprogramming and CRISPR-Cas9 genome editing

This chapter reports the research related to the third objective of this thesis, aiming to develop a non-perishable *in vitro* model for NF2-related vestibular schwannomas (VS). Herein, we present the generation and characterization of induced pluripotent stem cell (iPSC) lines harbouring single or bi-allelic inactivation of the *NF2* gene, obtained from both reprogramming vestibular schwannoma cells and gene editing. The generated iPSC lines were differentiated towards the Neural Crest – Schwann Cell axis.

Supplemental material is available at the end of the chapter.

Abstract

The appearance of bilateral vestibular schwannomas (VS) is one of the most characteristic features of Neurofibromatosis Type 2 (NF2), an autosomal dominant syndrome that predispose to the development of tumors of the nervous system. VS are caused by the bi-allelic inactivation of the *NF2* gene in a cell of the Schwann cell lineage. Our current understanding of VS initiation and progression as well as the development of new effective therapies is hampered by the absence of human non-perishable cell-based models. With this aim, we generated and characterized induced pluripotent stem cell (iPSC) lines with single o bi-allelic loss of function of *NF2* by combining the direct reprogramming of VS cells with the use of CRISPR/Cas9 editing. In our hands, *NF2* function seems to be essential for both reprograming and maintaining a pluripotent state. Despite the difficulty of maintaining pure pluripotent merlin-deficient cell clones, we were able to differentiate them into neural crests (NC) cells. However, at this stage, the spontaneous expression of S100B marker and the impossibility to generate Schwann cells in 2D cultures due to a lack of cell-plate attachment, denoted also an altered differentiation capacity of *NF2*-deficient cells towards the NC-SC axis, in these *in vitro* conditions. To overcome this deficiency, applying a 3D Schwann cell differentiation protocol, we successfully generated NF2(-/-) spheroids co-expressing p75 and S100B markers. If a Schwann-cell like identity is confirmed, these *NF2*(-/-) spheroids potentially represent a genuine VS model.

1. Introduction

Neurofibromatosis type 2 (NF2; MIM ID#101000) is a dominantly inherited autosomal syndrome characterized by the development of multiple tumours of the nervous system [1]. This condition is caused by pathogenic variants in the *NF2* tumour suppressor gene (22q12.2) that code for merlin, a scaffold protein that interacts with transmembrane receptors and intracellular effectors to mediate mitogenic and survival signalling pathways [2–4]. The incidence of the disease is estimated in 1 in 28.000 live birth with a complete penetrance by the age of 60, being 50–60% of cases due to *de novo* mutations [5].

The pathognomonic feature of the disease is the development of bilateral vestibular schwannomas, although affected individuals may also develop schwannomas in other cranial, spinal and peripheral nerves as well as meningiomas, both intracranial or intraspinal, and spinal ependymomas [6–10]. Cutaneous and ocular manifestations are also frequent [11,12]. Although histologically benign, these tumours are responsible for high morbidity and a reduced life expectancy due to their number and anatomical location [13].

Vestibular schwannomas (VSs) are benign and well-circumscribed intracranial tumours that arise from Schwann Cells (SCs) as a result of the bi-allelic *NF2* loss of function. They are found attached to the vestibulocochlear nerve, naturally growing over time [9,14–16], and are responsible for significant morbidity associated with NF2 which includes hearing loss, deafness and tinnitus that can eventually progress to facial paraesthesia, ataxia and vertigo [17]. Clinical management of VSs can be challenging due to side effects associated with treatment. Tumour size, growth rate and hearing loss are considered in the treatment decision-making process with the aim to balance between function preservation and patients' quality of life. The current gold standard for treatment of VSs include surveillance, surgery, radiotherapy and Bevacizumab [17]. The latter, an anti-angiogenic monoclonal antibody, a VEGF inhibitor, that has been shown to induce reduction of tumour growth and an improvement in hearing loss in some NF2 patients, although with associated toxicity when sustained over time [18]. As these tumours present a long disease course, there is the need to develop new treatments with minimal side effects.

The study of the *NF2* role in VSs and the development of potential therapies is still challenging due to the lack of non-perishable preclinical models that reproduce patients' genetics and the pathophysiology of NF2 related tumours. The first attempts to generate *in vivo* murine models revealed the essentiality of *NF2* during embryogenesis and early development [19]. While homozygous *NF2* mutant mice failed to develop extraembryonic structures impeding to reach a

gastrulation stage, mosaic *NF2^-/-* embryos showed defects in a variety of other embryonic tissues [19]. In *NF2^+/-* mutant mice, the deficiency of a single *NF2* allele caused the appearance of malignant epithelial tumours and sarcomas with an aggressive tendency to metastasize [20]. Conditional KO murine models can generate schwannomas and, in some cases, VSs, although differing histologically from human schwannomas [21,22]. Several xenograft mouse models have also been developed, with different success in recapitulating the biology of human NF2 traits [23].

At a cellular level, primary SC cultures derived from VSs have been established and demonstrated to preserve the pathophysiology of the tumour [24,25]. However, the limited life-span of primary cultures can severely constrain their use if significant quantities of SCs need to be used. Transformed and immortalized vestibular schwannoma derived cell lines have been developed in order to overcome this limitation, and have widely been used as platforms for drug screening (HEI-93, JEI-001) [26,27]. The concern with these models is the physiological changes immortalization may produce, compared to primary VSs cells.

Induced pluripotent stem cells (iPSCs) [28] models have been used in a wide range of diseases, representing an inexhaustible source of cells with diverse applications such as disease modelling, drug development, regenerative medicine or gene regulation [29–32]. The first related model reported for NF2 is an induced pluripotent stem cell (iPSC) line harbouring a homozygous variant in the *NF2* gene (UMi031-A-2), obtained through gene editing by CRISPR/Cas9 of a of a non-affected pluripotent cell line [33]. However, there is still the need to develop endurable *in vitro* models that recapitulate the genetic status of *NF2* derived VSs.

In the present study we have generated induced pluripotent stem cell (iPSC) lines harbouring single o bi-allelic loss of function of *NF2* by direct reprogramming of VS cells and the use of CRISPR/Cas9 editing. These cells were characterized and differentiated towards the NC-SC lineage and obtained *NF2* (+/-) and *NF2* (-/-) spheroids co-expressing classical markers of the NC-SC axis (p75 and S100B).

2. Materials and Methods

All procedures performed were in accordance with the ethical standards of the IGTP Institutional Review Board, that approved this study, and with the 1964 Helsinki declaration and its later amendments.

Patients and Vestibular Schwannoma samples

Tumour samples were obtained from NF2 patients clinically managed at the Spanish Reference Centre (CSUR) on Phacomatoses HUGTiP-ICO-IGTP, diagnosed according to standard diagnostic criteria [34]. Written informed consent to generate iPSC lines was obtained.

Tumour processing

Tumour samples were placed in DMEM medium (Gibco) with 1x Glx (Gibco) and 1x normocin antibiotic cocktail (InvivoGene) after surgery resection. VSs were digested with 160U/mL collagenase type 1 and 0.8U/mL dispase (Worthington, Lakewood, NJ) for 16 h at 37ºC. Dissociated cells were seeded on 0.1 mg/mL poly-L-lysine (Sigma) and 4mg/mL laminin (Gibco)-coated dishes in Schwann cell medium (SCM) and maintained at 37ºC and 10% CO_2 atmosphere. SCM consists of: DMEM (Gibco) with10% FBS, 500 U/mL penicillin/500mg/mL streptomycin (Gibco), 0.5mM 3-iso-butyl-1-methilxantine (Sigma), 2.5 mg/mL insulin (Sigma), 10nM hereguline-b1 (PeproTech), and 0.5mM forskolin (Sigma).

Reprogramming of Vestibular Schwannomas

Between $0,2 \cdot 10^6$-$1 \cdot 10^6$ of VS derived cells were reprogrammed using the CytoTune™-iPS 2.1 Sendai Reprogramming Kit (Thermo Fisher Scientific), a non-integrative cell reprogramming method containing the four Yamanaka factors (OCT4, SOX2, KLF4, and cMYC), following manufacturer's instructions. Reprogramming was performed at the Barcelona Stem Cell Bank (B-SCB) and as previously described [35].

Tumour and iPSCs molecular characterization

Genetic analysis were performed using the customized I2HCP panel as previously described [36] or Whole Exome Sequencing (WES). The latter were performed using KAPA HyperCap technology with KAPA HyperExome Probes (Roche) according to manufacturer's instructions and sequenced in a NextSeq instrument (Illumina). Analysis of small nucleotide variants was performed with Strelka [37] and annotated with annovar [38]. We considered exonic and splicing variants with a population frequency (PopFreqMax) below 1%. Variants classified as

benign or likely benign in ClinVar were excluded. We evaluated Mutation Taster, CADD and VEST3 predictors, and we used scores higher than 19 and 0.8 in the las two, respectively, in order to identify likely pathogenic variants. To detect *NF2* splicing variants, tumours were studied both at RNA and DNA levels. *NF2* variants were validated by Sanger Sequencing. SNP-array analysis was assessed using Illumina HumanOmniExpress v1 BeadChips (730,525 SNPs) according manufacturers' instructions. Raw data was processed with Illumina Genome Studio v2011.1 with the Genotyping module v1.9.4. All samples were analysed independently and treated as unpaired samples.

Variant analysis

Human Genome Variation Society (www.hgvs.org) nomenclature guidelines were used to name the mutation at the DNA level, its effect at the mRNA level, and the predicted resulting protein. The first nucleotide of the ATG translation initiation codon is denoted position þ1 according to the *NF2* mRNA sequence NM_000268.3 5. and NM_016418.

CRISPR/Cas9 gene edition in iPSC lines

CRISPR/Cas9 editing was performed with the ArciTect ribonucleoprotein (RNP) system (STEMCELL Technologies). The designed sgRNA targeted exon 2 of the *NF2* gene (GTACACAATCAAGGACACAG). TransIT-X2® Dynamic Delivery System (Mirus) was used for transfection according manufacturers' instructions. gDNA from single-cell clones was analysed to screen *NF2* mutations. In order to study cis o trans variants in *NF2, NF2* cDNA was cloned using Gateway Technology (Invitrogen). iPSC lines obtained from reprogrammed vestibular Schwannomas and the control *NF2*(+/+) line used in this study (FiPS Ctrl 1-SV4F-7, obtained from the Spanish National Stem Cell bank (BNLC)) were used to obtain isogenic *NF2*(-/-) iPSC lines.

iPSC culture

iPSCs established lines were grown on coated dishes with growth factor-reduced Matrigel (1:20) (BD Biosciences) and cultured in mTESR Plus medium (STEMCELL Technologies). Splits were performed using Accutase (Merk) and cells were seeded 24h with Rock Inhibitor (1:1000) (STEMCELL Technologies). When required, visibly differentiated cells were removed manually.

iPSC characterization

Complete characterization of the pluripotent stem cells in this work was performed or is currently being performed at the B-SCB. Pluripotency-associated markers were assessed by immunocytochemistry with antibodies listed in **Supplemental Table S3.1**. Alkaline Phosphatase

Blue Substrate Solution (Sigma) was used to demonstrate iPSC alkaline phosphatase activity. iPSC karyotype was assessed by treating cells with colcemide (Gibco) and processed as described [39], at the Cytogenetics Platform of the Haematology Department at Germans Trias I Pujol Hospital (Badalona). Ability of the iPSCs to differentiate to the three germinal layers was assessed though embryoid body (EB) formation (further described below). RT-PCR was performed to confirm the absence of the Sendai reprogramming virus and transgene expression (**Supplemental Table S3.2**). Merlin expression was analysed by Western Blot using NF2/Merlin antibody (**Supplemental Table S3.1**), described below.

Embryoid body formation

Differentiation towards the three germ layers was performed as previously described [41] in the B-SCB. Endoderm was induced by plating embryoid bodies (EBs) in 0.1% gelatin (Millipore) coated coverslips in culture with KODMEM (Gibco) supplemented with 20% fetal bovine serum (Hyclone), 1x penicillin/streptomycin (Gibco), 1x Glutamax (Gibco), 0.05 mM 2-mercaptoethanol (Gibco), non-essential aminoacids (Lonza). The same medium was used for mesoderm induction, supplemented with 0.5 mM L-ascorbic acid (Sigma). EBs were cultured in N2B27 medium (Neurobasal:DMEM:F12 50:50 v/v, 1x N2 supplement, 1x B27 supplement, 1x Glutamax) supplemented with b-FGF in suspension to induce ectoderm differentiation. After 10 days, EBs were plated on Matrigel (Corning) and cultured for three weeks in N2B27 medium without b-FGF.

Western Blotting

Cells were lysed with RIPA buffer (50 mM Tris-HCl (pH 7.4), 150 mM NaCl, 1mM EDTA, 0.5% Igepal CA-630) supplemented with 3mM DTT (Roche), 1mM PMSF (Fluka), 1mM sodium orthovanadate (Sigma), 5mM NaF (Honeywell), 10 ug/ml leupeptin (Sigma), 5ug/ml aprotinin (Sigma) and 1xPhosSTOP (Roche). 50 μg of protein extracted from iPSC cell lines was loaded to SDS-PAGE (150V) and transferred onto PVDF membranes (1 hour 350 mA at 4°C). Odyssey Blocking Buffer TBS (LI-COR) was used to block the membranes. Primary antibodies were incubated at 4°C overnight. Membranes were later incubated with IRDye 680LT and IRDye 800CW secondary antibodies (1:1000 dilution, LI-COR) for 1h at room temperature and scanned and analysed using the Odyssey Infrared Imaging System (LI-COR). Western Blot primary antibodies used were α-NF2: NF2/Merlin antibody (ab88957) α-mouse (Abcam) to target merlin and α-vinculin [EPR8185] (ab129002) − α − rabbit (Abcam) was used to normalize protein expression among samples.

Neural Crest differentiation

Differentiation of iPSCs lines towards NCSC was performed as previously described in Menendez et al. (2013) with minor modifications [40]. $9x10^4$ iPS cells were seeded on matrigel-coated dishes in mTESR Plus medium. The following day, the medium was replaced with Neural Crest Differentiation Media, which is composed of the following: DMEM:F12 (Gibco) 1:1; 5mg/mL BSA (Sigma); 500U/mL penicillin/ 500mg/mL streptomycin (Gibco); 2mM GlutaMAX (Gibco); 1x MEM non-essential amino acids (Gibco); 1x trace elements A; 1x trace elements B; 1x trace elements C (Corning); 2-mercaptoethanol (Gibco); 10 mg/mL transferrin (Sigma); 50mg/mL sodium L-ascorbate (Sigma); 10ng/mL heregulin-b1 (PeproTech); 200mg/mL LONG R3 IGFR (PeproTech); 8ng/mL basic fibroblast growth factor 2 (PeproTech), 2mM CHIR9902 (STEMCELL Technologies) and 20mM SB432542 (STEMCELL Technologies).

Differentiation towards SCs in 2D

To stablish SC differentiation, $0.4x10^6$ NC cells/well were plated onto 0.1mg/mL poly-L- lysine (Sigma) and 4mg/mL laminin (Gibco) and cultured in SC differentiation media (SCDM) as previously described [41]. SCDM is composed of DMEM:F12 (3:1); 500U/ml penicillin/ 500mg/mL streptomycin antibiotics (Gibco); 5mM forskolin (Sigma); 50ng/mL heregulin-b1; 2% N2 supplement (Gibco); 1% FBS (Gibco). Medium was changed twice a week.

Differentiation towards SC in 3D

Neural crest cells were detached with Accutase and, $2.25·10^6$ NC cells/well were seeded onto AggreWell TM800 24-well plates (Stem Cell Technologies) in 2mL SCDM (described above), 1mL of SCDM was replaced twice a week.

Flow cytometry

Cells in PBS-0.1% BSA were incubated with p75 primary antibody, conjugated with Alexa Fluor 568 secondary antibody, and Hnk1 primary antibody and detected with Alexa Fluor 488-conjugated secondary antibody. Antibodies were incubated 30 min on ice. Cells were analysed by flow cytometry using BD LSR Fortessa SORP and BD FACS Diva 6.2 software.

Immunocytochemistry

Cells or spheroids were fixed in 4% para-formaldehyde in PBS for 15min at room temperature (RT), permeabilized with 0.1%Triton-X 100 in PBS for 10 min at RT, blocked in 10% FBS in PBS for 15 min at RT, stained with the indicated antibodies (**Supplemental Table S3.1**) and incubated overnight at 4ºC. Secondary antibodies Alexa Fluor 488 and Alexa Fluor 568 were incubated 1h

at RT. Nuclei were stained with DAPI and images captured using LEICA DMIL6000 and LASAF software.

RT-qPCR analysis

Total RNA was reverse-transcribed using SuperScript III reverse transcriptase (Invitrogen) and random hexamers (Invitrogen, City,). qPCRs were performed using Roche Universal Probe Library (UPL) technology and analysed using the Light-Cycler® 480 Real-Time PCR System (Roche Diagnostics) as previously described [41]. Two housekeeping reference genes were used to normalize gene expression (EP300 and TBP) and results are expressed as Normalized Relative Expression (NRE). Primer sequences used are listed in **Supplemental Table S3.3**.

3. Results

Generation of induced pluripotent stem cells derived from vestibular schwannomas

Three VSs from NF2 patients meeting standard diagnostic criteria [28,42] were used for reprogramming (VS-25, VS-245 and VS-267). Molecular characterization of these tumours through the I2HCP panel [36] or Whole exome sequencing (WES) and SNP-array, uncovered *NF2* alterations reported in **Table 3.1.** WES analysis was performed for VS-25 and VS-245 and is currently being analysed for VS-267 (**Supplemental Tables S3.4 and S3.5**). No pathogenic variants were identified in known oncogenes or other tumour suppressor genes, as previously reported for VSs [43]. SNP-array analysis showed loss of heterozygosity (LOH) on chromosome 22q in VS-25, without the presence of complex rearrangements in any of the tumours analysed (**Supplemental Figure S3.4**).

Table 3.1. Information of patients and reprogramed tumours					
Patient ID	**Sex**	**Age at SV resection**	***NF2* Germline Mutation**	**Diagnostic**	***NF2* Somatic Mutation**
25	XY	48	g.83045A>G	NF2	LOH
245	XY	23	g.73341insG	Mosaic NF2	g.76297C>T
267	XY	15	g.62758C>T	NF2	g.73394G>A

The Sendai virus (SeV) vector encoding Yamanaka factors was used to induce pluripotency to dissociated cells of VSs, with the aim of generating iPSC *NF2* (-/-) clones that could recapitulate the genetic background of Schwann cells involved in tumorigenesis.

After VSs reprogramming, we determined the *NF2* genotype through Sanger sequencing of 38 clones for VS-25, 10 clones for VS-245 and 12 for VS-267 (**Supplemental Table S3.6**). From VS-25 and VS-267, only clones with the germline *NF2* pathogenic variant, *NF2* (+/-), were obtained. A clone derived from each tumour was selected for further characterization, referred as VSi-25(+/-) and VSi-267(+/-) from this point onwards. From VS-245, a resected tumour of a mosaic patient, *NF2* (+/+) and *NF2* (-/-) iPSC clones were obtained, for which selected clones were named as VSi-245(+/+) and VSi-245(-/-). SNP-array analysis of iPSCs selected clones showed no differences with respect to the tumour of origin, with the exception of VS-25 which had LOH on chromosome 22q as the second hit and clones obtained from this tumour only harboured the germline *NF2* variant, thus, not showing this alteration (**Supplemental Figure S3.4**).

The VSi-245(+/+) clone, since reprogrammed from an unaffected cell of the patient, was not further characterized. Distinctively, VSi-245(-/-) clones, harbouring the bi-allelic inactivation of *NF2*, showed to be Sendai-dependent even after 40 passages after reprogramming. Although SeV is a non-integrative retrovirus widely used for reprogramming which expression is lost due to dilution of the viral genome, no *NF2* (-/-) clones could be established directly from VSs without the presence of SeV over time. In addition, VSi-245(-/-) iPSCs showed aberrant morphologies and with a pronounced tendency to form aggregates, entailing complex experimental manipulation. VSi-245(-/-) was further characterized and differentiated through the NC-SC lineage (see full characterization in **Supplemental Material**). However, considering the aberrant morphology of these clones and the maintenance of the expression of SeV and the exogenous reprogramming genes, we determined that these iPS cells did not constitute a suitable study model.

Given the low efficiencies obtained in the generation of *NF2* (-/-) clones, their aberrant morphology and their dependence on exogenous reprogramming genes, we hypothesized that *NF2* was essential for the generation of iPSCs. Thus, it was suggested to edit the *NF2* gene from a pluripotency state.

Generation of isogenic *NF2* (-/-) iPSC lines through CRISPR/Cas9 gene editing

In order to obtain *NF2* (-/-) iPSC lines, we decided to edit the established tumour-derived iPSC lines as well as a control iPSC line (FiPS, *NF2*(+/+)) using CRISPR/Cas9 technology to target exon 2 of *NF2.*

Through the generation of single cell clones after the CRISPR/Cas9 edition, we obtained *NF2* (-/-) iPSC clones from tumour-derived lines (25-CasD7$^{(-/-)}$ from VSi-25$^{(+/-)}$, and 267-CasD2$^{(-/-)}$ from VSi-267$^{(+/-)}$) and isogenic *NF2* (+/-) and *NF2* (-/-) iPSC clones from the control line (FiPS-CasB2$^{(+/-)}$ and FiPS-CasH6$^{(-/-)}$). Pathogenic variants in *NF2* were fully characterized through PCR and Sanger sequencing and for each of them, the coding region of *NF2* was cloned to confirm compound heterozygous clones.

From this point on, we worked in the characterization of six iPSC lines: three with one pathogenic variant in *NF2* (two of which were obtained from VS reprogramming and one from the editing of unaffected control cells) and three carrying the bi-allelic inactivation of *NF2* (derived from the previous three). The FiPS line was used for all experiments as a control (*NF2* (+/+)). Information of the generated cell lines and the characterization of *NF2* genetic variants is detailed in **Table 3.2**.

Table 3.2. iPSCs lines information						
Generation method	Reprogramming VS		Editing iPSCs from VS		Editing FiPS Ctrl 1-SV4F-7	
iPS Cell line	**VSi-25**	**VSi-267**	**VSi-25-CasD7**	**VSi-267-CasD2**	**FiPS-CasB2**	**FiPS-CasH6**
NF2 **Genotype**	c.1736A>G	c.784C>T	Allele A: c.211dupA Allele B: c.212_213delCA and c.1736A>G *NF2* **(-/-)**	c. 212_213delCA c.784C>T *NF2* **(-/-)**	c.212_213delCA *NF2* **(+/-)**	c.211dupA c.212_213delCA *NF2* **(-/-)**
	NF2 **(+/-)**	*NF2* **(+/-)**				
p.	p.Lys529Asnfs*19	p.Arg262*	Allele A: p.Thr71Asnfs*15 Allele B: p.Thr71Serfs*14 p.Lys529Asnfs*19	p.Thr71Serfs*14 p.Arg262*	p.Thr71Serfs*14	p.Thr71Asnfs*15 p.Thr71Serfs*14
Effect	Splicing *NF2* (+/-)	Truncating *NF2* (+/-)	Splicing and truncating *NF2* (-/-)	Truncating *NF2* (-/-)	Truncating *NF2* (+/-)	Truncating *NF2* (-/-)
Affected exons	15	8	2 and 15	2 and 8	2	2

NF2 (+/-) and *NF2* (-/-) iPSC characterization

VS-iPSC derived clones were characterized at the Barcelona Stem Cell Bank (B-SCB). They expressed surface and transcription factors associated with pluripotency: Nanog, Tra-1-81, Oct4, SSEA-3 and Sox2 (**Figure 3.1A**) and showed karyotype stability after at least 20 passages (46, XY) (**Figure 3.1B**). They showed classical iPSC colony morphology (**Figure 3.1C**) and were positive for alkaline phosphatase staining (**Figure 3.1D**). The capacity to differentiate to the three primary germ layers *in vitro* (mesoderm, endoderm, ectoderm) was also assessed (**Figure 3.1E**). iPSC edited lines expressed the Oct4 pluripotency marker (**Figure 1A**, lower panels) and showed karyotypic stability (**Figure 3.1B**), although are currently under extended characterization at the B-SCB.

Morphology of *NF2* (-/-) iPSC colonies in culture showed some distinctive traits: *NF2* deficient clones presented less compact colony formation, eventually grew upwards and underwent major spontaneous differentiation compared with the iPSC control line (**Figure 3.1C**). Notably, the 267-CasD2$^{(-/-)}$ line required removal of visibly differentiated cells before each passage. Despite requiring particular culture conditions, these clones maintained a pluripotent morphology over time without the addition of external pluripotency markers. With the current evidence, the observed alterations in *NF2* (-/-) iPSC clones could be associated with the loss of *NF2* gene.

Merlin expression was assessed to confirm the genotype and revealed, as expected, that *NF2* (+/-) lines expressed half the levels of merlin compared with the control and that *NF2* (-/-) iPSC lines showed no expression of the protein (**Figure 3.1F**).
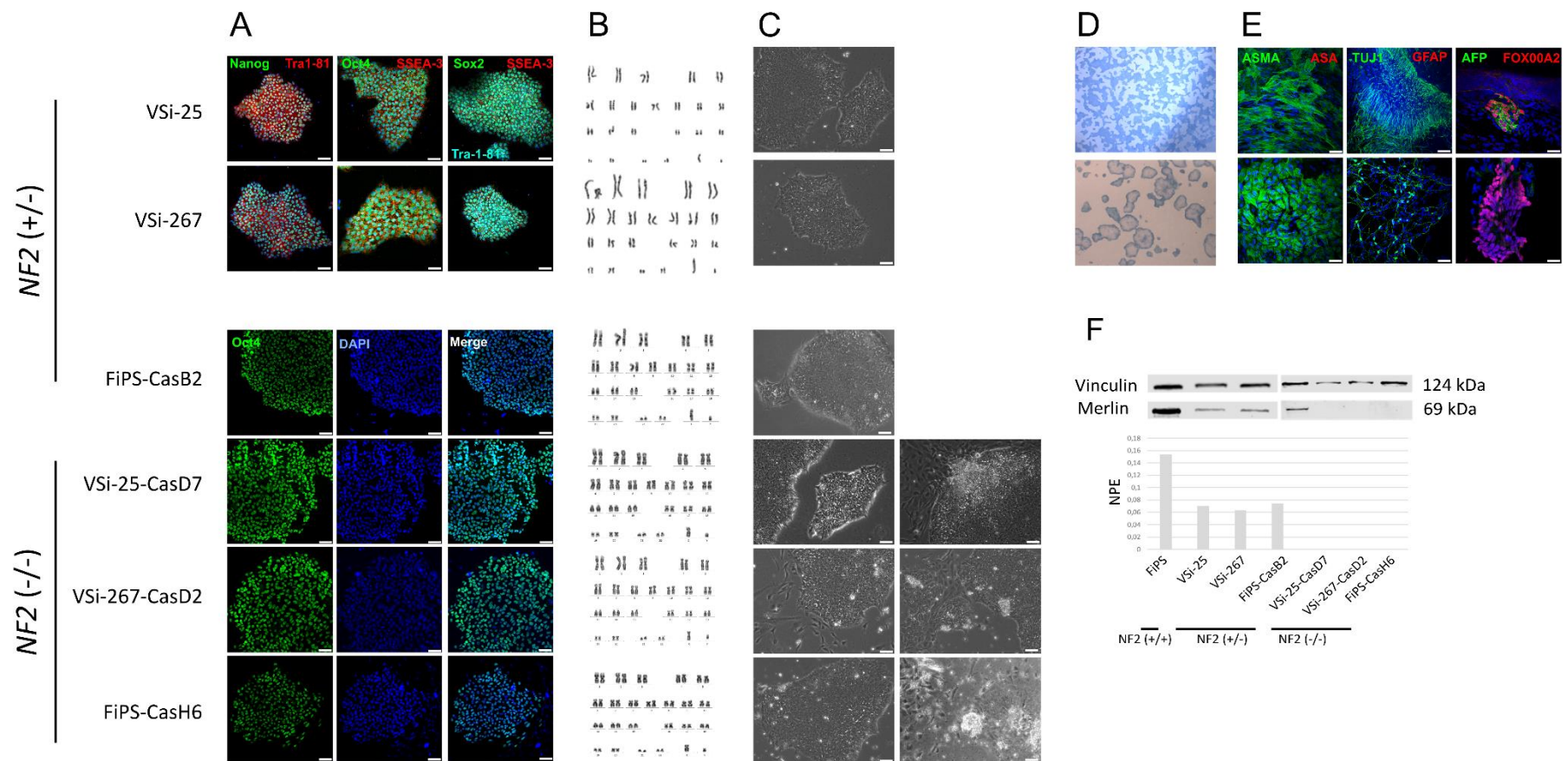
Figure 3.1. Characterization of iPSC lines. (A) Immunochemistry of pluripotency markers NANOG, OCT4, and SOX2 (in green), TRA-1-81, SSEA3 (in red); Scale bar, 75μM; Cell nuclei were stained DAPI; (B) Alkaline Phosphatase (ALP) Staining; (C) Karyotype of lines at passage 20 (46, XY); (D) Immunochemistry to demonstrate the capacity of the lines to *in vitro* differentiate to the three primary germ layers: mesoderm (ASMA in green and ASA in red), ectoderm (TUJ1 in green and GFAP in red) and endoderm (AFP in green and FOXA2 in red); Scale bar, 75μM; (E) Morphology of the cell colonies, Scale bar, 75μM; (F) Merlin expression analysed by Western Blot. The FiPS line generated from fibroblasts (*NF2* +/+) was used as a control cell line, NPE stands for Normalized Protein Expression.

Neural Crest differentiation from *NF2* (+/-) and *NF2* (-/-) iPSCs

The aim of this work was to obtain an unperishable Schwann-like cell model that genetically resembled cells composing VSs. With this purpose, iPSC lines were first differentiated towards a Neural Crest (NC) identity using a chemically defined medium, as previously reported [41], that mediates activation of Wnt singling and inhibition of TGFβ/activin/nodal signalling.

Cell morphology changed as days of differentiation progressed, achieving NC morphology approximately ten days after the initiation of the differentiation protocol (**Figure 3.2A**). Cell identity was first assessed by flow cytometry of NC characteristic markers, NGFR (p75) and Hnk, at early passages of the NC differentiation process (p4) and in a mature NC state (p8). The assay revealed that *NF2* (+/-) NC lines derived from VSs showed around >90% of cells expressing both markers, similar to the *NF2* (+/+) control line, although a lower percentage was detected for the edited *NF2* (+/-) NC line (FiPS-CasB2). Distinctively, reduced expression of p75 and Hnk was detected among the *NF2* deficient lines, with the average percentage of the three standing in 76,3%, showing more heterogeneity and a delayed capacity to differentiate (**Figure 3.2B**). Still, there was significant population expressing both p75 and Hnk.

Cell identity was further characterized through immunocytochemistry (**Figure 3.2C**), showing that all lines stained positive for the NC markers Sox10, AP2 and p75 and there was no expression of the pluripotency marker Oct4. Some cells from the NC culture of the *NF2* (-/-) lines were positive for S100B, a well characterized SC marker, correlating with the heterogeneity detected in cytometry assays. Differences of merlin-deficient NC cells were also observed in culture, as these required passages with low dilutions (1:2) to maintain a NC cell morphology.

Therefore, *NF2* (+/-) clones could be efficiently differentiated towards a NC identity although some differences were observed in the edited iPSC line FiPS-CasB2. On the other hand, *NF2* (-/-) NC-derived cultures required extensive care to maintain a NC morphology and showed alterations during differentiation, suggesting that *NF2* could have a relevant role for a successful differentiation towards a NC cell identity.
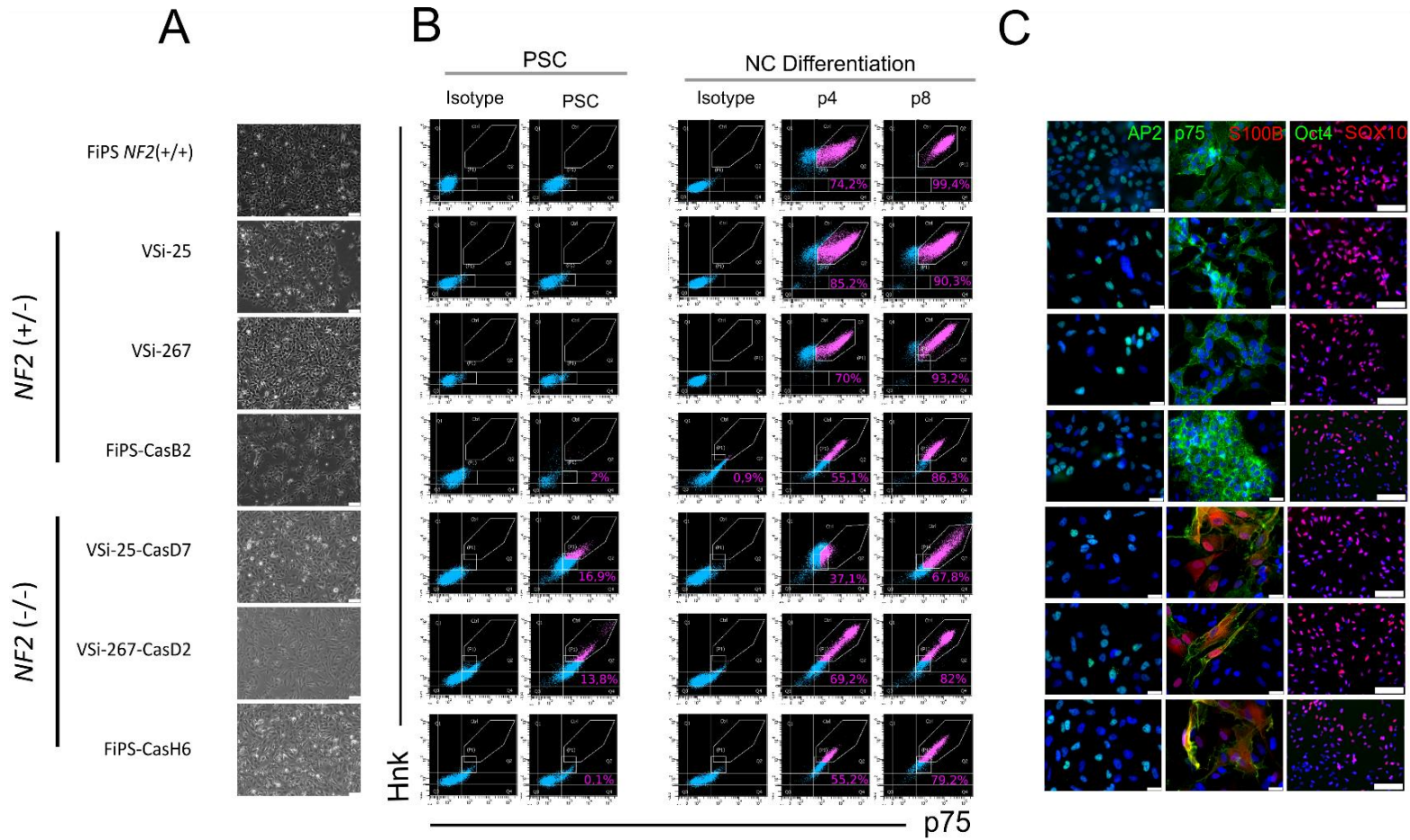
Figure 3.2. Neural Crest Characterization. (A) NC Morphology of *NF2* (+/-) and *NF2* (-/-) cell lines; Scale bar, 75µM; (B) Flow cytometry assays of the NC markers NGFR (p75) and Hnk1. The percentage of p75 and Hnk1-positive cells is shown in pink. P4 and P8 stand for passages 4 and 8, respectively; (C) Immunocytochemistry of AP2 (green), p75 (green) and S100B (red), Scale bars, 25µM; Oct4 (green) and SOX10 (red), Scale bar, 100µM; DAPI (blue) was used to stain cell nuclei.

Schwann Cell Differentiation of *NF2* (+/-) and *NF2* (-/-) from derived-NC cultures

The next step consisted of differentiating the established NC cultures towards a SC state. Thus, these cells were cultured in SC differentiation medium during 30 days, as previously described [41]. Three time points (7, 14 and 30 days) of the differentiation protocol were monitored through qRT-PCR assays and immunocytochemistry.

During the differentiation process towards a SC identity, significant differences were observed between the control line and the *NF2* (+/-) or *NF2* (-/-) lines, as barely five days after implementing the SC differentiation protocol, these presented difficulties in maintaining adherence to cell culture, in contrast to the control line, which already after seven days showed more elongated morphology resembling SC-like cells (**Supplemental Figure S3.5**). Lines VSi-25[(+/-)] and VSi-267[(+/-)] could be further characterized by RT-qPCR and immunocytochemistry as it was possible to maintain the culture during the 30 days of the protocol (**Figure 3.3**). Both cell lines showed expression of SOX10 and NGFR, characteristic markers of the NC-SC lineage. Furthermore, both lines managed to express SC precursor markers (IGTA4, CDH19, MPZ). GAP43 was expressed from the NC stage until the 30 days of differentiation, resembling the expression of the control line. The regulator of myelination EGR2 was expressed over the 30 days and both lines succeed in expressing SC markers at day 30 (PLP1, PMP22 and S100B) (**Figure 3.3A**). Immunocytochemistry assays showed expression of p75 and S100B at the three-point times studied of the SC differentiation protocol (**Figure 3.3B**). SC differentiating cells of both lines showed tendency to form aggregates and detached from the culture plate continuously.

For the rest of the lines, at seven days of culture most cells were completely detached and could not be further characterized. Thus, the poor adherence capacity compromised the ability of these cells to differentiate towards a SC identity. As described above, *NF2* (+/-) cell lines derived from VSs were able to reach the end of the differentiation protocol, although with clear alterations when compared with the control line. Here, the edited *NF2* (+/-) cell line showed again inconsistencies when compared with the other *NF2* (+/-) cell lines, as observed throughout NC differentiation. On the other hand, SC differentiation of *NF2* deficient lines, under the determined conditions, could not be accomplished.
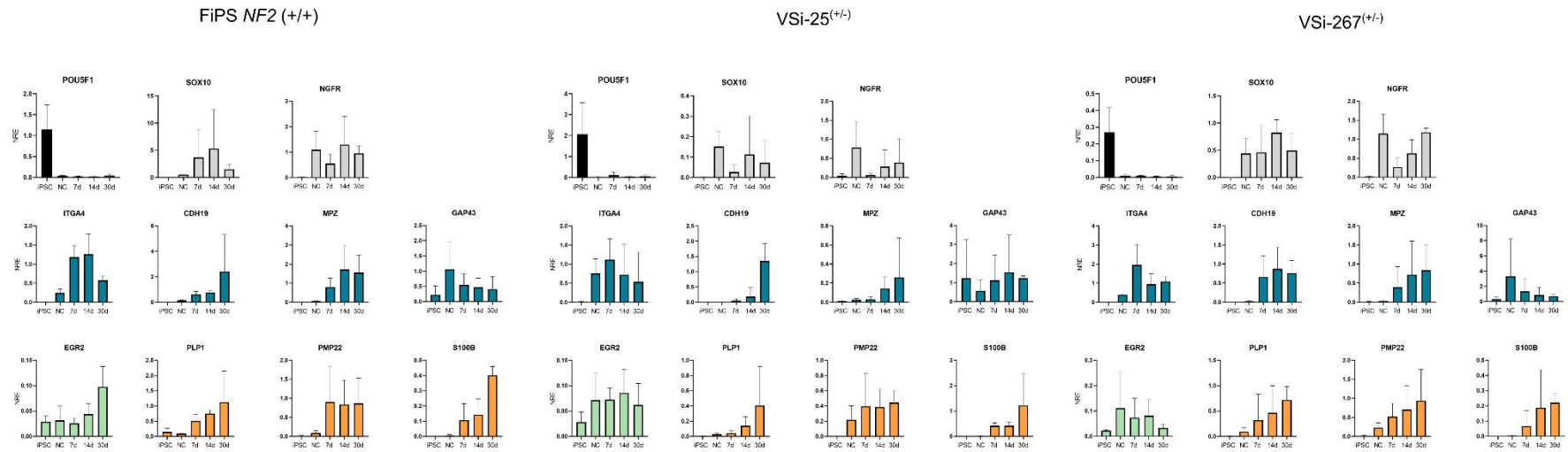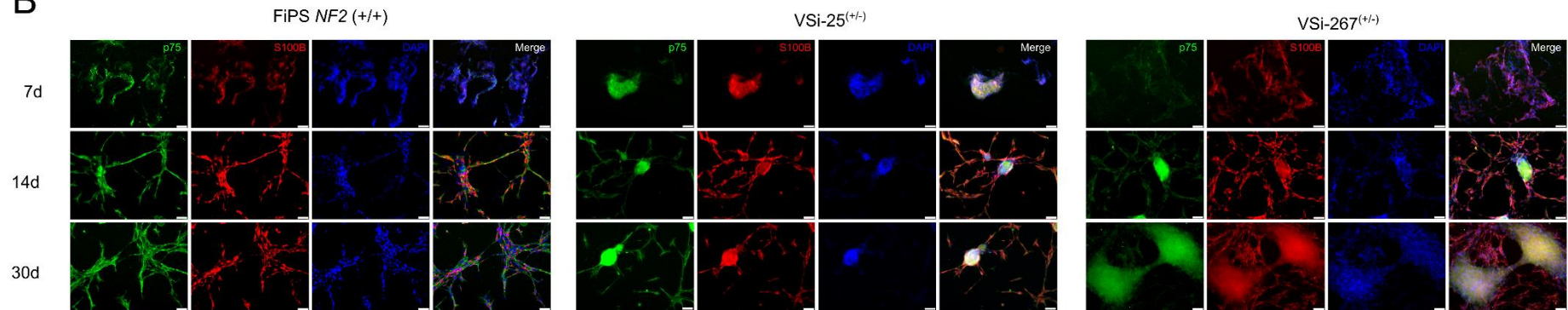
Figure 3.3. Characterization of VSi-25(+/-) and VSi-267(+/-) Schwann Cell Differentiation. (A) RT-qPCR analysis of classical markers of the SC-differentiation linage during five points of the differentiation protocol: iPSC, NC and SC differentiation at points 7, 14 and 30 days (7d, 14d and 30d). FiPS *NF2* (+/+) was used as a control. Bars represent the mean of NRE (Normalized Relative Expression) ±SEM of three independent experiments; (B) Immunochemistry of p75 (green) and S100B (red) markers at the time points of 7, 14 and 30 days; Scale bar, 75µM.

Schwann Cell Differentiation of *NF2* (+/-) and *NF2* (-/-) from derived NC in 3D

Considering the detachment behaviour of *NF2* mutant cells in the differentiation into SC, we tested the growth and differentiation capacity towards SC in 3D cultures, following the protocol established by Mazuelas et al. (2022) [44] with minor modifications. In brief, NC cells were seeded in uncoated culture plates during 30 days in SC differentiation medium. This procedure was monotorized at three time points (7, 14 and 30 days) through RNA-seq and immunocytechemistry analysis.

Control *NF2* (+/+) differentiating cells showed capacity to grow as spheroids and high expression of p75 and S100B markers after 7 days of differentiation, that was maintained throughout the 30 days of the protocol (**Figure 3.4A**). Both VSi-25$^{(+/-)}$ and VSi-267$^{(+/-)}$ lines succeeded in establishing spheroids that expressed p75 and S100B markers (**Figure 3.4A**). However, we were unable to obtain spheroids from the edited FiPS-CasB2($^{+/-}$) clone (**Supplemental Figure S3.6**). The three *NF2* (-/-) lines did manage to generate spheroids that highly expressed p75 and S100B markers after 7 days of SC differentiation and expression was maintained over 30 days. Further characterization of the generated spheroids from three independent experiments is currently being assessed through RNA-seq analysis.

Up to this point, the application of the 3D SC differentiation protocol resulted a successful approach for *NF2* deficient clones. We have been able to generate *NF2* (+/-) and *NF2* (-/-) spheroids that express classical markers of the NC-SC differentiation axis. Further transcriptome characterization will reveal if these could constitute SC-like spheroids to model NF2.

Overall, in this study we have generated *NF2* (+/-) and *NF2* (-/-) iPSCs lines through reprogramming VSs and *NF2* editing with CRISPR/Cas9. When these cells were differentiated into NC cells, *NF2* deficient cells denoted an altered differentiation capacity, showing heterogeneity in the expression of NC classic markers and spontaneous expression of S100B. In addition, these could not generate Schwann cells in 2D cultures. Thus, merlin-deficient cells showed an altered differentiation capacity towards de NC-SC axis, in the determined *in vitro* conditions. Through the application a 3D Schwann cell differentiation protocol, we have been able to generate *NF2* (+/-) and *NF2* (-/-) spheroids that successfully expressed the p75 and S100B markers, suggesting that these potentially represent a VS model (**Figure 3.4B**).
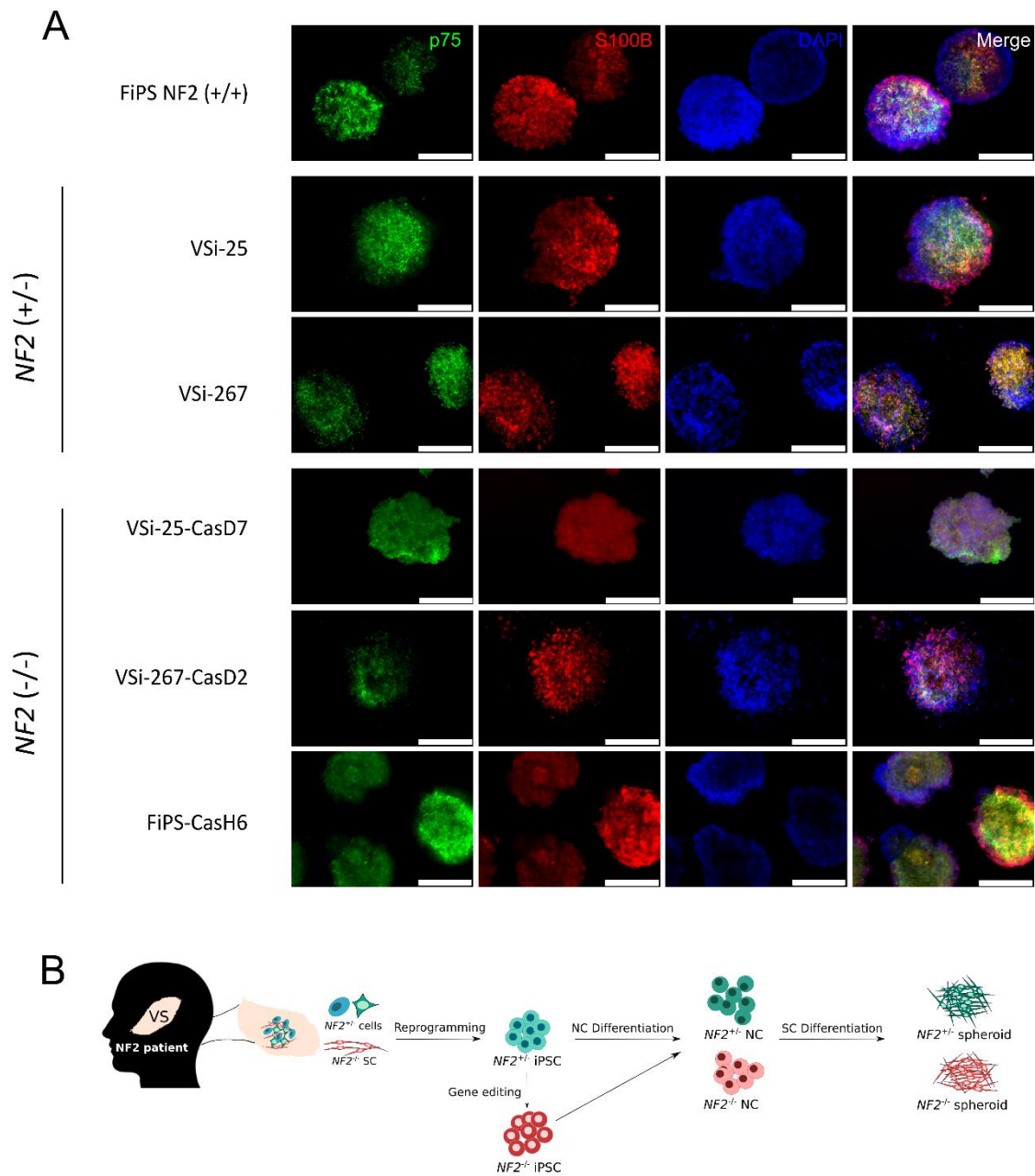
Figure 3.4. Schwann Cell Differentiation in 3D cultures. (A) Immunochemistry of p75 (green) and S100B (red) after 14 days of SC differentiation, Scale bar, 250µM. (B) Schematic representation of the experimental process.

4. Discussion

Bilateral vestibular schwannomas (VSs) are the main trait of Neurofibromatosis Type 2 (NF2), an autosomal dominant condition that predisposes to the development of nervous system neoplasia through the loss of function of the *NF2* gene [7]. VSs arise from a cell of the Schwann Cell (SC) lineage at the vestibular nerve, causing NF2 patients hearing loss or deafness, tinnitus, facial paraesthesia or vertigo [45]. There is the need to understand how these tumours originate and progress to be able to develop therapies that prevent their formation and growth. Currently, there is the possibility to derive primary cultures from the cells composing these tumours or use immortalized cell lines to study their pathogenicity. However, the limited number of passages that primary cells can achieve or the physiological changes that immortalization can impose to primary cells limit its use in experiments requiring many cells or a genuine resemblance to schwannoma cells, respectively.

In this study we have been able to generate *NF2* (+/-) and *NF2* (-/-) iPSC lines from a combination of direct reprogramming of VS cells and *NF2* gene editing. Specifically, it was possible to generate *NF2* (+/-) lines derived from two tumours (VS-25 and VS-267), and a *NF2* (-/-) line derived from a VS of a NF2 mosaic patient (VS-245), which maintained the expression of the non-integrative Sendai virus used for the reprogramming in the 9 clones analysed. Contrary to the previous experience in the generation of iPSCs derived from other NF2-independent SC arising tumours (plexiform neurofibromas) [41], it has not been possible to generate iPSCs derived from VSs with the bi-allelic inactivation of *NF2*. We hypothesize that *NF2* may have an inherent property required during the reprogramming process of the cells, related to its essential role in embryogenesis and early stages of development [19,46,47]. In our hands, generation of iPSC clones harbouring loss of *NF2* function was not viable, in accordance with what has been observed in other studies [46]. However, further evidences would be needed to support our findings and reach a definitive conclusion.

Through gene editing, we have demonstrated that once reprogrammed, pluripotency can be achieved in absence of *NF2,* both in VSs-derived and fibroblast-derived iPSCs, as recently reported [48]. However, the three *NF2* (-/-) iPSC lines required extensive experimental manipulation, showed aberrant morphologies with tendency to grow upwards and form aggregates, and were subjected to spontaneous differentiation. These observations suggest that the *NF2* gene could be responsible for these altered patterns, thus, it could have a relevant role in maintaining pluripotency. Despite all the inconveniences, the iPSCs lines generated in this study could constitute an inexhaustible source of cells harbouring single or bi-allelic inactivation

of *NF2,* that under determined culture conditions, could be used as a cellular model to develop further assays [49].

After testing the possibility of reprogramming VS and editing *NF2* in a pluripotent state, we assessed if the generated iPSCs lines could be differentiated towards the NC-SC axis. In the first step of differentiation, we showed that both *NF2* (+/-) and *NF2* (-/-) cells have the capacity to differentiate to a NC identity, although some dissimilarities were detected. While *NF2* (+/-) lines derived from VS showed high expression of NC markers, at this stage we identified distinctive features in the behaviour of the edited (*NF2* +/-) line with respect to the other two with which it shares the *NF2* genotype, as this line demonstrated reduced expression of the NC markers p75 and Hnk, that will be further discussed. In *NF2* (-/-) NC cultures, we detected more heterogeneity in the expression of NC markers by flow cytometry assays. These NC-derived cells showed a delayed differentiation capacity towards a NC identity and the expression of a classic SC marker (S100B). In addition, we highlight that iPSC-derived NCs with loss of *NF2* function seemed to require closer cell-cell contact to maintain this identity. Since this work is based in isogenic lines, we could attribute these differences to *NF2* deficiency, although further assays to assess expression profiles and multipotent capacity of the NC derived cultures should be performed.

The last aim of the work consisted of finding a cellular identity that resembled the cells from where VSs arise, and these are from the Schwann cell (SC) lineage. In the process of differentiation to SC from the established NC, we observed that both *NF2* (+/-) and *NF2* (-/-) cell lines were detached from the cell culture surface, eventually leading to cell death and preventing NC to generate SCs. Since the *NF2* gene product, merlin, is a tumour suppressor protein reported to be involved in cell-cell contact [50,51], we hypothesized that its function could be most notably required, or essential, in the differentiation process from NC to a SC stage in 2D cultures *in vitro*.

Thereafter, we performed a SC differentiation protocol in 3D so that SC-like cells spheroids could grow in suspension [44]. We succeed in generating spheroids from the control cell line (*NF2* +/+) that expressed classical SC markers already after seven days in SC differentiation medium, although we observed variability among *NF2* mutant cell lines. Two *NF2* (+/-) lines were able to reproduce the behaviour of the control line, while the line FiPS-CasB2[(+/-)] showed no viability to grow in suspension. Again, performance of this line differed from the other two *NF2* (+/-) lines. In light of all the results, and considering that this line was generated via CRISPR/Cas9 gene editing, we suggest the importance of performing WES or WGS (Whole Genome Sequencing) analysis to detect possible editing off-target effects, which could account for inconsistencies

found in this line throughout the study. If an off-target effect is confirmed, this line would not be eligible as a cellular model.

NF2 (-/-) lines were able to generate spheroids that co-expressed the well characterized NC-SC lineage markers p75 and S100B. Transcriptome analysis of these spheroids is currently being performed for the further characterization of these cells' identity. In addition, this assay could allow the identification of a putative differential expression of *NF2* (+/-) and *NF2* (-/-) spheroids and reveal relevant roles of the *NF2* gene.

Finally, it may be concluded that we generated *NF2* (+/-) and *NF2* (-/-) iPSC lines from reprogramming VS and gene editing. In our experience, the *NF2* gene seems to have a relevant role in reprogramming and in the maintenance of pluripotency. These cells were differentiated into NC cells, although *NF2* (-/-) cultures showed an altered differentiation capacity. The application of a 3D SC differentiation protocol resulted in the successful generation of *NF2* (+/-) and *NF2*(-/-) spheroids expressing NC-SC lineage markers (p75 and S100B). Transcriptome characterization will determine whether these spheroids constitute a valuable resource to assess the role of *NF2* in the biology of the tumours, study VSs pathogenicity and test therapeutic approaches for NF2 related tumours.

5. Acknowledgements

6. References

1   Evans DGR, Moran A, King A, *et al.* Incidence of vestibular schwannoma and neurofibromatosis 2 in the North West of England over a 10-year period: Higher incidence than previously thought. *Otology and Neurotology* 2005;**26**:93–7. doi:10.1097/00129492-200501000-00016

2   McClatchey AI, Giovannini M. Membrane organization and tumorigenesis - The NF2 tumor suppressor, Merlin. *Genes and Development* 2005;**19**:2265–77. doi:10.1101/gad.1335605

3   Gladden AB, Hebert AM, Schneeberger EE, *et al.* The NF2 Tumor Suppressor, Merlin, Regulates Epidermal Development through the Establishment of a Junctional Polarity Complex. *Developmental Cell* 2010;**19**:727–39. doi:10.1016/j.devcel.2010.10.008

4   Petrilli AM, Fernández-Valle C. Role of Merlin/NF2 inactivation in tumor biology. *Oncogene* 2015;**35**:537–48. doi:10.1038/onc.2015.125

5   Evans DG, Bowers NL, Tobi S, *et al.* Schwannomatosis: a genetic and epidemiological study. *Journal of Neurology, Neurosurgery & Psychiatry* 2018;**89**:1215–9. doi:10.1136/jnnp-2018-318538

6   Evans DGR, Huson SM, Donnai D, *et al.* A genetic study of type 2 neurofibromatosis in the United Kingdom. I. Prevalence, mutation rate, fitness, and confirmation of maternal transmission effect on severity. *Journal of Medical Genetics* 1992;**29**:841–6. doi:10.1136/jmg.29.12.841

7   Evans DGR, Huson SM, Donnai D, *et al.* A genetic study of type 2 neurofibromatosis in the United Kingdom . II . Guidelines for genetic counselling. 1992;:847–52.

8   Parry DM, Eldridge R, Kaiser-Kupfer MI, *et al.* Neurofibromatosis 2 (NF2): Clinical characteristics of 63 affected individuals and clinical evidence for heterogeneity. *American Journal of Medical Genetics* 1994;**52**:450–61. doi:10.1002/ajmg.1320520411

9   Baser ME, Makariou E v., Parry DM. Predictors of vestibular schwannoma growth in patients with neurofibromatosis Type 2. *Journal of Neurosurgery* 2002;**96**:217–22. doi:10.3171/jns.2002.96.2.0217

10   Forde C, King AT, Rutherford SA, *et al.* Disease course of neurofibromatosis type 2: A 30-year follow-up study of 353 patients seen at a single institution. *Neuro-Oncology* 2021;**23**:1113–24. doi:10.1093/neuonc/noaa284

11   Ragge NK, Baser ME, Klein J, *et al.* Ocular abnormalities in neurofibromatosis 2. *American Journal of Ophthalmology* 1995;**120**:634–41. doi:10.1016/S0002-9394(14)72210-X

12   Plana-Pla A, Bielsa-Marsol I, Carrato-Moñino C. Diagnostic and Prognostic Relevance of the Cutaneous Manifestations of Neurofibromatosis Type 2. *Actas Dermo-Sifiliograficas* 2017;**108**:630–6. doi:10.1016/j.ad.2016.12.007

13   Hexter A, Jones A, Joe H, *et al.* Clinical and molecular predictors of mortality in neurofibromatosis 2: a UK national analysis of 1192 patients. *Journal of Medical Genetics* 2015;**52**:699–705. doi:10.1136/jmedgenet-2015-103290

14   Dirks MS, Butman JA, Kim HJ, *et al.* Long-term natural history of neurofibromatosis Type 2-associated intracranial tumors: Clinical article. *Journal of Neurosurgery* 2012;**117**:109–17. doi:10.3171/2012.3.JNS111649

15   Peyre M, Goutagny S, Bah A, *et al.* Conservative management of bilateral vestibular schwannomas in neurofibromatosis type 2 patients: Hearing and tumor growth results. *Neurosurgery* 2013;**72**:907–13. doi:10.1227/NEU.0b013e31828bae28

16   Baser ME, Mautner VF, Parry DM, *et al.* Methodological issues in longitudinal studies: Vestibular schwannoma growth rates in neurofibromatosis 2. *Journal of Medical Genetics* 2005;**42**:903–6. doi:10.1136/jmg.2005.031302

17   Lloyd SKW, Evans DGR. *Neurofibromatosis type 2 (NF2): diagnosis and management.* 1st ed. Elsevier B.V. 2013. doi:10.1016/B978-0-444-52902-2.00054-0

18   Plotkin SR, Duda DG, Muzikansky A, *et al.* Multicenter, prospective, phase II and biomarker study of high-dose bevacizumab as induction therapy in patients with neurofibromatosis type 2 and progressive vestibular schwannoma. *Journal of Clinical Oncology* 2019;**37**:3446–54. doi:10.1200/JCO.19.01367

19   McClatchey AI, Saotome I, Ramesh V, *et al.* The Nf2 tumor suppressor gene product is essential for extraembryonic development immediately prior to gastrulation. *Genes and Development* 1997;**11**:1253–65. doi:10.1101/gad.11.10.1253

20   McClatchey AI, Saotome I, Mercer K, *et al.* Mice heterozygous for a mutation at the Nf2 tumor suppressor locus develop a range of highly metastatic tumors. *Genes and Development* 1998;**12**:1121–33. doi:10.1101/gad.12.8.1121

21   Stemmer-Rachamimov AO, Louis DN, Nielsen GP, *et al.* Comparative pathology of nerve sheath tumors in mouse models and humans. *Cancer Research* 2004;**64**:3718–24. doi:10.1158/0008-5472.CAN-03-4079

22   Giovannini M, Robanus-Maandag E, Van Der Valk M, *et al.* Conditional biallelic Nf2 mutation in the mouse promotes manifestations of human neurofibromatosis type 2. *Genes and Development* 2000;**14**:1617–30. doi:10.1101/gad.14.13.1617

23   Ren Y, Chari DA, Vasilijic S, *et al.* New developments in neurofibromatosis type 2 and vestibular schwannoma. *Neuro-Oncology Advances* 2021;**3**:1–13. doi:10.1093/noajnl/vdaa153

24   Dilwali S, Patel PB, Roberts DS, *et al.* Primary culture of human Schwann and schwannoma cells: Improved and simplified protocol. *Hearing Research* 2014;**315**:25–33. doi:10.1016/j.heares.2014.05.006

25   Rosenbaum C, Kluwe L, Mautner VF, *et al.* Isolation and Characterization of Schwann Cells from Neurofibromatosis Type 2 Patients. 1998.

26   Xue L, He W, Wang Z, *et al.* Characterization of a newly established schwannoma cell line from a sporadic vestibular schwannoma patient. *American Journal of Translational Research* 2021;**13**:8787–803.

27   Hung G, Li X, Faudoa R, *et al.* Establishment and characterization of a schwannoma cell line from a patient with neurofibromatosis 2. *International journal of oncology* 2002;**20**:475–82. doi:10.3892/ijo.20.3.475

28   Takahashi K, Yamanaka S. Induction of Pluripotent Stem Cells from Mouse Embryonic and Adult Fibroblast Cultures by Defined Factors. 2006;**2**:663–76. doi:10.1016/j.cell.2006.07.024

29   Lim WF, Inoue-Yokoo T, Tan KS, *et al.* Hematopoietic cell differentiation from embryonic and induced pluripotent stem cells. *Stem Cell Research and Therapy* 2013;**4**. doi:10.1186/scrt222

30   Yoshida Y, Yamanaka S. Induced Pluripotent Stem Cells 10 Years Later. *Circulation Research* 2017;**120**:1958–68. doi:10.1161/CIRCRESAHA.117.311080

31   Mungenast AE, Siegert S, Tsai LH. Modeling Alzheimer's disease with human induced pluripotent stem (iPS) cells. *Molecular and Cellular Neuroscience* 2016;**73**:13–31. doi:10.1016/j.mcn.2015.11.010

32   Chang CY, Ting HC, Liu CA, *et al.* Induced pluripotent stem cell (iPSC)-based neurodegenerative disease models for phenotype recapitulation and drug screening. *Molecules* 2020;**25**:1–21. doi:10.3390/molecules25082000

33   Nourbakhsh A, Gosstola NC, Fernandez-Valle C, *et al.* Characterization of UMi031-A-2 inducible pluripotent stem cell line with a neurofibromatosis type 2-associated mutation. *Stem Cell Research* 2021;**55**:102474. doi:10.1016/j.scr.2021.102474

34   Baser ME, Friedman JM, Wallace AJ, *et al.* Evaluation of clinical diagnostic criteria for neurofibromatosis 2. *Neurology* 2002;**59**:1759–65. doi:10.1212/01.WNL.0000035638.74084.F4

35   Raya Á, Rodríguez-Piz I, Guenechea G, *et al.* Disease-corrected haematopoietic progenitors from Fanconi anaemia induced pluripotent stem cells. *Nature* 2009;**460**:53–9. doi:10.1038/nature08129

36   Castellanos E, Gel B, Rosas I, *et al.* A comprehensive custom panel design for routine hereditary cancer testing : preserving control , improving diagnostics and revealing a complex variation landscape. *Nature Publishing Group* 2017;:1–12. doi:10.1038/srep39348

37   Saunders CT, Wong WSW, Swamy S, *et al.* Strelka: Accurate somatic small-variant calling from sequenced tumor-normal sample pairs. *Bioinformatics* 2012;**28**:1811–7. doi:10.1093/bioinformatics/bts271

38   Wang K, Li M, Hakonarson H. ANNOVAR: Functional annotation of genetic variants from high-throughput sequencing data. *Nucleic Acids Research* 2010;**38**. doi:10.1093/nar/gkq603

39   Campos PB, Sartore RC, Abdalla SN, *et al.* Chromosomal spread preparation of human embryonic stem cells for karyotyping. *Journal of Visualized Experiments* 2009;:4–7. doi:10.3791/1512

40   Park SS, Page AT, Kulik MJ, *et al.* Directed differentiation of human pluripotent cells to neural crest stem cells. *Nature Protocols* 2013;**8**:203–12. doi:10.1038/nprot.2012.156

41   Carrió M, Mazuelas H, Richaud-Patin Y, *et al.* Reprogramming Captures the Genetic and Tumorigenic Properties of Neurofibromatosis Type 1 Plexiform Neurofibromas. *Stem Cell Reports* 2019;**12**. doi:10.1016/j.stemcr.2019.01.001

42   Ban H, Nishishita N, Fusaki N, *et al.* Efficient generation of transgene-free human induced pluripotent stem cells (iPSCs) by temperature-sensitive Sendai virus vectors. *Proceedings of the National Academy of Sciences of the United States of America* 2011;**108**:14234–9. doi:10.1073/pnas.1103509108

43   Agnihotri S, Jalali S, Wilson MR, *et al.* The genomic landscape of schwannoma. Published Online First: 2016. doi:10.1038/ng.3688

44   Mazuelas H, Magallón-Lorenz M, Fernández-Rodríguez J, *et al.* Modeling iPSC-derived human neurofibroma-like tumors in mice uncovers the heterogeneity of Schwann cells within plexiform neurofibromas. *Cell Reports* 2022;**38**:110385. doi:10.1016/j.celrep.2022.110385

45   Asthagiri AR, Parry DM, Butman JA, *et al.* Neurofibromatosis type 2. *Lancet* 2009;**373**:1974–86. doi:10.1016/S0140-6736(09)60259-2

46   Yilmaz A, Peretz M, Aharony A, *et al.* Defining essential genes for human pluripotent stem cells by CRISPR-Cas9 screening in haploid cells. *Nature Cell Biology* 2018;**20**:610–9. doi:10.1038/s41556-018-0088-1

47   Blomen VA, Májek P, Jae LT, *et al.* Gene essentiality and synthetic lethality in haploid human cells. *Science* 2015;**350**:1092–6. doi:10.1126/science.aac7557

48   Nourbakhsh A, Gosstola NC, Fernandez-Valle C, *et al.* Characterization of UMi031-A-2 inducible pluripotent stem cell line with a neurofibromatosis type 2-associated mutation. *Stem Cell Research* 2021;**55**. doi:10.1016/j.scr.2021.102474

49   Rowe RG, Daley GQ. Induced pluripotent stem cells in disease modelling and drug discovery. Nature Reviews Genetics. 2019;**20**:377–88. doi:10.1038/s41576-019-0100-z

50   Curto M, McClatchey AI. Nf2/Merlin: A coordinator of receptor signalling and intercellular contact. *British Journal of Cancer* 2008;**98**:256–62. doi:10.1038/sj.bjc.6604002

51   Curto M, Cole BK, Lallemand D, *et al.* Contact-dependent inhibition of EGFR signaling by Nf2/Merlin. *Journal of Cell Biology* 2007;**177**:893–903. doi:10.1083/jcb.20070301

7. Supplemental Material: characterization of VSi-245$^{(-/-)}$ iPSCs, NC and SC

VSi-245$^{(-/-)}$ line was further characterized. It showed expression of pluripotency markers, NANOG, OCT4, and SOX2 (in green), TRA-1-81, SSEA3 (in red) (**Figure S3.1A**). Alkaline phosphatase staining was positive (**Figure S3.1B**) and the cell line showed karyotype stability after at least 20 passages (**Figure S3.1C**). It showed capacity to differentiate to the three germinal layers *in vitro* through the formation of embryoid bodies (EBs), mesoderm (ASMA in green and ASA in red), ectoderm (TUJ1 in green and GFAP in red) and endoderm (AFP in green and FOXA2 in red) (**Figure S3.1D**). In culture, this line showed differences in morphology and behaviour when compared with the *NF2* (+/+) control line (FiPS): VSi-245$^{(-/-)}$ colonies tend to regularly spontaneously differentiate, requiring to manually discard differentiated cells before each passage. In addition, *NF2* (-/-) iPSCs had less capacity to be tightly packed within the colonies and showed a shift to grow vertically (**Figure S3.1E**). Western Blot analysis revealed no expression of merlin (**Figure S3.1F**). SeV expression was assessed over time and it was still expressed at passage 20 after reprogramming (**Figure S3.1G**).

With the results obtained that far, the hypothesis that the *NF2* gene might be essential in the reprogramming procedure to reach a pluripotency state was considered, as all *NF2* (-/-) clones obtained were SeV-dependent. Thus, VSi-245$^{(-/-)}$ was differentiated towards NCSC-SC with the aim to achieve *NF2* (-/-) SC-like cells that were able to lose the expression of SeV and the reprogramming transgenes.

After 20 days of the NCSC differentiation protocol, or more than 10 passages, SeV was still expressed in VSi-245$^{(-/-)}$ derived NC. VSi-245$^{(-/-)}$ NC was obtained and succeed to show a NC-like morphology (**Figure S3.2A**), expression of the typical NC markers assessed though flow cytometry and immunocytochemistry, although remaining dependent on SeV expression. VSi-245$^{(-/-)}$ derived NC was a heterogeneous population compared with control (FiPS) and as can be seen in the expression markers Hnk and p75 analysed by flow cytometry (**Figure S3.2B**), although immunocytochemistry revealed expression of NC markers p75, AP2 and Sox10 (**Figure S3.2C**).

SC differentiation protocol was performed and a SC-like identity was achieved although the expression of the characteristic markers of the SC lineage showed differences when compared with the control (**Figure S3.3A**). VSi-245$^{(-/-)}$ SC-like cells expressed typical lineage and SC identity markers (p75 and S100B, **Figure S3.3B**) although maintained expression of SeV and the four Yamanaka factors (Oct3/4, Sox2, Klf4, and L-Myc).

Thus, cells continued receiving the factors for reprogramming and maintenance of pluripotency along with the differentiation signals that were induced with the NC-SC differentiation protocol, not representing a good model for further studies.

8. Supplemental Figures and Tables

Figure S3.1. Characterization of the VSi-245[(-/-)] iPSC. (A) Immunochemistry of pluripotency markers NANOG, OCT4, and SOX2 (in green), TRA-1-81, SSEA3 (in red); (B) Alkaline Phosphatase (ALP) Staining; (C) Karyotype at passage 20 (46, XY); Immunochemistry to demonstrate the capacity of the iPSCs to in vitro differentiate to the three primary germ layers: mesoderm (ASMA in green and ASA in red), ectoderm (TUJ1 in green and GFAP in red) and endoderm (AFP in green and FOXA2 in red); (E) Morphology of the cell colonies; (F) Merlin expression analysed by Western Blot. The FiPS lines generated from fibroblasts (NF2^{+/+}) was used as a control cell line, NPE stands for Normalized Protein Expression. (G) Expression of SeV and transgenes at different passages (p8 and p20) assessed by RT-PCR.
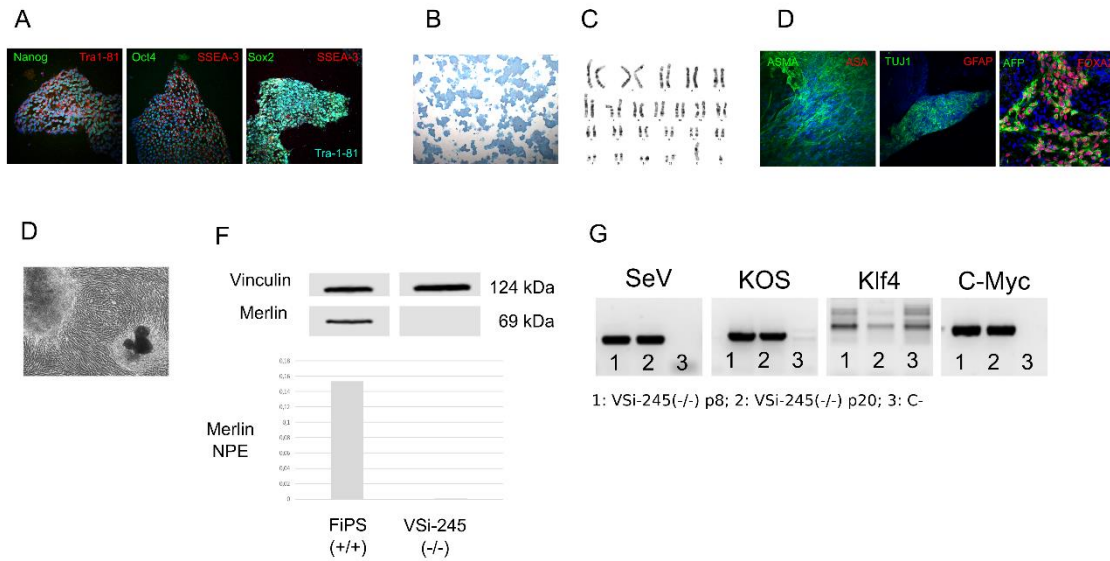
Figure S3.2. **Characterization of the VSi-245$^{(-/-)}$ NC.** (A) NC Morphology; Scale bar, 75μM; (B) Flow cytometry assays of the NC markers NGFR (p75) and Hnk1. The percentage of p75 and Hnk1-positive cells is shown in pink. P4 and P8, passages 4 and 8, respectively; (C) Immunocytochemistry of AP2 (green); Scale bar, 25μM, p75 (green) and S100B (red); Scale bar, 25μM; Oct4 (green) and SOX10 (red); Scale bar, 100μM; DAPI was used to stain cell nuclei.
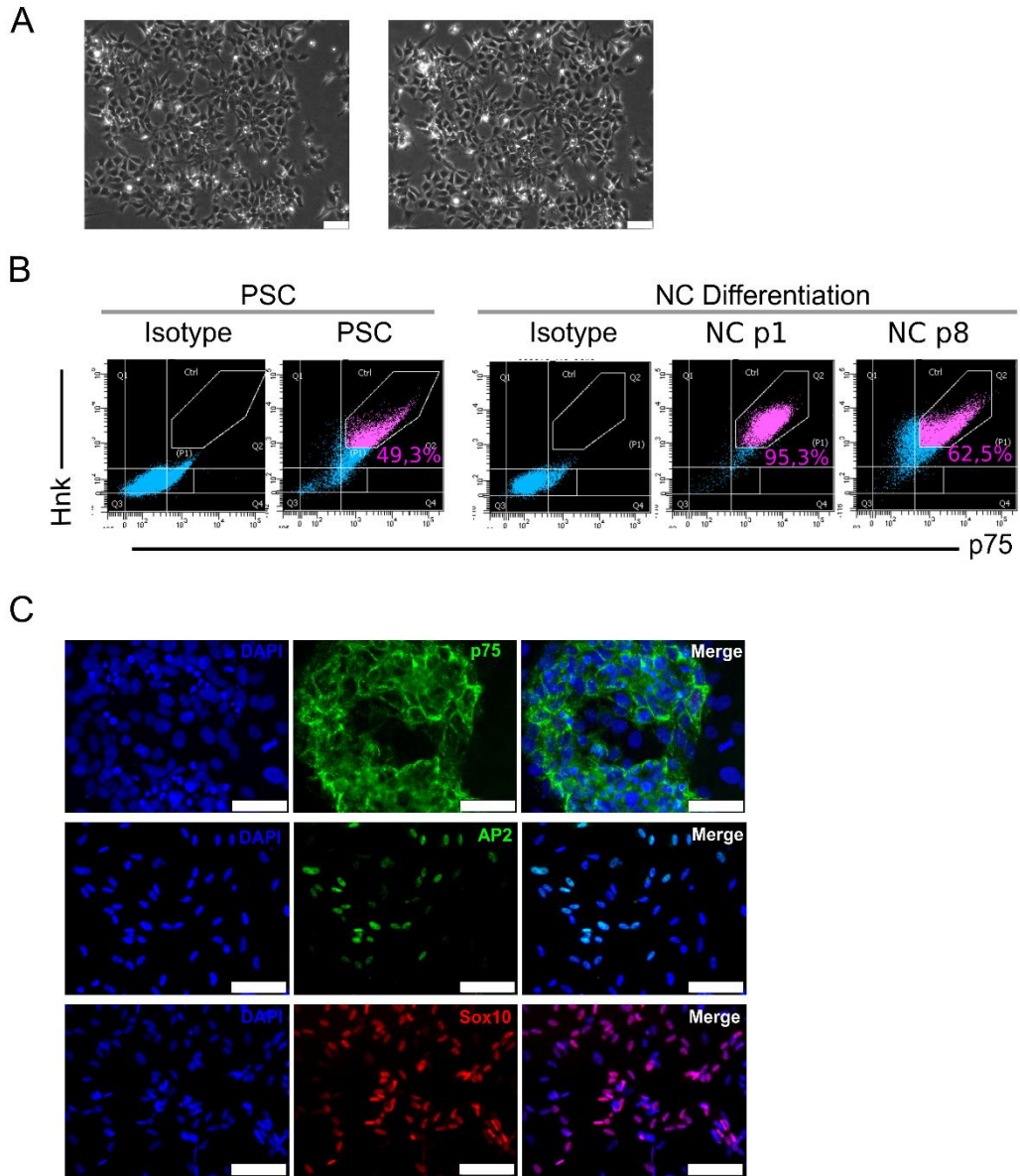
Figure S3.3. **Characterization of the VSi-245$^{(-/-)}$ SC.** (A) qRT-PCR expression analysis. Values are represented as the mean normalized relative expression (NRE) ±SEM from three independent differentiation experiments; (B) Immunocytochemistry analysis of p75 (green) and S100B (red) at the different time points of the SC differentiation protocol (7, 14 and 30 days); (C) Phase contrast images of the culture during the SC differentiation are shown. Scale bar, 75µM.
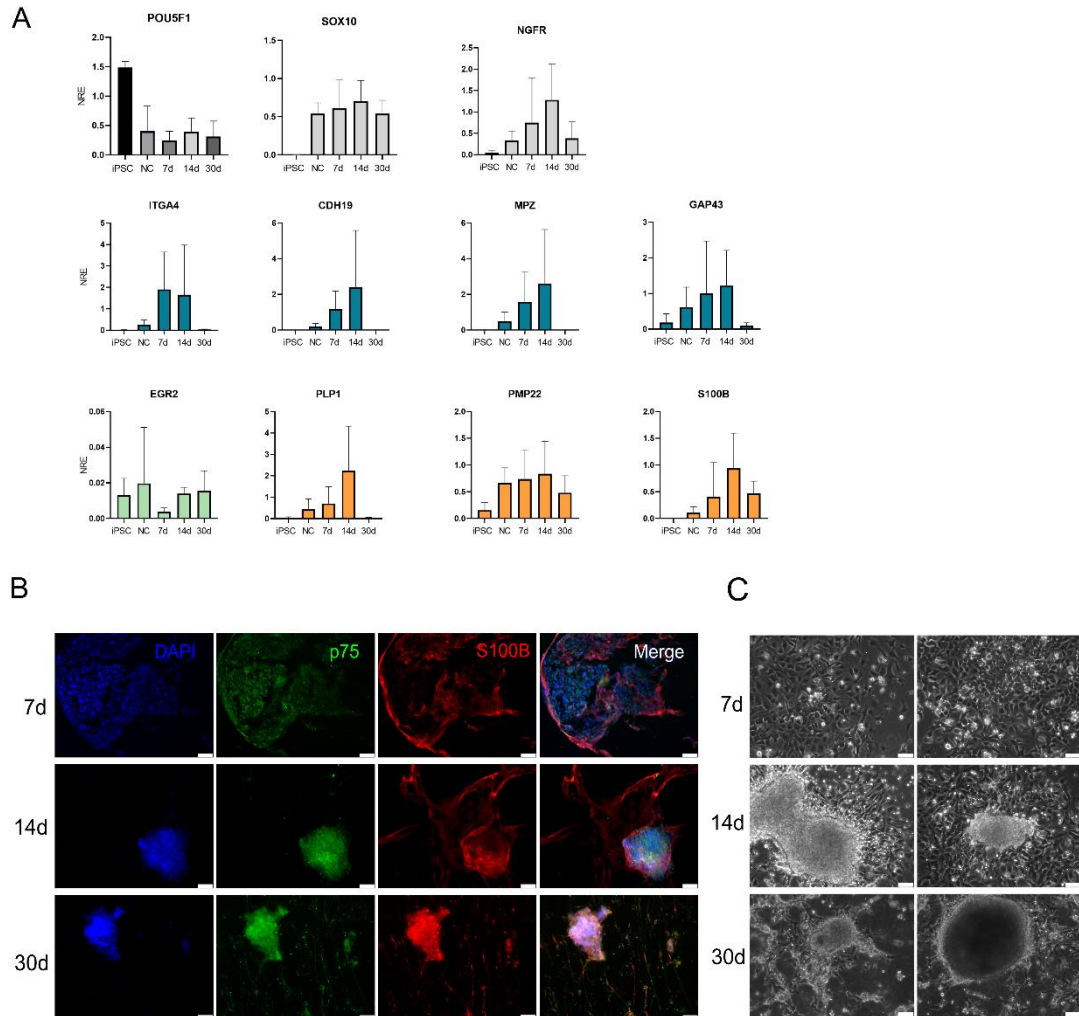
Figure S3.4. SNP-array analysis of VSs and the generated iPSC clones.

25-VS

VSi-25 (iPSC)

245-VS

VSi-245 (iPSC)

267-VS

VSi-267 (iPSC)
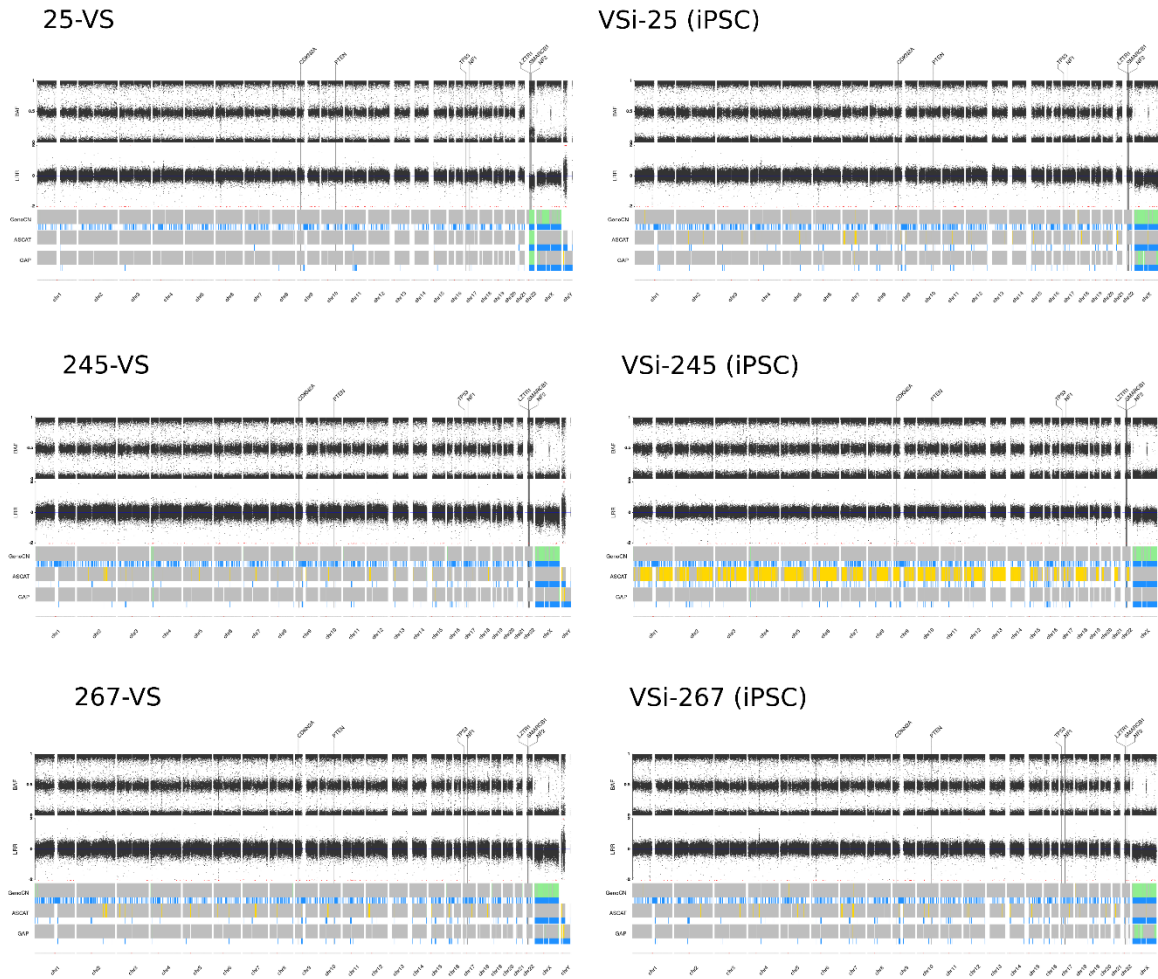
Figure S3.5. Phase-contrast images of *NF2* (+/-) and *NF2* (-/-) cell lines during SC differentiation. *NF2* deficient cells did not show capacity to maintain attachment to the cell culture. Scale bar, 75µM.
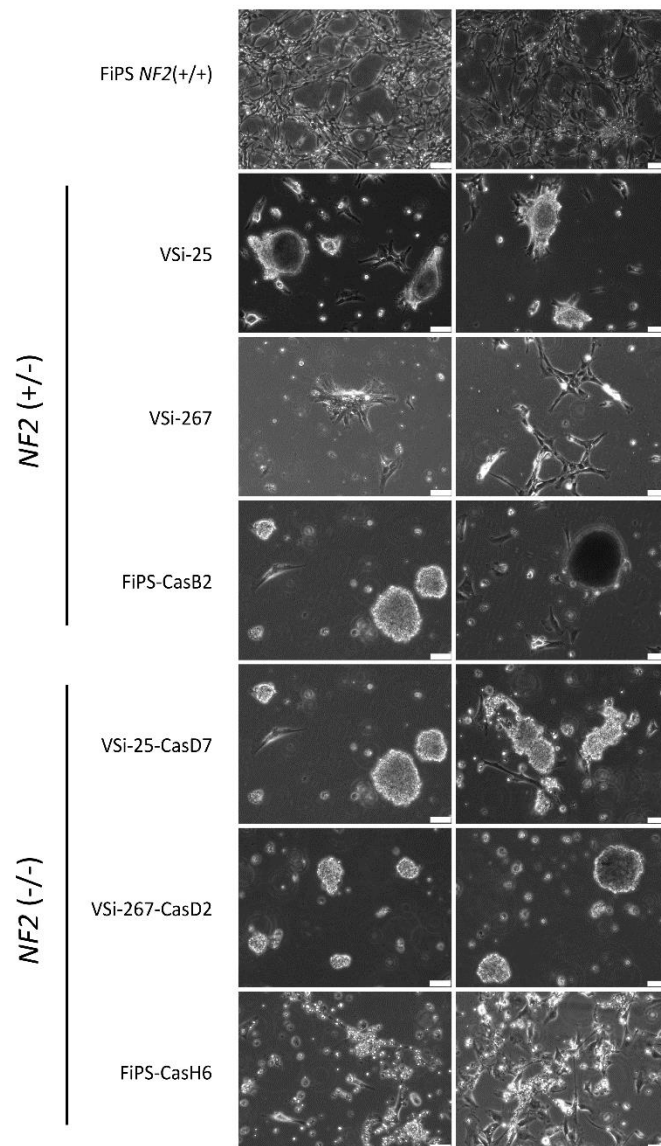
Figure S3.6. Phase contrast images of *NF2* (+/-) and *NF2* (-/-) 3D cultures during SC differentiation. No spheroids could be generated from the FiPS-CasB2 (*NF2* +/-) NC derived cells, Scale bar, 75µM (left panel) and 250µM (right panel).
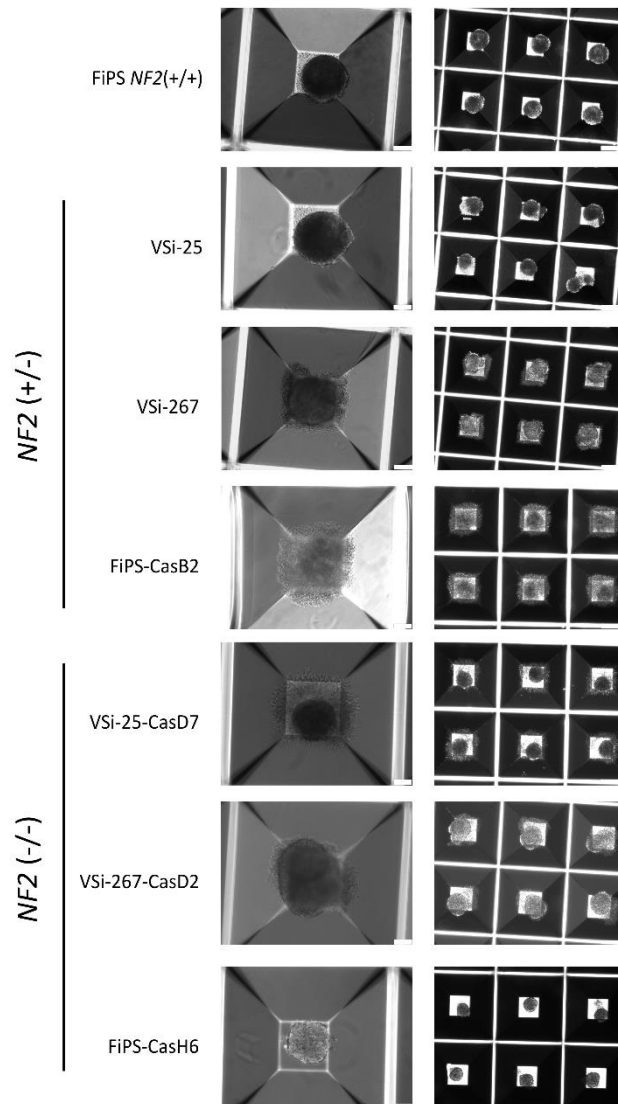
Table S3.1. List of antibodies.			
Antibody	**Supplier**	**Reference**	**Dilution**
Rabbit IgG anti-NF2 / Merlin	Abcam	ab109244	1:200
Rabbit IgG anti-Vinculin	Abcam	ab129002	1:1000
Mouse IgG anti-OCT3/4	Santa Cruz Biotechnology	Sc-5279	1:60
Mouse IgG anti OCT4 (OCT3)	Stem Cell Technologies	#60059	1:100
Rabbit IgG anti-SOX2	Pierce Antibodies	PA1-16968	1:100
Goat IgG anti-NANOG	R&D Systems	AF1997	1:25
Rat IgM anti-SSEA3	Hybridoma Bank	MC-631	1:3
Mouse IgG anti-SSEA4	Hybridoma Bank	MC-813-70	1:3
Mouse IgM anti TRA-1-81	Millipore	MAB4381	1:400
Goat IgG anti-FOXA2	R&D Systems	AF2400	1:50
Rabbit IgG anti-GATA4	Santa Cruz Biotechnology	Sc-9053	1:50
Mouse IgG anti SMA	Sigma	A5228	1:400
Mouse IgM anti-ASA	Sigma	A2172	1:400
Rabbit IgG anti GFAP	Dako	Z0334	1:500
Mouse IgG anti-TUJ1	Bio Legend	MMS-435P	1:500
Mouse IgG anti [NGFR5] to p75 NGF Receptor	Abcam	ab3125	1:100 (IF) 1:1000 (FACS)
Rabbit IgG anti-S100B	Dako	Z0311	1:1000
Mouse IgG anti-AP2	Thermo Scientific	MA1-872	1:50
Rabbit IgG anti-Sox10	Abcam	ab155279	1:50
Mouse IgG anti-HNK1	SIGMA	C6680	1:1000 (FACS)

Table S3.2. List of primers for RT-PCR to detect SeV genome and transgenes set			
Target		**Primer**	**Product size (bp)**
SeV	*Forward*	GGATCACTAGGTGATATCGAGC	181
	Reverse	ACCAGACAAGAGTTTAAGAGATATGTATC	
KOS	*Forward*	ATGCACCGCTACGACGTGAGCGC	528
	Reverse	ACCTTGACAATCCTGATGTGG	
Klf4	*Forward*	TTCCTGCATGCCAGAGGAGCCC	410
	Reverse	AATGTATCGAAGGTGCTCAA	
L-Myc	*Forward*	GAGAAGAGGATGGCTACAGAGA	237
	Reverse	GACGTGCAACTGTGCTATCT	

.

Table S3.3. List of primers for RT-qPCR.			
Gene	Sequence (5´-3´)		UPL
POU5F1	*Forward*	CTTCGCAAGCCCTCATTTC	60
	Reverse	GAGAAGGCGAAATCCGAAG	
POU3F1	*Forward*	TTCTCAAGTGCCCCAAGC	78
	Reverse	CCGGTTGCAGAACCAGAC	
NGFR	*Forward*	CCTTCCACGCTGTCTCCA	*60*
	Reverse	CCTAGGCAAGCATCCCATC	
SOX10	*Forward*	GACACGGTTTTCCACTTCCTA	25
	Reverse	GTCCTCGCAAAGAGTCCAAC	
TFAP2A	*Forward*	GGTGAACCCCAACGAAGTC	73
	Reverse	ACCGTGACCTTGTACTTCGAG	
S100B	*Forward*	GGAAGGGGTGAGACAAGGA	73
	Reverse	GGTGGAAAACGTCGATGAG	
CDH19	*Forward*	TGTACCAGAGGAAATGAATACGAC	78
	Reverse	CATATATGTCACCTGTTCTTTCATCA	
ITGA4	*Forward*	ATGCAGGATCGGAAAGAATC	78
	Reverse	CCACAAGGTTCTCCATTAGGG	
PLP1	*Forward*	CTTCAACACCTGGACCACCT	60
	Reverse	CCATGGGAGAACACCATACA	
GAP43	*Forward*	GCTCCAAGCCTGATGAGC	12
	Reverse	GCTCTGTGGCAGCATCAC	
EGR2	*Forward*	GCTGCTACCCAGAAGGCATA	60
	Reverse	GGATGAGGCTGTGGTTGAA	
PMP22	*Forward*	CTGTCGATCATCTTCAGCATTC	29
	Reverse	AGCACTCATCACGCACAGAC	
MPZ	*Forward*	TTCCCATCTCCTGCATCC	55
	Reverse	CTGGGCCACCTGGTAGAG	

Table S3.4. List of coding variants identified in 25-VS.

Gene	NM	c.	p.	Func.	ExonicFunc.	PopFreqMax	MutationTaster_	VEST3_score	CADD_phred
KCNA10	NM_005549	c.G1257A	p.M419I	nonsynonymous_SNV	exonic	0.001	D	0.914	26.6
AMPD1	NM_001172626	c.G1808A	p.G603E	nonsynonymous_SNV	exonic	0.0023	D	0.855	24.9
GUF1	NM_021927	c.G443T	p.S148I	nonsynonymous_SNV	exonic	0.0067	D	0.826	27.9
ALB	NM_000477	c.A323G	p.Y108C	nonsynonymous_SNV	exonic	0.0029	D	0.938	24.8
PADI4	NM_012387	c.G439A	p.G147S	nonsynonymous_SNV	exonic	0.0002	D	0.968	25.8
HIST1H2AJ	NM_021066	c.C143T	p.A48V	nonsynonymous_SNV	exonic	0.001	D	0.877	26.3
DARS2	NM_018122	c.A1577G	p.H526R	nonsynonymous_SNV	exonic	0.	D	0.909	26.4
KCNT2	NM_001287820	c.G2539A	p.G847R	nonsynonymous_SNV	exonic	0.	D	0.899	34
GCFC2	NM_001201334	c.A947G	p.Y316C	nonsynonymous_SNV	exonic	0.0002	D	0.96	26.9
CCDC74B	NM_001258307	c.T625C	p.C209R	nonsynonymous_SNV	exonic	.	D	0.824	23.3
ALPI	NM_001631	c.C1002G	p.I334M	nonsynonymous_SNV	exonic	.	D	0.853	23.4
HDLBP	NM_001243900	c.C1084T	p.P362S	nonsynonymous_SNV	exonic	0.	D	0.802	22.7
POLN	NM_181808	c.G998T	p.G333V	nonsynonymous_SNV	exonic	.	D	0.879	27.1
CLOCK	NM_004898	c.T1271C	p.F424S	nonsynonymous_SNV	exonic	.	D	0.814	24.6
TNPO1	NM_002270	c.C1442T	p.P481L	nonsynonymous_SNV	exonic	0.0001	D	0.807	26.2
ACTL7A	NM_006687	c.G640A	p.G214S	nonsynonymous_SNV	exonic	0.0099	D	0.86	28.4
FAM13B	NM_001101800	c.C2503T	p.R835W	nonsynonymous_SNV	exonic	0.0002	D	0.84	34
ENDOG	NM_004435	c.G734T	p.R245L	nonsynonymous_SNV	exonic	0.0071	D	0.811	24.4
C11orf49	NM_001003676	c.A56G	p.H19R	nonsynonymous_SNV	exonic	0.0043	D	0.878	25.6
TCIRG1	NM_006053	c.G601A	p.A201T	nonsynonymous_SNV	exonic	0.0049	D	0.895	33
GNAT3	NM_001102386	c.C532G	p.R178G	nonsynonymous_SNV	exonic	.	D	0.976	28.6
NCAPD3	NM_015261	c.G1981T	p.D661Y	nonsynonymous_SNV	exonic	0.007	D	0.928	25.4
EMP1	NM_001423	c.T32G	:p.V11G	nonsynonymous_SNV	exonic	0.0059	D	0.859	27.4
SLC20A2	NM_001257180	c.G1897A	p.A633T	nonsynonymous_SNV	exonic	.	D	0.861	21.9
NFIL3	NM_001289999	c.A770C	p.H257P	nonsynonymous_SNV	exonic	0.0005	D	0.803	22.5
ACTL7A	NM_006687	c.G944A	p.R315Q	nonsynonymous_SNV	exonic	0.0002	D	0.946	33
LRRC43	NM_001098519	c.A1031G	p.Y344C	nonsynonymous_SNV	exonic	0.0034	D	0.834	24.8
CHTF18	NM_022092	c.C2866T	p.R956C	nonsynonymous_SNV	exonic	0.0043	D	0.84	35
SLC17A8	NM_001145288	c.A221C	p.K74T	nonsynonymous_SNV	exonic	0.0002	D	0.87	24.3
TRAP1	NM_001272049	c.T1171A	p.Y391N	nonsynonymous_SNV	exonic	0.0091	D	0.928	27.9
STXBP2	NM_001127396	c.G1577C	p.R526P	nonsynonymous_SNV	exonic	0.0026	D	0.831	27.4
SYNDIG1	NM_024893	c.G511C	p.D171H	nonsynonymous_SNV	exonic	.	D	0.801	29.1
TTLL12	NM_015140	c.A1463G	p.Y488C	nonsynonymous_SNV	exonic	0.0043	D	0.947	22.8
NF2	NM_181830	c.A1487G	p.K496R	nonsynonymous_SNV	exonic	.	D	0.849	22.9

Table S3.5. List of coding variants identified in 245-VS.

Gene	NM	c.	p.	Func.	ExonicFunc.	PopFreqMax	MutationTaster_p	VEST3_score	CADD_phred
PADI4	NM_001114108	c.C568T	p.P190S	exonic	nonsynonymous_SNV	.	D	0.838	25.2
TTC22	NM_001114108	c.T959C	p.M320T	exonic	nonsynonymous_SNV	.	D	0.879	25.3
AGL	NM_000645	c.A2171G	p.Q724R	exonic	nonsynonymous_SNV	0.0003	D	0.804	26.0
IQGAP3	NM_178229	c.C4258T	p.R1420X	exonic	stopgain	0.0006	A	.	40
ZNF124	NM_001297568	c.997delC	p.L333fs	exonic	frameshift_deletion	.	.	.	.
ID2	NM_002166	c.252_254del	p.84_85del	exonic	nonframeshift_deletion	.	.	.	.
NBAS	NM_015909	c.C5110T	p.H1704Y	exonic	nonsynonymous_SNV	0.0005	D	0.901	25.1
ZNF804A	NM_194250	c.3322_3348del	p.1108_1116del	exonic	nonframeshift_deletion	.	.	.	.
MKRN2OS	NM_001195279	c.G86A	p.C29Y	exonic	nonsynonymous_SNV	.	D	0.97	29.3
ABHD18	NM_001039717	c.T611C	p.M204T	exonic	nonsynonymous_SNV	0.0006	D	0.939	26.9
GYPA	NM_001308187	c.72_73insT	p.V25fs	exonic	frameshift_insertion	.	.	.	.
FAM173B	NM_001258388	c.A464C	p.K155T	exonic	nonsynonymous_SNV	.	D	0.808	32
MSH3	NM_002439	c.G1778A	p.R593Q	exonic	nonsynonymous_SNV	0.0002	D	0.914	35
PCDHB13	NM_018933	c.C2392T	p.Q798X	exonic	stopgain	0.0001	N	.	35
SLC25A2	NM_031947	c.A572G	p.Y191C	exonic	nonsynonymous_SNV	0.0004	D	0.847	25.4
PSMB9	NM_002800	c.G295C	p.A99P	exonic	nonsynonymous_SNV	.	D	0.929	29.3
CD2AP	NM_012120	c.1568_1570del	p.523_524del	exonic	nonframeshift_deletion	0.0008	.	.	.
ROS1	NM_002944	c.C6124T	p.R2042W	exonic	nonsynonymous_SNV	0.0004	D	0.803	35
GPNMB	NM_001005340	c.G754T	p.D252Y	exonic	nonsynonymous_SNV	.	D	0.844	27.8
WIPF3	NM_001080529	c.871_872insCCC	p.A291delinsAP	exonic	nonframeshift_insertion	.	.	.	.
PEX1	NM_001282677	c.G2480C	p.G827A	exonic	nonsynonymous_SNV	.	D	0.959	29.5
TECPR1	NM_015395	c.31delC	p.L11fs	exonic	frameshift_deletion	.	.	.	.
TRPV6	NM_018646	c.G86A	p.R29Q	exonic	nonsynonymous_SNV	0.0009	.	.	.
PABPC1	NM_002568	c.C1805T	p.S602L	exonic	nonsynonymous_SNV	.	D	0.859	26.6
FSD1L	NM_001287191	c.418dupG	p.S139fs	exonic	frameshift_insertion	.	.	.	.
RBM18	NM_033117	c.A127T	p.K43X	exonic	stopgain	.	A	.	38
ABL1	NM_005157	c.G589A	p.E197K	exonic	nonsynonymous_SNV	0.0006	D	0.907	34
LOXL4	NM_032211	c.G1729A	p.G577R	exonic	nonsynonymous_SNV	0.0001	D	0.894	29.2
KRTAP5-7	NM_001012503	c.390_416del	p.130_139del	exonic	nonframeshift_deletion	.	.	.	.
PARPBP	NM_017915	c.A940T	p.K314X	exonic	stopgain	0.0001	A	.	42
COQ7	NM_001190983	c.T320C	p.I107T	exonic	nonsynonymous_SNV	.	D	0.979	27.8
EDC4	NM_014329	c.C3406T	p.Q1136X	exonic	stopgain	.	A	.	41
ARHGEF15	NM_025014	c.C1249A	p.R417S	exonic	nonsynonymous_SNV	0.0001	D	0.813	34
MYOCD	NM_153604	c.C2690T	p.P897L	exonic	nonsynonymous_SNV	0.0008	D	0.855	26.1
SPECC1	NM_001033554	c.C61T	p.R21W	exonic	nonsynonymous_SNV	0.0001	D	0.837	29.0
DHX58	NM_024119	c.C1892T	p.P631L	exonic	nonsynonymous_SNV	0.0002	D	0.821	26.3
ZNF519	NM_145287	c.1290_1373del	p.430_458del	exonic	nonframeshift_deletion	.	.	.	.
TPRX1	NM_198479	c.666_689del	p.222_230del	exonic	nonframeshift_deletion	.	.	.	.
SCAF1	NM_021228	c.1722_1727del	p.574_576del	exonic	nonframeshift_deletion	.	.	.	.
ZNF28	NM_006969	c.1849_1932del	p.617_644del	exonic	nonframeshift_deletion	.	.	.	.
ZIM3	NM_052882	c.941delA	p.K314fs	exonic	frameshift_deletion	0.	.	.	.
CDC45	NM_001178011	c.G614A	p.R205H	exonic	nonsynonymous_SNV	0.0001	D	0.844	29.2
NF2	NM_181830	c.819dupG	p.L273fs	exonic	frameshift_insertion	.	.	.	.
NF2	NM_181830	c.C1108T	p.Q370X	exonic	stopgain	.	A	.	48
SLC5A1	NM_001256314	c.1554_1555insAACGTC	p.L518delinsLNV	exonic	nonframeshift_insertion	.	.	.	.
LMF2	NM_033200	c.C1558T	p.P520S	exonic	nonsynonymous_SNV	.	D	0.814	28.5
TYMP	NM_001113756	c.1412dupC	p.S471fs	exonic	frameshift_insertion	.	.	.	.

Table S3.6. VSs Reprogramming information

Patient ID	Method	Number of Clones Analysed	iPSCs clones genotype		
			NF2(+/+)	*NF2*(+/-)	*NF2*(-/-)
25	SeV	12	0	12	0
267	SeV	3	0	3	0
245	SeV	10	1	0	9

Discussion

The overall objective of this thesis was to contribute to the development of tools required for advancing towards a personalized medicine for Neurofibromatosis type 2. For this purpose, we first worked on improving the prognosis capacity of the disease in order to contribute to an optimized, patient-based clinical management. In the second point of the study, a strategy has been developed to apply an antisense gene therapy *in vitro* for variants affecting the *NF2* gene, which represent a significant approximation in the advancement of targeted and personalized therapies for this disease. Finally, and addressing the need to develop new preclinical models for this condition, iPSCs lines harbouring single or bi-allelic inactivation of the *NF2* gene were generated. iPSCs lines were differentiated towards the NC-SC axis generating *NF2* mutant spheroids expressing NC-SC lineage markers. These spheroids could constitute a platform for the development of new therapies, as well as a valuable resource to deepen in the comprehension of the role of the *NF2* gene or its product, merlin, in tumorigenesis.

1. Refining prognosis capacity for Neurofibromatosis Type 2

Neurofibromatosis type 2 presents a broad phenotypic spectrum, as previously described throughout this thesis, making the clinical management of the disease complex and usually with the requirement of multidisciplinary approaches in specialized centres [62]. From the variability in the clinical manifestations emerges the relevance of stablishing prognostic markers and genotype-phenotype correlations, since they are tools that allow patients' prognosis prediction and therefore, could lead to a patient-centred clinical management and further genetic counselling support.

To date, several clinical prognostic markers and genotype-phenotype correlations have been described. At the clinical level, age of onset, extra-vestibular tumour burden and the presence of dermatologic or ophthalmologic lesions have been described as indicators of NF2 severity [26,40,42]. In addition, a reduced risk of mortality in patients treated at specialty centres has been reported, and thus, the centre where the patient is treated could contribute to prognosis [26]. At the molecular level, genotype-phenotype associations have evidenced that truncating variants in the *NF2* gene are responsible for a more severe disease, as opposed to missense variants and large or small in-frame deletions, which are related to milder forms [140,141]. Splice site variants present more phenotypic variability [142,143].

On this basis, the UK reference group established the Genetic Severity Score (GSS), by which it is possible to establish the prognosis of patients based on the *NF2* germline variant [146]. The

GSS groups the genetic variants of *NF2* into four categories. The first (group 1) considers any *NF2* variant in tissue mosaicism and is related to the mildest form of the disease. In contrast, in group 3 are included most of the truncating variants standing for the severest NF2 phenotypes. In between, categories 2A and 2B represent mild and moderate forms of the disease, respectively.

The application of the score in the Spanish cohort validated its prognostic potential for patients with severe phenotypes (group 3). Contrarily, results were not as satisfactory for groups associated with mild-moderate phenotypes. We found significant differences between groups 1 and 3 when analysing mean age at diagnosis and age at hearing loss, and although no significance was found in groups 2A and 2B, the same trend was identified when compared to the performance of the GSS in the UK cohort. The pattern was further observed in the presence of intracranial meningiomas in groups 3, 2B and 2A, albeit with a remarkably increased incidence of these tumours in group 1. Likewise, we found an unexpected high presence of spinal meningiomas within the mosaic group. No significant differences were identified in the development of spinal schwannomas or ependymomas, and in the need of major interventions. Therefore, in general terms, the GSS behaved as in the English cohort, although with significant variability and unexpected occurrences. As an example, we can mention a mosaic patient of our cohort, for whom a mild phenotype would predictably have been expected, although he developed multiple intracranial tumours during young adulthood and, since the GSS only considers genetic data, it cannot account for phenotypic variability observed among mosaic cases. Discrepancies have been also observed in patients in group 2A, including individuals diagnosed at early ages and presenting with high tumour burden.

There are several factors that could limit our study and that need to be considered when analysing the validation of the score. First, the small sample size of our study (n=52) and the fact that most of the patients were comprised in group 3 could suppose a significant bias. Patients included in our study are clinically managed at the Spanish reference centre, to which cases requiring complex clinical management are usually referred, thus more patients are found in group 3 than patients with mild manifestations. This is a notable distinction from the English cohort, given that NF2 patients in UK are centralized in specialized centres and studies are conducted in larger, in view of a rare disease, and more diverse cohorts [9]. Still, we have noticed, as reported in the literature, phenotypic heterogeneity among patients belonging to the same genetic severity group, even in patients harbouring the same genetic variant [9,76,216–220]. In addition, while presenting milder forms than individuals harbouring

truncating germline variants in general terms, we observed relevant variability in the disease presentation of mosaic patients.

These findings, although with the considered limitations of the study, suggested that the predictive capacity of the score for the mosaic or mild groups could still have room for improvement and could be potentially assessed with the integration of other factors that influence patients' phenotype. Nowadays, the GSS is scarcely used in clinical practice since, even being a valuable tool to determine prognostic trends, it is not yet accurate enough to define personalized clinical managements [148]. Therefore, the challenge remains in upgrading the prognostic capacity so that clinicians can determine the most optimal follow-up of patients in terms of expected outcomes.

In recent years, knowledge of merlin's involvement in several signalling pathways has increased [155,156], and we reasoned that expression of merlin interacting proteins could constitute a potential molecular prognostic factor. Expression of merlin and proteins of its downstream pathways was assessed in primary fibroblast cultures derived from NF2 patients. We observed that fibroblasts of individuals harbouring constitutional *NF2* variants expressed, on average, half the levels of merlin compared with non-affected control fibroblasts. This finding, although expected as a result of an inactivated allele, did not provide information on whether the type or location of the mutation within the gene could affect merlin expression and thus, could be related to severity. Furthermore, we observed that levels of phosphorylated ERK (pERK) were significantly lower expressed in patients harbouring truncating mutations, contrarily to what has been reported in schwannoma derived Schwann cells or immortalized tumour Schwann cells [116,122,124,125,159].

ERK is a downstream kinase in the Ras signalling pathway widely characterized for its role in regulation of cell growth and proliferation. ERK is activated through phosphorylation (pERK), activating its kinase activity which, in turn, allow phosphorylation of its downstream targets [221]. Although molecular mechanisms on how merlin modulate the Ras/Raf/MAPK pathway signalling through interactions with Ras and its effector proteins remain to be fully elucidated, it is found overactivated in merlin-deficient Schwann cells, consistent with the role of Ras oncogenes in neoplastic cells [159]. However, the mechanism by which pERK could be under expressed in merlin haploinsufficient fibroblasts cannot be determined in this study.

No significant differences were found in the expression of proteins related to other signalling pathways in which merlin interacts, although it should be noted that functional assays were performed in patient-derived fibroblasts due to their accessibility, but do not represent the

target cell of the disease. Thus, it is then more probable that assessing expression of merlin-interacting proteins in merlin deficient Schwann cells could provide more relevant data. Conversely, although fibroblasts constitute an approachable sample, the exeresis under local anaesthesia and sterile conditions of a skin punch represents inconvenience for patients. Therefore, the relevance of determining pERK levels in fibroblasts should be further evaluated before considering a practical clinical application. If our findings are confirmed in larger sample sets, the use of this data could be also indirectly applied to assess pathogenicity of missense variants. Otherwise, prognostic markers could be sought in more easily accessible tissues, such as blood. In addition, as a rare disease, sample collection is often challenging and even we have been able to complete functional assays in 27 patients, increasing the sample size with broader representation of *NF2* genetic variants could upgrade the study potential to identify significant correlations.

The next stage aimed to find a systematic approach to establish phenotype severity in an objective and quantitative manner, rather than referring to mild, moderate or severe phenotypes. We proposed a 10-scale system based on known prognostic markers to stablish phenotype quantification, accounting also for mosaic cases. Additionally, we reviewed the classification of genetic variants proposed in the GSS and suggested modifications to develop a new classification, named Functional Genetic Severity Score (FGSS). The FGSS consisted of six mutation classes, mostly differing from the GSS in the classification of large deletions and splicing variants. In the new suggested score, it was first considered reported evidences indicating that aberrant splicing affecting the N-terminal domain of *NF2* are related to severe phenotypes, while splice site mutations in C-terminal regions of *NF2* could present more moderate clinical manifestations [13,218,220,222,223]. We also took into consideration our experience with patients of the cohort harbouring variants close to the 3' region of the gene and the results obtained from the functional assays of pERK. Moreover, the maintenance of the gene reading frame was also contemplated, as in-frame variants could result in hypomorphic forms of merlin with potential functionality. Another differential point was in regard mosaicism extension, with mosaicism in blood or unaffected tissue (generalized mosaicism) rating distinctively from mosaic cases in which the variant can only be identified in tumours (tissue mosaicism).

The application of the FGSS in the Spanish cohort led to a reduced intragroup variability compared with the GSS, as well as to some improvement in the stratification of mosaic patients. In addition, it slightly upgraded the correlation among phenotype and clinical variables determined in the GSS. Outcome of the NF2 phenotype modelling according to the established

mutation classes revealed that the genetic variant could only partially explain the resulting phenotype, suggesting that other factors must be involved. Thus, the hypothesis was that incorporation of functional data could increase accuracy in the predictive model.

Merlin and pERK protein levels in fibroblasts were classified according to the FGSS and showed an increased correlation with the NF2 phenotype compared with the GSS, although with no significant differences. Likewise, the addition of the functional data did not significantly benefit the performance of the score. Here again, there is the need to consider the limiting sample size of the functional assay (n=27). In addition, we posit that since the genetic variant had much more influence in the model, the value of the functional data could not provide statistical significance.

Overall, we suggest that the observed trend in fibroblasts pERK levels constitutes a potential molecular prognostic factor, with the need to be tested in other independent cohorts and in larger sample sizes to support our findings. Furthermore, in this study we have proposed a score, the FGSS, with the aim of taking a step forward on the path towards a personalized medicine for NF2.

2. Testing the use of antisense oligonucleotides to modulate the effect of pathogenic variants causing Neurofibromatosis Type 2

As discussed so far, the genotype-phenotype association for NF2 could have great impact on the clinical management of patients, but may also represent a therapeutic opportunity to develop personalized therapies based on the type of *NF2* genetic variant. An example could be the use of antisense therapies, which have been extensively tested for many pathologies and have been approved by regulatory agencies, such as for Spinal Muscular Atrophy (SMA) or Duchenne Muscular Dystrophy (DMD), and for many other diseases are currently in clinical trials [224,225].

Herein, we proposed the use of antisense gene therapy to treat splice site and truncating variants in the *NF2* gene by the use of Phosphorodiamidate Morpholino Oligomers (PMOs) in primary fibroblasts derived from NF2 patients. PMOs are single-stranded, chemically modified DNA-like molecules designed to be efficient and resistant to nucleases, also associated with low toxicities. Because of their chemistry, they can exert a hindrance blocking function at pre-mRNA level, allowing the modulation of gene expression [226].

The use of these molecules for NF2 was first tested in 2013 in our laboratory to treat a *NF2* deep intronic mutation *in vitro*. In this study, PMO treatment allowed the correction of the aberrant splicing signal, which induced the inclusion of a cryptic exon and resulted in a truncating protein. Correcting the splice signal at RNA level led to the recovery of merlin expression levels, as well as an improvement in the organization of the actin cytoskeleton and a reduced proliferation rate in patient-derived fibroblasts [219].

In our study, the first approach targeted splice site variants, accounting for 25% of the point mutations of the *NF2* mutational spectrum and associated with variable clinical manifestations [80,143,144]. We designed mutation-specific PMOs targeting four splicing variants located near canonical splice sites with the aim to mask the aberrant splice signalling induced by the variant, without altering the transcription of the wild type allele (WT). For the four tested mutations, none of the designed PMOs allowed the recovery of the correct splice signalling. Contrarily, PMO treatment resulted in the induction of skipping of the following exon/s, affecting both the mutated and the WT alleles. We suggested that proximity of the mutations to canonical splice sites may lead PMOs to interfere with splicing machinery and exert the blocking effect on both alleles, preventing the recovery of the correct splice signal.

Distinctively, for truncating variants (nonsense or frameshift), largely associated with severe phenotypes, the strategy consisted of inducing skipping of the exon harbouring the mutation, insofar the gene reading frame was maintained. This would result in the synthesis of a shorter protein, with the absence of an exon, yet potentially functional and, therefore, its expression would contribute to mitigate the outcome phenotype. Truncating mutations in 9 exons (exons 1-5, 8-11), those that maintain the gene reading frame after skipped, from the 15 non-alternatively spliced exons in which truncating variants have been reported in the *NF2* gene, could be assessed with this approach. The use of PMOs to induce skipping has resulted successful in other pathologies, although most show a recessive inheritance pattern [179]. Thus, given the autosomal dominant inheritance pattern of *NF2*, it is worth noticing that there was the need to assess whether the effect of exon skipping on the two alleles was more beneficial on the phenotype than the presence of a truncating mutation in heterozygosis.

For this approach we were able to test truncating mutations located in exons 4, 8 and 11, and we designed exon-specific pairs of PMOs complementary to 5'- and 3'- of the intron-exon boundary regions. Results of dose-response and time-course experiments indicated that in-frame exon skipping was fully achieved for exons 4 and 8, and more that 50% was induced for exon 11, although the latter requiring higher doses of the treatment. Once exon skipping was

induced at RNA level, we studied the treatment effect on merlin levels. For exons 4 and 8, we observed a reduction of merlin expression during the 72h period assessed. In addition, the smaller form of merlin expected from the result of the skipping was not detected. In contrast, a shorter merlin was observed after inducing skipping of exon 11, which also resulted in a slight increase in merlin protein levels.

The common feature between exons 4 and 8, differing them from 11, is the protein domain they encode. In particular, exons 4 and 8 of *NF2* code for the FERM domain, reported to be the most relevant for the antimitogenic activity of merlin and responsible for intramolecular interactions with the C-terminal domain (CTD). Thus, we suggested that the outcome protein from the skipping of these exons could adopt an aberrant form, causing its synthesis prevention or rapid degradation. In contrast, exon 11 codes for the α-helical coiled-coil domain, this being a more flexible structure, so the lack of a fragment might not be as relevant in its folding.

We assessed merlin's potential functionality after the skipping of exon 11 (merlin-e11) in primary fibroblasts derived from two NF2 patients harbouring a truncating mutation in exon 11, an adult and a paediatric patient. For this purpose, we first considered the study of the actin cytoskeleton. Merlin has been extensively described as a scaffold protein with an important role in remodelling actin cytoskeleton through its link to adherens junctions, as well as in membrane ruffles and actin microspikes formation [103,227]. In this study we observed that expression of merlin-e11 could lead to an actin cytoskeleton organization improvement. In particular, fibroblasts from the adult patient showed substantial decrease in actin ruffles formation after treatment. Distinctively, merlin haploinsufficiency in paediatric fibroblasts led to foci formation in culture, condition reverted with the expression of merlin-e11, in which primary cells recovered the ability to grow as a monolayer, presumably due to an enhanced cell-cell contact inhibition capacity. Differences observed in response to merlin-e11 expression indicate the need of the treatment to be further tested in more samples to determine a general effect besides patient-dependent outcomes. Regarding the cases studied, we hypothesized that the difference in age of the patients could have influenced the response of primary cultures to treatment.

To extend the characterization of the phenotype resulting from expression of merlin-e11, we assessed the proliferation capacity of treated cells *in vitro*. As a tumour suppressor protein, it is expected that merlin recovery could have an effect in inhibiting proliferation [129,171,228,229]. Consistently, in our study, expression of merlin-e11 resulted in reduced proliferation rates, thus providing further evidence that its expression contributes to the recovery of cell-cell contact inhibition.

Much remains to be studied about possible strategies using antisense oligonucleotides for NF2. Firstly, in order to further investigate the use of antisense oligonucleotides to target splicing mutations, more variants should be tested. Additionally, a screening for effective sequences could be performed to target all the possible alternatives. This approach has been reported in other pathologies to find the most effective target sequence to induce exon skipping [230,231], although our strategy aims to specifically correct a specific variant, which restricts the range for variation in the PMO design. Likewise, the approach targeting truncating variants should be assessed for the other *NF2* in-frame exons to elucidate in which cases the skipping does not limit protein synthesis and could constitute a therapeutic strategy.

Another possibility arising from recent evidence suggesting that some mutant merlin forms could exert a dominant negative effect [114] would be the use of ASOs that depend on the activity of the RNAse H. The mechanism of action of these ASOs consists of the degradation of the hybrid formed between the pre-mRNA and the ASO, and thus leading to a reduced protein expression [179]. Therefore, a potential strategy to target both truncating and splicing variants, could be to design RNAse H-dependent ASOs that degrade the allele harbouring the pathogenic variant and potentially exerting a dominant negative effect.

Overall, according to our experience, PMOs did not seem appropriate to correct splice signals generated by variants closely located to the canonical splice sites. In addition, the use of PMOs did not enable to generate hypomorphic merlin forms when targeting exons 4 and 8. Conversely, expression of merlin-e11 showed encouraging results, providing an *in vitro* proof of concept on the use of antisense therapy for truncating variants located in exon 11 of the *NF2* gene. This approach could be considered for *in vivo* assays subsequent to further characterization.

3. Modelling Neurofibromatosis Type 2 with induced pluripotent stem cells

The previous *in vitro* studies mentioned in this thesis were performed in primary fibroblasts derived from NF2 patients. These are perishable cultures that do not constitute the cell target of the disease, representing a significant limitation. At the cellular level, the most suitable cells for the study of the disease would be tumour-derived Schwann cultures [189,190], although these samples are limited to those from patients that require intervention and, besides, have a finite proliferation capacity. To overcome the constraints of primary culture senescence, immortalized Schwann cell lines could be used, but they are not extensive and do not represent the broad mutational spectrum of *NF2* and the pathophysiology of NF2-related tumours

[191,192]. Hence, the lack of preclinical models that accurately reproduce the genetics and biology of NF2-related tumours hampers the understanding of the *NF2* role in vestibular schwannoma (VS) initiation and progression, as well as the development of new therapeutic approaches. In response to this need, the last part of this thesis aimed to settle an imperishable cellular model that captured the genetics and physiology underlying the development of VSs.

In this context, the generation of induced pluripotent stem cell (iPSC) lines with the bi-allelic inactivation of *NF2* could provide relevant advantages. First, an iPSC-based model would allow to overcome the senescence limitation associated with primary cultures derived from VSs. In addition, due to the iPSC potential differentiation capacity, it would be possible to differentiate these cells towards a Schwann cell identity, in which VSs arise, and reproduce the pathophysiology of the tumour.

iPSCs can be generated through the reprogramming of an affected cell or by the use of genetic engineering techniques, such as CRISPR/Cas9, that induce inactivation of the target gene with the added value of the feasibility to generate isogenic cell lines [196]. In this study we have been able to generate *NF2* mutant iPSC lines from the combination of reprogramming VSs and the use of CRISPR/Cas9 technology to edit the *NF2* gene. Specifically, two *NF2* (+/-) iPSCs lines (VSi-25 and VSi-267) and one *NF2* (-/-) line (VSi-245$^{-/-}$) were obtained from reprogrammed VSs cells. Reprogramming was achieved through the commonly used nonintegrating RNA Sendai virus vector (SeV) that induce the expression of the Yamanaka factors. As a non-integrating vector, its expression is loosened with culture passages. Unexpectedly, *NF2*(-/-) clones achieved from this approach resulted SeV dependent and as far as we know, there are no other cases reported in the literature with this phenomenon. Reprogramming of cancer cells has showed low efficiencies [232] and few cases of reprogramming of primary tumours have been reported in the literature [233,234]. However, this approach has succeeded in other pathologies such as Neurofibromatosis type 1, for which it was possible to reprogram benign plexiform neurofibromas with the same procedure [235]. In our experience, the failure in obtaining *NF2* (-/-) iPSC lines independent from SeV expression suggests that *NF2* may have a fundamental role during reprogramming, further discussed below.

With the aim to generate *NF2*(-/-) iPSC lines, the forming-tumour cells, we edited the *NF2* (+/-) iPSCs obtained from VSs and a control line *NF2* (+/+) via CRISPR/Cas9 system (Vsi-25-CasD7, Vsi-267-CasD2, FiPS-CasB2 and FiPS-CasH6). Thus, we achieved triplicates of isogenic iPSC lines. Pluripotency capacity of iPSCs derived from VSs was confirmed through the expression of pluripotency associated markers and ability to differentiate to the three germ lines. CRISPR-Cas9

derived lines were initially characterized and showed expression of pluripotent markers and karyotype stability, although complete characterization is currently on-going at the Barcelona Stem Cell Bank (B-SCB). However, in our hands, *NF2* deficient iPSCs showed aberrant morphologies, increased spontaneous differentiation and required particular culture conditions, suggesting a critical role of *NF2* in maintaining pluripotency.

Altogether, our results suggest an essential activity of the *NF2* gene during reprogramming and maintaining pluripotency. In line with our findings, *NF2* has been reported to be necessary for optimal fitness in haploid human pluripotent stem cells and other haploid cell lines cultures [236,237]. In addition, *NF2* has been shown to be required during embryogenesis, demonstrated through the lethality of NF2$^{-/-}$ KO mice in early developmental stages [184,185]. Thus, all of the above support the hypothesis that the failure to obtain *NF2* deficient clones through reprogramming VSs cells and the phenotype observed in merlin-deficient iPSCs could be attributable to the intrinsic function of *NF2*. Further evidences could contribute to draw definitive conclusions. Overall, we have been able to generate *NF2*-deficient iPSC lines, that although requiring particular experimental manipulation and indicating a critical function of the *NF2* gene in this state, represent an inexhaustible source of cells that could constitute an *in vitro* platform for the study of NF2*.*

In order to be develop a model for VSs, the aim was to obtain a cell identity that accounts for the cell from which the tumour originates, the Schwan cell. For this purpose, we first differentiated iPSCs lines into Neural Crest (NC) cells. After 20 days of differentiation, we were able to establish *NF2* (+/-) cultures that showed expression of characteristic markers of this cell identity similar to the control line. Distinctively, the edited *NF2* (+/-) line (FiPS-CasB2) presented distinct expression patterns when compared with the other *NF2* (+/-) lines derived from VSs, with a reduced expression of the studied markers. NC cultures of *NF2*(-/-) cells, although significantly expressing NC markers, showed more heterogeneity, a delayed differentiation capacity and the spontaneous expression of S100B, a well-defined SC marker. Since the same results were observed in the three *NF2* deficient lines, the denoted altered differentiation capacity of these cells towards a NC state could be associated with the lack of merlin expression.

Finally, a SC differentiation protocol was stablished in the NC derived cells. In the differentiation process, it was observed that the *NF2*(+/-) and *NF2*(-/-) cell lines had a tendency to detach from the surface, showing reduced adherence capacity, thus preventing the generation of SCs in the determined *in vitro* conditions. Given the known role of merlin in cell-cell contact and observations of foci formation in merlin deficient SC [96,126,229,238–240], we hypothesize that

lack of merlin expression may be responsible for cell detachment in the SC differentiation protocol *in vitro*.

In order to achieve a SC identity, and considering the inability of NC derived cells to differentiate towards SC in adherence cultures, we considered a 3D SC differentiation approach in which cells formed spheroids that were maintained in suspension [241]. Under these conditions, we were able to successful generate *NF2* (+/-) spheroids form the VSi-25 and VSi-267 lines, which co-expressed the NC-SC lineage markers p75 and S100B already at seven days upon differentiation, and the expression was maintained over the 30 days of the protocol. However, we were unable to generate viable spheroids from the edited, *NF2* (+/-), FiPS-CasB2 cell line. Considering all the results from the differentiation processes of this line, we consider that it should be further molecularly characterized to identify potential CRISPR-Cas9 off-target effects, as it showed distinct different expression patterns when compared to the other *NF2* (+/-) lines along the NC-SC differentiation.

The three *NF2* (-/-) lines (25-CasD7, VSi-267-CasD2 and FiPS-CasH6) were able to generate spheroids and stained positive for NC-SC lineage markers (p75 and S100B). An extensive study through RNA-seq analysis will provide a detailed characterization of the generated spheroids, allowing to precisely determine expression profiles of these cells. Therefore, the transcriptome analysis will determine if these spheroids resemble a SC-identity. In addition, it and could also reveal relevant data when comparing the differential expression of the *NF2* (+/-) and *NF2* (-/-) lines, leading to the potential identification of biological processes in which *NF2* is involved.

In summary, we have successfully generated spheroids from iPSC cell lines with the single or bi-allelic inactivation of *NF2* that could constitute a significant advance for the study of *NF2* in tumour development and a platform for the development of new therapies.

In conclusion, the results of this thesis contributed in developing tools for the advance in the path of a personalized medicine for NF2, with the need of additional research to be able to transfer the knowledge into clinical practice (**Figure D.1**).
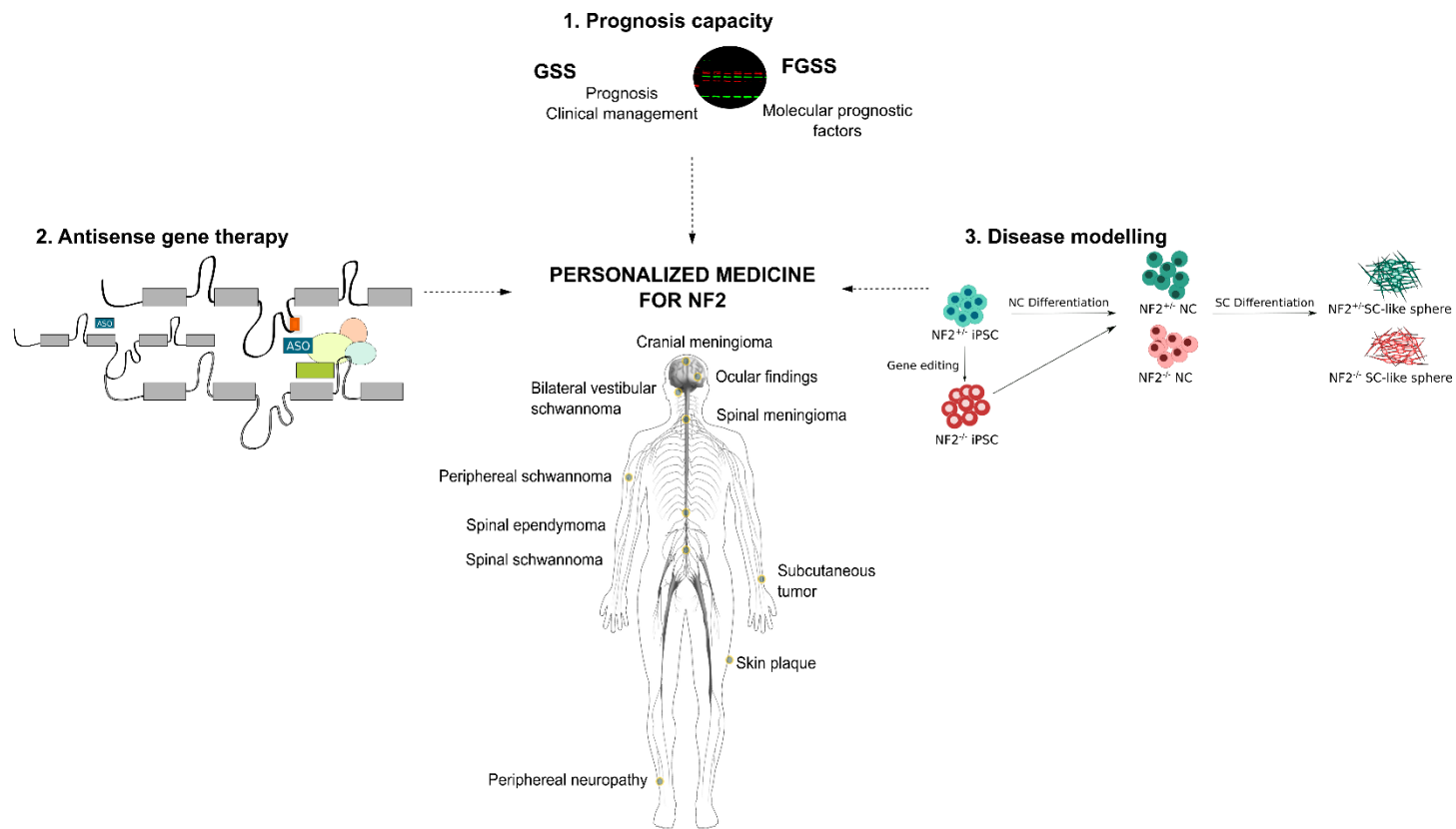
Figure D.1. Schematic representation of the work included in the thesis. (1) The study in NF2 prognosis, (2) an *in vitro* proof of concept of antisense gene therapy for NF2 and (3) disease modelling with an iPSC-based model. The dashed arrow indicates that there is still research to be done in order to reach the goal of a personalized medicine. *Adapted from: National Institutes of Health*.

Conclusions

The most significant conclusions of this thesis are the following:

- The Genetic Severity Score, published by the UK NF2 reference group, was validated in the cohort of NF2 patients from the Spanish National Reference Centre on Phacomatoses. This score allowed discrimination of patients with a severe disease from mild phenotypic forms. However, significant variability was observed among intermediate phenotypes and mosaic groups.

- Functional assays in primary fibroblasts cultures from NF2 patients revealed that levels of phosphorylated ERK (pERK) constitute a potential molecular prognostic factor.

- We proposed a revision of the Genetic Severity Score named Functional Genetic Severity Score. The FGSS considered the type of germline pathogenic variant in the *NF2* gene, the extent of mosaicism, genotype-phenotype reported evidences, the predicted effect of the genetic variant in merlin's function and the results of functional assays on merlin and pERK.

- The performance of the FGSS in the Spanish cohort showed reduced intragroup variability and increased correlations with NF2 phenotypes. The FGSS represents a tool to progress towards a patient-centred clinical management for patients with NF2.

- The use of variant-specific Phosphorodiamidate Morpholino Oligomers (PMOs) to correct aberrant splice signalling induced by genetic variants located near the canonical splice sites did not constitute a successful approach. It was not possible to modify the pathogenic effect of the four splicing variants tested.

- The proposed antisense strategy showed promising results for truncating variants located in exon 11. Exclusion of exon 11 generated an exon-less protein (merlin-e11) that partially rescued the *in vitro* phenotype in patient-derived fibroblasts by improving actin cytoskeleton organization and leading to a reduction of proliferation rates.

- We generated and characterized *NF2* (+/-) and *NF2* (-/-) iPSC lines from the combination of reprogramming VSs and CRISPR/Cas9 editing, in which *NF2* function seems to be essential for both reprograming and maintaining a pluripotent state.

- Merlin-deficient iPSC lines denoted an altered differentiation capacity to Neural Crest (NC) cells, showing heterogenous expression of NC markers, and a delayed differentiation capacity, possibly related to the role of *NF2*.

- We successfully generated *NF2*(+/-) and *NF2*(-/-) spheroids that express well-characterized Neural Crest-Schwann Cell lineage markers (p75 and S100B) and, if confirmed to recapitulate a Schwann cell-like expression pattern, potentially represent a genuine VS model.

References

1   Collins FS, Morgan M, Patrinos A. The Human Genome Project: Lessons from Large-Scale Biology. https://www.science.org

2   Finishing the euchromatic sequence of the human genome International Human Genome Sequencing Consortium*. 2004. http://www.genome.gov/10000923.

3   Ylie W, Urke B. Genetic Testing. 2002. http://www.cdc.gov/genomics/

4   NCI-NHGRI Working Group on Replication in Association Studies.

5   Evans DGR. Orphanet Journal of Rare Diseases. 2009;**2**:1–11. doi:10.1186/1750-1172-4-16

6   Evans DGR, Moran A, King A, *et al.* Incidence of vestibular schwannoma and neurofibromatosis 2 in the North West of England over a 10-year period: Higher incidence than previously thought. *Otology and Neurotology* 2005;**26**:93–7. doi:10.1097/00129492-200501000-00016

7   Evans DG, Howard E, Giblin C, *et al.* Birth incidence and prevalence of tumor-prone syndromes: Estimates from a UK family genetic register service. *American Journal of Medical Genetics, Part A* 2010;**152**:327–32. doi:10.1002/ajmg.a.33139

8   Jmg LTO. Somatic mosaicism in neurofibromatosis 2: prevalence and risk of disease transmission to offspring. 2003;:459–63.

9   Gareth Evans D, Hartley CL, Smith PT, *et al.* Incidence of mosaicism in 1055 de novo NF2 cases: much higher than previous estimates with high utility of next-generation sequencing. Published Online First: 2020. doi:10.1038/s41436

10   Baser ME, Kuramoto L, Joe H, *et al.* Genotype-Phenotype Correlations for Nervous System Tumors in Neurofibromatosis 2: A Population-Based Study. *The American Journal of Human Genetics* 2004;**75**:231–9. doi:10.1086/422700

11   Evans DGR, Ramsden RT, Shenton A, *et al.* Mosaicism in neurofibromatosis type 2: An update of risk based on uni/bilaterality of vestibular schwannoma at presentation and sensitive mutation analysis including multiple ligation-dependent probe amplification. *Journal of Medical Genetics* 2007;**44**:424–8. doi:10.1136/jmg.2006.047753

12   Forde C, King AT, Rutherford SA, *et al.* Disease course of neurofibromatosis type 2: A 30-year follow-up study of 353 patients seen at a single institution. *Neuro-Oncology* 2021;**23**:1113–24. doi:10.1093/neuonc/noaa284

13   Hexter A, Jones A, Joe H, *et al.* Clinical and molecular predictors of mortality in neurofibromatosis 2: a UK national analysis of 1192 patients. *Journal of Medical Genetics* 2015;**52**:699–705. doi:10.1136/jmedgenet-2015-103290

14   Asthagiri AR, Parry DM, Butman JA, *et al.* Neurofibromatosis type 2. *Lancet* 2009;**373**:1974–86. doi:10.1016/S0140-6736(09)60259-2

15   Helbing DL, Schulz A, Morrison H. Pathomechanisms in schwannoma development and progression. *Oncogene* Published Online First: 2020. doi:10.1038/s41388-020-1374-5

16   Wippold FJ, Lubner M, Perrin RJ, *et al.* Neuropathology for the neuroradiologist: Antoni A and Antoni B tissue patterns. American Journal of Neuroradiology. 2007;**28**:1633–8. doi:10.3174/ajnr.A0682

17   Mautner V-F, Lindenau M, Ais WW, *et al.* Clinical Studies.

18   Hilton DA, Hanemann CO. Schwannomas and their pathogenesis. Brain Pathology. 2014;**24**:205–20. doi:10.1111/bpa.12125

19   Gupta VK, Thakker A, Gupta KK. Vestibular Schwannoma: What We Know and Where We are Heading. Head and Neck Pathology. 2020;**14**:1058–66. doi:10.1007/s12105-020-01155-x

20   Mautner V-F, Baser ME, Thakkar SD, *et al.* Vestibular schwannoma growth in patients with neurofibromatosis Type 2: a longitudinal study. 2002.

21   Peyre M, Goutagny S, Bah A, *et al.* Conservative management of bilateral vestibular schwannomas in neurofibromatosis type 2 patients: Hearing and tumor growth results. *Neurosurgery* 2013;**72**:907–13. doi:10.1227/NEU.0b013e31828bae28

22   Baser ME, Mautner VF, Parry DM, *et al.* Methodological issues in longitudinal studies: Vestibular schwannoma growth rates in neurofibromatosis 2. *Journal of Medical Genetics* 2005;**42**:903–6. doi:10.1136/jmg.2005.031302

23   Dirks MS, Butman JA, Kim HJ, *et al.* Long-term natural history of neurofibromatosis Type 2-associated intracranial tumors: Clinical article. *Journal of Neurosurgery* 2012;**117**:109–17. doi:10.3171/2012.3.JNS111649

24   Fisher LM, Doherty K, Lev H, *et al.* Concordance of Bilateral Vestibular Schwannoma Growth and Hearing Changes in Neurofibromatosis 2: Neurofibromatosis 2 Natural History Consortium. http://journals.lww.com/otology-neurotology

25   Ren Y, Chari DA, Vasilijic S, *et al.* New developments in neurofibromatosis type 2 and vestibular schwannoma. *Neuro-Oncology Advances* 2021;**3**:1–13. doi:10.1093/noajnl/vdaa153

26   Baser ME, Friedman JM, Aeschliman D, *et al.* Predictors of the risk of mortality in neurofibromatosis 2. *American journal of human genetics* 2002;**71**:715–23. doi:10.1086/342716

27   Ruttledge MH, Sarrazin J, Rangaratnam\ S, *et al.* Evidence for the complete inactivation of the NF2 gene in the majority of sporadic • • men1ng1omas. 1994. http://www.nature.com/naturegenetics

28   Lomas J, Bello MJ, Arjona D, *et al.* Genetic and epigenetic alteration of the NF2 gene in sporadic meningiomas. *Genes Chromosomes and Cancer* 2005;**42**:314–9. doi:10.1002/gcc.20141

29   Patronas NJ, Courcoutsakis N, Bromley CM, *et al.* Index terms: Genes and genetics Neurofibromatosis, 30.1831 Spinal cord, MR, 30.121411, 30.12143 Spinal cord, neoplasms, 30.363, 30.364, 30. 2001.

30   Plotkin SR, O'Donnell CC, Curry WT, *et al.* Spinal ependymomas in neurofibromatosis type 2: A retrospective analysis of 55 patients: Clinical article. *Journal of Neurosurgery: Spine* 2011;**14**:543–7. doi:10.3171/2010.11.SPINE10350

31   Coy S, Rashid R, Stemmer-Rachamimov A, *et al.* An update on the CNS manifestations of neurofibromatosis type 2. Acta Neuropathologica. 2020;**139**:643–65. doi:10.1007/s00401-019-02029-5

32   Hagel C, Stemmer-Rachamimov AO, Bornemann A, *et al.* Clinical presentation, immunohistochemistry and electron microscopy indicate neurofibromatosis type 2-associated gliomas to be spinal ependymomas. *Neuropathology* 2012;**32**:611–6. doi:10.1111/j.1440-1789.2012.01306.x

33   Gareth Evans D, King AT, Bowers NL, *et al.* Identifying the deficiencies of current diagnostic criteria for neurofibromatosis 2 using databases of 2777 individuals with molecular testing The English Specialist NF2 Research Group. Published Online First: 2019. doi:10.1038/s41436

34   Hagel C, Lindenau M, Lamszus K, *et al.* Polyneuropathy in neurofibromatosis 2: Clinical findings, molecular genetics and neuropathological alterations in sural nerve biopsy specimens. *Acta Neuropathologica* 2002;**104**:179–87. doi:10.1007/s00401-002-0535-7

35   Sperfeld AD, Hein C, Schro Èder JM, *et al.* Occurrence and characterization of peripheral nerve involvement in neuro®bromatosis type 2.

36   Iseki C, Takahashi Y, Wada M, *et al.* A case of neurofibromatosis type 2 (NF2) presenting with late-onset axonal polyneuropathy. *Rinshō shinkeigaku = Clinical neurology* 2009;**49**:419–23. doi:10.5692/clinicalneurol.49.419

37   Hanemann CO, Diebold R, Kaufmann D. Role of NF2 haploinsufficiency in NF2-associated polyneuropathy. *Brain Pathology* 2007;**17**:371–6. doi:10.1111/j.1750-3639.2007.00086.x

38   Bosch MM, Boltshauser E, Harpes P, *et al.* Ophthalmologic Findings and Long-Term Course in Patients With Neurofibromatosis Type 2. *American Journal of Ophthalmology* 2006;**141**. doi:10.1016/j.ajo.2005.12.042

39   Meyers SM, Gutman FA, Kaye LD, *et al.* Retinal changes associated with neurofibromatosis 2. In: *Transactions of the American Ophthalmological Society*. 1995. 245–57. doi:10.1016/s0002-9394(14)70558-6

40   Painter SL, Sipkova Z, Emmanouil B, *et al.* Neurofibromatosis Type 2-Related Eye Disease Correlated With Genetic Severity Type. *Journal of Neuro-Ophthalmology* 2019;**39**:44–9. doi:10.1097/WNO.0000000000000675

41   Evans DGR. Neurofibromatosis 2 [Bilateral acoustic neurofibromatosis, central neurofibromatosis, NF2, neurofibromatosis type II]. *Genetics in Medicine* 2009;**11**:599–610. doi:10.1097/GIM.0b013e3181ac9a27

42   Plana-Pla A, Bielsa-Marsol I, Carrato-Moñino C. Diagnostic and Prognostic Relevance of the Cutaneous Manifestations of Neurofibromatosis Type 2. *Actas Dermo-Sifiliograficas* 2017;**108**:630–6. doi:10.1016/j.ad.2016.12.007

43   Mautner VF, Lindenau M, Baser ME, *et al.* Skin Abnormalities in Neurofibromatosis 2 Design: Case series. Setting: Hospital neurology department. Patients: Consecutive sample of 88 patients with NF2 re-ferred through workshops and publications, genetic coun-seling, and referral from neurosurgical departments; 81 pa-tients met the. http://archderm.jamanetwork.com/

44   Matsuo M, Ohno K, Ohtsuka F. Characterization of early onset neurofibromatosis type 2. *Brain and Development* 2014;**36**:148–52. doi:10.1016/j.braindev.2013.01.007

45   Ruggieri M, Iannetti P, Polizzi A, *et al.* Earliest clinical manifestations and natural history of neurofibromatosis type 2 (NF2) in childhood: A study of 24 patients. *Neuropediatrics* 2005;**36**:21–34. doi:10.1055/s-2005-837581

46   Castellanos E, Plana A, Carrato C, *et al.* Early genetic diagnosis of neurofibromatosis type 2 from skin plaque plexiform schwannomas in childhood. *JAMA Dermatology* 2018;**154**:341–6. doi:10.1001/jamadermatol.2017.5464

47   Evans DGR, Birch JM, Ramsden RT. Paediatric presentation of type 2 neurofibromatosis. 1999.

48   Ruggieri M, Praticò AD, Serra A, *et al.* Childhood neurofibromatosis type 2 (NF2) and related disorders: From bench to bedside and biologically targeted therapies. Acta Otorhinolaryngologica Italica. 2016;**36**:345–67. doi:10.14639/0392-100X-1093

49   Dhamija R, Plotkin S, Asthagiri A. Schwannomatosis. 2018.

50   Plotkin SR, Blakeley JO, Evans DG, *et al.* Update from the 2011 International Schwannomatosis Workshop: From genetics to diagnostic criteria. In: *American Journal of Medical Genetics, Part A*. 2013. 405–16. doi:10.1002/ajmg.a.35760

51   Patil S, Perry A, MacCollin M, *et al.* Immunohistochemical analysis supports a role for INI1/SMARCB1 in hereditary forms of schwannomas, but not in solitary, sporadic schwannomas. *Brain Pathology* 2008;**18**:517–9. doi:10.1111/j.1750-3639.2008.00155.x

52   Evans DG, Raymond FL, Barwell JG, *et al.* Genetic testing and screening of individuals at risk of NF2. *Clinical genetics* 2012;**82**:416–24. doi:10.1111/j.1399-0004.2011.01816.x

53   Boyd C, Mj S, Kluwe L, *et al.* Alterations in the SMARCB1 (INI1) tumor suppressor gene in familial schwannomatosis. 2008;**22**:358–66. doi:10.1111/j.1399-0004.2008.01060.x

54   Hadfield KD, Newman WG, Bowers NL, *et al.* Molecular characterisation of SMARCB1 and NF2 in familial and sporadic schwannomatosis. *Journal of Medical Genetics* 2008;**45**:332–9. doi:10.1136/jmg.2007.056499

55   Hulsebos TJM, Plomp AS, Wolterman RA, *et al.* Germline mutation of INI1/SMARCB1 in familial schwannomatosis. *American Journal of Human Genetics* 2007;**80**:805–10. doi:10.1086/513207

56   Paganini I, Chang VY, Capone GL, *et al.* Expanding the mutational spectrum of LZTR1 in schwannomatosis. *European Journal of Human Genetics* 2015;**23**:963–8. doi:10.1038/ejhg.2014.220

57   Piotrowski A, Xie J, Liu YF, *et al.* Germline loss-of-function mutations in LZTR1 predispose to an inherited disorder of multiple schwannomas. *Nature Genetics* 2014;**46**:182–7. doi:10.1038/ng.2855

58   Kehrer-Sawatzki H, Farschtschi S, Mautner VF, *et al.* The molecular pathogenesis of schwannomatosis, a paradigm for the co-involvement of multiple tumour suppressor genes in tumorigenesis. Human Genetics. 2017;**136**:129–48. doi:10.1007/s00439-016-1753-8

59   Smith MJ, Isidor B, Beetz C, *et al.* Mutations in LZTR1 add to the complex heterogeneity of schwannomatosis. 2014;:141–7.

60   Sestini R, Bacci C, Provenzano A, *et al.* Evidence of a four-hit mechanism involving SMARCB1 and NF2 in schwannomatosis-associated schwannomas. *Human Mutation* 2008;**29**:227–31. doi:10.1002/humu.20679

61   Rivera B, Nadaf J, Fahiminiya S, *et al.* DGCR8 microprocessor defect characterizes familial multinodular goiter with schwannomatosis. *Journal of Clinical Investigation* 2020;**130**:1479–90. doi:10.1172/JCI130206

62   Evans DGR, Baser ME, O'Reilly B, *et al.* Management of the patient and family with neurofibromatosis 2: A consensus conference statement. In: *British Journal of Neurosurgery*. 2005. 5–12. doi:10.1080/02688690500081206

63   Evans DGR, Huson SM, Donnai D, *et al.* A genetic study of type 2 neurofibromatosis in the United Kingdom . II . Guidelines for genetic counselling. 1992;:847–52.

64   Gareth Evans D, Donnai D, Harris RE. Article in The Quarterly journal of medicine. 1992. https://www.researchgate.net/publication/21670660

65   Smith MJ, Bowers NL, Bulman M, *et al.* Revisiting neurofibromatosis type 2 diagnostic criteria to exclude LZTR1-related schwannomatosis. 2016.

66   Evans DG, Bowers NL, Tobi S, *et al.* Schwannomatosis: a genetic and epidemiological study. *Journal of Neurology, Neurosurgery & Psychiatry* 2018;**89**:1215–9. doi:10.1136/jnnp-2018-318538

67   Evans DG, King AT, Bowers NL, *et al.* Identifying the deficiencies of current diagnostic criteria for neurofibromatosis 2 using databases of 2777 individuals with molecular testing. *Genetics in Medicine* 2018;**0**. doi:10.1038/s41436-018-0384-y

68   Evans G, Mary S, Legius E, *et al.* Revision of Diagnostic Criteria for Neurofibromatosis. 2019.

69   Dinh CT, Nisenbaum E, Chyou D, *et al.* Genomics, Epigenetics, and Hearing Loss in Neurofibromatosis Type 2. Otology and Neurotology. 2020;**41**:e529–37. doi:10.1097/MAO.0000000000002613

70   Trofatter JA, Maccoiin MM, Rutter JL, *et al.* A Novel Moesin-, Ezrin-, Radixin-like Gene Is a Candidate for the Neurofibromatosis 2 Tumor Suppressor. 1993.

71   Rouleau GA, Merel P, Lutchman M, *et al.* Alteration in a new gene encoding a putative membrane-organizing protein causes neuro-fibromatosis type 2. *Nature* 1993;**363**:515–21. doi:10.1038/363515a0

72   Pykett MJ, Murphy M, Harnlsh PR, *et al.* The neurofibromatosis 2 (NF2) tumor suppressor gene encodes multiple alternatively spliced transcripts. 1994.

73   Gardner WJ, Frazier CH, Philadelphia S. BILATERAL ACOUSTIC NEUROFIBROMAS A CLINICAL STUDY AND FIELD SURVEY OF A FAMILY OF FIVE GENERATIONS WITH BILATERAL DEAFNESS IN THIRTY-EIGHT MEMBERS *. http://archneurpsyc.jamanetwork.com/

74   Evans DGR, Huson SM, Donnai D, *et al.* A genetic study of type 2 neurofibromatosis in the United Kingdom. I. Prevalence, mutation rate, fitness, and confirmation of maternal transmission effect on severity. *Journal of Medical Genetics* 1992;**29**:841–6. doi:10.1136/jmg.29.12.841

75   Knudson AG. Mutation and Cancer: Statistical Study of Retinoblastoma. 1971.

76   Kluwe L, Mautner VF. Mosaicism in sporadic neurofibromatosis 2 patients. *Human molecular genetics* 1998;**7**:2051–5.

77   Kluwe L, Mautner V, Heinrich B, *et al.* Molecular study of frequency of mosaicism in neurofibromatosis 2 patients with bilateral vestibular schwannomas. *Journal of Medical Genetics* 2003;**40**:109–14. doi:10.1136/jmg.40.2.109

78   Moyhuddin A, Baser ME, Watson C, *et al.* Somatic mosaicism in neurofibromatosis 2: Prevalence and risk of disease transmission to offspring. *Journal of Medical Genetics* 2003;**40**:459–63. doi:10.1136/jmg.40.6.459

79   Evans DGR, Maher ER, Baser ME. Age related shift in the mutation spectra of germline and somatic NF2 mutations: Hypothetical role of DNA repair mechanisms. *Journal of Medical Genetics* 2005;**42**:630–2. doi:10.1136/jmg.2004.027953

80   Ahronowitz I, Xin W, Kiely R, *et al.* Mutational Spectrum of the NF2 Gene : A Meta-Analysis of 12 Years of Research and Diagnostic Laboratory Findings. 2007;**28**. doi:10.1002/humu

81   Baser ME, Evans DG. The distribution of constitutional and somatic mutations in the neurofibromatosis 2 gene. Human Mutation. 2006;**27**:297–306. doi:10.1002/humu.20317

82   Antinheimo1 J, Sallinen2 S-L, Sallinen2 P, *et al.* Genetic Aberrations in Sporadic and Neuro®bromatosis 2 (NF2)-Associated Schwannomas Studied by Comparative Genomic Hybridization (CGH).

83   Hexter AT, Evans DG. The Genetics of Vestibular Schwannoma. Current Otorhinolaryngology Reports. 2014;**2**:226–34. doi:10.1007/s40136-014-0061-x

84   Agnihotri S, Jalali S, Wilson MR, *et al.* The genomic landscape of schwannoma. Published Online First: 2016. doi:10.1038/ng.3688

85   Wellenreuther R, Kraus JA, Lenartz D, *et al.* Analysis of the Neurofibromatosis 2 Gene Reveals Molecular Variants of Meningioma. 1995.

86   Smith MJ, Higgs JE, Bowers NL, *et al.* Cranial meningiomas in 411 neurofibromatosis type 2 (NF2) patients with proven gene mutations: Clear positional effect of mutations, but absence of female severity effect on age at onset. *Journal of Medical Genetics* 2011;**48**:261–5. doi:10.1136/jmg.2010.085241

87   Clark VE, Harmancl AS, Bai H, *et al.* Recurrent somatic mutations in POLR2A define a distinct subset of meningiomas. *Nature Genetics* 2016;**48**:1253–9. doi:10.1038/ng.3651

88   Schroeder RD, Angelo LS, Kurzrock R. NF2 / Merlin in hereditary neurofibromatosis 2 versus cancer : biologic mechanisms and clinical associations ABSTRACT : 2013;**5**.

89   Sato T, Sekido Y. NF2/merlin inactivation and potential therapeutic targets in mesothelioma. *International Journal of Molecular Sciences* 2018;**19**. doi:10.3390/ijms19040988

90   Anand G, Vasallo G, Spanou M, *et al.* Diagnosis of sporadic neurofibromatosis type 2 in the paediatric population. *Archives of Disease in Childhood* 2018;**103**:463–9. doi:10.1136/archdischild-2017-313154

91   Kehrer-Sawatzki H, Kluwe L, Friedrich RE, *et al.* Phenotypic and genotypic overlap between mosaic NF2 and schwannomatosis in patients with multiple non-intradermal schwannomas. *Human Genetics* 2018;**137**:543–52. doi:10.1007/s00439-018-1909-9

92   Castellanos E, Bielsa I, Carrato C, *et al.* Segmental neurofibromatosis type 2:Discriminating two hit from four hit in a patient presenting multiple schwannomas confined to one limb. *BMC Medical Genomics* 2015;**8**. doi:10.1186/s12920-015-0076-2

93   Pasmant E, Louvrier C, Luscan A, *et al.* Neurofibromatosis type 2 French cohort analysis using a comprehensive NF2 molecular diagnostic strategy. *Neurochirurgie* 2018;**64**:335–41. doi:10.1016/j.neuchi.2015.01.004

94   Scherer SS, Gutmann DH. Rapid Communication Expression of the Neurofibromatosis 2 Tumor Suppressor Gene Product, Merlin, in Schwann Cells. 1996.

95   Stickney JT, Bacon WC, Rojas M, *et al.* Activation of the Tumor Suppressor Merlin Modulates Its Interaction with Lipid Rafts. 2004.

96   Okada T, Lopez-Lago M, Giancotti FG. Merlin/NF-2 mediates contact inhibition of growth by suppressing recruitment of Rac to the plasma membrane. *Journal of Cell Biology* 2005;**171**:361–71. doi:10.1083/jcb.200503165

97   Bianchp AB, Hara T, Ramesh V, *et al.* Mutations in transcript isoforms of the neurofibromatosis 2 gene in multiple human tumour types. 1994. http://www.nature.com/naturegenetics

98   Zoch A, Mayerl S, Schulz A, *et al.* Merlin isoforms 1 and 2 both act as tumour suppressors and are required for optimal sperm maturation. *PLoS ONE* 2015;**10**. doi:10.1371/journal.pone.0129151

99   Sher I, Hanemann OC, Karplus AP, *et al.* The Tumor Suppressor Merlin Controls Growth in Its Open State, and Phosphorylation Converts It to a Less-Active More-Closed State. Developmental Cell. 2012;**22**:703–5. doi:10.1016/j.devcel.2012.03.008

100   Johnson KC, Kissil JL, Fry JL, *et al.* Cellular transformation by a FERM domain mutant of the Nf2 tumor suppressor gene. *Oncogene* 2002;**21**:5990–7. doi:10.1038/sj.onc.1205693

101   Lajeunesse DR, Mccartney BM, Fehon RG. Structural Analysis of Drosophila Merlin Reveals Functional Domains Important for Growth Control and Subcellular Localization. 1998. http://www.jcb.org

102   McClatchey AI, Fehon RG. Merlin and the ERM proteins - regulators of receptor distribution and signaling at the cell cortex. Trends in Cell Biology. 2009;**19**:198–206. doi:10.1016/j.tcb.2009.02.006

103   Cooper J, Giancotti FG. Molecular insights into NF2/Merlin tumor suppressor function. FEBS Letters. 2014;**588**:2743–52. doi:10.1016/j.febslet.2014.04.001

104   Sivakumar KC, Thomas B, Karunagaran D. Three dimensional structure of the closed conformation (active) of human merlin reveals masking of actin binding site in the FERM domain. 2009. http://align.genome.jp

105   Gonzalez-Agosti C, Wiederhold T, Herndon ME, *et al.* Interdomain Interaction of Merlin Isoforms and Its Influence on Intermolecular Binding to NHE-RF*. 1999. http://www.jbc.org

106   Hennigan RF, Foster LA, Chaiken MF, *et al.* Fluorescence Resonance Energy Transfer Analysis of Merlin Conformational Changes. *Molecular and Cellular Biology* 2010;**30**:54–67. doi:10.1128/mcb.00248-09

107   Ali Khajeh J, Ju JH, Atchiba M, *et al.* Molecular conformation of the full-length tumor suppressor NF2/merlin - A small-angle neutron scattering study. *Journal of Molecular Biology* 2014;**426**:2755–68. doi:10.1016/j.jmb.2014.05.011

108   Lallemand D, Saint-Amaux AL, Giovannini M. Tumor-suppression functions of merlin are independent of its role as an organizer of the actin cytoskeleton in Schwann cells. *Journal of Cell Science* 2009;**122**:4141–9. doi:10.1242/jcs.045914

109   Shaw RJ, McClatchey AI, Jacks T. Regulation of the neurofibromatosis type 2 tumor suppressor protein, Merlin, by adhesion and growth arrest stimuli. *Journal of Biological Chemistry* 1998;**273**:7757–64. doi:10.1074/jbc.273.13.7757

110   The Nf2 Tumor Suppressor, Merlin, Functions in Rac-Dependent Signaling. http://www.developmental.

111   Alfthan K, Heiska L, Grönholm M, *et al.* Cyclic AMP-dependent Protein Kinase Phosphorylates Merlin at Serine 518 Independently of p21-activated Kinase and Promotes Merlin-Ezrin Heterodimerization. *Journal of Biological Chemistry* 2004;**279**:18559–66. doi:10.1074/jbc.M313916200

112   Jin H, Sperka T, Herrlich P, *et al.* Tumorigenic transformation by CPI-17 through inhibition of a merlin phosphatase. *Nature* 2006;**442**:576–9. doi:10.1038/nature04856

113   Chinthalapudi K, Mandati V, Zheng J, *et al.* Lipid binding promotes the open conformation and tumor-suppressive activity of neurofibromin 2. *Nature Communications* 2018;**9**. doi:10.1038/s41467-018-03648-4

114   Hennigan RF, Thomson CS, Ratner N. Merlin Tumor Suppressor Function is Regulated by PIP2-Mediated Dimerization. doi:10.1101/2021.11.11.468247

115 Lee S, Karas PJ, Hadley CC, *et al.* The role of merlin/NF2 loss in meningioma biology. Cancers. 2019;**11**. doi:10.3390/cancers11111633

116 Watt KI, Harvey KF, Gregorevic P. Regulation of tissue growth by the mammalian Hippo signaling pathway. Frontiers in Physiology. 2017;**8**. doi:10.3389/fphys.2017.00942

117 Hilton DA, Ristic N, Hanemann CO. Activation of ERK, AKT and JNK signalling pathways in human schwannomas *in situ*. *Histopathology* 2009;**55**:744–9. doi:10.1111/j.1365-2559.2009.03440.x

118 Rong R, Tang X, Gutmann DH, *et al.* inhibits phosphatidylinositol 3-kinase through binding to PIKE-L. 2004;**2**:3–8.

119 Jacob A, Lee TX, Neff BA, *et al.* Phosphatidylinositol 3-Kinase/AKT Pathway Activation in Human Vestibular Schwannoma.

120 Welling DB, Collier KA, Burns SS, *et al.* Early phase clinical studies of AR-42, a histone deacetylase inhibitor, for neurofibromatosis type 2-associated vestibular schwannomas and meningiomas. *Laryngoscope Investigative Otolaryngology* 2021;**6**:1008–19. doi:10.1002/lio2.643

121 Lopez-Lago MA, Okada T, Murillo MM, *et al.* Loss of the Tumor Suppressor Gene NF2, Encoding Merlin, Constitutively Activates Integrin-Dependent mTORC1 Signaling. *Molecular and Cellular Biology* 2009;**29**:4235–49. doi:10.1128/MCB.01578-08

122 James MF, Han S, Polizzano C, *et al.* NF2/Merlin Is a Novel Negative Regulator of mTOR Complex 1, and Activation of mTORC1 Is Associated with Meningioma and Schwannoma Growth. *Molecular and Cellular Biology* 2009;**29**:4250–61. doi:10.1128/mcb.01581-08

123 Petrilli AM, Fernández-Valle C. Role of Merlin/NF2 inactivation in tumor biology. *Oncogene* 2015;**35**:537–48. doi:10.1038/onc.2015.125

124 Fernandez-valle C, Tang Y, Ricard J, *et al.* Paxillin binds schwannomin and regulates its density-dependent localization and effect on cell morphology. 2002;**31**. doi:10.1038/ng930

125 Morrison H, Sperka T, Manent J, *et al.* Merlin / Neurofibromatosis Type 2 Suppresses Growth by Inhibiting the Activation of Ras and Rac. 2007;:520–8. doi:10.1158/0008-5472.CAN-06-1608

126 Cui Y, Groth S, Troutman S, *et al.* The NF2 tumor suppressor merlin interacts with Ras and RasGAP, which may modulate Ras signaling. *Oncogene* 2019;**38**:6370–81. doi:10.1038/s41388-019-0883-6

127 Cui Y, Ma L, Schacke S, *et al.* Merlin cooperates with neurofibromin and Spred1 to suppress the Ras-Erk pathway. *Human molecular genetics* 2021;**29**:3793–806. doi:10.1093/hmg/ddaa263

128 Carroll SL. Molecular mechanisms promoting the pathogenesis of Schwann cell neoplasms. Acta Neuropathologica. 2012;**123**:321–48. doi:10.1007/s00401-011-0928-6

129 MINIMO Jr L, Smith GM, Knauer D, *et al.* Overexpression of the NF2 gene inhibits schwannoma cell proliferation through promoting PDGFR degradation. 2003.

130 Mota M, Shevde LA. Merlin regulates signaling events at the nexus of development and cancer. *Cell Communication and Signaling* 2020;**18**:1–8. doi:10.1186/s12964-020-00544-7

131 Koutsimpelas D, Ruerup G, Mann WJ, *et al.* Lack of neurofibromatosis type 2 gene promoter methylation in sporadic vestibular schwannomas. *ORL* 2012;**74**:33–7. doi:10.1159/000334968

132 Lee JD, Kwon TJ, Kim UK, *et al.* Genetic and epigenetic alterations of the NF2 gene in sporadic vestibular schwannomas. *PLoS ONE* 2012;**7**. doi:10.1371/journal.pone.0030418

133 Kino T, Takeshima H, Nakao M, *et al.* Identification of the cis-acting region in the NF2 gene promoter as a potential target for mutation and methylation-dependent silencing in schwannoma.

134 Celis-Aguilar E, Lassaletta L, Torres-Martín M, *et al.* The Molecular Biology of Vestibular Schwannomas and Its Association with Hearing Loss: A Review. *Genetics Research International* 2012;**2012**:1–10. doi:10.1155/2012/856157

135 Lassaletta L, Bello †m Josefa, Río L del, *et al.* DNA Methylation of Multiple Genes in Vestibular Schwannoma: Relationship With Clinical and Radiological Findings.

136 Torres-Martín M, Lassaletta L, de Campos JM, *et al.* Genome-wide methylation analysis in vestibular schwannomas shows putative mechanisms of gene expression modulation and global hypomethylation at the HOX gene cluster. *Genes Chromosomes and Cancer* 2015;**54**:197–209. doi:10.1002/gcc.22232

137 Sahm F, Schrimpf D, Stichel D, *et al.* DNA methylation-based classification and grading system for meningioma: a multicentre, retrospective analysis. *The Lancet Oncology* 2017;**18**:682–94. doi:10.1016/S1470-2045(17)30155-9

138 Mater D, By H Wishart Esq BJ, S Ed FR, *et al.* Case of Tumours in the Skull, Dura Mater, and Brain.

139 Ruggieri M, Praticò AD, Evans DG. Diagnosis, Management, and New Therapeutic Options in Childhood Neurofibromatosis Type 2 and Related Forms. *Seminars in Pediatric Neurology* 2015;**22**:240–58. doi:10.1016/j.spen.2015.10.008

140 Ruggieri M, Gabriele AL, Polizzi A, *et al.* Natural history of neurofibromatosis type 2 with onset before the age of 1 year. *Neurogenetics* 2013;**14**:89–98. doi:10.1007/s10048-013-0354-0

141 Evans DGR, Trueman L, Wallace A, *et al.* Genotype / phenotype correlations in type 2 neurofibromatosis (NF2): evidence for more severe disease associated with truncating mutations. 1998;:450–5.

142 Selvanathan SK, Shenton A, Ferner R, *et al.* Further genotype - phenotype correlations in neurofibromatosis 2. *Clinical Genetics* 2010;**77**:163–70. doi:10.1111/j.1399-0004.2009.01315.x

143 Baser ME, Kuramoto L, Woods R, *et al.* The location of constitutional neurofibromatosis 2 (NF2) splice site mutations is associated with the severity of NF2. Journal of Medical Genetics. 2005;**42**:540–6. doi:10.1136/jmg.2004.029504

144 Evans DG, Bowers N, Huson SM, *et al.* Mutation type and position varies between mosaic and inherited NF2 and correlates with disease severity. Clinical Genetics. 2013;**83**:594–5. doi:10.1111/cge.12007

145 Baser ME, Wallace AJ, Strachan T, *et al.* Clinical and molecular correlates of somatic mosaicism in neurofibromatosis 2. Journal of Medical Genetics. 2000;**37**:542–3. doi:10.1136/jmg.37.7.542

146 Halliday D, Emmanouil B, Pretorius P, *et al.* Genetic severity score predicts clinical phenotype in NF2. *Journal of Medical Genetics* 2017;**54**:657–64. doi:10.1136/jmedgenet-2017-104519

147 Halliday D, Emmanouil B, Vassallo G, *et al.* Trends in phenotype in the English paediatric neurofibromatosis type 2 cohort stratified by genetic severity. *Clinical Genetics* 2019;**96**:151–62. doi:10.1111/cge.13551

148 Bettegowda C, Upadhayaya M, Evans DG, *et al.* Genotype-Phenotype Correlations in Neurofibromatosis and Their Potential Clinical Use. *Neurology* 2021;**97**:S91–8. doi:10.1212/WNL.0000000000012436

149 Halliday J, Rutherford SA, McCabe MG, *et al.* An update on the diagnosis and treatment of vestibular schwannoma. Expert Review of Neurotherapeutics. 2018;**18**:29–39. doi:10.1080/14737175.2018.1399795

150 Plotkin SR, Duda DG, Muzikansky A, *et al.* original reports abstract Multicenter , Prospective , Phase II and Biomarker Study of High-Dose Bevacizumab as Induction Therapy in Patients With Neuro fi bromatosis Type 2 and Progressive Vestibular Schwannoma. 2019.

151 Sverak P, Adams ME, Haines SJ, *et al.* Bevacizumab for Hearing Preservation in Neurofibromatosis Type 2: Emphasis on Patient-Reported Outcomes and Toxicities. *Otolaryngology - Head and Neck Surgery (United States)* 2019;**160**:526–32. doi:10.1177/0194599818809085

152 Nunes FP, Merker VL, Jennings D, *et al.* Bevacizumab Treatment for Meningiomas in NF2: A Retrospective Analysis of 15 Patients. *PLoS ONE* 2013;**8**. doi:10.1371/journal.pone.0059941

153   Morris KA, Afridi SK, Evans DG, *et al.* The response of spinal cord ependymomas to bevacizumab in patients with neurofibromatosis Type 2. *Journal of Neurosurgery: Spine* 2017;**26**:474–82. doi:10.3171/2016.8.SPINE16589

154   Bachir S, Shah S, Shapiro S, *et al.* Neurofibromatosis type 2 (NF2) and the implications for vestibular schwannoma and meningioma pathogenesis. International Journal of Molecular Sciences. 2021;**22**:1–12. doi:10.3390/ijms22020690

155   Molaie D, Leia Nghiemphu P. Neurofibromatosis Type 2: Current Trends and Future Directions for Targeted Biologic Therapies. In: *Neurofibromatosis - Current Trends and Future Directions*. IntechOpen 2020. doi:10.5772/intechopen.90163

156   Tamura R. Current understanding of neurofibromatosis type 1, 2, and schwannomatosis. International Journal of Molecular Sciences. 2021;**22**. doi:10.3390/ijms22115850

157   Plotkin SR, Merker VL, Halpin C, *et al.* Bevacizumab for Progressive Vestibular Schwannoma in Neurofibromatosis Type 2: A Retrospective Review of 31 Patients. Otology & Neurotology, Inc 2012. http://links.lww.com/MAO/A112

158   Morris KA, Golding JF, Axon PR, *et al.* Bevacizumab in Neurofibromatosis type 2 (NF2) related vestibular schwannomas: A nationally coordinated approach to delivery and prospective evaluation. *Neuro-Oncology Practice* 2016;**3**:281–9. doi:10.1093/nop/npv065

159   Ammoun S, Flaiz C, Ristic N, *et al.* Dissecting and targeting the growth factor-dependent and growth factor-independent extracellular signal-regulated kinase pathway in human schwannoma. *Cancer Research* 2008;**68**:5236–45. doi:10.1158/0008-5472.CAN-07-5849

160   Mukherjee J, Kamnasaran D, Balasubramaniam A, *et al.* Human schwannomas express activated platelet-derived growth factor receptors and c-kit and are growth inhibited by gleevec (imatinib mesylate). *Cancer Research* 2009;**69**:5099–107. doi:10.1158/0008-5472.CAN-08-4475

161   Karajannis MA, Legault G, Hagiwara M, *et al.* Phase II trial of lapatinib in adult and pediatric patients with neurofibromatosis type 2 and progressive vestibular schwannomas. *Neuro-Oncology* 2012;**14**:1163–70. doi:10.1093/neuonc/nos146

162   Osorio DS, Hu J, Mitchell C, *et al.* Effect of lapatinib on meningioma growth in adults with neurofibromatosis type 2. *Journal of Neuro-Oncology* 2018;**139**:749–55. doi:10.1007/s11060-018-2922-5

163   Troutman Scott, Moleirinho Susana, Kota Smitha, *et al.* Crizotinib inhibits NF2-associated schwannoma through inhibition of focal adhesion kinase 1. *Oncotarget* 2016;**Vol. 7, No. 34**:54515–25.

164   Chang LS, Oblinger JL, Smith AE, *et al.* Brigatinib causes tumor shrinkage in both NF2-deficient meningioma and schwannoma through inhibition of multiple tyrosine kinases but not ALK. *PLoS ONE* 2021;**16**. doi:10.1371/journal.pone.0252048

165   Giovannini M, Bonne NX, Vitte J, *et al.* MTORC1 inhibition delays growth of neurofibromatosis type 2 schwannoma. *Neuro-Oncology* 2014;**16**:493–504. doi:10.1093/neuonc/not242

166   Goutagny S, Giovannini M, Kalamarides M. A 4-year phase II study of everolimus in NF2 patients with growing vestibular schwannomas. Journal of Neuro-Oncology. 2017;**133**:443–5. doi:10.1007/s11060-017-2447-3

167   Beauchamp RL, James MF, DeSouza PA, *et al.* A high-throughput kinome screen reveals serum/glucocorticoidregulated kinase 1 as a therapeutic target for NF2-deficient meningiomas. *Oncotarget* 2015;**6**:16981–97. doi:10.18632/oncotarget.4858

168   Goutagny S, Raymond E, Esposito-Farese M, *et al.* Phase II study of mTORC1 inhibition by everolimus in neurofibromatosis type 2 patients with growing vestibular schwannomas. *Journal of Neuro-Oncology* 2015;**122**:313–20. doi:10.1007/s11060-014-1710-0

169   Karajannis MA, Legault G, Hagiwara M, *et al.* Phase II study of everolimus in children and adults with neurofibromatosis type 2 and progressive vestibular schwannomas. *Neuro-Oncology* 2014;**16**:292–7. doi:10.1093/neuonc/not150

170   Bush ML, Oblinger J, Brendel V, *et al.* AR42, a novel histone deacetylase inhibitor, as a potential therapy for vestibular schwannomas and meningiomas. *Neuro-Oncology* 2011;**13**:983–99. doi:10.1093/neuonc/nor072

171   Ammoun S, Ristic N, Matthies C, *et al.* Targeting ERK1/2 activation and proliferation in human primary schwannoma cells with MEK1/2 inhibitor AZD6244. *Neurobiology of Disease* 2010;**37**:141–6. doi:10.1016/j.nbd.2009.09.017

172   Wu L, Vasilijic S, Sun Y, *et al.* Losartan prevents tumor-induced hearing loss and augments radiation efficacy in NF2 schwannoma rodent models. 2021. https://www.science.org

173   Bulaklak K, Gersbach CA. The once and future gene therapy. Nature Communications. 2020;**11**. doi:10.1038/s41467-020-19505-2

174   Prabhakar S, Taherian M, Gianni D, *et al.* Regression of schwannomas induced by adeno-associated virus-mediated delivery of caspase-1. *Human Gene Therapy* 2013;**24**:152–62. doi:10.1089/hum.2012.094

175   Ahmed SG, Abdelnabi A, Maguire CA, *et al.* Gene therapy with apoptosis-associated speck-like protein, a newly described schwannoma tumor suppressor, inhibits schwannoma growth in vivo. *Neuro-Oncology* 2019;**21**:855–66. doi:10.1093/neuonc/noz065

176   Ren Y, Sagers JE, Landegger LD, *et al.* Tumor-Penetrating Delivery of siRNA against TNFα to Human Vestibular Schwannomas. *Scientific Reports* 2017;**7**. doi:10.1038/s41598-017-13032-9

177   Bennett CF. Therapeutic Antisense Oligonucleotides Are Coming of Age. *Annu Rev Med 2019* 2018;**70**:307–21. doi:10.1146/annurev-med-041217

178   Rinaldi C, Wood MJA. Antisense oligonucleotides: The next frontier for treatment of neurological disorders. Nature Reviews Neurology. 2018;**14**:9–22. doi:10.1038/nrneurol.2017.148

179   Dhuri K, Bechtold C, Quijano E, *et al.* Antisense oligonucleotides: An emerging area in drug discovery and development. Journal of Clinical Medicine. 2020;**9**:1–24. doi:10.3390/JCM9062004

180   Quemener AM, Bachelot L, Forestier A, *et al.* The powerful world of antisense oligonucleotides: From bench to bedside. Wiley Interdisciplinary Reviews: RNA. 2020;**11**. doi:10.1002/wrna.1594

181   Gagliardi M, Ashizawa AT. The challenges and strategies of antisense oligonucleotide drug delivery. Biomedicines. 2021;**9**. doi:10.3390/biomedicines9040433

182   Gleave ME, Monia BP. Antisense therapy for cancer. Nature Reviews Cancer. 2005;**5**:468–79. doi:10.1038/nrc1631

183   Castellanos E, Carrato C, Rosas I, *et al.* In vitro antisense therapeutics for a deep intronic mutation causing Neurofibromatosis type 2. 2013;:769–73. doi:10.1038/ejhg.2012.261

184   McClatchey AI, Saotome I, Ramesh V, *et al.* The Nf2 tumor suppressor gene product is essential for extraembryonic development immediately prior to gastrulation. *Genes and Development* 1997;**11**:1253–65. doi:10.1101/gad.11.10.1253

185   Giovannini M, Robanus-Maandag E, Niwa-Kawakita M, *et al.* Schwann cell hyperplasia and tumors in transgenic mice expressing a naturally occurring mutant NF2 protein. 1999. www.genesdev.org

186   Mcclatchey AI, Saotome I, Mercer K, *et al.* Mice heterozygous for a mutation at the Nf2 tumor suppressor locus develop a range of highly metastatic tumors. 1998. www.genesdev.org

187   Giovannini M, Robanus-Maandag E, van der Valk M, *et al.* Conditional biallelic Nf2 mutation in the mouse promotes manifestations of human neurofibromatosis type 2. 2000. www.genesdev.org

188   Kalamarides M, Niwa-Kawakita M, Leblois H, *et al.* Nf2 gene inactivation in arachnoidal cells is rate-limiting for meningioma development in the mouse. *Genes and Development* 2002;**16**:1060–5. doi:10.1101/gad.226302

189   Schularick NM, Clark JJ, Hansen MR. Primary culture of human vestibular schwannomas. *Journal of Visualized Experiments* Published Online First: 20 July 2014. doi:10.3791/51093

190   Dilwali S, Patel PB, Roberts DS, *et al.* Primary culture of human Schwann and schwannoma cells: Improved and simplified protocol. *Hearing Research* 2014;**315**:25–33. doi:10.1016/j.heares.2014.05.006

191   Hung G, Rhim JS, Slattery W, *et al.* Establishment and characterization of a schwannoma cell line from a patient with neurofibromatosis 2. 2002.

192   Xue L, He W, Wang Z, *et al.* Characterization of a newly established schwannoma cell line from a sporadic vestibular schwannoma patient. 2021. www.ajtr.org

193   Püttmann S, Senner V, Braune S, *et al.* Establishment of a benign meningioma cell line by hTERT-mediated immortalization. *Laboratory Investigation* 2005;**85**:1163–71. doi:10.1038/labinvest.3700307

194   Zakrzewski W, Dobrzyński M, Szymonowicz M, *et al.* Stem cells: Past, present, and future. Stem Cell Research and Therapy. 2019;**10**. doi:10.1186/s13287-019-1165-5

195   Takahashi K, Yamanaka S. Induction of Pluripotent Stem Cells from Mouse Embryonic and Adult Fibroblast Cultures by Defined Factors. 2006;**2**:663–76. doi:10.1016/j.cell.2006.07.024

196   Kim J, Koo BK, Knoblich JA. Human organoids: model systems for human biology and medicine. Nature Reviews Molecular Cell Biology. 2020;**21**:571–84. doi:10.1038/s41580-020-0259-3

197   González F, Boué S, Belmonte JCI. Methods for making induced pluripotent stem cells: Reprogramming à la carte. Nature Reviews Genetics. 2011;**12**:231–42. doi:10.1038/nrg2937

198   Okita K, Yamanaka S. Induced pluripotent stem cells: Opportunities and challenges. Philosophical Transactions of the Royal Society B: Biological Sciences. 2011;**366**:2198–207. doi:10.1098/rstb.2011.0016

199   Ebert AD, Yu J, Rose FF, *et al.* Induced pluripotent stem cells from a spinal muscular atrophy patient. *Nature* 2009;**457**:277–80. doi:10.1038/nature07677

200   Sundberg M, Bogetofte H, Lawson T, *et al.* Improved cell therapy protocols for Parkinson's disease based on differentiation efficiency and safety of hESC-, hiPSC-, and non-human primate iPSC-derived dopaminergic neurons. *Stem Cells* 2013;**31**:1548–62. doi:10.1002/stem.1415

201   Moretti A, Bellin M, Welling A, *et al.* Patient-Specific Induced Pluripotent Stem-Cell Models for Long-QT Syndrome. *New England Journal of Medicine* 2010;**363**:1397–409. doi:10.1056/nejmoa0908679

202   Liu GH, Suzuki K, Li M, *et al.* Modelling Fanconi anemia pathogenesis and therapeutics using integration-free patient-derived iPSCs. *Nature Communications* 2014;**5**. doi:10.1038/ncomms5330

203   Papapetrou EP. Patient-derived induced pluripotent stem cells in cancer research and precision oncology. Nature Medicine. 2016;**22**:1392–401. doi:10.1038/nm.4238

204   Nourbakhsh A, Gosstola NC, Fernandez-Valle C, *et al.* Characterization of UMi031-A-2 inducible pluripotent stem cell line with a neurofibromatosis type 2-associated mutation. *Stem Cell Research* 2021;**55**. doi:10.1016/j.scr.2021.102474

205   Ndubaku U, de Bellard ME. Glial cells: Old cells with new twists. Acta Histochemica. 2008;**110**:182–95. doi:10.1016/j.acthis.2007.10.003

206   le Douarin NM, Dupin E. Multipotentiality of the neural crest. Current Opinion in Genetics and Development. 2003;**13**:529–36. doi:10.1016/j.gde.2003.08.002

207   le Douarin NM, Creuzet S, Couly G, *et al.* Neural crest cell plasticity and its limits. Development. 2004;**131**:4637–50. doi:10.1242/dev.01350

208 Rogers CD, Jayasena CS, Nie S, *et al.* Neural crest specification: Tissues, signals, and transcription factors. Wiley Interdisciplinary Reviews: Developmental Biology. 2012;**1**:52–68. doi:10.1002/wdev.8

209 Srinivasan A, Toh YC. Human pluripotent stem cell-derived neural crest cells for tissue regeneration and disease modeling. Frontiers in Molecular Neuroscience. 2019;**12**. doi:10.3389/fnmol.2019.00039

210 Menendez L, Kulik MJ, Page AT, *et al.* Directed differentiation of human pluripotent cells to neural crest stem cells. *Nature Protocols* 2013;**8**:203–12. doi:10.1038/nprot.2012.156

211 Menendez L, Yatskievych TA, Antin PB, *et al.* Wnt signaling and a Smad pathway blockade direct the differentiation of human pluripotent stem cells to multipotent neural crest cells. *Proceedings of the National Academy of Sciences of the United States of America* 2011;**108**:19240–5. doi:10.1073/pnas.1113746108

212 Jessen KR, Mirsky R, Lloyd AC. Schwann cells: Development and role in nerve repair. *Cold Spring Harbor Perspectives in Biology* 2015;**7**:1–15. doi:10.1101/cshperspect.a020487

213 Simões-Costa M, Bronner ME. Establishing neural crest identity: a gene regulatory recipe. Development (Cambridge, England). 2015;**142**:242–57. doi:10.1242/dev.105445

214 Ma MS, Boddeke E, Copray S. Pluripotent Stem Cells for Schwann Cell Engineering. *Stem Cell Reviews and Reports* 2015;**11**:205–18. doi:10.1007/s12015-014-9577-1

215 Jessen KR, Mirsky R. The origin and development of glial cells in peripheral nerves. *Nature Reviews Neuroscience* 2005;**6**:671–82. doi:10.1038/nrn1746

216 Kluwe L, MacCollin M, Tatagiba M, *et al.* Phenotypic variability associated with 14 splice-site mutations in the NF2 gene. *American Journal of Medical Genetics* 1998;**77**:228–33. doi:10.1002/(SICI)1096-8628(19980518)77:3<228::AID-AJMG8>3.0.CO;2-L

217 Ruttledge MH, Andermann a a, Phelan CM, *et al.* Type of mutation in the neurofibromatosis type 2 gene (NF2) frequently determines severity of disease. *American Journal of Human Genetics* 1996;**59**:331–42.

218 Mautner VF, Baser ME, Kluwe L. Phenotypic variability in two families with novel splice-site and frameshift NF2 mutations. *Human Genetics* 1996;**98**:203–6. doi:10.1007/s004390050191

219 Castellanos E, Rosas I, Solanes A, *et al.* In vitro antisense therapeutics for a deep intronic mutation causing Neurofibromatosis type 2. *European Journal of Human Genetics* 2013;**21**:769–73. doi:10.1038/ejhg.2012.261

220 Heineman TE, Evans DGR, Campagne F, *et al.* In silico analysis of NF2 gene missense mutations in neurofibromatosis type 2: From genotype to phenotype. *Otology and Neurotology* 2015;**36**:908–14. doi:10.1097/MAO.0000000000000639

221 Molina JR, Adjei AA. The Ras/Raf/MAPK Pathway. *Journal of Thoracic Oncology* 2006;**1**:7–9. doi:10.1016/s1556-0864(15)31506-9

222 Baser ME, Friedman JM, Aeschliman D, *et al.* Predictors of the Risk of Mortality in Neurofibromatosis 2. 2002.

223 Kluwe L, Mautner VF. A missense mutation in the NF2 gene results in moderate and mild clinical phenotypes of neurofibromatosis type 2. *Human Genetics* 1996;**97**:224–7. doi:10.1007/BF02265270

224 Wurster CD, Ludolph AC. Nusinersen for spinal muscular atrophy. Therapeutic Advances in Neurological Disorders. 2018;**11**. doi:10.1177/1756285618754459

225 Antisense Oligonucleotide-Mediated Exon-skipping Therapies: Precision Medicine Spreading from Duchenne Muscular Dystrophy. *JMA Journal* 2021;**4**:232–40. doi:10.31662/jmaj.2021-0019

226 Summerton J, Weller D. Morpholino Antisense Oligomers: Design, Preparation, and Properties. 1997.

227 McClatchey AI, Giovannini M. Membrane organization and tumorigenesis - The NF2 tumor suppressor, Merlin. *Genes and Development* 2005;**19**:2265–77. doi:10.1101/gad.1335605

228   Hamaratoglu F, Willecke M, Kango-Singh M, *et al.* The tumour-suppressor genes NF2/Merlin and Expanded act through Hippo signalling to regulate cell proliferation and apoptosis. *Nature Cell Biology* 2006;**8**:27–36. doi:10.1038/ncb1339

229   Bosco EE, Nakai Y, Hennigan RF, *et al.* NF2-deficient cells depend on the Rac1-canonical Wnt signaling pathway to promote the loss of contact inhibition of proliferation. *Oncogene* 2010;**29**:2540–9. doi:10.1038/onc.2010.20

230   Takizawa H, Takeshita E, Sato M, *et al.* Highly sensitive screening of antisense sequences for different types of DMD mutations in patients' urine-derived cells. *Journal of the Neurological Sciences* 2021;**423**. doi:10.1016/j.jns.2021.117337

231   Echigoya Y, Lim KRQ, Trieu N, *et al.* Quantitative Antisense Screening and Optimization for Exon 51 Skipping in Duchenne Muscular Dystrophy. *Molecular Therapy* 2017;**25**:2561–72. doi:10.1016/j.ymthe.2017.07.014

232   Pan XY, Tsai MH, Wuputra K, *et al.* Application of cancer cell reprogramming technology to human cancer research. Anticancer Research. 2017;**37**:3367–77. doi:10.21873/anticanreS.11703

233   Kotini AG, Chang CJ, Chow A, *et al.* Stage-Specific Human Induced Pluripotent Stem Cells Map the Progression of Myeloid Transformation to Transplantable Leukemia. *Cell Stem Cell* 2017;**20**:315-328.e7. doi:10.1016/j.stem.2017.01.009

234   Kim J, Hoffman JP, Alpaugh RK, *et al.* An iPSC Line from Human Pancreatic Ductal Adenocarcinoma Undergoes Early to Invasive Stages of Pancreatic Cancer Progression. *Cell Reports* 2013;**3**:2088–99. doi:10.1016/j.celrep.2013.05.036

235   Carrió M, Mazuelas H, Richaud-Patin Y, *et al.* Reprogramming Captures the Genetic and Tumorigenic Properties of Neurofibromatosis Type 1 Plexiform Neurofibromas. *Stem Cell Reports* 2019;**12**. doi:10.1016/j.stemcr.2019.01.001

236   Yilmaz A, Peretz M, Aharony A, *et al.* Defining essential genes for human pluripotent stem cells by CRISPR-Cas9 screening in haploid cells. *Nature Cell Biology* 2018;**20**:610–9. doi:10.1038/s41556-018-0088-1

237   Blomen VA, Májek P, Jae LT, *et al.* Gene essentiality and synthetic lethality in haploid human cells. *Science* 2015;**350**:1092–6. doi:10.1126/science.aac7557

238   Curto M, Cole BK, Lallemand D, *et al.* Contact-dependent inhibition of EGFR signaling by Nf2/Merlin. *Journal of Cell Biology* 2007;**177**:893–903. doi:10.1083/jcb.200703010

239   Chiasson-MacKenzie C, Morris ZS, Baca Q, *et al.* NF2/Merlin mediates contact-dependent inhibition of EGFR mobility and internalization via cortical actomyosin. *Journal of Cell Biology* 2015;**211**:391–405. doi:10.1083/jcb.201503081

240   Morrison H, Sherman LS, Legg J, *et al.* The NF2 tumor suppressor gene product, merlin, mediates contact inhibition of growth through interactions with CD44. *Genes and Development* 2001;**15**:968–80. doi:10.1101/gad.189601

241   Mazuelas H, Magallón-Lorenz M, Fernández-Rodríguez J, *et al.* Modeling iPSC-derived human neurofibroma-like tumors in mice uncovers the heterogeneity of Schwann cells within plexiform neurofibromas. *Cell Reports* 2022;**38**:110385. doi:10.1016/j.celrep.2022.110385

Appendix A

Introduction: Supplementary tables

Categorization of NF2 genetic variants into severity groups according to the Genetic Severity Score

Table A1.1. Categorization of NF2 genetic variants into severity groups			
NF2 mutation detected in blood (Mosaic in blood determined on NGS as any level under 50%)	**2A Mild**	**2B Moderate**	**3 Severe**
Truncating mutation			
Exons 2-13			3
Exons 2-13 mosaic		2B	
Exons 14-15		2B	
Exons 14-15 mosaic	2A		
Exon 1/ Exon 1 mosaic	2A		
Splice site mutation			
Exons 1-7		2B	
Exons 1-7 mosaic	2A		
Exons 8-15	2A		
Exons 8-15 mosaic	2A		
Large deletion excluding promoter or exon 1		2B	
Large deletion excluding promoter or exon 1 mosaic	2A		
Large deletion including promoter or exon 1 non-mosaic or mosaic	2A		
Small in-frame deletion or duplication non-mosaic or mosaic	2A		
Missense mutation non-mosaic or mosaic	2A		
NF2, neurofibromatosis type 2; NGS, next-generation sequencing			

Extracted from: Halliday D, Emmanouil B, Pretorius P, et al. J Med Genet 2017;54:657–664

Drug candidates in clinical trials for Neurofibromatosis Type 2

		Table A1.2. Clinical trials of drug candidates for NF2-related tumours				
Drug	**Mechanisms of action**	**Title of the study**	**N**	**Phase**	**Primary outcome**	**NCT Number**
Bevacizumab (AvastinTM)	Anti-VEGF monoclonal antibody	Open-label, Phase 2 Study of Bevacizumab in Children and Young Adults with Neurofibromatosis 2 and Progressive Vestibular Schwannomas That Are Poor Candidates for Standard Treatment with Surgery or Radiation	22	II	Vestibular schwannoma volume	NCT01767792
Icotinib	EGFR inhibitor	Icotinib Hydrochloride Tablets Study for Patients with Neurofibromatosis Type 2 (NF2) and NF2-Related Tumours	10	II	Change from Baseline in volume of tumour	NCT02934256
Axitinib (InlytaTM)	VEGFR 1/2/3 inhibitor	Phase II Study of Axitinib in Patients with Neurofibromatosis Type 2 and Progressive Vestibular Schwannomas	13	II	Volumetric response rates	NCT02129647
Aspirin	Cox 2 inhibitor	Prospective, Randomized, Placebo-Controlled Phase II Trial of Aspirin for Vestibular Schwannomas	300	II	Progression-free survival	NCT03079999
Everolimus	mTORC1 inhibitor	Study of RAD001 for Treatment of NF2-related Vestibular Schwannoma	4	II	Vestibular schwannoma volume Hearing Number of adverse events	NCT01345136
AR-42	HDAC inhibitor	Exploratory Evaluation of AR-42 Histone Deacetylase Inhibitor in the Treatment of Vestibular Schwannoma and Meningioma	5	I	Expression levels of phospho-Akt (p-AKT) and p16INKA after 3 weeks of oral AR-42	NCT02282917

Crizotinib	FAK1 inhibitor	Open-label, Phase 2 Clinical Trial of Crizotinib for Children and Adults with Neurofibromatosis Type 2 and Progressive Vestibular Schwannomas	19	II	Volumetric response rate	NCT04283669
Selumetinib	MEK1/2 inhibitor	Phase 2 Trial of Selumetinib in Patients with Neurofibromatosis Type II Related Tumours	34	II	Hearing response Volumetric response rate	NCT03095248
AZD2014	mTORC1 and mTORC2 inhibitor	A Single Arm Phase 2 Study of the Dual mTORC1/mTORC2 Inhibitor AZD2014 Provided on an Intermittent Schedule for Neurofibromatosis 2 Patients with Progressive or Symptomatic Meningiomas	18	II	Volumetric response rate	NCT02831257
Brigatinib (ALUNBRIG®)	Multiple Tyr kinases inhibitor	Innovative Trial for Understanding the Impact of Targeted Therapies in NF2 (INTUITT-NF2)	80	II	Volumetric response rate	NCT04374305
REC-2282 (AR-42)	HDAC inhibitor	Efficacy and Safety of REC-2282 in Patients with Progressive Neurofibromatosis Type 2 (NF2) Mutated Meningiomas	89	II, III	Progression-free survival	NCT05130866

Source: ClinicalTrials.gov; U.S. National Library of Medicine

Antisense therapies approved by the FDA and EMA

Table A1.3. Antisense therapies approved by regulatory agencies				
Drug	**Approval**	**Indication**	**Mechanism**	**Chemistry**
Fomivirsen (VitraveneTM)	FDA (1998)	Cytomegalovirus (CMV) retinitis	Downregulate the gene encoding CMV immediate-early 2 protein	PS
Mipomersen (Kynamro®)	FDA (2013)	Familial hypercholesterolemia (FH)	Downregulate the gene APOB encoding apolipoprotein B	2'-O-MOE, PS, 5-methyl cytosine
Eteplirsen (Exondys 51®)	FDA (2016), EMA (2018)	Duchenne muscular dystrophy (DMD)	Rescue the expression of dystrophin through exon-51 skipping of the mRNA of DMD gene	PMO
Nusinersen (Spinraza®)	FDA (2016), EMA (2017)	Spinal muscular atrophy (SMA)	Increase the production of the survival motor neuron (SMN) protein by exon-7 inclusion of the mRNA of SMN2 gene	2'-O-MOE, PS, 5-methyl cytosine
Inotersen (Tegsedi®)	FDA and EMA (2018)	Hereditary transthyretin (TTR) amyloidosis	Downregulate the gene TTR encoding transthyretin	2'-O-MOE, PS,
Golodirsen (Vyondys 53®)	FDA (2019)	DMD	Rescue the expression of dystrophin through exon-53 skipping of the mRNA of DMD gene	PMO
Viltolarsen (Viltepso®)	FDA and EMA (2020)	DMD	Rescue the expression of dystrophin through exon-53 skipping of the mRNA of DMD gene	PMO
Casimersen (Amondys 45®)	FDA (2021)	DMD	Rescue the expression of dystrophin through exon-45 skipping of the mRNA of DMD gene	PMO
FDA: Food and Drug Administration; EMA: European Medicines Agency				

Adapted from: Li Y, Tan Y, Zhang R, et al. Antisense Oligonucleotide: A Potential Therapeutic Intervention for Chronic Kidney Disease. Kidney and Dialysis 2022;2:16–37 and Dhuri K, Bechtold C, Quijano E, et al. Antisense oligonucleotides: An emerging area in drug discovery and development. Journal of Clinical Medicine. 2020;9:1–24.

Appendix B

Chapter 1: Supplementary tables and figures

Figure S1.1. pMerlin and merlin levels in patient's fibroblasts. NPE stands for Normalized Protein Expression; Bars represent the SD from three independent experiments.
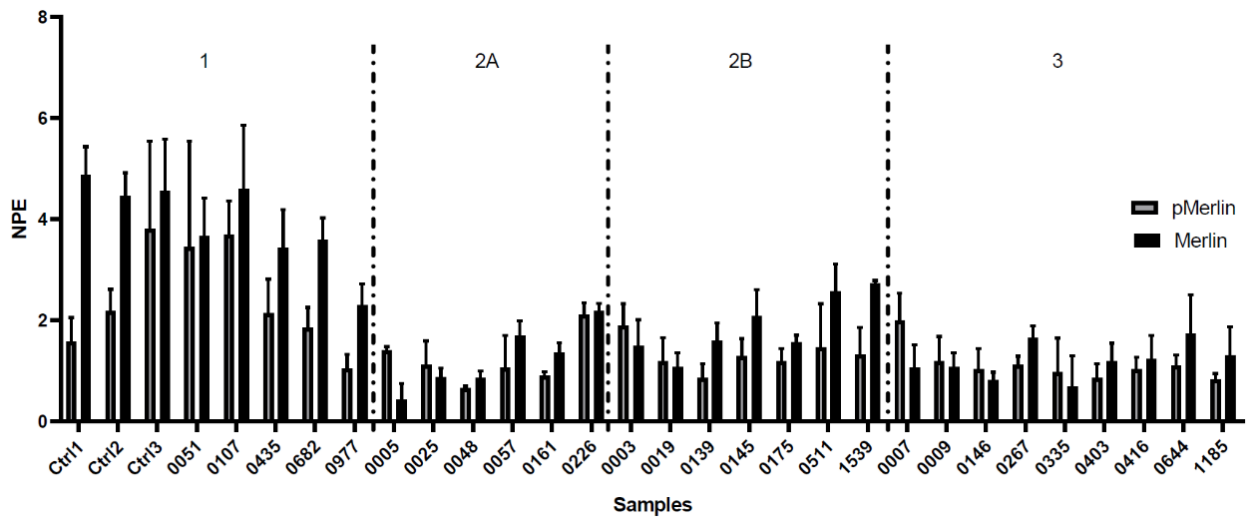
Figure S1.2. Levels of proteins involved in the NF2 downstream pathway in patients' fibroblasts. NPE stands for Normalized Protein Expression; Bars represent the SD from three independent experiments.

Figure S1.3. PCA-biplot of phenotypical NF2 data by NF2-mutation groups. VS: Vestibular Schwannoma; Age Dx: Age at diagnosis; PS: Peripheral Schwannoma; EVA: Extra vestibular Affection. Dim1 (Dimension 1); Dim2 (Dimension 1)

Figure S1.4. Sanger sequencing comparison between blood and fibroblast samples of a NF2 patient.

Table S1.1. NF2 Patients summary.

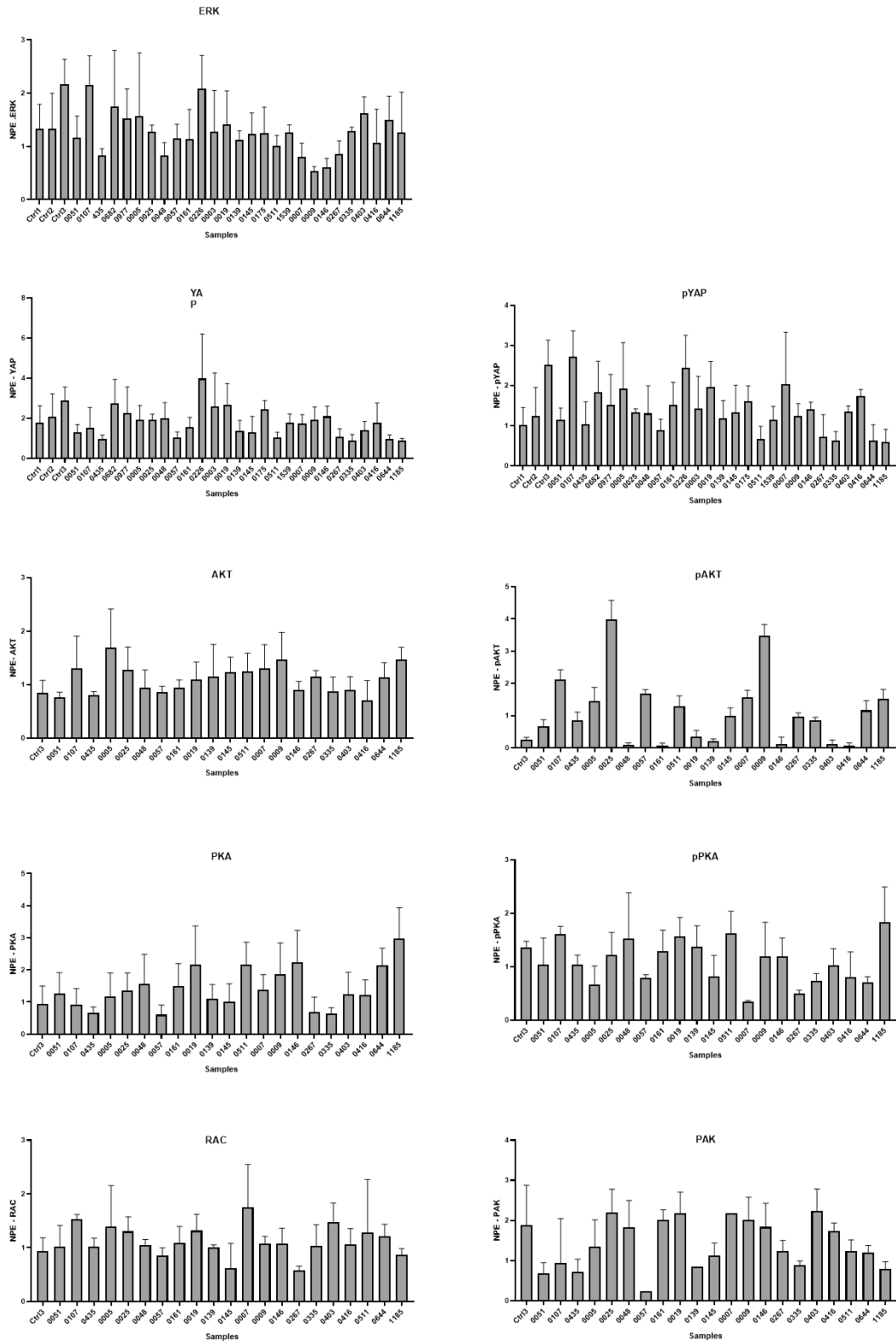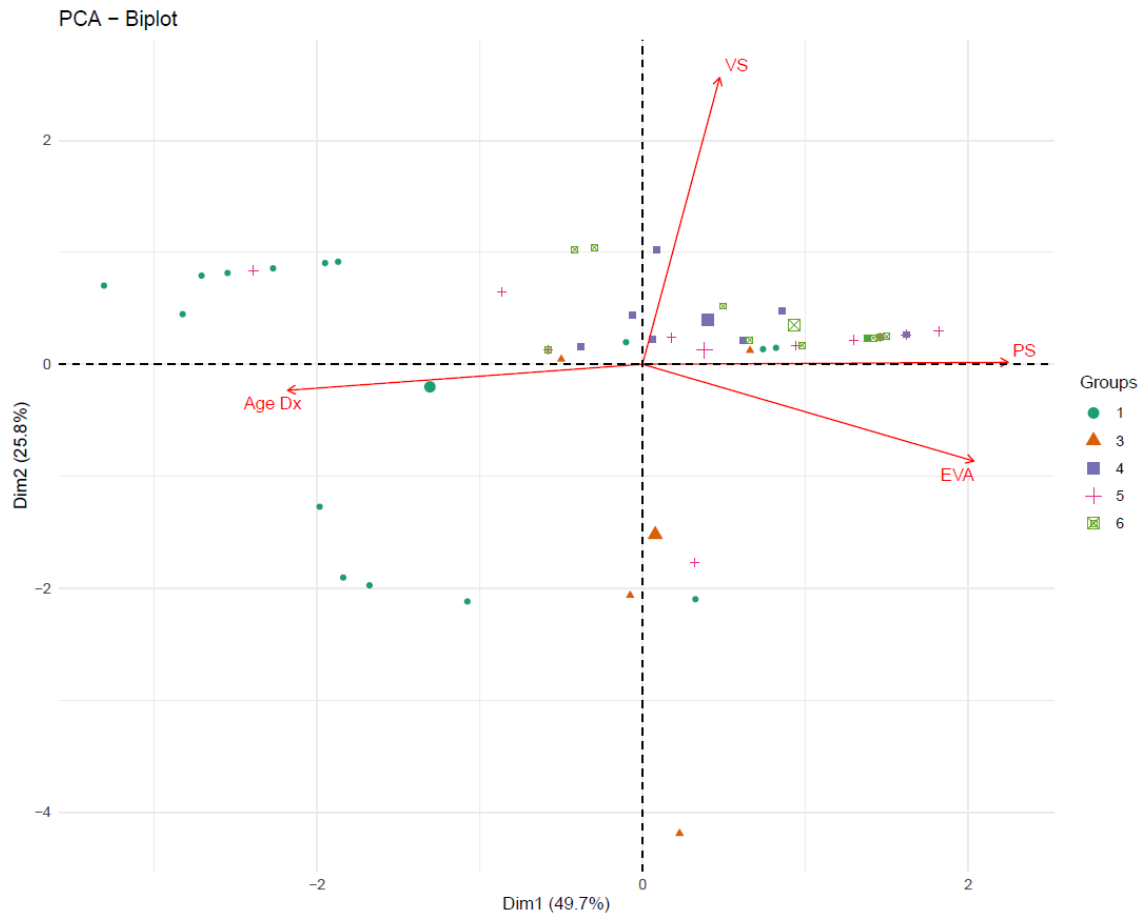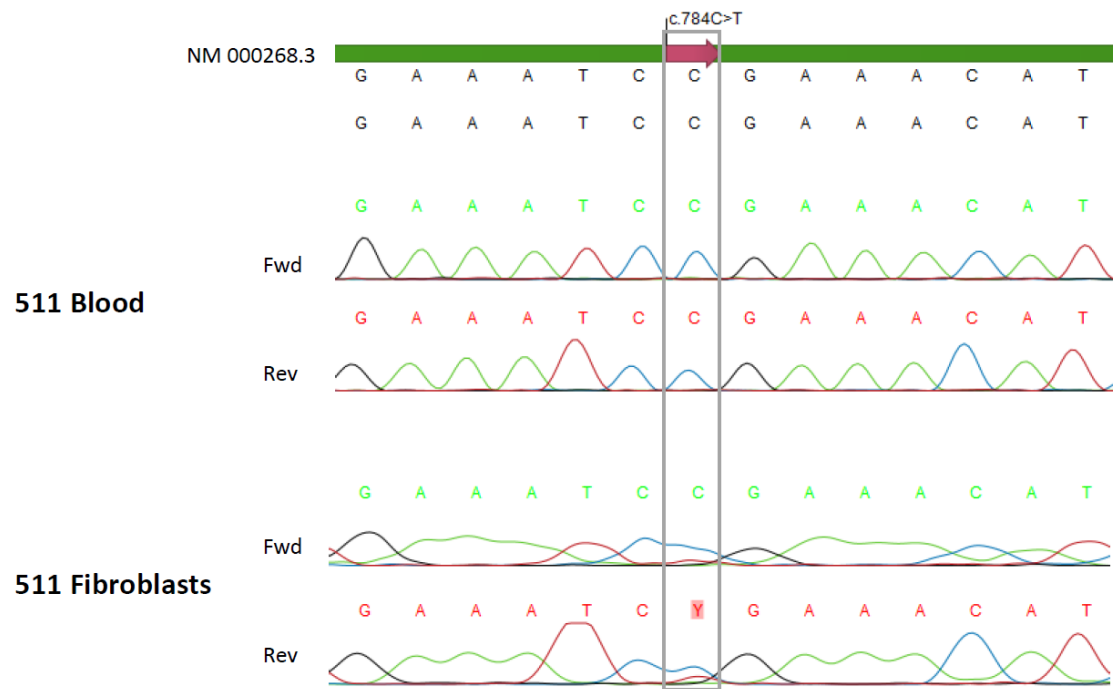| Identifier	Current Age	Age at diagnostic	Score	Vestibular Schwannomas Score (0= NO; 1=Unique, 2 = Multiple)	Peripheral schwannomas Score (0= NO; 1=Unique, 2 = Multiple)	Intracranial Meningioma	Intracraneal Schwannoma	Intraspinal Meningioma	Intraspinal Schwannoma	Ependymoma	Score (0,1,2,3)	Variant at cDNA	Variant at protein level	Inheritance	GSS	FGSS
1	28	19	3	2	2	No	No	No	No	No	0	Whole NF2 gene deletion. Mosaic present in blood		Sporadic	2A	4
2	46	23	3	2	0	Multiple	No	No	No	Single	3	Genetic test in blood inconclusive		Sporadic	1A	1
3	29	22	3	2	2	Multiple	No	No	No	No	2	c.115_363del	p.(Met39_Gln121del)	Sporadic	2B	4
5	53	16	3	2	0	No	No	No	Multiple	Multiple	3	c.1446_1477insNG_009057.1:g.74239_74405	p.(Pro482Profs*39)	Sporadic	2A	4
7	42	18	2	2	2	Multiple	No	No	Multiple	No	3	c.432C>G	p.(Tyr144*)	Sporadic	3	6
8	36	28	2	1	2	No	No	No	Multiple	No	2	c.592C>T. Present in two tumors	p.(Arg198*)	Sporadic	1B	5
9	29	19	3	2	2	Multiple	Multiple		Multiple	No	3	c.784C>T	p./Arg262*)	Sporadic	3	6
19	54	37	1	2	1	No	No	No	Single	No	1	Exons 15-16 deletion; r.1575_1747del	p.(Lys525Asnfs*19)	Sporadic	2B	4
24	54	40	1	1	0	Multiple	No	Multiple	Single	No	3	Genetic test in blood inconclusive		Sporadic	1A	1
25	55	47	1	2	0	No	No	No	No	No	0	c.1747A>G; r.1575_1747del	p.(Lys525Asnfs*19)	Sporadic	2A	4
48	25	14	3	2	2	Multiple	No	No	Multiple	No	3	c.810+1dupG	p.(Phe271Val4fs*)	Sporadic	2A	5
51	64	44	1	2	0	No	No	No	No	No	0	Genetic test in blood inconclusive		Sporadic	1A	1
57	50	22	3	2	1	No	Multiple	No	Multiple	No	3	Exons 1-5 deletion and 47 kb upstream (NIPSNAP1)		Familial	2A	4
69	58	30	2	2	0	No	Multiple	No	Multiple	No	3	Exons 1-5 deletion and 47 kb upstream (NIPSNAP1)		Familial	2A	4
106	70	61	1	1	1	No	No	No	Multiple	No	2	Exon 6 deletion in one tumor analyzed. Not detected in blood.		Sporadic	1A	1
107	70	38	1	2	2	Multiple	Multiple	Multiple	Multiple	No	3	c.592C>T in three tumors analyzed. Not detected in blood.	p.(Arg198*)	Sporadic	1B	3
139	12	9	3	2	2	No	Multiple	No	Multiple	No	3	c.241-9A>G	p.(Val81Phefs*44)	Sporadic	2B	5
144	79	69	1	2	0	Single	No	No	No	No	1	Genetic test in blood inconclusive		Sporadic	1A	1
145	43	31	2	2	2	Multiple	No	No	Multiple	Multiple	3	c.241-13T>A	p.(Val81Glnfs*45)	Sporadic	2B	5
146	28	17	3	2	2	Multiple	Single	No	Multiple	Multiple	3	c.1282C>T	p.(Gln428*)	Sporadic	3	6
161	34	28	2	2	1	No	No	No	Multiple	No	2	Exons 14-17 deletion. Mosaic present in blood		Sporadic	2A	4
175	25	19	3	2	0	Single	Single	No	Multiple	No	3	Exons 5-17 deletion and downstream CABP7 deletion		Sporadic	2B	4
226	55	50	1	2	1	Multiple	Single	No	Multiple	No	3	c.287T>C	p.(Phe96Ser)	Sporadic	2A	3
267	20	14	3	2	1	No	No	No	Multiple	No	2	c.784C>T	p.(Arg262*)	Sporadic	3	6
335	32	20	3	2	2	Multiple	Multiple	Single	Multiple	Multiple	3	c.380_396dupTAGATGAAAA	p.(Cys133*)	Sporadic	3	6
399	57	51	1	2	0	No	No	No	No	No	0	Genetic test in blood inconclusive		Sporadic	1A	1
403	31	18	3	2	2	Multiple	Single	Single	Multiple	No	3	c.784C>T	p.(Arg262*)	Sporadic	3	6
416	18	14	3	2	2	No	Multiple	Single	Multiple	Single	3	c.520dupA	p.(Ile174Asnfs*29)	Sporadic	3	6
435	21	17	3	0	1	No	Multiple	No	Multiple	No	3	c.970C>T in two tumors analyzed. Not detected in blood	p.(Gln324*)	Sporadic	1B	3
511	40	18	3	2	2	Multiple	No	Multiple	Multiple	Single	3	c.784C>T. Mosaic present in blood	p.(Arg262*)	Sporadic	2B	5
644	43	21	3	2	1	Multiple	Single	Single	Multiple	Single	3	c.784C>T	p.(Arg262*)	Sporadic	3	6
682	56	34	2	2	2	Multiple	Multiple	No	Multiple	Multiple	3	c.592C>T in one tumor analyzed. Not detected in blood		Sporadic	1A	1
806	38	20	3	2	2	Multiple	Multiple	Multiple	Multiple	Multiple	3	c.112G>T in one tumor analyzed. Not detected in blood		Sporadic	1A	1
824	40	36	1	2	0	Single	No	No	No	No	0	Ring 22		Sporadic	2A	1
833	67	55	1	2	0	No	No	No	No	No	0	Genetic test in blood inconclusive		Sporadic	1A	1
913	41	35	2	2	0	Multiple	Single	Single	No	No	3	c.169C>T detected at 7% in blood	p.(Arg57*)	Sporadic	2B	5
977	38	32	2	1	1	Multiple	No	No	Multiple	No	3	Exons 2-3 deletion in two tumors analyzed. Not detected in blood		Sporadic	1B	3
1040	39	18	3	2	2	No	Multiple	No	Multiple	Single	3	c.586C>T. Mosaic present in blood	p.(Arg196*)	Sporadic	2B	5
1073	27	18	3	2	2	Multiple	Multiple	Multiple	Single	Single	3	Genetic test in blood inconclusive		Sporadic	1A	1
1185	49	35	2	2	0	Single	No	No	Single	No	3	c.1096_1102del7	p.(Glu366Glnfs*7)	Familial, index	3	6
1190	55	39	1	1	2	Multiple	No	Multiple	Multiple	No	3	c.169C>T in one tumor analyzed. Not detected in blood	p.(Arg57*)	Sporadic	1A	1
1221	74	70	1	2	0	No	No	No	No	No	0	Genetic test in blood inconclusive		Sporadic	1A	1
1222	43	14	3	2	2	Multiple	No	Multiple	No	Multiple	3	c.448-2A>G		Sporadic	2B	4
1312	35	34	2	2	0	No	No	No	No	No	0	Genetic test in blood inconclusive		Sporadic	1A	1
1339	40	36	1	2	2	Multiple	No	Multiple	Multiple	No	3	Genetic test in blood inconclusive. Mosaic suspicion because her son is also NF2		Sporadic	1A	1
1536	15	14	3	2		No	No	No	No	No	0	c.1096_1102del7	p.(Glu366Glnfs*7)	Familial	3	6
1537	17	17	3	2		No	No	No	No	No	0	c.1096_1102del7	p.(Glu366Glnfs*7)	Familial	3	6
1539	40	22	3	2	2	Multiple	No	Multiple	No	No	3	c.169C>T. Mosaic present in blood	p.(Arg67*)	Sporadic	2B	5
1779	55	48	1	1	0	Multiple	No	No	No	No	2	Genetic test in blood inconclusive		Sporadic	1A	1
1802	21	18	3	2	2	Single	Multiple	Multiple	Multiple	No	3	c.1334_1337delAGAG	p.(Glu445Glyfs*9)	Sporadic	3	6
Patient 2	34	20	3	2	2	Multiple	No	No	Multiple	Single	3	c.1396C>T	p.(Arg466*)	Sporadic	3	6
Patient 5	52	30	2	2	2	Multiple	No	No	Multiple	No	3	c.634C>T	p.(Gln212*)	Sporadic	3	6

Table S1.2. Major interventions in relation to Genetic Severity Score							
Genetic Severity			**1 Tissue Mosaic**	**2A Mild**	**2B Moderate**	**3 Severe**	**Statistics**
N (%)	Proportion of patients whithin	VS surgery	7 (36,84%)	9 (100%)	5 (50%)	10 (71,4%)	$X^2(1) = 4.08$, $p = 0.043$
		Non-VS intracranial surgery	2 (10,5%)	0 (0%)	3 (30%)	5 (35,7%)	$X^2(1) = 3.99$, $p = 0.045$
		Spinal surgery	6 (31,58%)	1 (11,11%)	4 (40%)	2 (14,3%)	$X^2(1) = 0.72$, $p = 0.39$
		Shunt surgery	0 (0%)	0 (0%)	0 (0%)	1 (7,1%)	$X^2(1) = 1.73$, $p = 0.18$
		Radiotherapy	1 (5,26%)	3 (33,33%)	3 (30%)	8 (57,1%)	$X^2(1) = 8.9$, $p = 0.002$
		Bevacizumab	0 (0%)	1 (11,11%)	4 (40%)	6 (42,9%)	$X^2(1) = 10.2$, $p = 0.001$
	Total number of major interventions per person, grouped	0	7 (36,84%)	1 (11,11%)	0 (0%)	2 (14,3%)	$X^2(1) = 4.08$, $p = 0.043$
		1	5 (26,31%)	2 (22,22%)	3 (30%)	2 (14,3%)	$X^2(1) = 0.05$, $p = 0.82$
		2	2 (10,52%)	4 (44,44%)	2 (20%)	2 (14,3%)	$X^2(1) = 0$, $p = 1$
		3	1 (5,26%)	3 (33,33%)	1 (10%)	2 (14,3%)	$X^2(1) = 0.15$, $p = 0.69$
		4 or more	3 (15,79%)	0 (0%)	4 (40%)	6 (42,9%)	$X^2(1) = 4.10$, $p = 0.042$
Mean (SD)	Total number of major interventions per person, grouped		1,53 (1,91)	1,90 (0,99)	3,09 (2,34)	3,79 (3,36)	$r_s(50) = 0.35$, $p = 0.01$
	Number of total surgeries		1,53 (2,07)	1,50 (0,71)	1,91 (1,64)	2,64 (2,98)	$r_s(50) = 0.18$, $p = 0.19$
	Age at first radiotherapy session		23	37 (9,64)	30,33 (6,66)	24,29 (8,16)	$r_s(12) = -0.42$, $p = 0.13$
	Age started bevacizumab		-	32	26,67 (14,57)	23,67 (8,48)	$r_s(8) = -0.26$, $p = 0.46$
	Age at first surgery		35,44 (13,36)	29,78 (12,05)	26,67 (7,57)	20,80 (7,73)	$r_s(35) = -0.47$, $p = 0.003$
	Age at first major intervention		34,20 (13,20	29,78 (12,05)	25,55 (8,55)	20,55 (7,89)	$r_s(39) = -0.47$, $p = 0.001$
	Ratio of total number of major interventions to current age		0,03 (0,04)	0,04 (0,02)	0,08 (0,06)	0,13 (0,11)	$r_s(50) = 0.49$, $p < 0.001$

Table S1.3. Phenotype quantification		
Phenotypic feature		**Value**
Age at diagnosis	< 25 years	3
	< 35 years	2
	> 35 years	1
Vestibular Schwannoma	Unilateral	1
	Bilateral	2
Peripheral Schwannomas	Single	1
	Multiple	2
Extravestibular affection (Spinal/Cerebral)	Spinal and cerebral injury or spinal/cerebral different type of injury	3
	Cerebral or Spinal multiple injuries	2
	Single brain or spinal injury	1

Table S1.4. Revising pathogenicity associated with *NF2* mutations according to GSS. Patients with an unexpected phenotype according to GSS are highlighted in bold in the Reasoning column.

NF2-causing variant			GSS	Inheritance	Mosaicism		Phenotype Quantification	Merlin NPE levels	pERK NPE levels	Reasoning
cDNA (NM_00268.3)	Exon	Predicted protein			% in blood	Only in tissue				
c.169C>T & c.810+2T>A	exon 2; exon 8	p.(Arg57*) & p.(?)	1A	Sporadic	Not detected	One tumor analyzed	3	3,66129319	4,0767212	Mosaic patient. Very mild phenotype
c.1341-25_1377del62 +LOH	exon 13	p.(?)	1A	Sporadic	Not detected	One tumor analyzed	3			Mosaic patient. Very mild phenotype
Genetic test (NGS) in blood inconclusive			1A	Sporadic			3			Mosaic patient. Very mild phenotype
Genetic test (NGS) in blood inconclusive			1A	Sporadic			3			Mosaic patient. Very mild phenotype
Genetic test (NGS) in blood inconclusive			1A	Sporadic			4			Mosaic patient. Very mild phenotype
Genetic test (NGS) in blood inconclusive			1A	Sporadic			4			Mosaic patient. Very mild phenotype
Genetic test (NGS) in blood inconclusive			1A	Sporadic			4			Mosaic patient. Very mild phenotype
Genetic test in blood inconclusive			1A	Sporadic			5			Mosaic patient. Mild phenotype
exon 6 deletion + LOH	exon 6	p.(Val173Glyfs*2)	1A	Sporadic	Not detected	One tumor analyzed	5			Mosaic patient. Mild phenotype
c.169C>T + LOH	exon2	p.(Arg57*)	1A	Sporadic	Not detected	One tumor analyzed	7			**Mosaic patient. Unexpected mild-moderate phenotype**
Genetic test in blood inconclusive			1A	Sporadic			8			**Mosaic patient. Unexpected moderate phenotype**
Genetic test (NGS) in blood inconclusive			1A	Sporadic		Mosaic suspicion b	8			**Mosaic patient. Unexpected moderate phenotype**
c.592C>T + LOH	exon 6	p.(Arg198*)	1A	Sporadic	2% in fibroblas	One tumor analyzed	9	3,57902164	9,08179524	**Mosaic patient. Unexpected severe phenotype**

Mutation	Exon	Protein	Class	Inheritance	Detection	Tumor	Number	Value 1	Value 2	Comments
c.112G>T + LOH	exon 1	P.(Glu38*)	1A	Sporadic	Not detected	One tumor analyzed	10			Mosaic patient. Unexpected severe phenotype
Genetic test (NGS) in blood inconclusive			1A	Sporadic			10			Mosaic patient. Unexpected severe phenotype
exons 2-3 deletion	exon 2 & 3	p.(?)	1B	Sporadic	Not detected	Two tumors analyze	7	2,28870175	3,0376054	Mosaic patient. Unexpected mild-moderate phenotype
c.970C>T	exon 10	p.(Gln324*)	1B	Sporadic	Not detected	Two tumors analyze	7	3,42502203	0,33804115	Mosaic patient. Unexpected mild-moderate phenotype
c.592C>T	exon 6	p.(Arg198*)	1B	Sporadic	Not detected	Three tumors analyz	8	4,58749871	4,55488321	Mosaic patient. Unexpected moderate phenotype
c.592C>T	exon 6	p.(Arg198*)	1B	Sporadic	Not detected	Two tumors analyze	7			Mosaic patient. Unexpected mild-moderate phenotype
c.1747A>G; r.1575_1747del	exon 15	p.(Lys525Asnfs*19)	2A	Sporadic			3	0,65585897	1,75666641	Splicing variant at exon 15. Mild phenotype
Ring 22			2A	Sporadic			3			
exons 14-17 deletion	exons 14-17	p.(?)	2A	Sporadic	20% (MLPA kit P044)		7	0,82372417	0,34586901	Large deletion excluding promoter in mosaicism. Unexpected mild-moderate phenotype. Merlin and pERK levels below threshold.
c.287T>C	exon 3	p.(Phe96Ser)	2A	Sporadic			7	2,18077529	2,23406472	Missense variant. Unexpected mild-moderate phenotype.
Whole NF2 gene deletion in mosaicism	whole gene		2A	Sporadic	~10% (MLPA kit P044)		7			Large deletion including promoter in mosaicism. Unexpected mild-moderate phenotype.
exons 1-5 deletion and 47 kb upstream (NIPSNAP1)	exon 1-5	Merlin synthesis altered	2A	Familial			7			Large deletion including promoter. Unexpected mild-moderate phenotype.
c.1446_1477insNG_009057.1:g.74239_74405	Deep intronic mutation between exons 13 - 14	p.(Pro482Profs*39)	2A	Sporadic			8	0,41335449	4,7636402	Splicing variant at exon 14. Unexpected moderate phenotype. pERK levels above threshold.

exons 1-5 deletion and 47 kb upstream (NIPSNAP1)	exon 1-5	Merlin synthesis altered	2A	Familial			9	1,68851611	5,7267768	**Large deletion including promoter. Unexpected severe phenotype.**
c.810+1dupG	exon 8	p.(Phe271Val4fs*)	2A	Sporadic			10	0,7651892	0,66179798	**Splicing variant at exon 8. Unexpected severe phenotype. Merlin and pERK levels below threshold.**
exons 15-16 deletion; r.1575_1747del	exon15-16	p.(Lys525Asnfs*19)	2B	Sporadic			5	0,98880623	5,64437297	**Large deletion excluding promoter. Unexpected mild phenotype. At functional level this deletion alters exon 15 splicing. pERK levels are above threshold**
c.169C>T	exon 2	p.(Arg57*)	2B	Sporadic	Detected at 7% in blood (NGS)		7			Nonsense variant at mosaicism. Mild-moderate phenotype
exons 5-17 deletion and downstream CABP7 deletion	exons 5-17	p.(?)	2B	Sporadic			8	1,55439894	2,65118931	Large deletion excluding promoter. Moderate phenotype. pERK levels are above threshold
c.115_363del	Exon 2&3 skipping	p.(Met39_Gln121del)	2B	Sporadic			9	1,48734671	3,14955982	Splicing variant at exon 2&3. Unexpected severe phenotype. pERK levels above threshold.
c.241-13T>A	exon 3	p.(Val81Glnfs*45)	2B	Sporadic			9	2,06863943	1,09999436	Splicing variant at exon 3. Unexpected severe phenotype. pERK levels below threshold.
c.241-9A>G	exon 3	p.(Val81Phefs*44)	2B	Sporadic			10	1,57827175	2,46664781	Splicing variant at exon 3. Unexpected severe phenotype. pERK levels below threshold.
c.784C>T	exon 8	p.(Arg262*)	2B	Sporadic	Detected at ~ 10% in fibroblasts, n		10	2,56486969	0,81433044	**Nonsense variant at mosaicism. Unexpected severe phenotype. pERK levels below threshold**

c.	exon	p.								
c.169C>T	exon 2	p.(Arg67*)	2B	Sporadic	5,6% in blood (NGS)		10	2,71920859	1,74534982	**Nonsense variant at mosaicism. Unexpected severe phenotype. pERK levels below threshold**
c.586C>T	exon 6	p.(Arg196*)	2B	Sporadic	Detected at >20% in blood (externa		10			**Nonsense variant at mosaicism. Unexpected severe phenotype**
c.448-2A>G	exon 5	p.(?), splicing	2B	Sporadic			10			Splicing variant at exon 3. Unexpected severe phenotype
c.1096_1102del7	exon11	p.(Glu366Glnfs*7)	3	Familial, index			7	1,28967814	1,45881049	Nonsense variant. Unexpected mild-moderate phenotype. Protein levels below threshold
c.784C>T	exon 8	p.(Arg262*)	3	Sporadic			8	1,64843072	1,12977722	Nonsense variant. Unexpected moderate phenotype. Protein levels below threshold
c.784C>T	exon 8	p.(Arg262*)	3	Sporadic			9	1,72710678	0,74796226	Nonsense variant. Severe phenotype. Protein levels below threshold
c.634C>T	exon 7	p.(Gln212*)	3	Sporadic			9			Nonsense variant. Severe phenotype
c.380_396dupTAGATGAAAA	exon 4	p.(Cys133*)	3	Sporadic			10	0,6773879	0,81003198	Nonsense variant. Severe phenotype. Protein levels below threshold

c.1282C>T	exon 12	p.(Gln428*)	3	Sporadic			10	0,80455913	0,66749818	Nonsense variant. Severe phenotype. Protein levels below threshold
c.432C>G	exon 4	p.(Tyr144*)	3	Sporadic			10	1,04771615	1,90213891	Nonsense variant. Severe phenotype. Protein levels below threshold
c.784C>T	exon 8	p./Arg262*)	3	Sporadic			10	1,0694117	1,74014287	Nonsense variant. Severe phenotype. Protein levels below threshold
c.784C>T	exon 8	p.(Arg262*)	3	Sporadic			10	1,17909458	0,32191149	Nonsense variant. Severe phenotype. Protein levels below threshold
c.520dupA	exon 6	p.(Ile174Asnfs*29)	3	Sporadic			10	1,23139075	0,29106762	Nonsense variant. Severe phenotype. Protein levels below threshold
c.1334_1337delAGAG	Small Deletion	p.(Glu445Glyfs*9)	3	Sporadic			10			Nonsense variant. Severe phenotype
c.1396C>T	exon 13	p.(Arg466*)	3	Sporadic			10			Nonsense variant. Severe phenotype

Table S1.5. Demographic data according to Functional Genetic Severity Score

Functional Genetic Severity Score			1	2	3	4	5	6	Correlation
N (% total)	Number of patients		16 (30,7%)	0	4 (7,7%)	10 (19,23%)	8 (15,38%)	14 (26,9%)	
N (% gender)	Gender	Male	12 (36,4%)		3 (9,1%)	6 (18,18%)	3 (9%)	9 (27,3%)	
		Female	4 (21,1%)		2 (10,5%)	4 (21,1%)	4 (21,1%)	5 (26,3%)	$X^2(4)$ = 1.81, p = 0.77
Mean (SD)	Age at diagnosis		40,94 (16,11)		36,6 (12,99)	23 (7,37)	24 (12,90)	18,79 (6,5)	$r_s(50)$ = -0.64, p < 0.001
	Current age		52,25 (15,56)		46,8 (18,43)	41,56 (12,76)	36,88 (12,91)	30,79 (12,07)	$r_s(50)$ = -0.54, p < 0.001
	Years since diagnosis		11,25 (6,86)		10,2 (12,21)	18,56 (12,09)	12,88 (6,69)	12 (8,26)	$r_s(50)$ = 0.04, p = 0.75
	Age at NF2-related death					53	40	42	
N (% score category)	NF2-related deaths					1 (10%)	1 (12,5%)	1 (7,2%)	
	Familial NF2		0 (0%)		1 (20%)	3 (30%)	0 (0%)	3 (21,4%)	
	Sporadic NF2		16 (100%)		4 (80%)	7 (70%)	7 (87,5%)	11 (78,6%)	X2(4) = 7.73, p = 0.10

Table S1.6. Tumor burden, presence of ocular features and hearing outcome according to Functional Genetic Severity Score									
Functional Genetic Severity Score			**1**	**2**	**3**	**4**	**5**	**6**	**Statistics**
N (% total)	Number of patients		16	0	4	10	8	14	
Tumor load	N (%)	Bilateral VS	11 (68,7%)	0 (0%)	3 (75%)	10 (100%)	8 (100%)	14 (100%)	$X^2(1)$ = 8.9, p = 0.002
		Unilateral VS	5 (31,2%)	0 (0%)	1 (25%)	0 (0%)	0 (0%)	0 (0%)	$X^2(1)$ = 8.9, p = 0.002
		Intracranial meningioma	9 (56,2%)	0 (0%)	3 (75%)	3 (30%)	5 (62,5%)	10 (71,4%)	$X^2(1)$ = 0.35, p = 0.55
		Intracranial Schwannoma	3 (18,7%)	0 (0%)	3 (75%)	3 (30%)	3 (37,5%)	7 (50%)	$X^2(1)$ = 1.8, p = 0.17
		Spinal meningioma	5 (31,2%)	0 (0%)	1 (25%)	1 (10%)	3 (37,5%)	5 (45,5%)	$X^2(1)$ = 0.10, p = 0.74
		Spinal Schwannoma	8 (50%)	0 (0%)	4 (100%)	6 (60%)	6 (75%)	11 (100%)	$X^2(1)$ = 1.7, p = 0.17
		Spinal ependymoma	4 (25%)	0 (0%)	0 (0%)	2 (20%)	3 (37,5%)	5 (45,5%)	$X^2(1)$ = 0.8, p = 0.35
Ocular Features	N (%)	Epiretinal membranes	0 (0%)	0 (0%)	0 (0%)	0 (0%)	0 (0%)	0 (0%)	NA
		Cataract	3 (37,5%)	0 (0%)	1 (50%)	3 (30%)	1 (12,5%)	3 (42,9%)	$X^2(1)$ = 0, p = 1
		Combined hamartoma	0 (0%)	0 (0%)	0 (0%)	0 (0%)	0 (0%)	2 (28,6%)	$X^2(1)$ = 3.1, p = 0.07
		Optic nerve meningioma	0 (0%)	0 (0%)	0 (0%)	0 (0%)	1 (12,5%)	0 (0%)	$X^2(1)$ = 0.3, p = 0.53
	Mean (SD)	Total eye features		0 (0%)					$r_s(49)$ = 0.06, p = 0.67
Hearing Outcomes	N (%)	Hearing grade 1	12 (75%)	0 (0%)	4 (100%)	3 (30%)	3 (37,5%)	6 (42,9%)	$X^2(1)$ = 5.4, p = 0.019
		2	1 (6,2%)	0 (0%)	0 (0%)	0 (0%)	0 (0%)	0 (0%)	$X^2(1)$ = 1.5, p = 0.20
		3 o 4	0 (0%)	0 (0%)	0 (0%)	0 (0%)	2 (25%)	1 (7,1%)	$X^2(1)$ = 2.1, p = 0.14
		5	2 (12,5%)	0 (0%)	0 (0%)	3 (30%)	1 (12,5%)	4 (28,6%)	$X^2(1)$ = 1.6, p = 0.20
		6	2 (12,5%)	0 (0%)	0 (0%)	4 (40%)	2 (25%)	3 (21,4%)	$X^2(1)$ = 0.6, p = 0.42
	Mean (SD)	Age of loss of useful hearing	48,31 (17,16)	0 (0%)	46,8 (18,43)	32,38 (8,43)	29,38 (11,89)	26,23 (12,58)	$r_s(48)$ = -0.58, p < 0.001
Cutaneus manifestations	N (%)		4 (25%)	0 (0%)	0 (0%)	0 (0%)	4 (50%)	9 (75%)	$X^2(1)$ = 6.2, p = 0.012

* For group 1 and 6, only 4 out 16 and 11 out of 14 patients, respectively, have been tested by a spinal magnetic resonance

Table S1.7. Major interventions in relation to Functional Genetic Severity Score								
Functional Genetic Severity Score			**1**	**2**	**3**	**4**	**5**	**6**	**Statistics**
N (%)	Proportion of patients	VS surgery	6 (37,5%)		3 (60%)	9 (90%)	3 (37,5%)	10 (71,4%)	$X^2(1) = 2.16$, p = 0.14
		Non-VS intracranial surgery	1 (6,3%)		1 (20%)	0 (0%)	3 (37,5%)	5 (35,7%)	$X^2(1) = 4.5$, p = 0.032
		Spinal surgery	3 (18,8%)		4 (80%)	1 (10%)	3 (37,5%)	2 (14,3%)	$X^2(1) = 0.4$, p = 0.51
		Shunt surgery	0 (0%)		0 (0%)	0 (0%)	0 (0%)	1 (7,1%)	$X^2(1) = 1.5$, p = 0.21
		Radiotherapy	1 (6,3%)		0 (0%)	3 (30%)	3 (37,5%)	8 (57,1%)	$X^2(1) = 10.1$, p = 0.001
		Bevacizumab	0 (0%)		0 (0%)	2 (20%)	3 (37,5%)	6 (42,9%)	$X^2(1) = 9.6$, p = 0.002
	Total number of major interventions per person, grouped	0	8 (50%)		0 (0%)	0 (0%)	0 (0%)	2 (14,3%)	$X^2(1) = 7.1$, p = 0.007
		1	3 (18,8%)		3 (60%)	2 (20%)	2 (25%)	2 (14,3%)	$X^2(1) = 0.4$, p = 0.51
		2	2 (12,5%)		1 (20%)	4 (40%)	1 (12,5%)	2 (14,3%)	$X^2(1) = 0.03$, p = 0.86
		3	1 (6,3%)		0 (0%)	4 (40%)	0 (0%)	2 (14,3%)	$X^2(1) = 0.22$, p = 0.63
		4 or more	2 (12,5%)		1 (20%)	0 (0%)	4 (50%)	6 (42,9%)	$X^2(1) = 4.5$, p = 0.033
Mean (SD)	Total number of major interventions per person, grouped		1,25 (1,77)		2 (1,73)	2,22 (0,83)	3,63 (2,50)	3,79 (3,36)	$r_s(50) = 0.39$, p = 0.003
	Number of total surgeries		1,19 (1,80)		2,2 (2,17)	1,67 (0,50)	2,13 (1,89)	2,64 (2,98)	$r_s(50) = 0.22$, p = 0.11
	Age at first radiotherapy session		23		0	37 (9,64)	30,33 (6,66)	24,29 (8,16)	$r_s(12) = -0.42$, p = 0.13
	Age started bevacizumab		0		0	32	26,67 (14,57)	23,67 (8,48)	$r_s(8) = -0.26$, p = 0.46
	Age at first surgery		36,71 (13,90)		34,8 (10,62)	25,67 (7,55)	27,50 (11,93)	20,80 (7,73)	$r_s(35) = -0.51$, p = 0.001
	Age at first major intervention		35,00 (13,75)		34,8 (10,62)	25,67 (7,55)	25,75 (11,93)	20,55 (7,89)	$r_s(39) = -0.51$, p < 0.001
	Ratio of total number of major interventions to current age		0,03 (0,04)		0,04 (0,02)	0,05 (0,02)	0,10 (0,06)	0,13 (0,11)	$r_s(50) = 0.54$, p < 0.001

Score	GSS					FGSS					
Group/Class	1	2A	2B	3	Mean	1	3	4	5	6	Mean
Merlin Protien Levels (σ)	3,11	0,54	0,29	0,12	1,02	1,76	2,01	0,27	0,55	0,12	0,94
pERK Protien Levels(σ)	6,88	3,99	5,43	0,54	4,21	3,54	3,27	2,01	0,44	0,34	1,92
Age at diagnosis (σ)	216,97	169,78	99,46	33,27	129,87	202,77	149,08	54,29	182,25	35,62	124,80
Age at hearing loss (σ)	324,72	144	110,88	148,1	181,925	262,11	365,19	71,47	148,35	117,93	193,01

Table S1.8. Intragroup Variability of Merlin, pERK, age at diagnosis and age at hearing loss.

Appendix C

Article

Revisiting the UK Genetic Severity Score for NF2: a proposal for the addition of a functional genetic component

N.Catasús, B.Garcia, I.Galván-Femenía, A.Plana, A.Negro, I.Rosas, A.Ros, E.Amilibia, J.L. Becerra,

C.Hostalot, F.Rocaribas, I.Bielsa, C.L.Garcia. R. de Cid, E.Serra, I.Blanco, E.Castellanos (2021).

Original research

Revisiting the UK Genetic Severity Score for NF2: a proposal for the addition of a functional genetic component

Núria Catasús,[1] Belen Garcia,[1,2] Iván Galván-Femenía,[3] Adrià Plana,[4] Alejandro Negro [ORCID],[1,2] Inma Rosas [ORCID],[1,5] Andrea Ros,[1,2] Emilio Amilibia,[6] Juan Luis Becerra,[7] Cristina Hostalot,[8] Francesc Rocaribas,[6] Isabel Bielsa,[4] Conxi Lazaro Garcia [ORCID],[9] Rafael de Cid [ORCID],[3] Eduard Serra,[10] Ignacio Blanco,[1,2] Elisabeth Castellanos [ORCID],[1,5] On behalf of NF2 Spanish National Reference Centre HUGTP-ICO-IGTP

ABSTRACT

Background Neurofibromatosis type 2 (NF2) is an autosomal dominant disorder characterised by the development of multiple schwannomas, especially on vestibular nerves, and meningiomas. The UK NF2 Genetic Severity Score (GSS) is useful to predict the progression of the disease from germline *NF2* pathogenic variants, which allows the clinical follow-up and the genetic counselling offered to affected families to be optimised.

Methods 52 Spanish patients were classified using the GSS, and patients' clinical severity was measured and compared between GSS groups. The GSS was reviewed with the addition of phenotype quantification, genetic variant classification and functional assays of Merlin and its downstream pathways. Principal component analysis and regression models were used to evaluate the differences between severity and the effect of *NF2* germline variants.

Results The GSS was validated in the Spanish NF2 cohort. However, for 25% of mosaic patients and patients harbouring variants associated with mild and moderate phenotypes, it did not perform as well for predicting clinical outcomes as it did for pathogenic variants associated with severe phenotypes. We studied the possibility of modifying the mutation classification in the GSS by adding the impact of pathogenic variants on the function of Merlin in 27 cases. This revision helped to reduce variability within *NF2* mutation classes and moderately enhanced the correlation between patient phenotype and the different prognosis parameters analysed ($R^2 = 0.38$ vs $R^2 = 0.32$, $p > 0001$).

Conclusions We validated the UK NF2 GSS in a Spanish NF2 cohort, despite the significant phenotypic variability identified within it. The revision of the GSS, named Functional Genetic Severity Score, could add value for the classification of mosaic patients and patients showing mild and moderate phenotypes once it has been validated in other cohorts.

INTRODUCTION

Neurofibromatosis type 2 (NF2) (MIM 101000) is an autosomal dominant syndrome caused by mutations in the *NF2* gene that affects 1 in 28 000–40 000 births worldwide.[1 2] Approximately 50% of the cases are due to de novo variants, while the other 50% are familial cases. NF2 typically presents with vestibular schwannomas (VS) on addition to multiples schwannomas in other cranial, peripheral and spinal nerves, as well as meningiomas, ependymomas, congenital cataracts, and it is also associated with focal neurological deficits. Due to the development of bilateral VS, NF2 disease will progress in most patients causing hearing loss, tinnitus and balance problems.[3] Despite the benign nature of these tumours, their multiplicity and anatomical location causes highly increased morbidity and early death. Therapeutic management is challenging in these patients due to the recurrence of treated tumours. Surgery, radiotherapy and bevacizumab are the current gold standard treatments.[4 5]

The clinical expression of the disease is highly variable, which makes the clinical management of these patients complex and challenging.[6] Phenotype differences found among patients led to a clinical classification in which two subgroups of adult patients were established into Gardner and Wishart subtypes (mild and severe phenotypes, respectively). Further studies have resulted in the identification of several prognostic markers[7 8] and a good genotype-phenotype correlation.[9–11]

In this context, the UK NF2 Reference Group established a Genetic Severity Score (GSS) to predict the severity of the disease based on the type of *NF2* germline variant in the patient.[12] This score stratifies patients with NF2 into four groups: in groups 1A and 1B no pathogenic variant is identified in blood and patients show a very mild phenotype, while patients in group 3 carry truncating variants in exons 2–13 of the *NF2* gene and present a severe phenotype. Group 2B harbour mosaic in blood for a truncating variant in exons 2–13, splicing variant involving exons 1–7, large deletions not including the promoter or exon 1, truncating variants in exons 14–15 and patients present a moderate phenotype. Finally, group 2A includes full or mosaic *NF2* variants identified in blood, excluding those found in group 2B or 3, and is associated with mild phenotype. Therefore,

the GSS represents a tool by which it is possible to establish a trend in NF2 prognosis from the patient' germline variant and thus, improve the clinical follow-up and the genetic counselling offered to affected families.[12 13]

Around 50% of NF2 de novo cases are mosaic (groups 1A and 1B) and present highly variable phenotypes.[14 15] Specifically, >15% of the patients with de novo NF2 show bilateral VS before the age of 20 and with no variant identified in blood.[14 16] Therefore, despite the good performance of the UK NF2 GSS, this complicates the day-to-day application of it in the clinical context, as some mosaic cases may develop multiple tumours at early ages.[8 17–19] Similarly, some patients harbouring splicing and missense variants could also show significant differences in their clinical manifestations.[7 9 10 20–24] Hence, the GSS is useful for classifying patients with NF2 in general terms but there is room for improvement in stratifying some patients.

The NF2 gene encodes for the protein Merlin. Merlin can be considered to be a scaffold protein as it indirectly links F-actin, transmembrane receptors and intracellular effectors to modulate receptor-mediated signalling pathways and integrates extracellular signals to modulate morphology, motility, proliferation and survival.[25–27] Understanding the impact of the pathogenic NF2 variant on the stability of Merlin, and on the regulation of its associated signalling pathways could be a better way of accounting for variant pathogenicity. In this context, analysing the status of small GTPases (Rac1 and Ras), mammalian target of rapamycin, phosphoinositide 3-kinase/Akt and Hippo pathways in patients with NF2 could help to determine the functional impact of the germline variant and therefore these data could be used to improve the capacity to predict the prognosis of patients with NF2.

In this study, we present the validation of the UK NF2 GSS[12] in the patients with NF2 from the Spanish National Reference Centre (CSUR) of Phacomatoses and we propose a revised version, called Functional Genetic Severity Score (FGSS), considering data obtained from functional assays and the predicted mutational effect on Merlin. We describe here the performance of the FGSS in comparison to GSS and show the changes observed in the behaviour of some clinical prognosis markers analysed in our cohort.

MATERIALS AND METHODS
Patients
Written informed consent was obtained from all individuals included in the study. Clinical diagnosis was established following the Manchester Criteria.[28] Clinical data were recorded, five domains were assessed: patient demographics, tumour load, ocular features, hearing capacity and major interventions. Genetic testing was performed using the customised I2HCP panel[29] in blood or tissue when available.

Functional assay
The pathways downstream of Merlin were analysed in 27 out of 52 patients with NF2 through a western blot assay. Cultured fibroblasts from skin biopsies were processed as described by Castellanos et al.[23] Three primary cultures from healthy donors were included as control samples (Ctrl1, Ctrl2 and Ctrl3) and grouped together with the tissue mosaic patients for the statistical analysis. Primary antibodies (online supplemental materials and methods 1) were incubated at 4°C overnight and secondary antibodies during 1 hour at room temperature (IRDye 680LT and IRDye 800CW, 1:1000 dilution, LI-COR). The statistical threshold that allowed the differentiation between controls or

mosaic patients and the patients in group 3 (severe) was established through the ±2 SD limits method.

Statistics
All statistical analyses of the validation of the GSS were reproduced from the study of Halliday et al[12] with minor modifications. In order to study differences between protein expression levels in the functional assay, Kruskal-Wallis and Mann-Whitney U statistical tests were performed among genetic severity groups and pathogenic variant classes. Analysis of variance (ANOVA) of FGSS and NF2 mutations was performed to test differences of severity between NF2 mutations groups. Backward stepwise regression analysis was performed to evaluate the contribution of Merlin and pERK levels in the ANOVA model. Spearman's correlation (ρ) was used to calculate the correlation between Merlin and phosphorylated Merlin (pMerlin). Statistical analyses were performed using R software. For more information, see online supplemental materials and methods 1.

RESULTS
Validation of the UK NF2 GSS in a Spanish cohort
Fifty-two patients with NF2 from the CSUR for Phacomatoses cohort were included in the GSS validation group. This cohort consisted of 19 men and 33 women, all of them with a clinical diagnosis of NF2[28] at a mean age of 28.9 (range 9–70), 44 patients showed bilateral VS, 39 presented spinal tumours and 30 had intracranial meningiomas with a mean age of the cohort of 41.87 (range 12–79). We stratified the whole cohort following the GSS classification. Nineteen cases of the cohort (35%) were assigned to group 1, including 4 confirmed tissue mosaics (group 1B, two or more affected tissue samples studied) and 15 to group 1A as presumed mosaics, since no variant was identified in blood and affected tissues were not available. Twelve out of 19 patients were clinically diagnosed by the presence of bilateral vestibular schwannomas, while 6 cases (4 from 1A and 2 from 1B) showed a unilateral vestibular schwannoma in addition to multiple schwannomas and/or meningiomas. Only one case did not develop vestibular schwannomas at the moment of data collection and NF2 diagnosis was confirmed by genetic testing (patient 435) (online supplemental table 1). Finally, the 33 patients with a constitutional NF2 pathogenic variant were classified in group 2A, 2B or 3 following GSS criteria (tables 1–2).

When analysing demographic data (table 1), we observed the mean age at diagnosis in individuals in group 1 (39.88±16.48, range: 17–70) was significantly statistically different from that of patients in group 3 (18.79±6.45, range: 14–35; p<0.001). The mean age at diagnosis for the group 2A was ~31 (range 14–50) and lower in group 2B~23 (range 9–37) with no significant differences between these groups. Regarding the age at hearing loss, significant differences were also found between groups 1 and 3 (p<0.0005); we observed a linear correlation between the age at hearing loss and the severity group as established by the GSS (table 2). Therefore, these results showed the same tendency as the English cohort and that features related to poor prognosis such as the age at diagnosis and age at hearing loss correlated with the four groups established.

When studying tumour burden, the highest incidence of intracranial meningiomas was found in groups 2B and 3 (~70%), with a lower incidence in group 2A (22.2%) and a remarkably high incidence in group 1 (58%). Similarly, intracranial schwannomas were also present in patients classified into groups associated with mild phenotypes. Spinal meningioma was reported in groups 1, 2B and 3 of our cohort, specifically, six mosaic patients

Table 1 Demographic data according to Genetic Severity Score

Genetic severity			1 Tissue mosaic	2A Mild	2B Moderate	3 Severe	Correlation
N (% total)	Number of patients		19 (36.54%)	9 (17.3%)	10 (19.23%)	14 (26.9%)	
N (% gender)	Gender	Male	4 (21.1%)	3 (15.8%)	7 (36.8%)	5 (26.3%)	
		Female	15 (45.45%)	6 (18.2%)	3 (9%)	9 (27.3%)	$\chi^2(3)=4.91$, p=0.17
Mean (SD)	Age at diagnosis		39.88 (16.48)	30.80 (13.40)	22.82 (9.13)	18.79 (6.45)	$r_s(50)=-0.60$, p<0.001
	Current age		52.29 (17.16)	44.80 (12.10)	36.55 (11.09)	30.79 (12.07)	$r_s(50)=-0.53$, p<0.001
	Years since diagnosis		12.35 (8.41)	14 (12.18)	13.73 (8.13)	12 (8.26)	$r_s(50)=0.02$, p=0.89
	Age at NF2-related death			53	40	42	
N (% score category)	NF2-related deaths			1	1	1 (7.14%)	
	Familial NF2		0 (0%)	2 (22.22)	1 (9.09%)	3 (21.43%)	
	Sporadic NF2		19 (100%)	7 (77.77%)	9 (90%)	11 (78.57%)	$\chi^2(3)=5.93$, p=0.11

NF2, neurofibromatosis type 2.

from our cohort developed multiple spinal meningiomas. A fairly even distribution of the presence of spinal schwannomas was seen in the groups 1 and 2 (52 to 66%) and a higher incidence was found in group 3 (79%) with no statistically significant differences. Regarding spinal ependymomas, a higher incidence was found in patients from groups 2B and 3 (40% and 36%, respectively), but there was also considerable variability in the other groups and no clear linear trend was observed. Finally, considering the number of major interventions in our cohort we did not observe significant differences between groups (table 2, online supplemental tables 1; 2).

Functional analysis of Merlin and associated signalling pathways in patient skin fibroblasts

To better interpret the pathogenicity of NF2 constitutional variants in relation to the phenotype variability observed within GSS categories, a functional assay in primary cultured fibroblasts from patients was developed to analyse the activation state of

Merlin and some of its downstream pathways. In particular, we analysed PAK1 and RAC total protein amount, and total protein and the phosphorylated forms of Merlin, ERK, PKA, YAP and AKT.

As expected, all patients that harboured a germline pathogenic variant, and therefore had one NF2 mutated allele, showed lower Merlin levels compared with healthy controls or tissue mosaics (p<0.05). No significant differences were found intergroups with a pathogenic variant in the NF2 gene, regardless the variant type or location within the gene, meaning that the effect on Merlin levels were very similar in patients carrying truncating and splicing variants or large deletions (figure 1A and B, online supplemental table 1). When studying the status of pMerlin, we observed the same tendency as Merlin, suggesting that decreased levels of pMerlin could be due to the lower levels of Merlin rather than a dysregulation of Merlin activation (online supplemental figure 1).

Table 2 Tumour burden, presence of ocular features and hearing outcome according to Genetic Severity Score

Genetic severity				1 Tissue Mosaic	2A Mild	2BModerate	3 Severe	Statistics
Number of patients				19	9	10	14	
Tumour load	N (%)	Bilateral VS		11 (57.89%)	9 (100%)	10 (100%)	14 (100%)	$\chi^2(1)=8.38$, p=0.003
		Unilateral VS		6 (31.58%)	0 (0%)	0 (0%)	0 (0%)	$\chi^2(1)=5.18$, p=0.022
		Intracranial meningioma		11 (57.89%)	2 (22.2%)	7 (70%)	10 (71.4%)	$\chi^2(1)=0.79$, p=0.37
		Intracranial schwannoma		5 (26.3%)	3 (33.3%)	4 (40%)	7 (50%)	$\chi^2(1)=1.56$, p=0.21
		Spinal meningioma		6 (31.58%)	0 (0%)	4 (40%)	5 (35.7%)	$\chi^2(1)=0.23$, p=0.62
		Spinal schwannoma		10 (52.63%)	6 (66.7%)	6 (60%)	11 (78.6%)	$\chi^2(1)=2.46$, p=0.11
		Spinal ependymoma		4 (21.05%)	1 (11.1%)	4 (40%)	5 (35.7%)	$\chi^2(1)=1.23$, p=0.26
Ocular features	N (%)	Epiretinal membranes		0 (0%)	0 (0%)	0 (0%)	0 (0%)	NA
		Cataract		4 (21.05%)	2 (22.2%)	2 (22.2%)	3 (21.42%)	$\chi^2(1)=0.01$, p=0.90
		Combined hamartoma		0 (0%)	0 (0%)	0 (0%)	2 (14.28%)	$\chi^2(1)=3.35$, p=0.06
		Optic nerve meningioma		0 (0%)	0 (0%)	1 (10%)	0 (0%)	$\chi^2(1)=0.24$, p=0.62
	Mean (SD)	Total eye features		0.27	0.2	0.33	0.4	$r_s(49)=0.05$, p=0.69
Hearing outcomes	N (%)	Hearing grade	1	13 (68.4%)	5 (55.5%)	4 (40%)	6 (42.9%)	$\chi^2(1)=2.05$, p=0.15
			2	1 (5.26%)	0 (0%)	0 (0%)	0 (0%)	$\chi^2(1)=1.33$, p=0.24
			3					
			4	0 (0%)	0 (0%)	2 (20%)	1 (7.1%)	$\chi^2(1)=1.83$, p=0.17
			5	2 (10.52%)	2 (22.2%)	1 (10%)	4 (28.6%)	$\chi^2(1)=1.01$, p=0.31
			6	2 (10.52%)	3 (33.3%)	3 (30%)	3 (21.4%)	$\chi^2(1)=0.50$, p=0.47
	Mean (SD)	Age of loss of useful hearing		48.59 (18.57)	38 (11.96)	30.27 (9.88)	26.23 (12.58)	$r_s(48)=-0.56$, p<0.001
Cutaneous manifestations	N (%)			6 (31.57%)	2 (22.2%)	6 (60%)	9 (64.3%)	$\chi^2(1)=3,94$, p=0.047

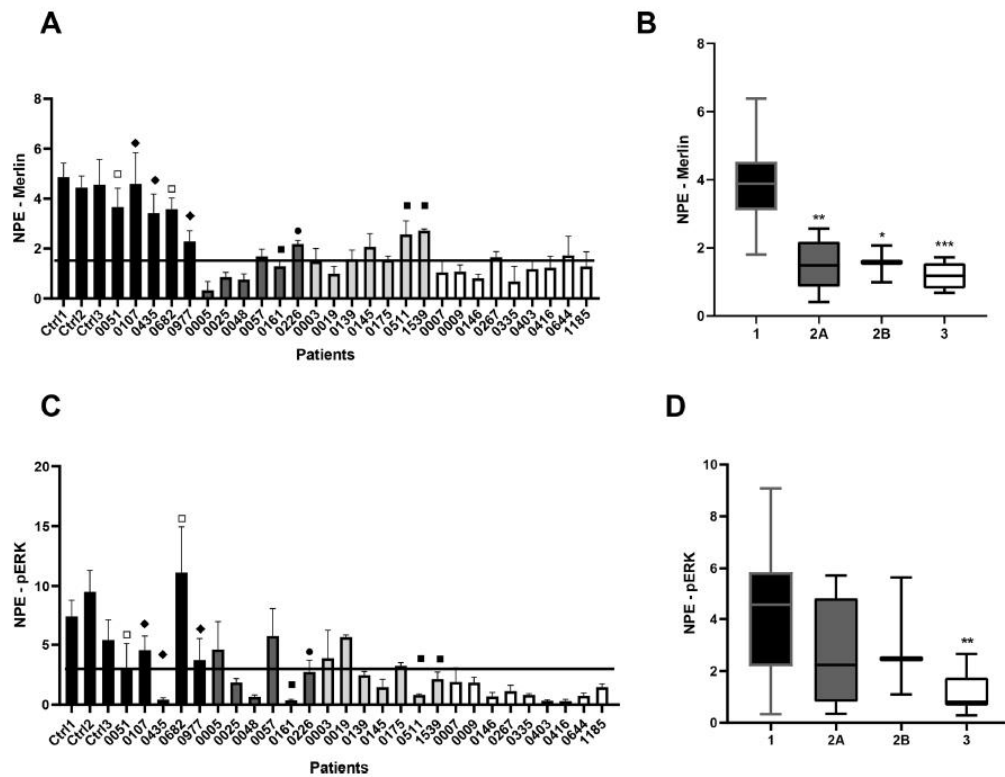NA, not available; VS, Vestibular Schwannoma.

Figure 1 Merlin and pERK levels in patient's fibroblasts according to the Genetic Severity Score. (A) Merlin levels in fibroblasts of patients with NF2. (B) Average of Merlin levels according to Genetic Severity Groups. (C) pERK levels in fibroblasts of patients with NF2. (D) Average of pERK levels according to Genetic Severity Groups. Column's grey scale indicates the Genetic Severity Group; NPE, normalised protein expression; bars represent the SD from three independent experiments (*$p<0.05$; **$p<0.005$; ***$p<0.001$). ☐ Presumed mosaicism; ■ generalised mosaicism; ◆ tissue mosaicism; ○ missense.

Results did not indicate any differences in the status of the PI3K, PAK, YAP or RAC pathways, neither in the total protein levels nor in the phosphorylated forms. In contrast, pERK levels in patients' fibroblasts with truncating variants were statistically significantly lower than pERK levels in tissue mosaics or healthy controls, while ERK levels remained constant between groups (figure 1C,D, online supplemental figure 2). These results allowed a statistically significant discrimination of patients with severe phenotypes from healthy controls ($p=0.0042$). The group with intermediate phenotype showed greater variability, as did the group of mosaic patients (SD 2A=1.999, SD 2B=2.332, 1AB=2.624).

Reviewing GSS mutation categorisation

Due to the unexpected tendency among groups 1 and 2 in the clinical manifestations of the studied cohort, we revised the GSS considering the predicted mutation effect on Merlin, its position within the gene and its effect on Merlin and pERK activity based on functional assays results.

First, qualitative clinical data recorded were coded to quantitative variables in order to measure the NF2 phenotype, independently of the NF2 variant type and the mosaicism status. Quantification of the phenotype was based on well-known NF2 prognosis markers (online supplemental table 3) and was presented in a numeric 10-scale based on the sum of the transformed quantitative variables. In this way, a patient younger than 25 years, presenting bilateral VS, peripheral schwannomas and multiple spinal/cerebral tumours was classified with the most severe score (10).

Second, we analysed the relation between the GSS predicted phenotype and the outcome of the phenotype quantification in the patients of our cohort. We observed that some tissue mosaic patients did not show the expected very mild phenotype. In addition, patients carrying large deletions including or excluding the 5' of the gene did not show phenotypic differences and neither did the patients harbouring splice variants in exons 1–7 or 8–13 (online supplemental table 4).

Taking into account the mentioned observations, we revised the GSS categorisation of NF2 mutations and propose a modified criteria based on six mutation classes (1–6), which was referred to as FGSS. In general terms, presumed mosaics or patients carrying a Ring22 were scored as 1 and related to very mild phenotypes, while truncating variants in exons 2–13 were associated with a severe phenotype and scored as 6. Other types of pathogenic variants were scored in between considering the proportion of cells carrying the mutation and when the variant induced a frameshift alteration. However, we did not take into account the position of the altered exons, except for exon 1, since no differences were observed in Merlin levels when comparing variants affecting 5' or 3' of the NF2 gene (table 3 and online supplemental table 4, materials and methods 1).

Table 3 Categorisation of *NF2* mutation according to Functional Genetic Severity Score

NF2 germline variants	GSS subcategory	FGSS mutation class	Phenotype quantification	Disease severity
Ring22 (n=1)	NA	1	<5	Very mild phenotype
Missense variants (n=1)	2A	3	6–7	Mild
Large and small deletions				
Small in-frame deletion or duplication (n=1)	2A	3	6–7	Mild
*Large deletion (>1 exon) including promoter or exon 1				
Maintaining reading frame	2A	3	6–7	Mild
Causing frameshift alteration (n=2)	2A	4	7–7,8	Moderate
Whole *NF2* gene	2A	4	7–7,8	Moderate
*Large deletion (>1 exon) excluding promoter or exon 1				
Maintaining reading frame	2B	3	6–7	Mild
Causing frameshift alteration (n=2)	2B	4	7–7,8	Moderate
Whole *NF2* gene	2B	4	7–7,8	Moderate
Splicing mutation				
Exons 1–7 (in frame)	2B	4	7–7,8	Moderate
Exons 8–13 (in frame)	2A	4	7–7,8	Moderate
Exons 1–7 (frameshift) (n=3)	2B	5	7,8–8,5	Moderate-to-severe
Exons 8–13 (frameshift) (n=1)	2A	5	7,8–8,5	Moderate-to-severe
Exons 14–17 (n=2)	2A	4	7–7,8	Moderate
Truncating mutation				
Exon 1	2A	5	7,8–8,5	Moderate-to-severe
Exons 2–13 (n=14)	3	6	>8,5–10	Severe
Exons 14–15	2B	5	7,8–8,5	Moderate-to-evere
NF2 generalised mosaic variants*	**GSS subcategory**	**FGSS mutation class**	**Phenotype quantification**	**Disease severity**
Ring22	NA	1	<5	Very mild phenotype
Missense variants	2A	2	<5	Very mild phenotype
Large and small deletions				
Small in-frame deletion or duplication	2A	2	<5	Very mild phenotype
*Large deletion (>1 exon) including promoter or exon 1				
Maintaining reading frame	2A	2	<5	Very mild phenotype
Causing frameshift alteration	2A	3	6–7	Mild
Whole *NF2* gene (n=1)		3	6–7	Mild
*Large deletion (>1 exon) excluding promoter or exon 1				
Maintaining reading frame	2A	2	<5	Very mild phenotype
Causing frameshift alteration (n=1)	2A	3	6–7	Mild
Splicing mutation				
Exons 1–7 (in frame)	2A	3	6–7	Mild
Exons 8–13 (in frame)	2A	3	6–7	Mild
Exons 1–7 (frameshift)	2A	4	7–7,8	Moderate
Exons 8–13 (frameshift)	2A	4	7–7,8	Moderate
Exons 14–17	2A	3	6–7	Mild
Truncating mutation				
Exon 1 mosaic	2A	4	7–7,8	Moderate
Exons 2–13 mosaic (n=4)	2B	5	7,8–8,5	Moderate-to-severe
Exons 14–15 mosaic	2A	4	7–7,8	Moderate
NF2 tissue mosaic variants†	**GSS subcategory**	**FGSS mutation class**	**Phenotype quantification**	**Disease severity**
Variants classified as 3	1B	1	<5	Very mild phenotype
Variants classified as 4 (n=1)	1B	2	<5	Very mild phenotype
Variants classified as 5–6 (n=3)	1B	3	6–7	Mild

*Generalised mosaic variants: >2,5% of reads, 5% of cells.
†Detected in two affected tissues. In addition, 15 patients with an inconclusive genetic test.
FGSS, Functional Genetic Severity Score; GSS, Genetic Severity Score; NF2, neurofibromatosis type 2.

Analysis of the added value of incorporating functional genetic information to GSS

When stratifying our cohort with the proposed criteria, patients harbouring genetic variants scored as 5 or 6 showed a severe phenotype, while patients harbouring *NF2* mutation class 4 behaved in a fairly similar way, although fewer extravestibular lesions were observed. In contrast, patients classified as class 3 presented a greater clinical heterogeneity, because class 3
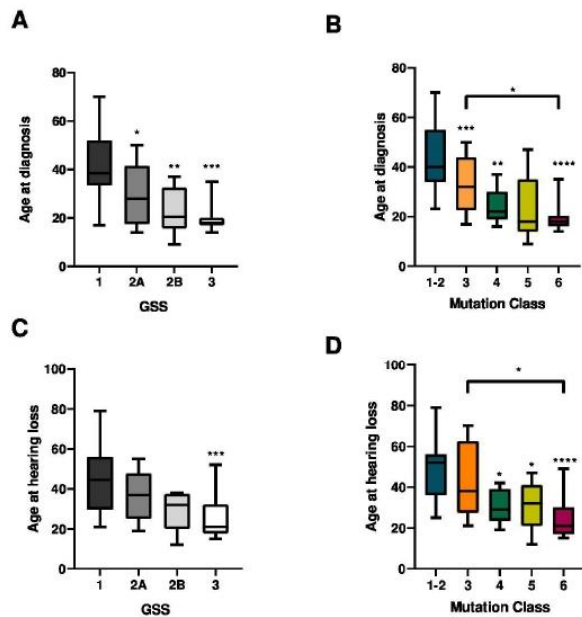
Figure 2 Comparison of the age at diagnosis and age at hearing loss according to Genetic Severity Score (GSS) or Functional Genetic Severity Score (FGSS). (A) Average age at diagnosis according to the GSS classification. (B) Average age at diagnosis according to the FGSS. (C) Average age at hearing loss according to the GSS. (D) Average age at hearing loss according to the FGSS. Column's grey scale indicates the Genetic Severity Group; Blue stands for the healthy controls and mutation classes 1 and 2; orange stands for mutation class 3; dark green stands for mutation class 4; light green stands for mutation class 5 and purple stands for mutation class 6. Bars represent the SD (*p<0.05; **p<0.005; ***p<0.001; ****p<0.0005).

included generalised and tissue mosaicisms as well as patients carrying constitutional variants associated with a mild phenotype. Finally, patients of classes 1 or 2 showed very mild phenotypes since these groups contain presumed mosaic and tissue mosaic patients, who harbour less deleterious variants. The FGSS showed stronger correlation between classes when studying the appearance of vestibular schwannomas, the presence of intracranial meningiomas as well as in hearing outcomes and cutaneous manifestations. The age at first surgery and several of the parameters related to major interventions analysed also showed larger means between classes when compared with the GSS (table 2, online supplemental tables 1; 5–7). In addition, the proposed revision to classify patient phenotype based on the NF2 genetic variant reduced the intragroup variability, improved the classification of mosaic patients and moderately improved the correlation between patient phenotype and some of the prognostic parameters analysed (figure 2, online supplemental tables 4–7). All these phenomena could indicate that the revised criteria could add value to the GSS.

Similarly, Merlin and pERK levels showed the same trend when classified through the GSS but the intragroup variability decreased in classes associated with mild phenotypes. In addition, Merlin levels were similar in groups 4–6, and significantly lower in groups 1–3 (p<0.005), since these three last groups contained mosaic patients. Furthermore, the levels of pERK in classes 5 and 6 were statistically significantly lower compared with class 4 and below (p<0.005). As mentioned before, class

3 showed higher variability due to the phenotypic variability detected in tissue mosaic patients (σ=1.884) (figure 3, online supplemental table 8).

In addition, we explored the variability of phenotypical data by principal component analysis (PCA) (online supplemental figure 3). The PCA-biplot suggested that patients in the first quadrant mainly had NF2 mutations of classes 4, 5 and 6; early age at diagnosis and presented extravestibular affection, vestibular and peripheral schwannomas, whereas patients with negative values in the PCA-biplot presented late age at diagnosis and mainly NF2 variants of class 1. To evaluate the tendency observed using the FGSS and taking into account the different number of genetic subcategories between GSS and FGSS, we performed a regression model (ANOVA) between the quantitative phenotype and NF2 disease-causing variant class to evaluate quantitatively the NF2 phenotype in base of the NF2 variant (online supplemental table 9A, Shapiro-Wilk test p=0.67, Levene test p=0.16). We observed that NF2 phenotype could be explained partially by the NF2 germline variant, specifically by variants classified as 3 or higher scores (R^2=0.38, p=0.0001). Therefore, variants classified as 6 were associated with patients showing the severest phenotypes (phenotype >8.5), while variants classified as 3 were associated with patients presenting milder phenotypes (phenotype ~7). These results agreed with the observations that some mosaic patients showed a severe phenotype. In this regard, the fact that the NF2 pathogenic variant could explain no more than 40% of the phenotype, indicated that many other variables could explain the resulting phenotype of the patient. Due to the differences observed in ERK activation, the incorporation of functional data from 27 patients to the statistical model was analysed. Yet, using this sample set, the incorporation of pERK levels into the ANOVA model in addition to NF2 germline mutation class data did not seem to improve the capacity to explain the NF2 phenotype (p>0.05, online supplemental table 9).

In contrast, the regression model between GSS and NF2 disease-causing variant showed an R^2=0.32 (p=0.001) and was only statistically significant in groups 2B and 3 (online supplemental table 9B). Unfortunately, none of these models could explain presumed mosaics or some of the tissue mosaic patients. However, taken overall, these results indicate that FGSS would improve the contribution of the NF2 variant in predicting the NF2 phenotype and could improve the prognosis prediction capacity of patients with NF2 in comparison with GSS.

DISCUSSION

The clinical management of NF2 is complex, it requires a specialised multidisciplinary team, andpresents challenges due to the phenotypic variability found among patients. A huge effort has been made to determine NF2 prognosis markers[7 8] and to establish a good genotype-phenotype relationship in order to be able to predict NF2 prognosis.[9–11] Improvement in determining patient prognosis allows an optimisation of the patients' clinical follow-up and ameliorate the genetic counselling offered to affected families.

The UK NF2 GSS[12] is an objective tool for predicting the trend of NF2 prognosis based on the patient germline genetic variant type. The application of the GSS in our Spanish cohort confirmed significant differences in several prognostic markers between groups 1 and 3, thus, allowing the GSS validation to determine the prognosis of patients carrying variants associated with the severest phenotypes. However, in our cohort the GSS had difficulty in classifying patients harbouring variants associated with mild or moderate NF2 phenotypes accurately
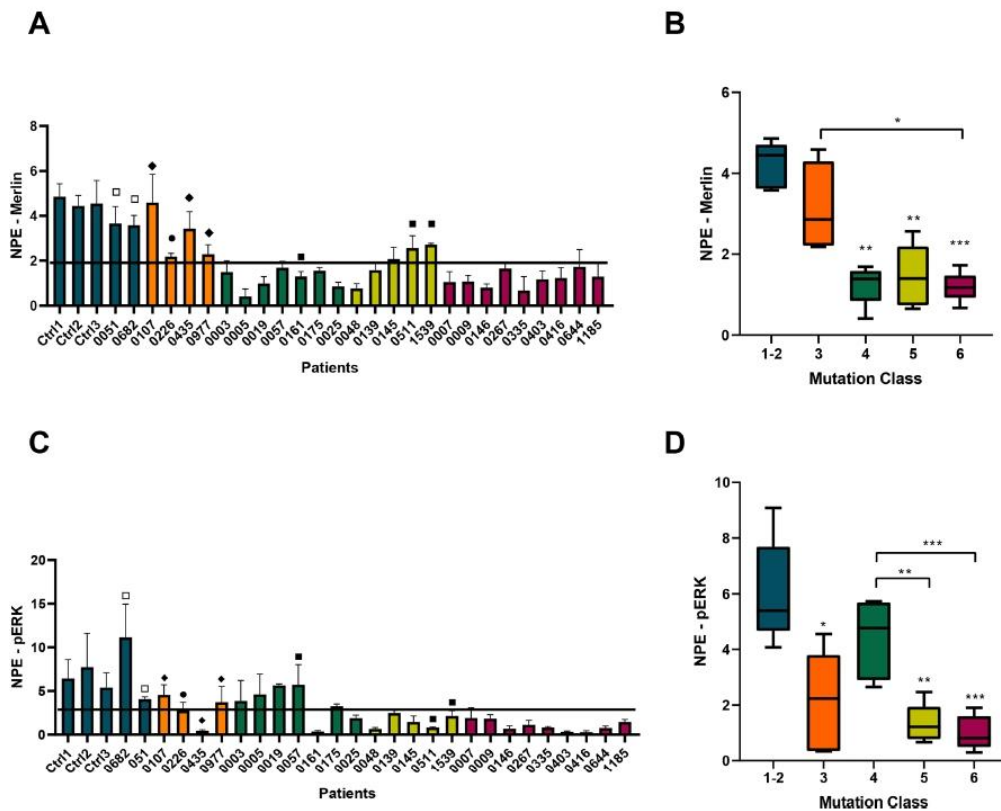
Figure 3 Merlin and pERK levels in patient's fibroblasts according to the Functional Genetic Severity Score (FGSS). (A) Merlin levels in fibroblasts of patients with NF2. (B) Average of Merlin levels according to mutation class. (C) pERK levels in fibroblasts of patients with NF2. (D) Average of pERK levels according to mutation class. Blue stands for the healthy controls and mutation classes 1 and 2; orange stands for mutation class 3; dark green stands for mutation class 4; light green stands for mutation class 5 and purple stands for mutation class 6. NPE, normalised protein expression. Bars represent the SD from three independent experiments ($*p<0.05$; $**p<0.005$; $***p<0.001$). □ presumed mosaicism; ■ generalised mosaicism; ◆ tissue mosaicism; ○ missense.

enough, and neither could it differentiate the mosaic patients among them, since not all of this group presented a mild clinical presentation. Certain inconsistencies have been detected, as in the case of four patients from group 2A and one mosaic patient (group 1B), who were clinically diagnosed close to the age of 20 and who have recently developed multiple central nervous system tumours in addition to vestibular schwannomas, three of them before their 30s. These disparities could be due to the cohort size (n=52) or due to a possible bias since the largest number of patients in the cohort belong to the severe phenotype group. In contrast to the UK health system, the Spanish Reference Center is responsible for the management of patients with NF2 in its healthcare region, and patients attending their region centre are generally only referred to the CSUR when their clinical management is complex. Hence, our cohort could be biased due to the low representation of mild phenotypes. In addition, other factors need to be taken into consideration in addition to *NF2* pathogenic variant, as there is a wide range of evidence for heterogeneity in the mild-to-moderate phenotypes, even in patients harbouring the same *NF2* variant,[10 11 14 15 21–23] which was also observed in our statistical model. Although the GSS is entirely appropriate for establishing general trends, there is scope for improvement by harnessing other types of data to establish a personalised NF2 prognosis score.

Understanding the status of Merlin and its regulated pathways might provide data that could help in the interpretation of the NF2 genotype-phenotype relationship. With this aim, a functional assay in primary cultured fibroblast from patients was developed. As expected, Merlin levels showed significant differences between group 1 (no variant identified in blood), compared with the groups harbouring a constitutional *NF2* genetic variant. Furthermore, no differences were found regardless of the type or the location of variant within the gene. Although evidence in Schwann cells or immortalised tumour cells show the opposite effect, in this study, significantly lower levels of pERK in Merlin haploinsufficient primary fibroblasts were observed in comparison with healthy controls and tissue mosaics.[26 30–32] Hence, these results, if validated in other cohorts and in larger sample sizes, would establish that pERK levels in patient fibroblast are associated with severe phenotype, and thus are susceptible for use as an NF2 prognostic marker.

In this study, we decided to quantify the NF2 phenotype using a 10-scale system based on well-known NF2 prognostic markers.[7] This scale allows an easy quantification of the NF2 phenotype, which is held to be more accurate than using a qualitative system (mild-moderate-severe), and the quantification of mosaic phenotypes. Additionally, this quantitative method makes it possible to model the NF2 phenotypes according to the *NF2* genetic variant, as has been done in other studies.[33–35]

Subsequently, with the aim of improving the NF2 prognostic capacity based on the germline variant, and also to assess if functional data could be incorporated into the UK NF2 GSS, we reviewed the classification of variants proposed by Halliday et al.[12] Similar to GSS, we propose that in addition to the predicted mutation effect on Merlin function and the functional assays results, the mosaicism extension and the published NF2 genotype-phenotype evidence[9 10 12 14 16] be taken into account. We classified NF2 genetic variants in six classes, where truncating variants in exons 2–13 were scored 6, missense and in-frame deletions as 3, presumed mosaics or patients carrying a Ring22 as 1, while the other type of pathogenic variants were scored in between. The main dissimilarities to GSS are the classification of large deletions and splicing variants, where the position in the NF2 gene were contemplated differently, because considerable evidence indicates that splicing variants affecting the N-term or C-term of NF2 gene are associated with both severe and moderate phenotypes, respectively,[5 7 8 20–22] and variants that do not alter the reading frame have lower scores in comparison to those generating a frameshift alteration, assuming that in-frame alterations could generate a hypomorphic Merlin preventing the activation of nonsense-mediated mRNA decay.

Within our cohort, the reviewed GSS, called FGSS seems to reduce the intragroup variability, to improve mosaic patient stratification and slightly upgrade the correlation between patient phenotype and the different prognostic parameters analysed in relation to the GSS. Furthermore, the modelling of the NF2 phenotype in terms of the NF2 mutation classification in our cohort corroborates that NF2 variants can partially explain patient phenotype therefore, the GSS with this added value could be more precise when determining a prognosis trend in patients with NF2.

Similar to the GSS, FGSS is unable to properly classify presumed and some tissue mosaic patients. Although mosaic patients are generally associated with mild phenotypes, some of these patients show a rather severe phenotype, indicating that the extension of mosaicism should also be considered. Regarding this point, we observed that NF2 analysis on blood may not represent the degree of affectation, given that in some patients the NF2 variant was undetectable in blood, but was present in the skin fibroblasts (online supplemental figure 4). In addition, it is known that tissue mosaic patients with NF2 are at risk of transmitting the disease, even though the variant was not detected in blood.[14 16] These outcomes could indicate that haematopoietic primordial stem cells harbouring NF2 mutations may have a selective growth disadvantage over normal stem cells, reducing their representation in this tissue, contrarily to what it has been shown for NF1 mutations.[36 37]

In addition, both GSS and FGSS identify similar levels of Merlin and pERK, but using FGSS there is an increased correlation with the NF2 phenotype and a decreased intragroup variability in groups associated with mild phenotypes. However, although pERK levels could represent a potential NF2 prognosis marker, its incorporation into the genetic score does not improve the capacity to explain NF2 phenotype. This could be due to the small sample set included in the model (n=27) or because the contribution of pERK on NF2 phenotype is too low when compared with the contribution of the NF2 variant in the phenotype description, thus, its addition does not increase the statistical significance of the model. Although discouraging, these results should be tested in larger sets of samples because the inclusion tendency of pERK levels does appear to be a promising approach.

To conclude, with the data obtained from this study, we propose a review of the UK NF2 GSS to continue the advance towards a personalised assessment of) NF2 prognosis. This revision considers the type of germline pathogenic variant, the extent of mosaicism, genotype-phenotype evidence and statistically significant correlations already published, and the predicted effect of mutation on the function of Merlin and its effect on Merlin and pERK activity.

Author affiliations
[1]Clinical Genomics Research Unit, Fundació Institut d'Investigació en Ciències de la Salut Germans Trias i Pujol (IGTP-PMPPC), Badalona, Spain
[2]Genetic Counseling Unit, Clinical Genetics Service, Northern Metropolitan Clinical Laboratory, Hospital Universitari Germans Trias i Pujol, Badalona, Spain
[3]Genomes for Life—GCAT lab Group, Fundació Institut d'Investigació en Ciències de la Salut Germans Trias i Pujol, Badalona, Spain
[4]Dermatology Department, Hospital Universitari Germans Trias i Pujol, Badalona, Spain
[5]Clinical Genomics Unit, Clinical Genetics Service, Northern Metropolitan Clinical Laboratory, Hospital Universitari Germans Trias i Pujol, Badalona, Spain
[6]Otorhinolaryngology, Hospital Universitari Germans Trias i Pujol, Badalona, Spain
[7]Neurology, Hospital Universitari Germans Trias i Pujol, Badalona, Spain
[8]Neurosurgery, Hospital Universitari Germans Trias i Pujol, Badalona, Spain
[9]Hereditary Cancer Program, ICO-IDIBELL-CIBERONC, Catalan Institute of Oncology, L'Hospitalet de Llobregat, Barcelona, Spain
[10]Hereditary Cancer Group, Fundació Institut d'Investigació en Ciències de la Salut Germans Trias i Pujol (IGTP-PMPPC), Badalona, Spain

Twitter Núria Catasús @- and Elisabeth Castellanos @elishabeba82

ORCID iDs
Alejandro Negro http://orcid.org/0000-0002-4654-077X
Inma Rosas http://orcid.org/0000-0003-4238-0227
Conxi Lazaro Garcia http://orcid.org/0000-0002-7198-5906
Rafael de Cid http://orcid.org/0000-0003-3579-6777
Elisabeth Castellanos http://orcid.org/0000-0002-8133-5325

REFERENCES

1 Evans DG, Bowers NL, Tobi S, Hartley C, Wallace AJ, King AT, Lloyd SKW, Rutherford SA, Hammerbeck-Ward C, Pathmanaban ON, Freeman SR, Ealing J, Kellett M, Laitt R, Thomas O, Halliday D, Ferner R, Taylor A, Duff C, Harkness EF, Smith MJ. Schwannomatosis: a genetic and epidemiological study. *J Neurol Neurosurg Psychiatry* 2018;89:1215–9.

2 Evans DG, Huson SM, Donnai D, Neary W, Blair V, Teare D, Newton V, Strachan T, Ramsden R, Harris R. A genetic study of type 2 neurofibromatosis in the United Kingdom. I. prevalence, mutation rate, fitness, and confirmation of maternal transmission effect on severity. *J Med Genet* 1992;29:841–6.

3 Ferner RE, Bakker A, Elgersma Y, Evans DGR, Giovannini M, Legius E, Lloyd A, Messiaen LM, Plotkin S, Reilly KM, Schindeler A, Smith MJ, Ullrich NJ, Widemann B, Sherman LS. From process to progress—2017 international conference on neurofibromatosis 1, neurofibromatosis 2 and schwannomatosis. *AJMG* 2019:1098–106.

4 Lloyd SKW, Evans DGR. Neurofibromatosis type 2 (NF2): diagnosis and management. *Handb Clin Neurol* 2013;115:957–67.

5 Plotkin SR, Duda DG, Muzikansky A, Allen J, Blakeley J, Rosser T, Campian JL, Clapp DW, Fisher MJ, Tonsgard J, Ullrich N, Thomas C, Cutter G, Korf B, Packer R, Karajannis MA, Multicenter KMA. Multicenter, prospective, phase II and biomarker study of high-dose bevacizumab as induction therapy in patients with neurofibromatosis type 2 and progressive vestibular schwannoma. *J Clin Oncol* 2019;37:3446–54.

6 Asthagiri AR, Parry DM, Butman JA, Kim HJ, Tsilou ET, Zhuang Z, Lonser RR. Neurofibromatosis type 2. *Lancet* 2009;373:1974–86.

7 Hexter A, Jones A, Joe H, Heap L, Smith MJ, Wallace AJ, Halliday D, Parry A, Taylor A, Raymond L, Shaw A, Afridi S, Obholzer R, Axon P, King AT, Friedman JM, Evans DGR, English Specialist NF2 Research Group. Clinical and molecular predictors of mortality in neurofibromatosis type 2: a UK national analysis of 1192 patients. *J Med Genet* 2015;52:699–705.

8 Baser ME, Friedman JM, Aeschliman D, Joe H, Wallace AJ, Ramsden RT, Evans DGR. Predictors of the risk of mortality in neurofibromatosis 2. *Am J Hum Genet* 2002;71:715–23.

9 Baser ME, Kuramoto L, Joe H, Friedman JM, Wallace AJ, Gillespie JE, Ramsden RT, Evans DGR. Genotype-phenotype correlations for nervous system tumors in neurofibromatosis 2: a population-based study. *Am J Hum Genet* 2004;75:231–9.

10 Kluwe L, MacCollin M, Tatagiba M, Thomas S, Hazim W, Haase W, Mautner V-F. Phenotypic variability associated with 14 splice-site mutations in the NF2 gene. *Am J Med Genet* 1998;77:228–33.

11 Ruttledge MH, Andermann AA, Phelan CM, Claudio JO, Han FY, Chretien N, Rangaratnam S, MacCollin M, Short P, Parry D, Michels V, Riccardi VM, Weksberg R, Kitamura K, Bradburn JM, Hall BD, Propping P, Rouleau GA. Type of mutation in the neurofibromatosis type 2 gene (NF2) frequently determines severity of disease. *Am J Hum Genet* 1996;59:331–42 http://www.ncbi.nlm.nih.gov/pubmed/8755919%5Cnhttp://www.pubmedcentral.nih.gov/articlerender.fcgi?artid=PMC1914741%5Cnhttp://www.pubmedcentral.nih.gov/articlerender.fcgi?artid=1914741&tool=pmcentrez&rendertype=abstract

12 Halliday D, Emmanouil B, Pretorius P, MacKeith S, Painter S, Tomkins H, Evans DG, Parry A. Genetic severity score predicts clinical phenotype in NF2. *J Med Genet* 2017;54:657–64.

13 Halliday D, Emmanouil B, Vassallo G, Lascelles K, Nicholson J, Chandratre S, Anand G, Wasik M, Pretorius P, Evans DG, Parry A, Axon P, Gair J, Smyth C, Afridi SK, Obholzer R, Everett V, Jarvis N, Henshaw K, Hanemann CO, Howard W, May A, Redman C, Rattihalli R, Tomkins H, English NF2 research group. Trends in phenotype in the English paediatric neurofibromatosis type 2 cohort stratified by genetic severity. *Clin Genet* 2019;96:151–62.

14 Evans DG, Hartley CL, Smith PT, King AT, Bowers NL, Tobi S, Wallace AJ, Perry M, Anup R, Lloyd SKW, Rutherford SA, Hammerbeck-Ward C, Pathmanaban ON, Stapleton E, Freeman SR, Kellett M, Halliday D, Parry A, Gair JJ, Axon P, Laitt R, Thomas O, Afridi SK, Obholzer R, Duff C, Stivaros SM, Vassallo G, Harkness EF, Smith MJ, English Specialist NF research group. Incidence of mosaicism in 1055 de novo NF2 cases: much higher than previous estimates with high utility of next-generation sequencing. *Genet Med* 2020;22:53–9.

15 Kluwe L, Mautner VF. Mosaicism in sporadic neurofibromatosis 2 patients. *Hum Mol Genet* 1998;7:2051–5 http://www.ncbi.nlm.nih.gov/pubmed/9817921

16 Evans DG, Raymond FL, Barwell JG, Halliday D. Genetic testing and screening of individuals at risk of NF2. *Clin Genet* 2012;82:416–24.

17 Hagel C, Lindenau M, Lamszus K, Kluwe L, Stavrou D, Mautner V-F. Polyneuropathy in neurofibromatosis 2: clinical findings, molecular genetics and neuropathological alterations in sural nerve biopsy specimens. *Acta Neuropathol* 2002;104:179–87.

18 Otsuka G, Saito K, Nagatani T, Yoshida J. Age at symptom onset and long-term survival in patients with neurofibromatosis type 2. *J Neurosurg* 2003;99:480–3.

19 Baser ME, Makariou EV, Parry DM. Predictors of vestibular schwannoma growth in patients with neurofibromatosis type 2. *J Neurosurg* 2002;96:217–22.

20 Kluwe L, Mautner VF. A missense mutation in the NF2 gene results in moderate and mild clinical phenotypes of neurofibromatosis type 2. *Hum Genet* 1996;97:224–7.

21 Heineman TE, Evans DGR, Campagne F, Selesnick SH. In silico analysis of NF2 gene missense mutations in neurofibromatosis type 2: from genotype to phenotype. *Otol Neurotol* 2015;36:908–14.

22 Mautner VF, Baser ME, Kluwe L. Phenotypic variability in two families with novel splice-site and frameshift NF2 mutations. *Hum Genet* 1996;98:203–6.

23 Castellanos E, Rosas I, Solanes A, Bielsa I, Lázaro C, Carrato C, Hostalot C, Prades P, Roca-Ribas F, Blanco I, Serra E, NF2 Multidisciplinary Clinics HUGTiP-ICO-IMPPC. In vitro antisense therapeutics for a deep intronic mutation causing neurofibromatosis type 2. *Eur J Hum Genet* 2013;21:769–73.

24 Baser ME, Kuramoto L, Woods R, Joe H, Friedman JM, Wallace AJ, Ramsden RT, Olschwang S, Bijlsma E, Kalamarides M, Papi L, Kato R, Carroll J, Lázaro C, Joncourt F, Parry DM, Rouleau GA, Evans DGR. The location of constitutional neurofibromatosis 2 (NF2) splice site mutations is associated with the severity of NF2. *J Med Genet* 2005;42:540–6.

25 Li W, Cooper J, Karajannis MA, Giancotti FG. Merlin: a tumour suppressor with functions at the cell cortex and in the nucleus. *EMBO Rep* 2012;13:204–15.

26 Petrilli AM, Fernández-Valle C. Role of Merlin/NF2 inactivation in tumor biology. *Oncogene* 2016;35:537–48.

27 Cooper J, Giancotti FG. Molecular insights into *NF2*/Merlin tumor suppressor function. *FEBS Lett* 2014;588:2743–52.

28 Baser ME, Friedman JM, Wallace AJ, Ramsden RT, Joe H, Evans DGR. Evaluation of clinical diagnostic criteria for neurofibromatosis 2. *Neurology* 2002;59:1759–65.

29 Castellanos E, Gel B, Rosas I, Tornero E, Santín S, Pluvinet R, Velasco J, Sumoy L, Del Valle J, Perucho M, Blanco I, Navarro M, Brunet J, Pineda M, Feliubadaló L, Capellá G, Lázaro C, Serra E. A comprehensive custom panel design for routine hereditary cancer testing: preserving control, improving diagnostics and revealing a complex variation landscape. *Sci Rep* 2017;7:39348.

30 Cui Y, Groth S, Troutman S, Carlstedt A, Sperka T, Riecken LB, Kissil JL, Jin H, Morrison H. The NF2 tumor suppressor merlin interacts with Ras and RasGAP, which may modulate Ras signaling. *Oncogene* 2019;38:6370–81.

31 Morrison H, Sperka T, Manent J, Giovannini M, Ponta H, Herrlich P. Merlin/neurofibromatosis type 2 suppresses growth by inhibiting the activation of Ras and Rac. *Cancer Res* 2007;67:520–7.

32 Hilton DA, Ristic N, Hanemann CO. Activation of ERK, AKT and JNK signalling pathways in human schwannomas *in situ*. *Histopathology* 2009;55:744–9.

33 Painter SL, Sipkova Z, Emmanouil B, Halliday D, Parry A, Elston JS. Neurofibromatosis type 2–Related eye disease correlated with genetic severity type. *J Neuro-Ophthalmology* 2019;39:44–9.

34 Abi Jaoude S, Peyre M, Degos V, Goutagny S, Parfait B, Kalamarides M. Validation of a scoring system to evaluate the risk of rapid growth of intracranial meningiomas in neurofibromatosis type 2 patients. *J Neurosurg* 2020:1377–85.

35 Emmanouil B, Houston R, May A, Ramsden JD, Hanemann CO, Halliday D, Parry A, Mackeith S. Progression of hearing loss in neurofibromatosis type 2 according to genetic severity. *Laryngoscope* 2019;129:974–80.

36 Roehl AC, Mussotter T, Cooper DN, Kluwe L, Wimmer K, Josef H, Zetzmann M, Vogt J, Mautner V, Kehrer-sawatzki H. Tissue-Specific differences in the proportion of mosaic large NF1 deletions are suggestive of a selective growth advantage of hematopoietic del (+ / −) stem cells. *Hum Mutat* 2011;33.

37 Fernández-Rodríguez J, Castellsagué J, Benito L, Benavente Y, Capellá G, Blanco I, Serra E, Lázaro C. A mild neurofibromatosis type 1 phenotype produced by the combination of the benign nature of a leaky NF1-splice mutation and the presence of a complex mosaicism. *Hum Mutat* 2011;32:705–9.

Supplementary Methods and Materials:

NF2 diagnosis and clinical data collection:

Patients included in the study are clinically followed-up in the NF2 Spanish reference center. Our multidisciplinary team consists of physicians with different specialities responsible for NF2 patients follow-up in their area of expertise (Neurologists, Neurosurgeons, Otolaryngologists, Dermatologists, Pediatricians, Oncologists, Clinical Geneticist, Genetic Counselling, Radiotherapists, Radiologists, etc.). Neurofibromatosis and Schwannomatosis (probable) patients are followed-up yearly by all clinical specialists required and when the patient informs of new symptomatology or clinical problem. Records from patient's follow-up were reviewed according to five domains: patient demographics, tumor load, ocular features, hearing capacity and major interventions. All clinical data collected was from the last clinical patient assessment. Patients included met the Manchester NF2 diagnostic criteria NF2 [Baser et al 2002]. The age at diagnosis also include patients that were detected asymptomatically on scan although most of them were symptomatic.

Tumor burden was determined by reviews of gadolinium-enhanced brain and spine MRI scans performed. In case of NF2 patients, a brain and spine MRI scan is usually offered once the patient is clinically diagnosed and afterwards, a yearly brain scan is performed. In addition, a spine or whole body scan is offered if the patient needs tumor growth follow-up or shows new symptomatology related to the development or growth of a tumor. Type of lesions was determined taking into account the most likely lesion radiologically although histological diagnosis was used when available. Hearing was evaluated at every appointment using speech audiometry and pure tone audiometry. Hearing grade was classified on a score of 1-6 according to Halliday et al. Grades 1, 2, 3-4 represents those patients with an optimum Speech Discrimination Score (SDS) in the better hearing ear of >70%, 50%–70% and below 50%, respectively. Patients with hearing implant are classified as grade 5 and those with bilaterally dead ears as grade 6. Hearing loss was defined as the age of loss of useful hearing which it was described by Halliday et al. as hearing grade 3 or worse.

The clinical assessment of cutaneous abnormalities consisted of examination for CAL spots as well as the type, location and number of dermal tumors clinically suggestive of cutaneous schwannomas. However, for this study only the number of patients that present tumors suggestive of cutaneous schwannomas, most of them confirmed by a histopathological analysis are considered. Tumor histopathological features were classified using the World Health Organization criteria for central nervous system and soft tissue tumors. Schwannomas were defined as encapsulated tumors composed of spindle-shaped neoplastic Schwann cells. The study was based on hematoxylin and eosin–stained slides and the immunocytochemical analysis of S100 and MelanA.

The number and type of major interventions for each patient was also collected. The indication of intervention is decided by the multidisciplinary team committee, taking into account patient's symptomatology, tumor location and growth rate. In the case of vestibular schwannomas, the hearing grade of the affected ear and the contralateral one is considered.

Genetic NF2 test: Genetic test was performed using the customized I2HCP panel (Castellanos et al 2017) in blood or tissue when available and validated by Sanger sequencing in all primary cultures established. In

1

mosaic patients, a deep sequencing with a >700 depth of coverage was performed in primary culture fibroblasts. Only variants detected above 5% of the cells were considered.

Functional assay, Western Blot analysis: Merlin's downstream pathways were analyzed in 27 out of 30 NF2 patients included in the validation of the Genetic Severity Score. We obtained cultured fibroblasts from skin biopsies that were processes as described in [29]. 50 μg of protein extracted from these primary cultures at 50%, 80% and 100% of confluence was load to SDS-PAGE (150V) and transferred onto PVDF membranes (1 hour 350 mA at 4°C). Odyssey Blocking Buffer TBS (LI-COR) was used to block the resulting membranes. Three primary cultures from healthy donors were included as control samples (Ctrl1, Ctrl2 and Ctrl3). When grouping for the statistical studies, the control healthy donors and the mosaics as a control group were been taken into account, since none of these show the constitutional *NF2* mutation in the analyzed tissue. Primary antibodies were incubated at 4°C overnight. Membranes were later incubated with IRDye 680LT and IRDye 800CW secondary antibodies (1:1000 dilution, LI-COR) for 1h at room temperature and scanned and analyzed using the Odyssey Infrared Imaging System (LI-COR). The statistical threshold that allows the differentiation between healthy controls or mosaic patients and the patients in group 3 (severe) is established through the ±2SD limits method.

Primary antibodies: α-pERK: phospho-p44/42; APK (Erk1/2) (Thr202/Tyr204) (E10) #9106 α-mouse (Cell Signaling Technology), **α-ERK**: p44/42; APK (Erk1/2) Antibody #9102 − α − rabbit (Cell Signaling Technology, **α-pAKT:** Phospho Akt (Ser 473) (587F11) Mouse ab #4051 α-mouse (Cell Signaling Technology), **α-AKT** Akt Antibody #9272− α −rabbit (Cell Signaling Technology, **α-pNF2:** Phospho NF2/Merlin (phospho S518) antibody (ab131473) α-rabbit (Abcam), **α-NF2:** NF2/Merlin antibody (ab88957) α-mouse (Abcam), **α -PAK1:** Anti-PAK1 antibody (ab154284) α-rabbit (Abcam), **α -RAC1:** Anti-RAC1 antibody (ab33186) α-mouse (Abcam), **α-pYAP1**: anti-YAP1 (phospho S127) antibody [EP1675Y] (ab76252) − α − rabbit (Abcam), **α-YAP1**: anti-YAP1 antibody (ab56701) − α − mouse (Abcam), **α-pPKA:** Phospho PKA. Anti PKA alpha+beta (phospho T197) antibody (ab5815) −α −rabbit (Abcam), **α-PKA:** PKA C alpha beta antibody Clone #515741 (MAB5908) − α − mouse (Abcam). **α-vinculin:** anti-vinculin antibody [EPR8185] (ab129002) − α − rabbit (Abcam) was used to normalize protein expression among samples

NF2 phenotype quantification: Clinical phenotype was recorded as follows: age of diagnosis was rated as 3 if it was below 25, 2 between 25 and 35 and 1 if patient was diagnosed after the age of 35; the presence of peripheral and vestibular schwannomas were scored as 0, 1 or 2 if they were absent, unique or multiple, while extravestibular lesions were scored between 1 if we detected single intracranial or intra-spinal lesion, 2 if the patients showed multiple intracranial or intra-spinal schwannomas or meningiomas, or 3 when patient developed multiple intra-spinal or intracerebral different lesion types or multiple intra-spinal and intracerebral schwannomas or meningiomas (Supplementary Table 3).

NF2 pathogenic variant score: Truncating mutations in exons 2-13 were scored 6, missense and in frame deletions as 3, presumed mosaics or patients carrying a Ring22 as 1. Based on [7,10,14,41], the predicted effect of *NF2* mutation on the function of Merlin, and our observations on the phenotype shown by patients harboring mutations in the most terminal region of the gene and the results from the pERK functional analysis, we decided to rate differently when mutations are located in first exons, as Merlin could start its translation using another methionine, or if the variant does not alter *NF2* reading frame because some Merlin residual function could be maintained. In addition, when the variant affects exon 14 or the followings due to its association to good prognosis was also considered (Supplementary Table 4) [7,8]. In addition, in the absence of more evidence, we scored all missense variants as 3, since in our functional

2

assays and as published before [42], missense mutations result in the quantitative loss of Merlin proteins, and we assume they might minimally affect the intrinsic protein function unless when altering specific positions, which would be rated differently once the association to a severe phenotype is demonstrated. In contrast to GSS, we scored those splicing and copy number alterations (CNA) at exon level that do not alter the reading frame as less severe, in comparison to those generating a frameshift alteration assuming that in frame alterations could generate an hypomorphic Merlin, although we do not consider them different when variants are located at exons 1-7 or 8-13. We also scored generalized mosaicism, if *NF2* variant was detected in blood or unaffected tissue, differently from tissue mosaicism if it was detected only in two independent tumors, since the degree of affectation could be different. Finally, patients with an inconclusive blood test without any tumor analyzed were considered presumed tissue mosaics and scored as 1 (Table 3).

Statistics: All statistical analyses of the validation of the GSS were reproduced from the study of Halliday et al. In brief, an NF2 Genetic Severity Score (GSS) was determined based on the phenotype of patients. Genetic Severity Score consists of a 3-point classification into tissue mosaicism, classic and severe disease. χ2 statistics were used to compare the distribution of GSS by gender and NF2-related deaths (sporadic or familial). Trends with genetic severity were investigated using Mantel-Haenszel linear-by-linear χ2 tests of association for tumor load, ocular features, hearing outcomes and major interventions of the patients. Spearman's rank-order correlations were run to assess the relationship between age of patients, eye features, number of interventions, ratio of interventions to age and genetic severity. In our study, minor variations were applied in comparison to Halliday et al. and quality of life was not considered. Principal component analysis (PCA) of age at diagnosis, extravestibular affection, vestibular and peripheral schwannomas was performed to explore variability of NF2 type mutations of patients.

In our study, minor variations were applied. Mutation data, tumor load, ocular features, hearing outcomes and major interventions of the patients were defined as categorical variables. Quality of life was not considered in our study. Principal component analysis (PCA) of age at diagnosis, extravestibular affection, vestibular and peripheral schwannomas was performed to explore variability of NF2 type mutations of patients.

In order to study differences between protein expression levels in the functional assay, Kruskal-Wallis and Mann-Whitney U statistical tests were performed among genetic severity groups and mutation classes. Fibroblast protein levels from healthy controls have been included in group 1 for the statistics analysis. Analysis of variance (ANOVA) of FGSS and NF2 mutations was performed to test differences of severity between NF2 mutations groups. Shapiro Wilk and Levene tests were applied for testing Normality of residuals and homoscedasticity of groups respectively. Backward stepwise regression analysis was performed to evaluate the contribution of Merlin and pERK levels in the ANOVA model. Statistical analyses were performed using R software.

3

Supplementary Methods and Materials:

Supplementary Figures and Tables:

Supplementary Figure 1. pMerlin and Merlin levels in patient's fibroblasts. NPE stands for Normalized Protein Expression; Bars represent the SD from three independent experiments.

Supplementary Figure 2. Levels of proteins involved in the NF2 downstream pathway in patients' fibroblasts. NPE stands for Normalized Protein Expression; Bars represent the SD from three independent experiments.

Supplementary Figure 3. PCA-biplot of phenotypical NF2 data by NF2-mutation groups. VS: Vestibular Schwannoma; Age Dx: Age at diagnosis; PS: Peripheral Schwannoma; EVA: Extra vestibular Affection. Dim1 (Dimension 1); Dim2 (Dimension 1)

Supplementary Figure 4. Sanger sequencing comparison between blood and fibroblast samples of a NF2 patient.

Supplementary Table 1. NF2 Patients summary.

Supplementary Table 2. Major interventions in relation to Genetic Severity Score.

Supplementary Table 3. NF2 Phenotype quantification.

Supplementary Table 4. Revising pathogenicity associated to *NF2* mutations according to GSS. Patients with an unexpected phenotype according to GSS are highlighted in bold in the Reasoning column.

Supplementary Table 5. Demographic data according to Functional Genetic Severity Score.

Supplementary Table 6. Tumor burden, presence of ocular features and hearing outcome according to Functional Genetic Severity Score.

Supplementary Table 7. Major interventions in relation to Functional Genetic Severity Score.

Supplementary Table 8. Intragroup Variability of Merlin, pERK, age at diagnosis and age at hearing loss.

Supplementary Table 9. A) FGSS and *NF2* disease-causing variant regression model. B) FGSS and *NF2* disease-causing variant regression model.

Supplementary Methods:

NF2 diagnosis and clinical data collection: Patients included in the study are clinically followed-up in the NF2 Spanish reference center. Our multidisciplinary team consists of physicians with different specialties responsible for NF2 patients' follow-up in their area of expertise (Neurologists, Neurosurgeons, Otolaryngologists, Dermatricians, Paediatricians, Oncologists, Clinical Geneticist, Genetic Counselling, Radiotherapists, Radiologists, etc.). Neurofibromatosis and Schwannomatosis (probable) patients are followed-up yearly by all clinical specialists required and when the patient informs of new symptomatology or clinical problem. Records from patient's follow-up were reviewed according to five

domains: patient demographics, tumor load, ocular features, hearing capacity and major interventions. All clinical data collected was from the last clinical patient assessment. Patients included met the Manchester NF2 diagnostic criteria NF2 [Baser et al 2002]. The age at diagnosis also include patients that were detected asymptomatically on scan although most of them were symptomatic.

Tumor burden was determined by reviews of gadolinium-enhanced brain and spine MRI scans performed. In case of NF2 patients, a brain and spine MRI scan is usually offered once the patient is clinically diagnosed and afterwards, a yearly brain scan is performed. In addition, a spine or whole body scan is offered if the patient needs tumor growth follow-up or shows new symptomatology related to the development or growth of a tumor. Type of lesions was determined taking into account the most likely lesion radiologically although histological diagnosis was used when available. Hearing was evaluated at every appointment using speech audiometry and pure tone audiometry. Hearing grade was classified on a score of 1-6 according to Halliday et al. Grades 1, 2, 3-4 represents those patients with an optimum Speech Discrimination Score (SDS) in the better hearing ear of >70%, 50%–70% and below 50%, respectively. Patients with hearing implant are classified as grade 5 and those with bilaterally dead ears as grade 6. Hearing loss was defined as the age of loss of useful hearing which it was described by Halliday et al. as hearing grade 3 or worse.

The clinical assessment of cutaneous abnormalities consisted of examination for CAL spots as well as the type, location and number of dermal tumors clinically suggestive of cutaneous schwannomas. However, for this study only the number of patients that present tumors suggestive of cutaneous schwannomas, most of them confirmed by a histopathological analysis are considered. Tumor histopathological features were classified using the World Health Organization criteria for central nervous system and soft tissue tumors. Schwannomas were defined as encapsulated tumors composed of spindle-shaped neoplastic Schwann cells. The study was based on hematoxylin and eosin–stained slides and the immunocytochemical analysis of S100 and MelanA.

The number and type of major interventions for each patient was also collected. The indication of intervention is decided by the multidisciplinary team committee, taking into account patient's symptomatology, tumor location and growth rate. In the case of vestibular schwannomas, the hearing grade of the affected ear and the contralateral one is considered.

Genetic NF2 test: Genetic test was performed using the customized I2HCP panel (Castellanos et al 2017) in blood or tissue when available and validated by Sanger sequencing in all primary cultures established. In mosaic patients, a deep sequencing with a >700 depth of coverage was performed in primary culture fibroblasts. Only variants detected above 5% of the cells were considered.

Functional assay, Western Blot analysis: Merlin's downstream pathways were analyzed in 27 out of 30 NF2 patients included in the validation of the Genetic Severity Score. We obtained cultured fibroblasts from skin biopsies that were processes as described in [29]. 50 µg of protein extracted from these primary cultures at 50%, 80% and 100% of confluence was load to SDS-PAGE (150V) and transferred onto PVDF membranes (1 hour 350 mA at 4°C). Odyssey Blocking Buffer TBS (LI-COR) was used to block the resulting membranes. Three primary cultures from healthy donors were included as control samples (Ctrl1, Ctrl2 and Ctrl3). When grouping for the statistical studies, the control healthy donors and the mosaics as a control group were been taken into account, since none of these show the constitutional *NF2* mutation in

2

Supplemental material

BMJ Publishing Group Limited (BMJ) disclaims all liability and responsibility arising from any reliance
placed on this supplemental material which has been supplied by the author(s)

J Med Genet

the analyzed tissue. Primary antibodies were incubated at 4°C overnight. Membranes were later incubated with IRDye 680LT and IRDye 800CW secondary antibodies (1:1000 dilution, LI-COR) for 1h at room temperature and scanned and analyzed using the Odyssey Infrared Imaging System (LI-COR). The statistical threshold that allows the differentiation between healthy controls or mosaic patients and the patients in group 3 (severe) is established through the ±2SD limits method.

Primary antibodies: α-pERK: phospho-p44/42; APK (Erk1/2) (Thr202/Tyr204) (E10) #9106 α-mouse (Cell Signaling Technology), **α-ERK**: p44/42; APK (Erk1/2) Antibody #9102 – α – rabbit (Cell Signaling Technology, **α-pAKT:** Phospho Akt (Ser 473) (587F11) Mouse ab #4051 α-mouse (Cell Signaling Technology), **α-AKT** Akt Antibody #9272– α –rabbit (Cell Signaling Technology, **α-pNF2:** Phospho NF2/Merlin (phospho S518) antibody (ab131473) α-rabbit (Abcam), **α-NF2:** NF2/Merlin antibody (ab88957) α-mouse (Abcam), **α -PAK1:** Anti-PAK1 antibody (ab154284) α-rabbit (Abcam), **α -RAC1:** Anti-RAC1 antibody (ab33186) α-mouse (Abcam), **α-pYAP1**: anti-YAP1 (phospho S127) antibody [EP1675Y] (ab76252) – α – rabbit (Abcam), **α-YAP1:** anti-YAP1 antibody (ab56701) – α – mouse (Abcam), **α-pPKA:** Phospho PKA. Anti PKA alpha+beta (phospho T197) antibody (ab5815) – α – rabbit (Abcam), **α-PKA:** PKA C alpha beta antibody Clone #515741 (MAB5908) – α – mouse (Abcam). **α-vinculin:** anti-vinculin antibody [EPR8185] (ab129002) – α – rabbit (Abcam) was used to normalize protein expression among samples

NF2 phenotype quantification: Clinical phenotype was recorded as follows: age of diagnosis was rated as 3 if it was below 25, 2 between 25 and 35 and 1 if patient was diagnosed after the age of 35; the presence of peripheral and vestibular schwannomas were scored as 0, 1 or 2 if they were absent, unique or multiple, while extravestibular lesions were scored between 1 if we detected single intracranial or intra-spinal lesion, 2 if the patients showed multiple intracranial or intra-spinal schwannomas or meningiomas, or 3 when patient developed multiple intra-spinal or intracerebral different lesion types or multiple intra-spinal and intracerebral schwannomas or meningiomas (Supplementary Table 3).

NF2 pathogenic variant score: Truncating mutations in exons 2-13 were scored 6, missense and in frame deletions as 3, presumed mosaics or patients carrying a Ring22 as 1. Based on [7,10,14,41], the predicted effect of *NF2* mutation on the function of Merlin, and our observations on the phenotype shown by patients harboring mutations in the most terminal region of the gene and the results from the pERK functional analysis, we decided to rate differently when mutations are located in first exons, as Merlin could start its translation using another methionine, or if the variant does not alter *NF2* reading frame because some Merlin residual function could be maintained. In addition, when the variant affects exon 14 or the followings due to its association to good prognosis was also considered (Supplementary Table 4) [7,8]. In addition, in the absence of more evidence, we scored all missense variants as 3, since in our functional assays and as published before [42], missense mutations result in the quantitative loss of Merlin proteins, and we assume they might minimally affect the intrinsic protein function unless when altering specific positions, which would be rated differently once the association to a severe phenotype is demonstrated. In contrast to GSS, we scored those splicing and copy number alterations (CNA) at exon level that do not alter the reading frame as less severe, in comparison to those generating a frameshift alteration assuming that in frame alterations could generate an hypomorphic Merlin, although we do not consider them different when variants are located at exons 1-7 or 8-13. We also scored generalized mosaicism, if *NF2* variant was detected in blood or unaffected tissue, differently from tissue mosaicism if it was detected only in two independent tumors, since the degree of affectation could be different.

3

Supplemental material

BMJ Publishing Group Limited (BMJ) disclaims all liability and responsibility arising from any reliance
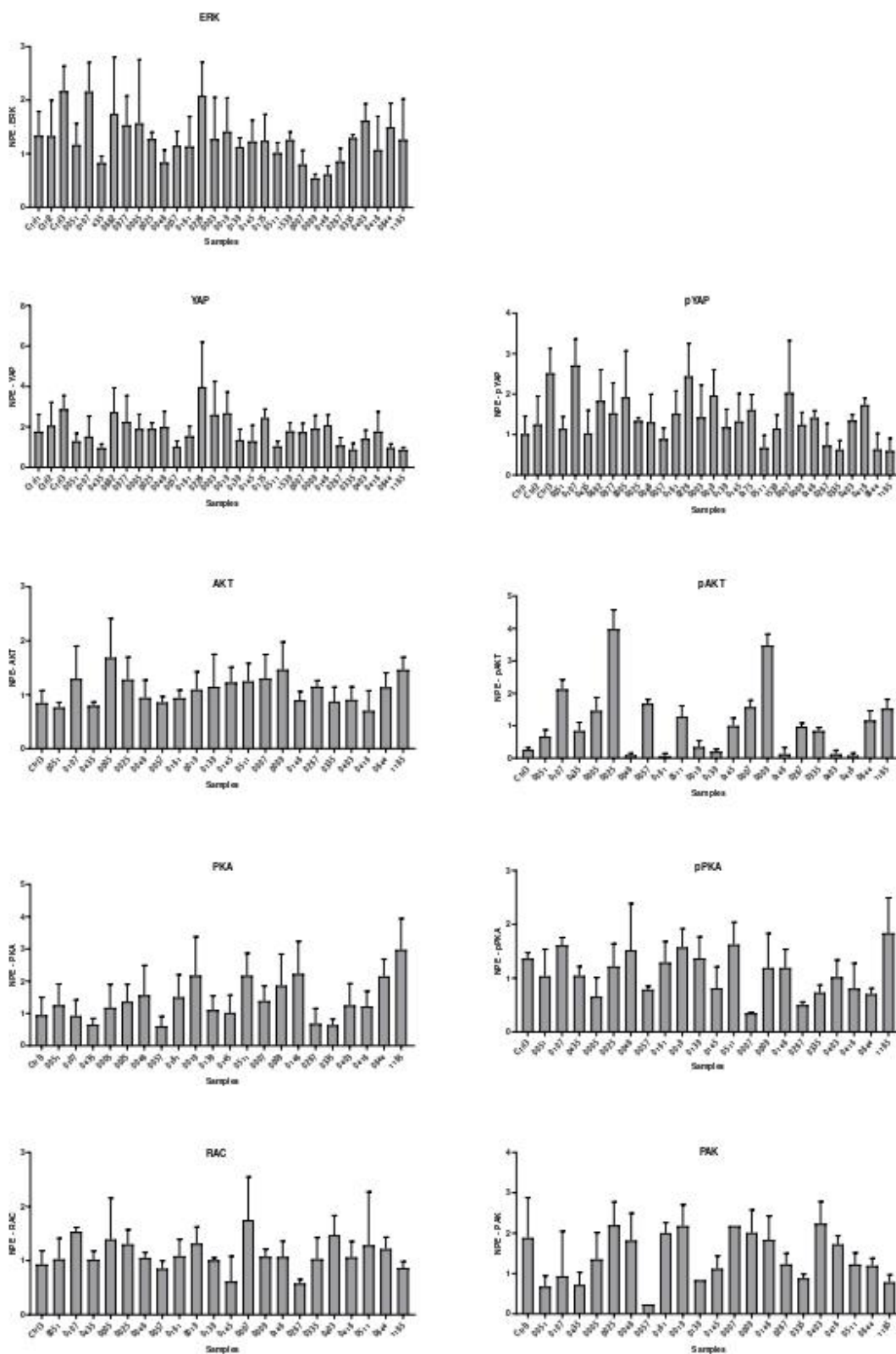placed on this supplemental material which has been supplied by the author(s)

J Med Genet

Finally, patients with an inconclusive blood test without any tumor analyzed were considered presumed tissue mosaics and scored as 1 (Table 3).
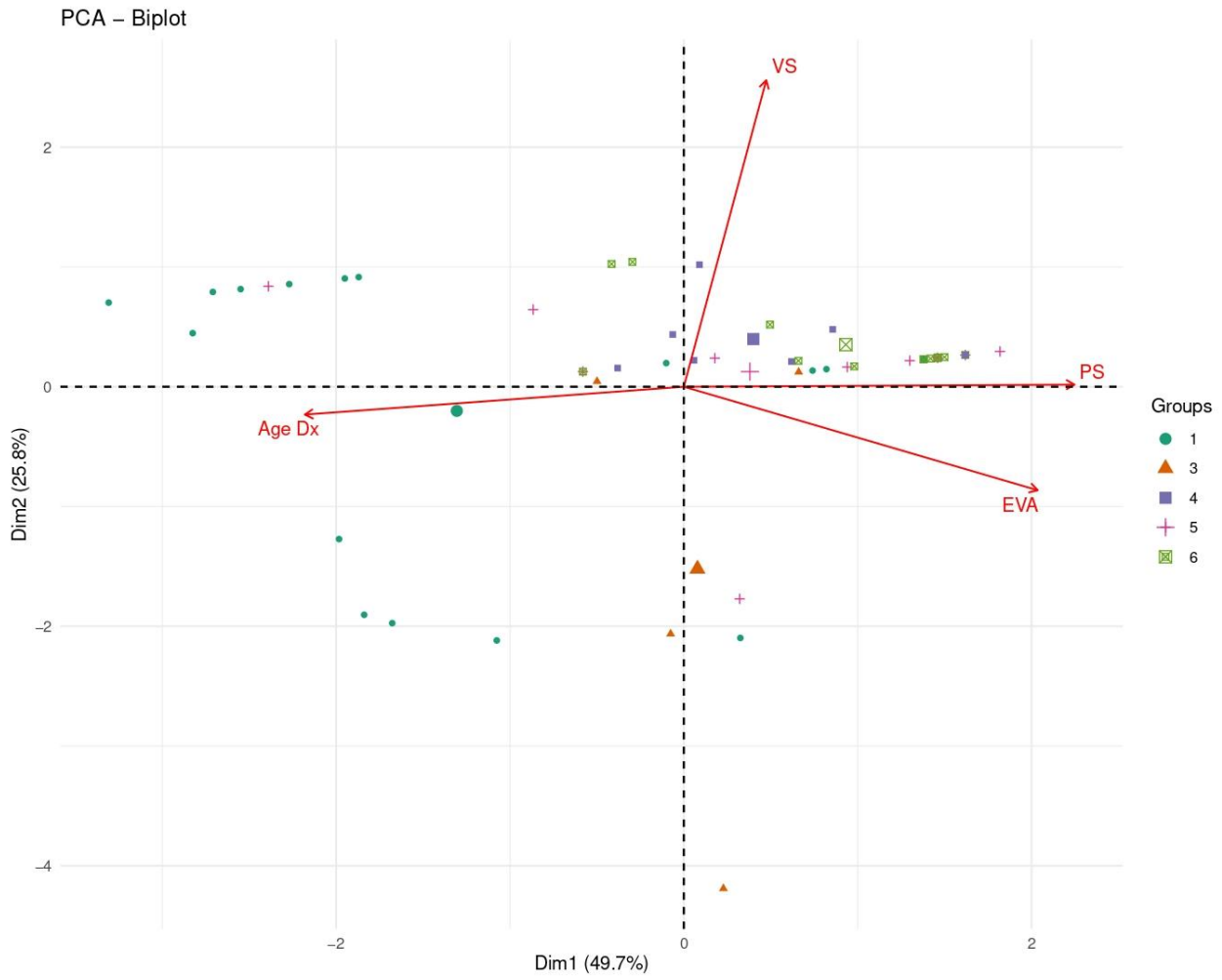
Statistics: All statistical analyses of the validation of the GSS were reproduced from the study of Halliday et al. In brief, an NF2 Genetic Severity Score (GSS) was determined based on the phenotype of patients. Genetic Severity Score consists of a 3-point classification into tissue mosaicism, classic and severe disease. χ2 statistics were used to compare the distribution of GSS by gender and NF2-related deaths (sporadic or familial). Trends with genetic severity were investigated using Mantel-Haenszel linear-by-linear χ2 tests of association for tumor load, ocular features, hearing outcomes and major interventions of the patients. Spearman's rank-order correlations were run to assess the relationship between age of patients, eye features, number of interventions, ratio of interventions to age and genetic severity. In our study, minor variations were applied in comparison to Halliday et al. and quality of life was not considered. Principal component analysis (PCA) of age at diagnosis, extravestibular affection, vestibular and peripheral schwannomas was performed to explore variability of NF2 type mutations of patients.

In our study, minor variations were applied. Mutation data, tumor load, ocular features, hearing outcomes and major interventions of the patients were defined as categorical variables. Quality of life was not considered in our study. Principal component analysis (PCA) of age at diagnosis, extravestibular affection, vestibular and peripheral schwannomas was performed to explore variability of NF2 type mutations of patients.

In order to study differences between protein expression levels in the functional assay, Kruskal-Wallis and Mann-Whitney U statistical tests were performed among genetic severity groups and mutation classes. Fibroblast protein levels from healthy controls have been included in group 1 for the statistics analysis. Analysis of variance (ANOVA) of FGSS and NF2 mutations was performed to test differences of severity between NF2 mutations groups. Shapiro Wilk and Levene tests were applied for testing Normality of residuals and homoscedasticity of groups respectively. Backward stepwise regression analysis was performed to evaluate the contribution of Merlin and pERK levels in the ANOVA model. Statistical analyses were performed using R software.

4

PCA – Biplot

Identifier	Current Age	Age at diagnostic	Score	Vestibular Schwannomas Score (0=NO; 1=Unique, 2=Multiple)	Peripheral schwannomas Score (0=NO; 1=Unique, 2=Multiple)	Intracranial Meningioma	Intracranial Schwannoma	Intraspinal Meningioma	Intraspinal Schwannoma	Ependymoma	Score (0,1,2,3)	Variant at cDNA	Variant at protein level	Inheritance	GSS	FGSS
1	28	19		2	2	No	No	No	No	No	0	Whole NF2 gene deletion. Mosaic present in blood		Sporadic	2A	3
2	46	23		2	0	Multiple	No	No	No	Single	3	Genetic test in blood inconclusive		Sporadic	1A	1
3	29	22		2	2	Multiple	No	No	No	No	2	c.115_363del	p.(Met39_Gln121del)	Sporadic	2B	3
5	53	16		2	0	No	No	No	Multiple	Multiple		c.1446_1477insNG_009057.1 g.74239_74405	p.(Pro482Profs*39)	Sporadic	2A	4
7	42	18		2	2	Multiple	No	No	Multiple	No	3	c.432C>G	p.(Tyr144*)	Sporadic	3	6
8	36	28		1	2	No	No	No	Multiple	No	2	c.592C>T. Present in two tumors	p.(Arg198*)	Sporadic	1B	3
9	29	19		2	2	Multiple	Multiple	No	Multiple	No	3	c.784C>T	p.(Arg262*)	Sporadic	3	6
19	54	37		2	2	1	No	No	Single	No	1	Exons 15-16 deletion; r.1575_1747del	p.(Lys525Asnfs*19)	Sporadic	2B	4
24	54	40		1	1	Multiple	No	Multiple	Single	No	3	Genetic test in blood inconclusive		Sporadic	1A	1
25	55	47		2	2	No	No	No	No	No	0	r.1575_1747del	p.(Lys525Asnfs*19)	Sporadic	2A	4
48	25	14		3	2	Multiple	No	No	Multiple	No	3	c.810+1dupG	p.(Phe271Valfs*)	Sporadic	2A	5
51	64	44		2	0	No	No	No	No	No	0	Genetic test in blood inconclusive		Sporadic	1A	1
57	50	22		3	0	No	Multiple	No	Multiple	No	3	Exons 1-5 deletion and 47 kb upstream (NIPSNAP1)		Familial	2A	4
69	58	30		2	0	No	Multiple	No	Multiple	No	3	Exons 1-5 deletion and 47 kb upstream (NIPSNAP1)		Familial	2A	4
106	70	61		1	1	No	No	No	Multiple	No		Exon 6 deletion in one tumor analyzed. Not detected in blood.		Sporadic	1A	1
107	70	38		2	2	Multiple	Multiple	Multiple	Multiple	No	3	c.592C>T in three tumors analyzed. Not detected in blood.	p.(Arg198*)	Sporadic	1B	3
139	12	9		3	2	No	Multiple	No	Multiple	No	3	c.241-9A>G	p.(Val81Phefs*44)	Sporadic	2B	5
144	79	69		1	2	Single	No	No	No	No	1	Genetic test in blood inconclusive		Sporadic	1A	1
145	43	31		2	2	Multiple	No	No	Multiple	Multiple	3	c.241-13T>A	p.(Val81Glnfs*45)	Sporadic	2B	5
146	28	17		3	2	Multiple	Single	No	Multiple	Multiple	3	c.1282C>T	p.(Gln428*)	Sporadic	3	6
161	34	28		2	2	No	No	No	Multiple	No	2	Exons 14-17 deletion. Mosaic present in blood		Sporadic	2A	3
175	25	19		3	0	Single	Single	No	Multiple	No	3	Exons 5-17 deletion and downstream CABP7 deletion		Sporadic	2B	4
226	55	50		1	2	Multiple	Single	No	Multiple	No	3	c.2875T>C	p.(Phe965Ser)	Sporadic	2A	3
267	20	14		3	2	No	No	No	No	No	0	c.784C>T	p.(Arg262*)	Sporadic	3	6
335	32	20		3	2	Multiple	Multiple	Single	Multiple	Multiple	3	c.380_396dupTAGATGAAAA	p.(Cys133*)	Sporadic	3	6
399	57	51		2	2	No	No	No	No	No	0	Genetic test in blood inconclusive		Sporadic	1A	1
403	31	18		3	2	Multiple	Single	Single	Multiple	No	3	c.784C>T	p.(Arg262*)	Sporadic	3	6
416	18	14		3	2	Multiple	Single	Single	Multiple	Single	3	c.520dupA	p.(Ile174Asnfs*29)	Sporadic	3	6
435	21	17		3	0	1	No	Multiple	No	Multiple	No	3	c.970C>T in two tumors analyzed. Not detected in blood	p.(Gln324*)	Sporadic	1B	3
511	40	18		3	2	Multiple	No	Multiple	Multiple	Single	3	c.784C>T. Mosaic present in blood	p.(Arg262*)	Sporadic	2B	5
644	43	21		3	1	Multiple	Single	Single	Multiple	Single	3	c.784C>T	p.(Arg262*)	Sporadic	3	6
682	56	34		2	2	Multiple	Multiple	No	Multiple	Multiple	3	c.592C>T in one tumor analyzed. Not detected in blood		Sporadic	1A	1
806	38	20		2	2	Multiple	Multiple	Multiple	Multiple	Multiple	3	c.112G>T in one tumor analyzed. Not detected in blood		Sporadic	1A	1
824	40	36		1	0	Single	No	No	No	No	0	Ring 22		Sporadic	2A	1
833	67	55		2	0	No	No	No	No	No	0	Genetic test in blood inconclusive		Sporadic	1A	1
913	41	35		2	0	Multiple	Single	Single	No	No	3	c.169C>T detected at 7% in blood	p.(Arg57*)	Sporadic	2B	5
977	38	32		1	2	Multiple	No	No	Multiple	No	3	Exons 2-8 deletion in two tumors analyzed. Not detected in blood		Sporadic	1B	2
1040	39	18		3	2	No	No	No	Multiple	Single	3	c.586C>T. Mosaic present in blood	p.(Arg196*)	Sporadic	2B	5
1073	27	18		2	2	Multiple	Multiple	Multiple	Single	Single	3	Genetic test in blood inconclusive		Sporadic	1A	1
1185	49	35		3	0	Single	No	No	Single	No	3	c.1096_1102del7	p.(Glu366Glnfs*7)	Familial, index	3	6
1190	55	39		1	2	Multiple	No	Multiple	Multiple	No	3	c.169C>T in one tumor analyzed. Not detected in blood	p.(Arg57*)	Sporadic	1A	1
1221	74	70		1	2	No	No	No	No	No	0	Genetic test in blood inconclusive		Sporadic	1A	1
1222	43	14		3	2	Multiple	No	Multiple	No	Multiple	3	c.448-2A>G		Sporadic	2B	5
1312	35	34		2	2	No	No	No	No	No	0	Genetic test in blood inconclusive		Sporadic	1A	1
1339	40	36		2	2	Multiple	No	Multiple	Multiple	No	3	Genetic test in blood inconclusive. Mosaic suspicion because her son is also NF2		Sporadic	1A	1
1536	15	14		3	2	No	No	No	No	No	0	c.1096_1102del7	p.(Glu366Glnfs*7)	Familial	3	6
1537	17	17		3	2	No	No	No	No	No	0	c.1096_1102del7	p.(Glu366Glnfs*7)	Familial	3	6
1539	40	22		3	2	Multiple	No	No	Multiple	No	3	c.169C>T. Mosaic present in blood	p.(Arg57*)	Sporadic	2B	5
1779	55	48		1	0	Multiple	No	No	No	No	2	Genetic test in blood inconclusive		Sporadic	1A	1
1802	21	18		3	2	Single	Multiple	Multiple	Multiple	No	3	c.1334_1337delAGAG	p.(Glu445Glyfs*9)	Sporadic	3	6
Patient2	34	20		3	2	Multiple	No	No	Multiple	Single	3	c.1396C>T	p.(Arg466*)	Sporadic	3	6
Patient5	52	30		2	2	Multiple	No	No	Multiple	No	3	c.634C>T	p.(Gln212*)	Sporadic	3	6

Supplementary Table 2. Major interventions in relation to Genetic Severity Score						
Genetic Severity		**1 Tissue Mosaic**	**2A Mild**	**2B Moderate**	**3 Severe**	**Statistics**
N (%)	Proportion of patients whithin — VS surgery	7 (36,84%)	9 (100%)	5 (50%)	10 (71,4%)	$X^2(1) = 4.08$, p = 0.043
	Non-VS intracranial surgery	2 (10,5%)	0 (0%)	3 (30%)	5 (35,7%)	$X^2(1) = 3.99$, p = 0.045
	Spinal surgery	6 (31,58%)	1 (11,11%)	4 (40%)	2 (14,3%)	$X^2(1) = 0.72$, p = 0.39
	Shunt surgery	0 (0%)	0 (0%)	0 (0%)	1 (7,1%)	$X^2(1) = 1.73$, p = 0.18
	Radiotherapy	1 (5,26%)	3 (33,33%)	3 (30%)	8 (57,1%)	$X^2(1) = 8.9$, p = 0.002
	Bevacizumab	0 (0%)	1 (11,11%)	4 (40%)	6 (42,9%)	$X^2(1) = 10.2$, p = 0.001
	Total number of major interventions per person, grouped — 0	7 (36,84%)	1 (11,11%)	0 (0%)	2 (14,3%)	$X^2(1) = 4.08$, p = 0.043
	1	5 (26,31%)	2 (22,22%)	3 (30%)	2 (14,3%)	$X^2(1) = 0.05$, p = 0.82
	2	2 (10,52%)	4 (44,44%)	2 (20%)	2 (14,3%)	$X^2(1) = 0$, p = 1
	3	1 (5,26%)	3 (33,33%)	1 (10%)	2 (14,3%)	$X^2(1) = 0.15$, p = 0.69
	4 or more	3 (15,79%)	0 (0%)	4 (40%)	6 (42,9%)	$X^2(1) = 4.10$, p = 0.042
Mean (SD)	Total number of major interventions per person, grouped	1,53 (1,91)	1,90 (0,99)	3,09 (2,34)	3,79 (3,36)	$r_s(50) = 0.35$, p = 0.01
	Number of total surgeries	1,53 (2,07)	1,50 (0,71)	1,91 (1,64)	2,64 (2,98)	$r_s(50) = 0.18$, p = 0.19
	Age at first radiotherapy session	23	37 (9,64)	30,33 (6,66)	24,29 (8,16)	$r_s(12) = -0.42$, p = 0.13
	Age started bevacizumab	-	32	26,67 (14,57)	23,67 (8,48)	$r_s(8) = -0.26$, p = 0.46
	Age at first surgery	35,44 (13,36)	29,78 (12,05)	26,67 (7,57)	20,80 (7,73)	$r_s(35) = -0.47$, p = 0.003
	Age at first major intervention	34,20 (13,20	29,78 (12,05)	25,55 (8,55)	20,55 (7,89)	$r_s(39) = -0.47$, p = 0.001
	Ratio of total number of major interventions to current age	0,03 (0,04)	0,04 (0,02)	0,08 (0,06)	0,13 (0,11)	$r_s(50) = 0.49$, p < 0.001

Supplementary Table 3. Phenotype quantification		
Phenotypic feature		**Value**
Age at diagnosis	< 25 years	3
	< 35 years	2
	> 35 years	1
Vestibular Schwannoma	Unilateral	1
	Bilateral	2
Peripheral Schwannomas	Single	1
	Multiple	2
Extravestibular affection (Spinal/Cerebral)	Spinal and cerebral injury or spinal/cerebral different type of injury	3
	Cerebral or Spinal multiple injuries	2
	Single brain or spinal injury	1

Suppplementary Table 4. Revising mutation associated pathogenicity according to GSS

NF2-causing variant			GSS	Inheritance	Mosaicism		Phenotype Quantification	Merlin NPE levels	pERK NPE levels	Reasoning
cDNA (NM_00268.3)	Exon	Predicted protein			% in blood	Only in tissue				
c.169C>T & c.810+2T>A	exon 2; exon 8	p.(Arg57*) & p.(?)	1A	Sporadic	Not detected	One tumor analyzed	3	3,66129319	4,0767212	Mosaic patient. Very mild phenotype
c.1341-25_1377del62 +LOH	exon 13	p.(?)	1A	Sporadic	Not detected	One tumor analyzed	3			Mosaic patient. Very mild phenotype
Genetic test (NGS) in blood inconclusive			1A	Sporadic			3			Mosaic patient. Very mild phenotype
Genetic test (NGS) in blood inconclusive			1A	Sporadic			3			Mosaic patient. Very mild phenotype
Genetic test (NGS) in blood inconclusive			1A	Sporadic			4			Mosaic patient. Very mild phenotype
Genetic test (NGS) in blood inconclusive			1A	Sporadic			4			Mosaic patient. Very mild phenotype
Genetic test (NGS) in blood inconclusive			1A	Sporadic			4			Mosaic patient. Very mild phenotype
Genetic test in blood inconclusive			1A	Sporadic			5			Mosaic patient. Mild phenotype
exon 6 deletion + LOH	exon 6	p.(Val173Glyfs*2)	1A	Sporadic	Not detected	One tumor analyzed	5			Mosaic patient. Mild phenotype
c.169C>T + LOH	exon2	p.(Arg57*)	1A	Sporadic	Not detected	One tumor analyzed	7			**Mosaic patient. Unexpected mild-moderate phenotype**
Genetic test in blood inconclusive			1A	Sporadic			8			**Mosaic patient. Unexpected moderate phenotype**
Genetic test (NGS) in blood inconclusive			1A	Sporadic		Mosaic suspicion b	8			**Mosaic patient. Unexpected moderate phenotype**
c.592C>T + LOH	exon 6	p.(Arg198*)	1A	Sporadic	2% in fibroblas	One tumor analyzed	9	3,57902164	9,08179524	**Mosaic patient. Unexpected <u>severe</u> phenotype**

c.112G>T + LOH	exon 1	P.(Glu38*)	1A	Sporadic	Not detected	One tumor analyzed	10			Mosaic patient. Unexpected severe phenotype
Genetic test (NGS) in blood inconclusive			1A	Sporadic			10			Mosaic patient. Unexpected severe phenotype
exons 2-3 deletion	exon 2 & 3	p.(?)	1B	Sporadic	Not detected	Two tumors analyze	7	2,28870175	3,0376054	Mosaic patient. Unexpected mild-moderate phenotype
c.970C>T	exon 10	p.(Gln324*)	1B	Sporadic	Not detected	Two tumors analyze	7	3,42502203	0,33804115	Mosaic patient. Unexpected mild-moderate phenotype
c.592C>T	exon 6	p.(Arg198*)	1B	Sporadic	Not detected	Three tumors analyz	8	4,58749871	4,55488321	Mosaic patient. Unexpected moderate phenotype
c.592C>T	exon 6	p.(Arg198*)	1B	Sporadic	Not detected	Two tumors analyze	7			Mosaic patient. Unexpected mild-moderate phenotype
c.1747A>G; r.1575_1747del	exon 15	p.(Lys525Asnfs*19)	2A	Sporadic			3	0,65585897	1,75666641	Splicing variant at exon 15. Mild phenotype
Ring 22			2A	Sporadic			3			
exons 14-17 deletion	exons 14-17	p.(?)	2A	Sporadic	20% (MLPA kit P044)		7	0,82372417	0,34586901	Large deletion excluding promoter in mosaicism. Unexpected mild-moderate phenotype. Merlin and pERK levels below threshold.
c.287T>C	exon 3	p.(Phe96Ser)	2A	Sporadic			7	2,18077529	2,23406472	Missense variant. Unexpected mild-moderate phenotype.
Whole NF2 gene deletion in mosaicism	whole gene		2A	Sporadic	~10% (MLPA kit P044)		7			Large deletion including promoter in mosaicism. Unexpected mild-moderate phenotype.
exons 1-5 deletion and 47 kb upstream (NIPSNAP1)	exon 1-5	Merlin synthesis altered	2A	Familial			7			Large deletion including promoter. Unexpected mild-moderate phenotype.
c.1446_1477insNG_009057.1:g.74239_74405	Deep intronic mutation between exons 13 - 14	p.(Pro482Profs*39)	2A	Sporadic			8	0,41335449	4,7636402	Splicing variant at exon 14. Unexpected moderate phenotype. pERK levels above threshold.

exons 1-5 deletion and 47 kb upstream (NIPSNAP1)	exon 1-5	Merlin synthesis altered	2A	Familial			9	1,68851611	5,7267768	Large deletion including promoter. Unexpected severe phenotype.
c.810+1dupG	exon 8	p.(Phe271Val4fs*)	2A	Sporadic			10	0,7651892	0,66179798	Splicing variant at exon 8. Unexpected severe phenotype. Merlin and pERK levels below threshold.
exons 15-16 deletion; r.1575_1747del	exon 15-16	p.(Lys525Asnfs*19)	2B	Sporadic			5	0,98880623	5,64437297	Large deletion excluding promoter. Unexpected mild phenotype. At functional level this deletion alters exon 15 splicing. pERK levels are above threshold
c.169C>T	exon 2	p.(Arg57*)	2B	Sporadic	Detected at 7% in blood (NGS)		7			Nonsense variant at mosaicism. Mild-moderate phenotype
exons 5-17 deletion and downstream CABP7 deletion	exons 5-17	p.(?)	2B	Sporadic			8	1,55439894	2,65118931	Large deletion excluding promoter. Moderate phenotype. pERK levels are above threshold
c.115_363del	Exon 2&3 skipping	p.(Met39_Gln121del)	2B	Sporadic			9	1,48734671	3,14955982	Splicing variant at exon 2&3. Unexpected severe phenotype. pERK levels above threshold.
c.241-13T>A	exon 3	p.(Val81Glnfs*45)	2B	Sporadic			9	2,06863943	1,09999436	Splicing variant at exon 3. Unexpected severe phenotype. pERK levels below threshold.
c.241-9A>G	exon 3	p.(Val81Phefs*44)	2B	Sporadic			10	1,57827175	2,46664781	Splicing variant at exon 3. Unexpected severe phenotype. pERK levels below threshold.
c.784C>T	exon 8	p.(Arg262*)	2B	Sporadic	Detected at ~ 10% in fibroblasts, n		10	2,56486969	0,81433044	Nonsense variant at mosaicism. Unexpected severe phenotype. pERK levels below threshold

c.169C>T	exon 2	p.(Arg67*)	2B	Sporadic	5,6% in blood (NGS)	10	2,71920859	1,74534982	Nonsense variant at mosaicism. Unexpected severe phenotype. pERK levels below threshold
c.586C>T	exon 6	p.(Arg196*)	2B	Sporadic	Detected at >20% in blood (externa	10			Nonsense variant at mosaicism. Unexpected severe phenotype
c.448-2A>G	exon 5	p.(?), splicing	2B	Sporadic		10			Splicing variant at exon 3. Unexpected severe phenotype
c.1096_1102del7	exon11	p.(Glu366Glnfs*7)	3	Familial, index		7	1,28967814	1,45881049	Nonsense variant. Unexpected mild-moderate phenotype. Protein levels below threshold
c.784C>T	exon 8	p.(Arg262*)	3	Sporadic		8	1,64843072	1,12977722	Nonsense variant. Unexpected moderate phenotype. Protein levels below threshold
c.784C>T	exon 8	p.(Arg262*)	3	Sporadic		9	1,72710678	0,74796226	Nonsense variant. Severe phenotype. Protein levels below threshold
c.634C>T	exon 7	p.(Gln212*)	3	Sporadic		9			Nonsense variant. Severe phenotype
c.380_396dupTAGAT GAAAA	exon 4	p.(Cys133*)	3	Sporadic		10	0,6773879	0,81003198	Nonsense variant. Severe phenotype. Protein levels below threshold

c.1282C>T	exon 12	p.(Gln428*)	3	Sporadic			10	0,80455913	0,66749818	Nonsense variant. Severe phenotype. Protein levels below threshold
c.432C>G	exon 4	p.(Tyr144*)	3	Sporadic			10	1,04771615	1,90213891	Nonsense variant. Severe phenotype. Protein levels below threshold
c.784C>T	exon 8	p./Arg262*)	3	Sporadic			10	1,0694117	1,74014287	Nonsense variant. Severe phenotype. Protein levels below threshold
c.784C>T	exon 8	p.(Arg262*)	3	Sporadic			10	1,17909458	0,32191149	Nonsense variant. Severe phenotype. Protein levels below threshold
c.520dupA	exon 6	p.(Ile174Asnfs*29)	3	Sporadic			10	1,23139075	0,29106762	Nonsense variant. Severe phenotype. Protein levels below threshold
c.1334_1337delAGAG	Small Deletion	p.(Glu445Glyfs*9)	3	Sporadic			10			Nonsense variant. Severe phenotype
c.1396C>T	exon 13	p.(Arg466*)	3	Sporadic			10			Nonsense variant. Severe phenotype

Supplementary Table 5. Demographic data according to Functional Genetic Severity Score									
Functional Genetic Severity Score			1	2	3	4	5	6	Correlation
N (% total)	Number of patients		16 (30,7%)	0	4 (7,7%)	10 (19,23%)	8 (15,38%)	14 (26,9%)	
N (% gender)	Gender	Male	12 (36,4%)		3 (9,1%)	6 (18,18%)	3 (9%)	9 (27,3%)	
		Female	4 (21,1%)		2 (10,5%)	4 (21,1%)	4 (21,1%)	5 (26,3%)	$X^2(4) = 1.81, p = 0.77$
Mean (SD)	Age at diagnosis		40,94 (16,11)		36,6 (12,99)	23 (7,37)	24 (12,90)	18,79 (6,5)	$r_s(50) = -0.64, p < 0.001$
	Current age		52,25 (15,56)		46,8 (18,43)	41,56 (12,76)	36,88 (12,91)	30,79 (12,07)	$r_s(50) = -0.54, p < 0.001$
	Years since diagnosis		11,25 (6,86)		10,2 (12,21)	18,56 (12,09)	12,88 (6,69)	12 (8,26)	$r_s(50) = 0.04, p = 0.75$
	Age at NF2-related death					53	40	42	
N (% score category)	NF2-related deaths					1 (10%)	1 (12,5%)	1 (7,2%)	
	Familial NF2		0 (0%)		1 (20%)	3 (30%)	0 (0%)	3 (21,4%)	
	Sporadic NF2		16 (100%)		4 (80%)	7 (70%)	7 (87,5%)	11 (78,6%)	$X2(4) = 7.73, p = 0.10$

Supplementary Table 6. Tumor burden, presence of ocular features and hearing outcome according to Functional Genetic Severity Score									
Functional Genetic Severity Score			**1**	**2**	**3**	**4**	**5**	**6**	**Statistics**
N (% total)	Number of patients		16	0	4	10	8	14	
Tumor load	N (%)	Bilateral VS	11 (68,7%)	0 (0%)	3 (75%)	10 (100%)	8 (100%)	14 (100%)	$X^2(1) = 8.9$, p = 0.002
		Unilateral VS	5 (31,2%)	0 (0%)	1 (25%)	0 (0%)	0 (0%)	0 (0%)	$X^2(1) = 8.9$, p = 0.002
		Intracranial meningioma	9 (56,2%)	0 (0%)	3 (75%)	3 (30%)	5 (62,5%)	10 (71,4%)	$X^2(1) = 0.35$, p = 0.55
		Intracranial Schwannoma	3 (18,7%)	0 (0%)	3 (75%)	3 (30%)	3 (37,5%)	7 (50%)	$X^2(1) = 1.8$, p = 0.17
		Spinal meningioma	5 (31,2%)	0 (0%)	1 (25%)	1 (10%)	3 (37,5%)	5 (45,5%)	$X^2(1) = 0.10$, p = 0.74
		Spinal Schwannoma	8 (50%)	0 (0%)	4 (100%)	6 (60%)	6 (75%)	11 (100%)	$X^2(1) = 1.7$, p = 0.17
		Spinal ependymoma	4 (25%)	0 (0%)	0 (0%)	2 (20%)	3 (37,5%)	5 (45,5%)	$X^2(1) = 0.8$, p = 0.35
Ocular Features	N (%)	Epiretinal membranes	0 (0%)	0 (0%)	0 (0%)	0 (0%)	0 (0%)	0 (0%)	NA
		Cataract	3 (37,5%)	0 (0%)	1 (50%)	3 (30%)	1 (12,5%)	3 (42,9%)	$X^2(1) = 0$, p = 1
		Combined hamartoma	0 (0%)	0 (0%)	0 (0%)	0 (0%)	0 (0%)	2 (28,6%)	$X^2(1) = 3.1$, p = 0.07
		Optic nerve meningioma	0 (0%)	0 (0%)	0 (0%)	0 (0%)	1 (12,5%)	0 (0%)	$X^2(1) = 0.3$, p = 0.53
	Mean (SD)	Total eye features		0 (0%)					$r_s(49) = 0.06$, p = 0.67
Hearing Outcomes	N (%)	Hearing grade	1 12 (75%)	0 (0%)	4 (100%)	3 (30%)	3 (37,5%)	6 (42,9%)	$X^2(1) = 5.4$, p = 0.019
			2 1 (6,2%)	0 (0%)	0 (0%)	0 (0%)	0 (0%)	0 (0%)	$X^2(1) = 1.5$, p = 0.20
		3 o 4	0 (0%)	0 (0%)	0 (0%)	0 (0%)	2 (25%)	1 (7,1%)	$X^2(1) = 2.1$, p = 0.14
			5 2 (12,5%)	0 (0%)	0 (0%)	3 (30%)	1 (12,5%)	4 (28,6%)	$X^2(1) = 1.6$, p = 0.20
			6 2 (12,5%)	0 (0%)	0 (0%)	4 (40%)	2 (25%)	3 (21,4%)	$X^2(1) = 0.6$, p = 0.42
	Mean (SD)	Age of loss of useful hearing	48,31 (17,16)	0 (0%)	46,8 (18,43)	32,38 (8,43)	29,38 (11,89)	26,23 (12,58)	$r_s(48) = -0.58$, p < 0.001
Cutaneus manifestations	N (%)		4 (25%)	0 (0%)	0 (0%)	0 (0%)	4 (50%)	9 (75%)	$X^2(1) = 6.2$, p = 0.012

* For group 1 and 6, only 4 out 16 and 11 out of 14 patients, respectively, have been tested by a spinal magnetic resonance

Supplementary Table 7. Major interventions in relation to Functional Genetic Severity Score								
Functional Genetic Severity Score			**1**	**2**	**3**	**4**	**5**	**6**	**Statistics**
N (%)	Proportion of patients	VS surgery	6 (37,5%)		3 (60%)	9 (90%)	3 (37,5%)	10 (71,4%)	$X^2(1) = 2.16$, p = 0.14
		Non-VS intracranial surgery	1 (6,3%)		1 (20%)	0 (0%)	3 (37,5%)	5 (35,7%)	$X^2(1) = 4.5$, p = 0.032
		Spinal surgery	3 (18,8%)		4 (80%)	1 (10%)	3 (37,5%)	2 (14,3%)	$X^2(1) = 0.4$, p = 0.51
		Shunt surgery	0 (0%)		0 (0%)	0 (0%)	0 (0%)	1 (7,1%)	$X^2(1) = 1.5$, p = 0.21
		Radiotherapy	1 (6,3%)		0 (0%)	3 (30%)	3 (37,5%)	8 (57,1%)	$X^2(1) = 10.1$, p = 0.001
		Bevacizumab	0 (0%)		0 (0%)	2 (20%)	3 (37,5%)	6 (42,9%)	$X^2(1) = 9.6$, p = 0.002
	Total number of major interventions per person, grouped	0	8 (50%)		0 (0%)	0 (0%)	0 (0%)	2 (14,3%)	$X^2(1) = 7.1$, p = 0.007
		1	3 (18,8%)		3 (60%)	2 (20%)	2 (25%)	2 (14,3%)	$X^2(1) = 0.4$, p = 0.51
		2	2 (12,5%)		1 (20%)	4 (40%)	1 (12,5%)	2 (14,3%)	$X^2(1) = 0.03$, p = 0.86
		3	1 (6,3%)		0 (0%)	4 (40%)	0 (0%)	2 (14,3%)	$X^2(1) = 0.22$, p = 0.63
		4 or more	2 (12,5%)		1 (20%)	0 (0%)	4 (50%)	6 (42,9%)	$X^2(1) = 4.5$, p = 0.033
Mean (SD)	Total number of major interventions per person, grouped		1,25 (1,77)		2 (1,73)	2,22 (0,83)	3,63 (2,50)	3,79 (3,36)	$r_s(50) = 0.39$, p = 0.003
	Number of total surgeries		1,19 (1,80)		2,2 (2,17)	1,67 (0,50)	2,13 (1,89)	2,64 (2,98)	$r_s(50) = 0.22$, p = 0.11
	Age at first radiotherapy session		23		0	37 (9,64)	30,33 (6,66)	24,29 (8,16)	$r_s(12) = -0.42$, p = 0.13
	Age started bevacizumab		0		0	32	26,67 (14,57)	23,67 (8,48)	$r_s(8) = -0.26$, p = 0.46
	Age at first surgery		36,71 (13,90)		34,8 (10,62)	25,67 (7,55)	27,50 (11,93)	20,80 (7,73)	$r_s(35) = -0.51$, p = 0.001
	Age at first major intervention		35,00 (13,75)		34,8 (10,62)	25,67 (7,55)	25,75 (11,93)	20,55 (7,89)	$r_s(39) = -0.51$, p < 0.001
	Ratio of total number of major interventions to current age		0,03 (0,04)		0,04 (0,02)	0,05 (0,02)	0,10 (0,06)	0,13 (0,11)	$r_s(50) = 0.54$, p < 0.001

Supplementary Table 8. Intragroup Variability of Merlin, pERK, age at diagnosis and age at hearing loss.											
Score	GSS					FGSS					
Group/Class	1	2A	2B	3	Mean	1	3	4	5	6	Mean
Merlin Protien Levels (σ)	3,11	0,54	0,29	0,12	1,02	1,76	2,01	0,27	0,55	0,12	0,94
pERK Protien Levels(σ)	6,88	3,99	5,43	0,54	4,21	3,54	3,27	2,01	0,44	0,34	1,92
Age at diagnosis (σ)	216,97	169,78	99,46	33,27	129,87	202,77	149,08	54,29	182,25	35,62	124,80
Age at hearing loss (σ)	324,72	144	110,88	148,1	181,925	262,11	365,19	71,47	148,35	117,93	193,01

Suppplementary Table 9A. FGSS and NF2 disease-causing variant regression model

	Model 1 (N=52)				Model 2 (N=27)			
	beta	se	t	p	beta	se	t	p
Intercept	5062	0.519	9739	7.46e-13	5141	18612	2762	0.012
Type 3	2187	1162	1882	0.066				
Type 4	3080	0.942	3269	0.002	2419	14691	1647	0.116
Type 5	2837	0.838	3385	0.001	2035	13829	1472	0.157
Type 6	3804	0.747	5091	6.18e-06	3352	13817	2426	0.025
pERK					-0.135	0.241	-0.562	0.580
NF2					0.786	0.499	1574	0.132
			R^2=0.381	0.0001			R^2=0.143	0.161

The outcome in both models is FGSS. The patients in Model 2 only have mutations of type 3, 4, 5 and 6. Then, the base category of this model is Type 3.

Suppplementary Table 9B. GSS and NF2 disease-causing variant regression model

	Model GSS (N=52)			
	beta	se	t	p
Intercept	5428	0.565	9603	2.3e-12
1B	1904	1345	1415	0.163
2A	1349	0.903	1493	0.142
2B	3207	0.852	3764	0.0004
3	3238	0.832	3891	0.0003
			R^2=0.322	0.001

The outcome in the model is GSS.

Appendix D

Article

Neurofibromatosis Type 1 families with first-degree relatives harbouring distinct *NF1* pathogenic variants. Genetic counselling and familial diagnosis: what should be offered?

B.Garcia[*], N.Catasús[*], A.Ros, I.Rosas, A.Negro, M.Guerrero-Murillo, A.M. Valero, A.Duat-Rodriguez, J.L.Becerra, S.Bonache, C.Lázaro-Garcia, C.Comas, I.Bielsa, E.Serra, C.Hernández-Chico, Y.Martin, E.Castellanos, I.Blanco (2022). Journal of Medical Genetics, jmedgenet-2021-108301. https://doi.org/10.1136/jmedgenet-2021-108301

This article is presented as other research performed in the course of the doctoral thesis period. *Contributed equally.

Original research

Neurofibromatosis type 1 families with first-degree relatives harbouring distinct *NF1* pathogenic variants. Genetic counselling and familial diagnosis: what should be offered?

Belen Garcia,[1,2] Nuria Catasus,[2] Andrea Ros,[1,2] Inma Rosas ,[2,3]
Alejandro Negro ,[2,3] Mercedes Guerrero-Murillo,[2,3] Ana Maria Valero,[4]
Anna Duat-Rodriguez,[5] Juan Luis Becerra,[6] Sandra Bonache,[2,3]
Conxi Lázaro Garcia ,[7,8] Carmina Comas,[9] Isabel Bielsa,[10] Eduard Serra,[8,11]
Concepción Hernández-Chico,[12,13] Yolanda Martin,[12,13] Elisabeth Castellanos ,[2,3]
Ignacio Blanco[1,2]

ABSTRACT

Neurofibromatosis type 1 (NF1) is an autosomal dominant disorder caused by pathogenic variants in *NF1*. Recently, *NF1* testing has been included as a clinical criterion for NF1 diagnosis. Additionally, preconception genetic counselling in patients with NF1 focuses on a 50% risk of transmitting the familial variant as the risk of having a sporadic NF1 is considered the same as the general population.

Methods 829 individuals, 583 NF1 sporadic cases and 246 patients with NF1 with documented family history, underwent genetic testing for NF1. Genotyping and segregation analysis of *NF1* familial variants was determined by microsatellite analysis and *NF1* sequencing.

Results The mutational analysis of NF1 in 154 families with two or more affected cases studied showed the co-occurrence of two different *NF1* germline pathogenic variants in four families. The estimated mutation rate in those families was 3.89×10^{-3}, 20 times higher than the *NF1* mutation rate ($\sim 2 \times 10^{-4}$) (p=0.0008). Furthermore, the co-occurrence of two different *NF1* germline pathogenic variants in these families was 1:39, 60 times the frequency of sporadic NF1 (1:2500) (p=0.003). In all cases, the de novo NF1 pathogenic variant was present in a descendant of an affected male. In two cases, variants were detected in the inherited paternal wild-type allele.

Conclusions Our results, together with previous cases reported, suggest that the offspring of male patients with NF1 could have an increased risk of experiencing de novo NF1 pathogenic variants. This observation, if confirmed in additional cohorts, could have relevant implications for NF1 genetic counselling, family planning and *NF1* genetic testing.

INTRODUCTION

Neurofibromatosis type 1 (NF1; MIM #162200) is a neurocutaneous genetic disorder that affects 1:2500-1:3000 live births.[1] The hallmarks of the disease are café-au-lait macules (CALMs), skin-fold freckling, cutaneous neurofibromas (NFs) and Lisch nodules. NF1 presents with complete penetrance in adults,[2 3] although there is notable variability in the clinical expression.[4–6] Other tumours of the central and peripheral nervous system are also common among patients with NF1, like optic pathway gliomas and plexiform neurofibromas, the latter may occasionally transform to malignant peripheral nerve sheath tumours. In addition, patients with NF1 can also show skeletal abnormalities such as scoliosis, tibial pseudarthrosis and sphenoid wing dysplasia. Learning difficulties, social and behavioural problems are also present in some individuals as well as attention deficit/hyperactivity disorder traits.[7] Therefore, NF1 syndrome is a classical example of a chronic and complex genetically determined condition requiring a lifelong multidisciplinary healthcare approach.

NF1 is caused by loss-of-function variants in the *NF1* tumour suppressor gene (MIM #613113), located on chromosome 17q11.2, which encodes for neurofibromin, a negative regulator of the Ras GTPase.[8] Diagnostic criteria for NF1 have been recently revised.[9] Currently, sporadic patients with NF1 are diagnosed when presenting two or more of the most characteristic clinical NF1 features or with only one for children, usually CALMs, and a *NF1* pathogenic variant. For familial cases, the presence of one clinical NF1 feature and an affected parent would be sufficient to clinically diagnose the patient, although the *NF1* test is recommended to confirm the clinical diagnosis.

NF1 is one of the genes with the highest mutation rate reported in humans. The germline mutation rate for *NF1* was first estimated as 1×10^{-4} per gamete per generation,[10] but later it was defined as $3–6 \times 10^{-5}$, 10-fold to 100-fold higher than the average mutation rate for hereditary conditions.[11–13] Hence, approximately 50% of patients with NF1 show no family history, with the disorder arising from de novo loss-of-function variants in the *NF1* gene.[14]

Paternal age effect has been well described as a risk factor for NF1, similarly as it is for other genetic disorders, so that the risk of de novo occurrence of NF1 in offspring increases with increasing paternal age, although statistical demographic demonstration remains to be seen on large cohorts.[15 16] In addition, a paternal age effect of mutated gametes has been observed for specific genes, some of them components of the RAS-MAPK pathway, which are positively selected in spermatogonia lineages.[17–19] This effect might positively select and clonally expand NF1-affected spermatogonia lineages. Furthermore, the type of pathogenic variant correlates with its parental origin: whole gene deletion occurs preferentially in oogenesis, while other types of small mutations appear to account for most of the paternally derived inherited mutations.[18 20–22]

As NF1 is inherited following an autosomal dominant pattern, the risk of an affected offspring for an NF1 individual is 50% in every pregnancy. To avoid transmission of the disorder, there are several reproductive options that are discussed with a couple throughout the process of genetic counselling, such as prenatal diagnostic testing or preimplantation genetic testing for monogenic disorders (PGT-M), among others. In both cases, it is necessary that the NF1-causing variant had been determined in the affected parent.[23] In familial cases, it is usually assumed that members of a family harbour an identical molecular aetiology. However, some studies have reported affected members of the same NF1 family harbouring different NF1 germline variants.[5 24–27] These data might suggest that offspring of NF1 individuals could be at an increased risk of having a de novo mutation in the NF1 gene, higher than that estimated in the general population, which would pose a new challenge for genetic counselling of NF1 families, specifically for prenatal and PGT-M testing. In addition, the current diagnosis of NF1 is established in any child with a parent with NF1 when the child presents with one or more of the NF1 criteria. Since the NF1 genetic test has been included in the revised clinical criteria[9] as a new criterion, affected children could be misdiagnosed as healthy if they did not share the same NF1 disease-causing variant as their affected progenitor.

This study presents four families from two independent cohorts, in which two different NF1 germline pathogenic variants were identified in the affected members, from a total of 154 families. In all cases, the family member harbouring the new NF1 pathogenic variant was a descendant of an affected male individual, and in two of them we were able to demonstrate that the new NF1 variant occurred in the father's wild-type NF1 allele. If confirmed in other larger cohorts, these results would support the possibility that descendants of NF1 males could have a higher risk than previously expected of inheriting a de novo NF1 variant, which would affect preconception genetic counselling. In addition, this should also be considered when genetic testing is performed to confirm NF1 in familial cases, as the absence of the familial NF1 variant could erroneously rule out its de novo presence.

MATERIALS AND METHODS
Patients and samples
Patients and their relatives were attended in two Spanish public hospitals, the National Reference Center (CSUR) of Phakomatoses (Hospital Universitari Germans Trias i Pujol-ICO-Germans Trias i Pujol Research Institute, Badalona) and the Hospital Universitario Ramón y Cajal, Madrid.

NF1 genetic testing
DNA and RNA was obtained from blood lymphocytes using standard protocols. Each centre applied a distinct protocol for mutation detection, both previously described.[28 29] Variants were classified following American College of Medical Genetics guidelines with minor modifications.[30] NF1 reference sequences: NM_000267.3; NG_009018.1; LRG_214.

Microsatellite analysis
Several microsatellite markers located at chromosome 17 were studied to determine the parental origin of mutated NF1 allele. Families 1 and 2 were studied using MMPA,[31] while families 3 and 4 as described in the study by Valero et al.[29]

De novo NF1 frequency estimation in NF1 families
The estimated frequency of de novo NF1 cases within NF1 families was calculated considering the observed frequency of families with two affected members harbouring different NF1 pathogenic variants among all families attended. Statistical significance was established by comparison with NF1 de novo expected frequency (1:2500).

Estimated de novo NF1 mutation rate in NF1 families
To estimate the frequency of de novo mutations in NF1 that occur per gamete per generation, we counted the number of de novo mutant alleles transmitted from patients with NF1 to their offspring in relation to all NF1 offspring (de novo mutant/total offspring from NF1 familial cases×2).[12 32] Statistical significance was established by comparison with NF1 mutation rate (1×10^{-4} and $3–6\times10^{-5}$) by Fisher's exact test.

Determination of allele-carrying de novo NF1 variant
We identified SNPs located close to the de novo mutations in the coding sequence of the NF1 gene. A fragment of the cDNA coding sequence containing both the de novo variant and the identified polymorphisms, were cloned using the Gateway Gene Cloning system (Invitrogen) and analysed by Sanger sequencing to determine the paternal origin of the allele in which the de novo mutation originated. Primers used were (5' to 3'): (family 1: GGGGACAAGTTTGTACAAAAAAGCAGGCTGCTCAGT AAAGTAAACATATAGCTGTG and GGGGACCACTTTGTAC AAGAAAGCTGGGTCATATGTGAATGCTTATTATACAGTC; family 2: GGGGACAAGTTTGTACAAAAAAGCAGGC TGTGCCGTCGAAGGAAAAAGC and GGGGACCACTTT GTACAAGAAAGCTGGGTAAGCAAGAGCTTTGGATCTGC).

Statistical analysis
The different groups were compared using the χ^2 or Fisher's exact test for binary data. The level of statistical significance was $p<0.05$. All statistical analyses were performed using R software (V.3.6.1).

RESULTS
Genetic characterisation of the Spanish cohort
A total of 829 individuals who had confirmed or suspected NF1 were diagnosed and given genetic counselling. Of these, 583 (66%) were sporadic NF1 cases, while 246 (34%) were index cases of NF1 families. We were able to genetically test two or more affected individuals in 154 out of the 246 NF1 families, including 154 index cases and 375 affected relatives (n=529) (table 1). There were no significant differences in age and sex between the different groups of patients: the sex ratio among both cohorts was very similar: 47% of men and 53% of women

Table 1 NF1 patient cohort

	A series (HRYC)	B series (CSUR HGTP-ICO)	Total	% women/men
NF1 individuals	590	239	829	53/47
Sporadic NF1	426	157	583	53/47
NF1 families (index cases)	166	80	246	54/46
NF1 families (index cases) with >1 affected individual tested	126	28	154	54/46

*Men proportion χ^2, p=0.07, 95% CI 0.437 to 0.503.
CSUR, National Reference Center; HGTP, Hospital Universitari Germans Trias i Pujol; HRYC, Hospital Universitario Ramón y Cajal; NF1, neurofibromatosis type 1.

in sporadic cases and 46% of men and 54% of women in familial index cases (table 1, χ^2, p>0.05). Unexpectedly, familial cases were under-represented in both cohorts. However, the frequencies of the different types of *NF1*-causing variants identified agreed with the previously reported (expected) distribution,[33] with nearly 90% of the cases due to point mutations, 4% single or multiple exon deletions and 6% whole *NF1* gene deletions (online supplemental table 1).

Families harbouring two *NF1* pathogenic variants

Among the 154 families with two or more affected individuals genetically analysed, 4 families harbouring two different *NF1* disease-causing variants were detected (figure 1).

Family 1

A man aged 35 years (figure 1A, II.3) was diagnosed with NF1 during childhood due to the presence of café-au-lait macules (CALMs) and a family history of NF1. The genetic test identified the pathogenic variant c.6792C>A (r.[6757_6858del,6792c>a], p.[Ala2253_Lys2286del,Tyr2264*]) in the *NF1* gene. The patient consulted when his partner was pregnant and they declined prenatal genetic testing after genetic counselling was provided. On the birth of a daughter (figure 1A, III.2), the familial c.6792C>A variant was studied and NF1 was discarded due to the negative genetic test results. Some months later, in routine paediatric follow-ups, more than six CALMs were identified, alerting the paediatrician to the possibility of NF1. After genetic counselling, a comprehensive *NF1* gene test was performed for the daughter (III.2) identifying a different *NF1* pathogenic variant (c.2990G>A; r.2851_2990del; p.Leu952Cysfs*22). In
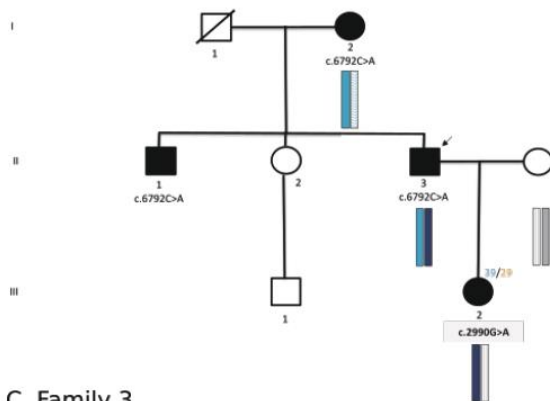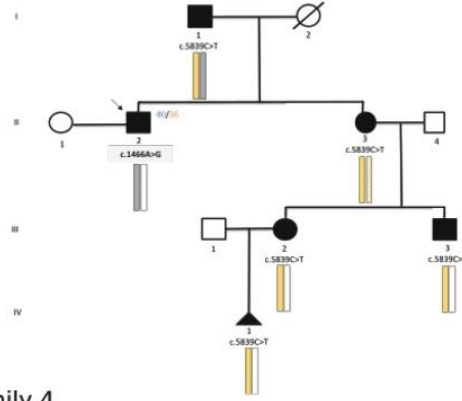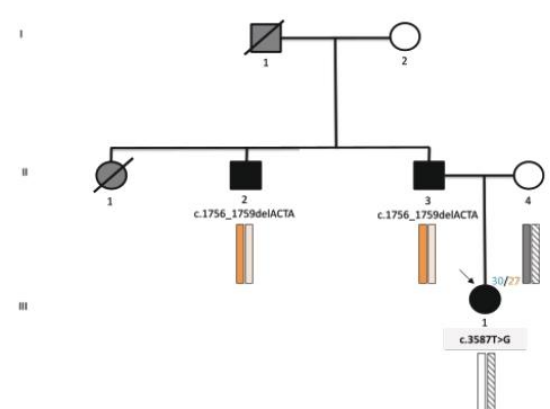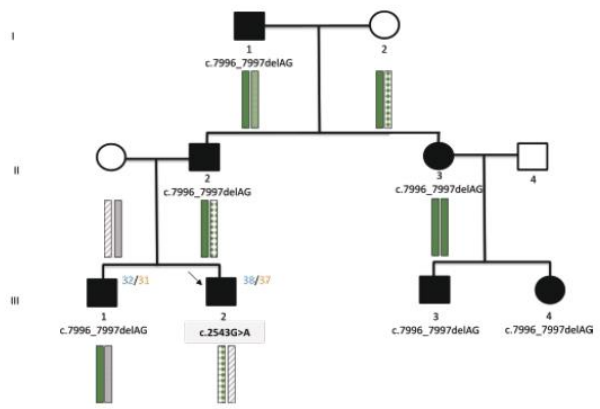

Figure 1 Pedigree of families 1–4. Families 1 and 2 were diagnosed at the Spanish National Reference Center (CSUR) of Phakomatoses while families 3 and 4 at Hospital Ramón y Cajal. Family members clinically diagnosed with neurofibromatosis type 1 (NF1) are depicted with blackened symbols. Grey denotes possibly affected subjects referred by their relatives, and white denotes healthy individuals. Polymorphism analyses determine that in families 1, 2 and 4, de novo mutation has originated in the paternal allele. Paternal and maternal ages at conception are indicated above the patient in blue and orange, respectively. De novo variant is shown in bold and highlighted in grey. Arrow indicates the index case in each family.

addition, we determined that III.2 inherited the wild-type NF1 allele from her father.

Family 2

A man aged 43 years (figure 1B, II.2) was clinically diagnosed with NF1. His father (I.1), sister (II.3) and niece and nephew (III.2 and III.3) were also affected. The genetic test identified the pathogenic genetic variant c.1466A>G (p.Tyr489*) in the NF1 gene in the index case (II.2). His niece (III.2) got pregnant and she asked for prenatal diagnosis. After genetic counselling, the genetic study showed that she did not carry the variant detected in the index case (c.1466A>G), but a different pathogenic variant was identified through a comprehensive NF1 study (c.5839C>T; p.(Arg1947*)). After prenatal testing, the pregnancy was interrupted as the same pathogenic variant was identified in the fetus. The other affected members of the family (I.1, II.3 and III.3) also carried the variant c.5839C>T, indicating it as the familial variant. The study of microsatellites showed that the index case (II.2) inherited the wild-type NF1 paternal allele, contrary to the rest of affected individuals of the family.

Family 3

A woman aged 20 years (figure 1C, III.1) with family history of NF1, diagnosed with NF1 during childhood and presenting a Noonan-like phenotype was referred for genetic testing along with her parents. The genetic test identified a de novo pathogenic genetic variant in the NF1 gene, c.3587T>G (p.Leu1196Arg). Her father (II.3), clinically diagnosed of NF1 did not harbour the same variant. Thus, a comprehensive NF1 gene test was performed on the family. Her father (II.3) and paternal uncle (II.2) were carrying a different pathogenic genetic variant c.1756_1759del (p.Thr586Valfs*18) in the NF1 gene, showing that in this case, the patient (III.1) was carrying a de novo pathogenic NF1 mutation. The study of microsatellites in this family did not allow us to determine which paternal allele III.1 had inherited.

Family 4

A boy aged 6 years (figure 1D, III.2) was clinically diagnosed with NF1 with a Noonan-like phenotype. His father (II.2), brother (III.1), aunt (II.3) and cousins (III.3 and III.4) were also affected. A comprehensive NF1 genetic test was performed on patient II.3 identifying the pathogenic variant c.7996_7997delAG (p.Ser2666Cysfs*5). When the test was extended to other members of the family, the genetic test showed that the individual III.2 diagnosed with NF1 did not carry the familial variant, but a de novo mutation was identified through a comprehensive NF1 study (c.2543G>A; p.Gly848Glu). In addition, we determined III.2 inherited the wild-type NF1 allele from his father.

In all four cases, paternity was confirmed by microsatellite analysis and the de novo NF1 variants detected in their offspring in a proportion of 50%. In addition, these de novo variants not detected in blood in affected fathers, although germline mosaicism could not be confirmed.

Parental origin of new NF1 mutated alleles

It is known that parental age and gender influence both mutation type and de novo occurrence of NF1 pathogenic variants. Thus, we studied the parental origin of the de novo mutations in these four families. In all of them, the de novo NF1 cases occurred in the offspring of an affected male (figure 1). Microsatellite analysis confirmed paternity and in three families, de novo NF1 individuals inherited the wild-type allele from the affected father (family 1, 2 and 4), although the analysis was not informative in family 3. Furthermore, in families 1 and 2, we were able to analyse the NF1 coding region of parents and affected children to determine the differential polymorphisms surrounding familial and de novo NF1 pathogenic variants. We then cloned and sequenced the NF1 coding region harbouring both the NF1 variants and the closest polymorphisms, allowing us to determine the allele carrying the de novo NF1 variant. In both cases, we demonstrated that the de novo NF1 pathogenic variants were present in the wild-type NF1 allele inherited from the affected father, thus discarding a de novo sporadic mutation in the maternal allele (figure 2).

Incidence of the de novo NF1 mutations in familial cases

In 154 out of 246 families in our cohort, we were able to analyse whether the pathogenic NF1 variant co-segregated in more than one affected individual in the same family. Additionally, the 154 families analysed had a total of 514 offspring, of which 164 individuals were diagnosed as healthy due to the absence of any clinical NF1 manifestation and by NF1 DNA testing, 346 were diagnosed with NF1 and carrying the familial NF1 pathogenic variant and 4 affected NF1 individuals were cases in which a different NF1 variant was identified (table 2). In the light of these transmission results, we estimated that the de novo mutation rate per gamete and per generation was 3.89×10^{-3}, around 20 times the first NF1 mutation rate to be described ($\sim 2 \times 10^{-4}$)[10] and 100 times higher considering the most recent NF1 mutation rate estimates of $3-6 \times 10^{-5}$.[11–13] In both scenarios, this difference is statistically significant. Similarly, if we considered the 246 families present in our cohort and assuming that not all tested NF1 individuals (n=100) harbour the familial NF1-causig variant, the estimated NF1 mutation rate per gamete and generation was 2.81×10^{-3}, 100 times higher considering the lowest NF1 mutation rate and 14 times considering the highest NF1 mutation rate described ($\sim 2 \times 10^{-4}$) (table 2).

Furthermore, given that the increased risk of transmission in individuals with NF1, due to their higher de novo mutation rate, could be appreciated as negligible considering the 50% risk of inheriting the familial variant, we estimated the co-occurrence of de novo NF1 cases in NF1 families to quantify the possible risk for these families of presenting a similar situation. In our cohort, we identified four families where the NF1 pathogenic variant detected in the index case did not co-segregate within the family. These results correspond to a frequency of 1:39 of familial cases with two or more genetically tested individuals (4 of 154), considerably higher than the expected de novo cases by chance assumed to be similar to those in the general population ($\sim$1:2500) about 60 times the frequency of sporadic NF1 ($p < 0.05$).

DISCUSSION

Our results highlight the fact that de novo NF1 pathogenic variants may appear more frequently than expected in NF1-affected families. One hundred fifty-four families of our cohort with familial NF1 in which two or more individuals were genetically tested were attended and in four of the families, two independent pathogenic variants in NF1 gene have been described. Several evidences have been published considering a possible higher mutation rate in NF1 in individuals with NF1 and, to date, 11 NF1 families with two or more independent mutations in the NF1 gene have already been reported.[5 25–27] More specifically, considering NF1 offspring data from our cohort, the estimated mutation rate of NF1 gene within NF1 families could be
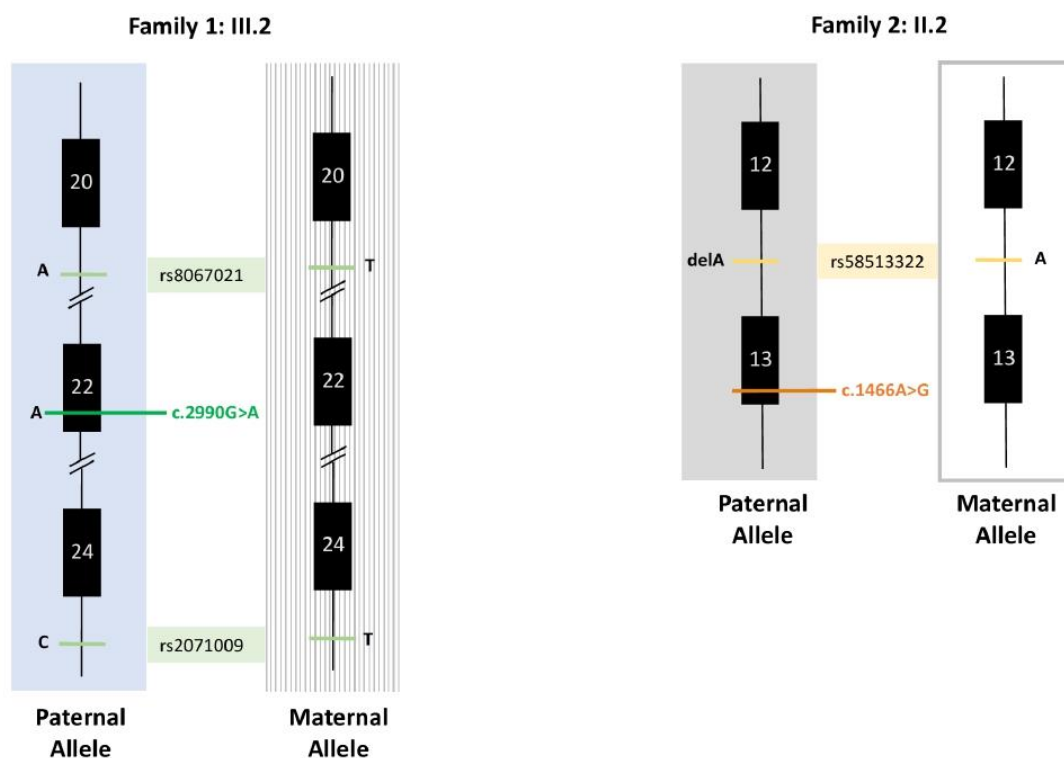
Figure 2

Figure 2 Diagram of the analysed neurofibromatosis type 1 region in families 1 and 2. Polymorphism analyses determine that in both families de novo mutation has originated in the paternal allele.

at least 14 times higher the highest *NF1* mutation rate previously described ($\sim 2 \times 10^{-4}$). However, these data could be biased due to the small cohorts studied and it needs to be confirmed in larger cohorts.

Further evidence is needed to consider an elevated *NF1* mutation rate in NF1 families compared with the general population. A possible explanation was that the presence of an inheritable defect in DNA repair segregating in the family, which is unlinked to the *NF1* gene, could be responsible for the occurrence of independent *NF1* pathogenic variants within a family.[26] The results obtained from the patients attended at the HGTP-ICO CSUR show that the de novo mutation occurs in the healthy allele of the affected progenitor and we can discard alterations in the most common genes related to DNA repair in the families studied there, since the next-generation sequencing (NGS) panel

used to genetically diagnose them also contains >130 genes involved in other cancer predisposition syndromes,[28] many caused by defects in DNA repair genes. Thus, our data do not support the hypothesis of a DNA repair defect unlinked to *NF1* gene as the molecular cause of this increased *NF1* mutation rate.

On the other hand, these de novo NF1 variants could be associated with both paternal origin and paternal age in addition to some intrinsic effect of NF1. In our cohort, four families showed de novo pathogenic variants in the offspring of NF1-affected males, all of whom were older than 30 years. In addition, in two of these families, the de novo mutation was found to be in the wild-type male allele. Studies of de novo mutations in humans have estimated the mutation rate of single-nucleotide variants to be $\sim 10^{-8}$ mutations per generation, giving rise to 45–60 de novo mutations per genome, mostly from paternal

Table 2 Estimation of the de novo NF1 mutation rate in NF1 families

	NF1 offspring				De novo *NF1* mutation rate in NF1 families
	Healthy*	Familial NF1 variant	New NF1 variant	Total	
Familial NF1 (n=246)	260	446†	4	710	Observed: 2.81×10^{-3} Expected: 2×10^{-4}; p=6.55×10^{-3} Expected: 3×10^{-5}; p=1.9×10^{-5}
NF1 families with >1 affected individuals tested (n=154)	164	346	4	514	Observed: 3.89×10^{-3} Expected: 2×10^{-4}; p=8.88×10^{-4} Expected: 3×10^{-5}; p=3.31×10^{-7}

*Paediatric cases, clinically determined by the absence of NF1 features.
†100 patients without genetic testing. Assumed to harbour the familial variant; n indicates the total number of families studied.
NF1, neurofibromatosis type 1.

origin and very variable within families.[34 35] It is established that the cumulative number of de novo variants transmitted by 20-year-old parents is around 45 and it increases by a factor of 1.3 per year, reaching around 90 at a parental age of 45.[36] In the case of NF1, similar evidences have been established: point de novo pathogenic variants have been previously associated with a paternal origin,[22 37] and the risk of de novo occurrence of NF1 in offspring increases with increasing paternal age.[15 16 20 24 38] In addition to this genome-wide paternal age effect, an additional paternal age effect has been observed for specific genes (eg, components of the RAS-MAPK pathway), which are positively selected in spermatogonia lineages.[17–19] As a consequence, the effective germline mutation rate in these genes is up to four orders of magnitude higher than the genome-wide rate.[18] In these cases, the association of these mutations with paternal age is stronger than the linear genome-wide paternal age effect. Therefore, the increased mutation rate in NF1 families could be affected by both gender and age of affected parent.

Regardless of the underlying cause of this higher *NF1* mutation rate, the data reported suggest that NF1 families are at an increased risk of experiencing a de novo mutation in *NF1* (1:39; 1,64%) compared with the general population (1:2500; 0.04%), especially in families in which the father is the affected member (p=0.0034). This observation, if confirmed in larger cohorts, would have relevant implications in genetic counselling and family planning, and also for genetic studies offered to NF1 relatives. Therefore, a negative result for a familial variant genetic test would not ensure the absence of the disease in antenatal tests. Furthermore, this should also be considered when genetic testing is performed to confirm NF1 in familial cases, as the absence of the familial *NF1* variant could erroneously rule out its de novo presence. Hence, without additional data, it is very important to reinforce the message during genetic counselling that all members of an affected family may not harbour the same variant, especially when considering family planning. In this context, the current approach to antenatal testing for the familial variant should be reconsidered, particularly if the father is the affected parent. There is the need to assess whether it could be more advantageous to propose to the family that they undertake a prenatal comprehensive study of the *NF1* gene (NGS panel and copy-number alterations detection) or genotyping of the sperm of fathers, as proposed by Pasmant and Pacot,[39] while considering all the implications, such as family stress, response time, incidental findings, technical limitation and cost-effectiveness. In the era of NGS, the sequencing of a gene takes on average 3 weeks, and consequently could be done in the context of prenatal diagnosis.

CONCLUSION

In summary, an unexpected number of NF1 families with two independent pathogenic variants in the *NF1* gene have been identified in our cohort, which comprises families from two expert NF centres. Moreover, 11 families with two different NF1-causing variants have been described in the literature. These findings suggest that NF1 individuals could present a *NF1* mutation rate of 3.89×10^{-3}, 20 times the highest *NF1* mutation rate described in the general population ($\sim 2 \times 10^{-4}$), and could be at risk of 1:39 of experiencing de novo mutations in the *NF1* gene. The knowledge of the estimated NF1 recurrence risk, together with a gender and age effect, is an essential component in genetic counselling when deciding on antenatal and familial NF1 testing strategies. Therefore, if this observation could be confirmed in other cohorts, would have relevant implications in *NF1* testing, genetic counselling and family planning for families affected with NF1.

Author affiliations
[1]Genetic Counseling Unit, Clinical Genetics Service, Northern Metropolitan Clinical Laboratory, Hospital Universitari Germans Trias i Pujol, Badalona, Spain
[2]Clinical Genomics Research Unit, Foundation Institute of Research in Health Sciences Germans Trias i Pujol, Badalona, Spain
[3]Clinical Genomics Unit—Genetics Service, Hospital Universitari Germans Trias i Pujol, Badalona, Spain
[4]Servicio de Genética, Hospital Universitario Ramon y Cajal, Madrid, Spain
[5]Neurology Service, Hospital Infantil Universitario Niño Jesús, Madrid, Spain
[6]Neurology, Hospital Universitari Germans Trias i Pujol, Badalona, Spain
[7]Hereditary Cancer Program, Program in Molecular Mechanisms and Experimental Therapy in Oncology (Oncobell), IDIBELL, Catalan Institute of Oncology, L'Hospitalet de Llobregat, Spain
[8]Centro de Investigación Biomédica en Red de Cáncer, CIBERONC, Madrid, Spain
[9]Department of Obstetrics, Hospital Universitari Germans Trias i Pujol, Badalona, Spain
[10]Dermatology, Hospital Universitari Germans Trias i Pujol, Badalona, Spain
[11]Hereditary Cancer Group, Fundació Institut d'Investigació en Ciències de la Salut Germans Trias i Pujol, Badalona, Spain
[12]Servicio de Genética, IRYCIS, Hospital Universitario Ramon y Cajal, Madrid, Spain
[13]Centro de Investigación Biomédica en Red de Enfermedades Raras, CIBERER, Valencia, Spain

ORCID iDs
Inma Rosas http://orcid.org/0000-0003-4238-0227
Alejandro Negro http://orcid.org/0000-0002-4654-077X
Conxi Lázaro Garcia http://orcid.org/0000-0002-7198-5906
Elisabeth Castellanos http://orcid.org/0000-0002-8133-5325

REFERENCES

1 Evans DG, Howard E, Giblin C, Clancy T, Spencer H, Huson SM, Lalloo F. Birth incidence and prevalence of tumor-prone syndromes: estimates from a UK family genetic register service. *Am J Med Genet A* 2010;152A:327–32.
2 Boyd KP, Korf BR, Theos A. Neurofibromatosis type 1. *J Am Acad Dermatol* 2009;61:1–14.
3 DeBella K, Szudek J, Friedman JM. Use of the National Institutes of health criteria for diagnosis of neurofibromatosis 1 in children. *Pediatrics* 2000;105:608–14.
4 Szudek J, Joe H, Friedman JM. Analysis of intrafamilial phenotypic variation in neurofibromatosis 1 (NF1). *Genet Epidemiol* 2002;23:150–64.
5 Sabbagh A, Pasmant E, Imbard A, Luscan A, Soares M, Blanché H, Laurendeau I, Ferkal S, Vidaud M, Pinson S, Bellanné-Chantelot C, Vidaud D, Parfait B, Wolkenstein P. Nf1 molecular characterization and neurofibromatosis type I genotype-phenotype correlation: the French experience. *Hum Mutat* 2013;34:1510–8.
6 Easton DF, Ponder MA, Huson SM, Ponder BA. An analysis of variation in expression of neurofibromatosis (NF) type 1 (NF1): evidence for modifying genes. *Am J Hum Genet* 1993;53:305.
7 Ferner RE. Neurofibromatosis 1 and neurofibromatosis 2: a twenty first century perspective. *Lancet Neurol* 2007;6:340–51.
8 Ratner N, Miller SJ. A RASopathy gene commonly mutated in cancer: the neurofibromatosis type 1 tumour suppressor. *Nat Rev Cancer* 2015;15:290–301.
9 Legius E, Messiaen L, Wolkenstein P, Pancza P, Avery RA, Berman Y, Blakeley J, Babovic-Vuksanovic D, Cunha KS, Ferner R, Fisher MJ, Friedman JM, Gutmann DH, Kehrer-Sawatzki H, Korf BR, Mautner V-F, Peltonen S, Rauen KA, Riccardi V, Schorry E, Stemmer-Rachamimov A, Stevenson DA, Tadini G, Ullrich NJ, Viskochil D, Wimmer K, Yohay K, Huson SM, Evans DG, Plotkin SR, International Consensus Group on Neurofibromatosis Diagnostic Criteria (I-NF-DC). Revised diagnostic criteria for neurofibromatosis type 1 and Legius syndrome: an international consensus recommendation. *Genet Med* 2021;23:1506–13.
10 Crowe FW, Schull WJ. *A clinical, pathological and genetic study of multiple neurofibromatosis*. Springfield, Illinois Charles C Thomas, 1956.
11 Sergeyev AS. On the mutation rate of neurofibromatosis. *Humangenetik* 1975;28:129–38.
12 Huson SM, Compston DA, Clark P, Harper PS, Huson SM, Compston DA, Clark P, Harper SM PS PS, DA C. A genetic study of von Recklinghausen neurofibromatosis in South East Wales. I. prevalence, fitness, mutation rate, and effect of parental transmission on severity. *J Med Genet* 1989;26:704–11.
13 Clementi M, Barbujani G, Turolla L, Tenconi R, Medica G, Pediatria D, Giustiniani V, Padova U, Loredan V. Neurofibromatosis-1: a maximum likelihood estimation of mutation rate. *Hum Genet* 1990;84:116–8.
14 Upadhyaya M, Ruggieri M, Maynard J, Osborn M, Hartog C, Mudd S, Penttinen M, Cordeiro I, Ponder M, Ponder BA, Krawczak M, Cooper DN. Gross deletions of the neurofibromatosis type 1 (NF1) gene are predominantly of maternal origin and commonly associated with a learning disability, dysmorphic features and developmental delay. *Hum Genet* 1998;102:591–7.
15 Adel Fahmideh M, Tettamanti G, Lavebratt C, Talbäck M, Mathiesen T, Lannering B, Johnson KJ, Feychting M. Parental age and risk of genetic syndromes predisposing to nervous system tumors: nested case-control study. *Clin Epidemiol* 2018;10:729–38.
16 Bunin GR, Needle M, Riccardi VM. Paternal age and sporadic neurofibromatosis 1: a case-control study and consideration of the methodologic issues. *Genet Epidemiol* 1997;14:507–16.
17 Tartaglia M, Cordeddu V, Chang H, Shaw A, Kalidas K, Crosby A, Patton MA, Sorcini M, van der Burgt I, Jeffery S, Gelb BD, a PM, Gelb BD, Jeffery S, Burgt vander I. Paternal germline origin and sex-ratio distortion in transmission of PTPN11 mutations in Noonan syndrome. *Am J Hum Genet* 2004;75:492–7.
18 Goriely A, Wilkie AOM. Paternal age effect mutations and selfish spermatogonial selection: causes and consequences for human disease. *Am J Hum Genet* 2012;90:175–200.
19 Penrose LS. Parental age and mutation. *Lancet* 1955;269:312–3.
20 Riccardi VM, Dobson CE, Chakraborty R, Bontke C. The pathophysiology of neurofibromatosis: IX. paternal age as a factor in the origin of new mutations. *Am J Med Genet* 1984;18:169–76.
21 Lázaro C, Gaona A, Ainsworth P, Tenconi R, Vidaud D, Kruyer H, Ars E, Volpini V, Estivill X. Sex differences in mutational rate and mutational mechanism in the NF1 gene in neurofibromatosis type 1 patients. *Hum Genet* 1996;98:696–9.
22 Jadayel D, Fain P, Upadhyaya M, Ponder MA, Huson SM, Carey J, Fryer A, Mathew CG, Barker DF, Ponder BA. Paternal origin of new mutations in von Recklinghausen neurofibromatosis. *Nature* 1990;343:558–9.
23 Brabbing-Goldstein D, Ben-Shachar S. Ante-Natal counseling in phacomatoses. *Childs Nerv Syst* 2020;36:2269–77.
24 Dubov T, Toledano-Alhadef H, Bokstein F, Constantini S, Ben-Shachar S. The effect of parental age on the presence of de novo mutations - Lessons from neurofibromatosis type I. *Mol Genet Genomic Med* 2016;4:480–6.
25 Klose A, Peters H, Hoffmeyer S, Buske A, Lüder A, Hess D, Lehmann R, Nürnberg P, Tinschert S. Two independent mutations in a family with neurofibromatosis type 1 (NF1). *Am J Med Genet* 1999;83:6–12.
26 Upadhyaya M, Majounie E, Thompson P, Han S, Consoli C, Krawczak M, Cordeiro I, Cooper DN. Three different pathological lesions in the NF1 gene originating de novo in a family with neurofibromatosis type 1. *Hum Genet* 2003;112:12–17.
27 Pacot L, Burin des Roziers C, Laurendeau I, Briand-Suleau A, Coustier A, Mayard T, Tlemsani C, Faivre L, Thomas Q, Rodriguez D, Blesson S, Dollfus H, Muller Y-G, Parfait B, Vidaud M, Gilbert-Dussardier B, Yardin C, Dauriat B, Derancourt C, Vidaud D, Pasmant E. One NF1 mutation may conceal another. *Genes* 2019;10:633.
28 Castellanos E, Gel B, Rosas I, Tornero E, Santín S, Pluvinet R, Velasco J, Sumoy L, Del Valle J, Perucho M, Blanco I, Navarro M, Brunet J, Pineda M, Feliubadaló L, Capellá G, Lázaro C, Serra E. A comprehensive custom panel design for routine hereditary cancer testing: preserving control, improving diagnostics and revealing a complex variation landscape. *Sci Rep* 2017;7:39348.
29 Valero MC, Martín Y, Hernández-Imaz E, Marina Hernández A, Meléan G, Valero AM, Javier Rodríguez-Álvarez F, Tellería D, Hernández-Chico C. A highly sensitive genetic protocol to detect NF1 mutations. *J Mol Diagn* 2011;13:113–22.
30 Castellanos E, Rosas I, Negro A, Gel B, Alibés A, Baena N, Pineda M, Pi G, Pintos G, Salvador H, Lázaro C, Blanco I, Vilageliu L, Brems H, Grinberg D, Legius E, Serra E. Mutational spectrum by phenotype: panel-based NGS testing of patients with clinical suspicion of RASopathy and children with multiple café-au-lait macules. *Clin Genet* 2020;97:264–75.
31 Garcia-Linares C, Fernández-Rodríguez J, Terribas E, Mercadé J, Pros E, Benito L, Benavente Y, Capellà G, Ravella A, Blanco I, Kehrer-Sawatzki H, Lázaro C, Serra E. Dissecting loss of heterozygosity (LOH) in neurofibromatosis type 1-associated neurofibromas: importance of copy neutral LOH. *Hum Mutat* 2011;32:78–90.
32 Peter D, Turnpenny SE. *Emery's Elements of Medical Genetics*. 15th Editi. Elsevier, 1900.
33 Messiaen LM, Wimmer K. NF1 mutational spectrum. *Neurofibromatosis Kaufmann D* 2008;16:63–77.
34 Conrad DF, Keebler JEM, DePristo MA, Lindsay SJ, Zhang Y, Casals F, Idaghdour Y, Hartl CL, Torroja C, Garimella KV, Zilversmit M, Cartwright R, Rouleau GA, Daly M, Stone EA, Hurles ME, Awadalla P, 1000 Genomes Project. Variation in genome-wide mutation rates within and between human families. *Nat Genet* 2011;43:712–4.
35 Goldmann JM, Wong WSW, Pinelli M, Farrah T, Bodian D, Stittrich AB, Glusman G, Vissers LELM, Hoischen A, Roach JC, Vockley JG, Veltman JA, Solomon BD, Gilissen C, Niederhuber JE. Parent-Of-Origin-Specific signatures of de novo mutations. *Nat Genet* 2016;48:935–9.
36 Goldmann JM, Veltman JA, Gilissen C. De novo mutations reflect development and aging of the human germline. *Trends Genet* 2019;35:828–39.
37 Stephens K, Kayes L, Riccardi VM, Rising M, Sybert VP, Pagon RA. Preferential mutation of the neurofibromatosis type 1 gene in paternally derived chromosomes. *Hum Genet* 1992;88:279–82.
38 Liu Q, Zoellner S, Gutmann DH, Johnson KJ. Parental age and neurofibromatosis type 1: a report from the NF1 patient registry initiative. *Fam Cancer* 2015;14:317–24.
39 Pasmant E, Pacot L. Should we genotype the sperm of fathers from patients with 'de novo' mutations? *Eur J Endocrinol* 2019;182:C1–3.

Supplementary Table 1: Type of NF1 pathogenic variant						
	A Series (H. Ramon & Cajal)	**B Series** (CSUR)	**Total (%)**	**Expected proportion***	**p-val**	**Statistical Method^**
Sporadic NF1						
Nonsense	107	21	128 (0,25)	0,207	0,043	1
Frameshift	124	21	145 (0,29)	0,256	**0,229**	1
Splicing	95	18	113 (0,22)	0,270	0,030	1
Missense / in frame variants	47	17	64 (0,13)	0,159	**0,069**	1
First Methionine	1	1	2 (0.004)	1,734	**0,621**	2
Single or multiple exon deletions	16	4	20 (0,04)	0,022	0,047	1
Whole NF1 gene deletion	34	5	39 (0,07)	0,050	0,032	1
Familial NF1 (index cases)						
Nonsense	38	12	50 (0,23)	0,207	**0,506**	1
Frameshift	50	18	68 (0,31)	0,256	**0,091**	1
Splicing	52	9	61 (0,13)	0,270	**0,822**	1
Missense / in frame variants	18	11	29 (0,13)	0,159	**0,363**	1
First Methionine	1	0	1 (0.005)	2,034	**0,441**	2
Single or multiple exon deletions	2	0	2 (0,01)	0,411	**0,310**	2
Whole NF1 gene deletion	5	2	7 (0,03)	0,050	**0,311**	1

* Messiaen & Wimmer, 2008   ^ 1) 2-sample test for equality of proportions with continuity correction; 2) Fisher's Exact Test for Count Data

Appendix E

Directors' report

As the co-directors of the doctoral thesis of Núria Catasús Segura, entitled "Refining prognosis capacity and implementing principles of personalized therapies for Neurofibromatosis Type 2", Elisabeth Castellanos Pérez and Ignacio Blanco Guillermo certify that the PhD candidate has actively participated in the design and the main performance of the experimental work, analysis of the results and their discussion, drawing conclusions and preparing publications presented in this thesis.

The work of the candidate is summarized below:

- The PhD candidate settled primary cultures and functional analysis performed in order to identify new molecular prognostic markers for Neurofibromatosis Type 2. She contributed in stablishing the data base of NF2 patients from the Spanish cohort to validate the Genetic Severity Score and the analysis of the results.

- She prepared the figures and actively participated in writing the manuscript for the publication: *N.Catasús, B.Garcia, I.Galván-Femenía, A.Plana, A.Negro, I.Rosas, A.Ros, E.Amilibia, JL.Becerra, C.Hostalot, F.Rocaribas, I.Bielsa, CL.Garcia, R.de Cid, E.Serra, I.Blanco, E.Castellanos (2021). Journal of Medical Genetics, 1–9* (Impact Factor 6.318).

- The candidate designed PMOs, settled fibroblasts primary cultures and experimental conditions to perform the assays required to test the antisense approaches presented in this work based on previous works from the group. She performed the functional assays and results analysis.

- She prepared the figures and contributed in preparing the manuscript for publication: *N.Catasús, I.Rosas, S.Bonache, A.Negro, A.Plana, H.Salvador, E.Serra, I.Blanco, E.Castellanos. Molecular Therapy. Submitted.* (bioRxiv: https://doi.org/10.1101/2022.02.11.479859).

- The candidate performed the experimental procedures to set up iPSC cultures. She designed and performed the CRISPR-Cas9 experiments included in this thesis. She performed all experimental procedures included in the NC and SC differentiation processes, as well as the main work in the cellular characterization, including flow cytometry and immunofluorescence assays. She has prepared the figures and wrote the adapted manuscript presented in this thesis as Chapter 3.

While the main contribution in this work was conducted by the PhD candidate, the projects presented in this thesis benefit from expertise and collaboration of other professionals and core facilities as described as follows:

- Clinical data and sample collection for the research projects carried out in this thesis have been made in the context of CSUR (National unit of expertise for genetic neurocutaneous syndromes (Phacomatoses) at HUGTP-ICO-IGTP.
- Genetic analysis and diagnosis have been performed in collaboration with the Clinical Genomics Unit.
- All the members of the Clinical Genomics Research Group have been involved in the research projects described in this thesis.
- Eduard Serra and Meritxell Carrió (Hereditary Cancer Lab at IGTP) have contributed with their expertise in the field of pluripotent stem cells and NFs.
- Bioinformatic analysis of this thesis have been mainly performed by Mercedes Guerrero (HUGTP), Rafael de Cid and Ivan Galván (Genomes for Life-GCAT Lab Group, IGTP).
- Generation and main characterization of iPSCs was performed at the Barcelona Stem Cell Bank (B-SCB).
- Several techniques were performed at the Cytometry and Translational Genomics IGTP Core Facilities.

Dr. Elisabeth Castellanos Pérez, co-director   Dr. Ignacio Blanco Guillermo, co-director

Barcelona 2022